GASTROINTESTINAL CANCER IMMUNE RESPONSE AND IMMUNE RELATED ADVERSE EFFECTS

EDITED BY: Ti Wen, Yanhong Deng and Bo Qin
PUBLISHED IN: Frontiers in Immunology and Frontiers in Oncology

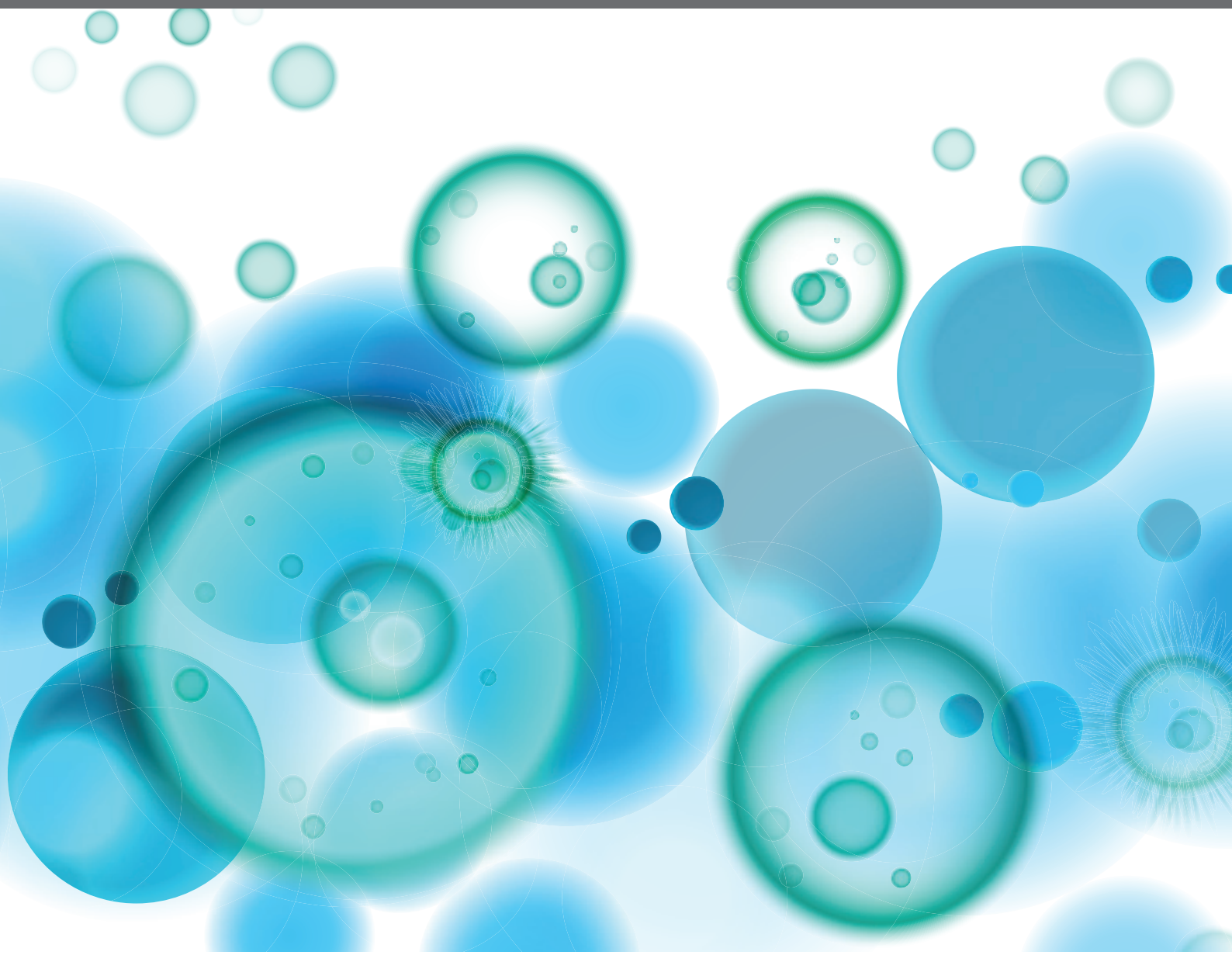

frontiers Research Topics

frontiers

ISSN 1664-8714
ISBN 978-2-83250-671-4
DOI 10.3389/978-2-83250-671-4

About Frontiers

Frontiers is more than just an open-access publisher of scholarly articles: it is a pioneering approach to the world of academia, radically improving the way scholarly research is managed. The grand vision of Frontiers is a world where all people have an equal opportunity to seek, share and generate knowledge. Frontiers provides immediate and permanent online open access to all its publications, but this alone is not enough to realize our grand goals.

Frontiers Journal Series

The Frontiers Journal Series is a multi-tier and interdisciplinary set of open-access, online journals, promising a paradigm shift from the current review, selection and dissemination processes in academic publishing. All Frontiers journals are driven by researchers for researchers; therefore, they constitute a service to the scholarly community. At the same time, the Frontiers Journal Series operates on a revolutionary invention, the tiered publishing system, initially addressing specific communities of scholars, and gradually climbing up to broader public understanding, thus serving the interests of the lay society, too.

Dedication to Quality

Each Frontiers article is a landmark of the highest quality, thanks to genuinely collaborative interactions between authors and review editors, who include some of the world's best academicians. Research must be certified by peers before entering a stream of knowledge that may eventually reach the public - and shape society; therefore, Frontiers only applies the most rigorous and unbiased reviews.
Frontiers revolutionizes research publishing by freely delivering the most outstanding research, evaluated with no bias from both the academic and social point of view. By applying the most advanced information technologies, Frontiers is catapulting scholarly publishing into a new generation.

What are Frontiers Research Topics?

Frontiers Research Topics are very popular trademarks of the Frontiers Journals Series: they are collections of at least ten articles, all centered on a particular subject. With their unique mix of varied contributions from Original Research to Review Articles, Frontiers Research Topics unify the most influential researchers, the latest key findings and historical advances in a hot research area! Find out more on how to host your own Frontiers Research Topic or contribute to one as an author by contacting the Frontiers Editorial Office: frontiersin.org/about/contact

GASTROINTESTINAL CANCER IMMUNE RESPONSE AND IMMUNE RELATED ADVERSE EFFECTS

Topic Editors:
Ti Wen, The First Affiliated Hospital of China Medical University, China
Yanhong Deng, The Sixth Affiliated Hospital of Sun Yat-sen University, China
Bo Qin, Mayo Clinic, United States

Citation: Wen, T., Deng, Y., Qin, B., eds. (2022). Gastrointestinal Cancer Immune Response and Immune Related Adverse Effects. Lausanne: Frontiers Media SA. doi: 10.3389/978-2-83250-671-4

Table of Contents

frontiers | Frontiers in Oncology

TYPE Editorial
PUBLISHED 18 October 2022
DOI 10.3389/fonc.2022.1034890

OPEN ACCESS

EDITED AND REVIEWED BY
Francesco Sabbatino,
University of Salerno, Italy

*CORRESPONDENCE
Ti Wen
wenti@cmu.edu.cn

SPECIALTY SECTION
This article was submitted to Cancer Immunity and Immunotherapy, a section of the journal Frontiers in Oncology

RECEIVED 02 September 2022
ACCEPTED 28 September 2022
PUBLISHED 18 October 2022

CITATION
Wen T, Deng Y and Qin B (2022) Editorial: Gastrointestinal cancer immune response and immune related adverse effects. *Front. Oncol.* 12:1034890. doi: 10.3389/fonc.2022.1034890

Editorial: Gastrointestinal cancer immune response and immune related adverse effects

Ti Wen[1]*, Yanhong Deng[2,3] and Bo Qin[4]

[1]Department of Medical Oncology, The First Hospital of China Medical University, Shenyang, China, [2]Department of Medical Oncology, The Sixth Affiliated Hospital of Sun Yat-sen University, Guangzhou, China, [3]Department of Gastroenterology, The Sixth Affiliated Hospital of Sun Yat-sen University, Guangzhou, China, [4]Mayo Clinic, Rochester, MN, United States

KEYWORDS

immune response, GI cancers, immune related adverse effects, tumor microenvironment, biomarker

Editorial on the Research Topic
Gastrointestinal cancer immune response and immune related adverse effects

Gastrointestinal (GI) cancers, including the cancers originating from esophagus, stomach, liver, biliary system, small intestine, colon and pancreas, (1), are among the most common and lethal solid tumors worldwide, and emerge as major health burdens, especially in China. Surgery, chemotherapy, and radiotherapy are the traditional treatments for GI cancers, but many patients have poor outcome with low 5-year survival rate (2). Recently, treatments for solid tumors targeting the crosstalk between tumor and immune system have achieved significant success in gastrointestinal cancer. Immune checkpoint inhibitor (ICI) therapy and related combination therapy have become new treatment options for gastric cancer (3), colon cancer (4), liver cancer (5), and esophageal cancer (6).

However, many questions following the application of immunotherapy raise, such as, the dynamic immune response within tumor microenvironment (TME) during cancer development and treatment. Understanding the responses of the immune system in different periods and/or changes of immune response caused by multiple treatments are necessary to reveal potential molecules as novel immune targets or biomarkers and guide personal medicine in the future.

Within this context, we proposed the research topic, aiming to publish advances in the field of the immune regulation during different cancer stages or treatment that may significantly contribute to shed light on the immunotherapy of GI cancer. After almost one year, we had received more than 50 article submissions, and 12 of them were accepted including 6 original articles, 4 review articles and 2 case reports.

Therapeutic strategies and efficacy for GI cancers

In gastric cancer with serosal invasion, Lin et al. reported that camrelizumab combined with nab-paclitaxel plus S-1 can improve the rate of tumor regression grade (TRG 1a/1b) and pCR (pathological complete response) significantly. Duan et al. demonstrated that the combination of neoadjuvant immunotherapy and chemotherapy is correlated with high pathological and immunologic response in the tumor microenvironment (TME) of esophageal squamous cell carcinoma (ESCC). Lv et al. reported a case of advanced Epstein-Barr virus-associated gastric cancer (EBVaGC) patient, with high tumor mutation burden (TMB), positive expression of PD-L1 and PD-L1+ CD68+ macrophages enrichment, who had a long-term manageable toxicity and partial response to the combination of camrelizumab and oxaliplatin plus oral S-1 (SOX). Wang et al. reported a case of HER2-positive gallbladder cancer (GBC) patients who were resistance to trastuzumab-based targeted therapy and chemotherapy may benefit from trastuzumab plus anti-PD-1. A network meta-analysis (NMA) comparing the efficacy and safety of immunotherapy plus oxaliplatin- or cisplatin- based chemotherapy in the first-line treatment of advanced gastric cancer (AGC) was conducted by Guo et al. It suggested that the progression free survival (PFS) was prolonged significantly in patients treated with PD-1 inhibitor plus oxaliplatin- based chemotherapy. In addition, a review by Westdorp et al. discussed pathways that were altered in ICI-mediated colitis (IMC) in both human colon biopsy samples and mouse models, and revealed a complicated interplay between the gut microbiome and several types of immune cells. Thus, understanding the cellular mechanisms that induce immune related adverse events (irAEs) may provide opportunities for prevention and management.

Identification of biomarkers in GI cancer for diagnosis and prognosis

Xu et al identified a nine-lncRNA-based signature as the ferroptosis-related prognostic model for hepatocellular carcinoma (HCC) patients. According to the prognostic signature, patients were divided into high and low risk groups, and the regulation of several immune-associated signaling pathways were correlated with the low-risk group shown by GSEA analysis. In HCC patients, Huang et al. reported that H2AFY expression was an independent unfavorable prognostic factor and correlated with immune infiltration in TME. Moreover, mitosis, cell cycle, chromatin assembly and spliceosome may be regulated by H2AFY and its co-expressed genes through E2F family and cancer-related kinases pathways shown by functional network analysis. Knockdown H2AFY inhibited the migration and proliferation of HCC cells, promoted apoptosis and cycle arrest of cells *in vitro*.

Studies by Yue et al. indicated that CX3CR1, expressed in colorectal cancer (CRC) patients and cell lines, was chosen as a TME-related hub gene. It was positively correlated with CD8+T cells, CD4+T cells, B cells, macrophages, dendritic cells and neutrophils and negatively correlated with tumor purity. Moreover, CX3CR1 expression correlated with the recruitment of immune-infiltrating cells, and it might control CRC progression through inhibiting tumor-associated macrophage (TAM) polarization. These findings suggested that CX3CR1 indicate better survival in CRC. Xie et al. reported that for CRC patient`s peripheral blood immune cells (PBIC) m^6A RNA was a diagnostic biomarker. Compared with those in the healthy controls, the PBIC m^6A RNA levels in the CRC group were apparently elevated, even higher in progressed and metastasized CRC, while reduced after treatment. Impressively, the area under the curve (AUC) of the PBIC m6A levels was 0.946, which was higher than the AUCs for CA125, CA19-9, and CEA. Gene set variation analysis implied that monocytes resulted as the specific immune cells most correlated with high PBIC m^6A levels in CRC patients.

Reviews in GI cancer progression and immunotherapy

Dugage et al. highlighted three immunotherapeutic strategies in Gastrointestinal stromal tumors (GIST). Firstly, patients involved in clinical trials must be better screened, according to the driver mutation and the tertiary lymphoid structures (TLS) or PD-L1 expression. Secondly, during imatinib therapy, indoleamine 2,3-dioxygenase (IDO) targeting should be explored after disease progression. Finally, combination of *c-kit* inhibition with ICI is recommended.

Kim and Lee. described the gut microbiome strains such as Salmonella, E. coli, F. nucleatum, B. fragilis and P. anaerobius in each stage of the tumorigenesis process of CRC. This review provided an overview of the microbiota species involved in the associations between the gut microbiome and CRC. It also indicated treatments which regulate the gut microbiome could improve the efficacy of CRC treatment.

Conclusion

In conclusion, a group of original and review articles are collected in this Research Topic "*Gastrointestinal Cancer*

Immune Response and Immune Related Adverse Effects". We believe that this published knowledge can help us to understand the immune response in each stage of cancer development or during different types of treatment more deeply, find biomarkers and develop new therapeutic approaches for GI cancer which will contribute to improve immunotherapeutic efficacy and prognosis for GI cancer patients.

Author contributions

All authors listed have made a substantial, direct, and intellectual contribution to the work and approved it for publication.

Conflict of interest

The authors declare that the research was conducted in the absence of any commercial or financial relationships that could be construed as a potential conflict of interest.

Publisher's note

References

1. Gonzalez RS, Raza A, Propst R, Adeyi O, Bateman J, Sopha SC, et al. Recent advances in digestive tract tumors: Updates from the 5th edition of the world health organization "Blue book". *Arch Pathol Lab Med* (2021) 145(5):607–26. doi: 10.5858/arpa.2020-0047-RA

2. Siegel RL, Miller KD, Fuchs HE, Jemal A. Cancer statistics, 2021. *CA Cancer J Clin* (2021) 71(1):7–33. doi: 10.3322/caac.21654

3. Janjigian YY, Shitara K, Moehler M, Garrido M, Salman P, Shen L, et al. First-line nivolumab plus chemotherapy versus chemotherapy alone for advanced gastric, gastro-oesophageal junction, and oesophageal adenocarcinoma (CheckMate 649): a randomised, open-label, phase 3 trial. *Lancet* (2021) 398 (10294):27–40. doi: 10.1016/S0140-6736(21)00797-2

4. Fukuoka S, Hara H, Takahashi N, Kojima T, Kawazoe A, Asayama M, et al. Regorafenib plus nivolumab in patients with advanced gastric or colorectal cancer: An open-label, dose-escalation, and dose-expansion phase ib trial (REGONIVO, EPOC1603). *J Clin Oncol* (2020) 38(18):2053–61. doi: 10.1200/JCO.19.03296

5. Llovet JM, Castet F, Heikenwalder M, Maini MK, Mazzaferro V, DJ P, et al. Immunotherapies for hepatocellular carcinoma. *Nat Rev Clin Oncol* (2021) 19 (3):151–72. doi: 10.1038/s41571-021-00573-2

6. Kato K, Shah MA, Enzinger P, Bennouna J, Shen L, Adenis A, et al. KEYNOTE-590: Phase III study of first-line chemotherapy with or without pembrolizumab for advanced esophageal cancer. *Future Oncol* (2019) 15 (10):1057–66. doi: 10.2217/fon-2018-0609

frontiers in Immunology

REVIEW
published: 20 August 2021
doi: 10.3389/fimmu.2021.715727

Beyond the Driver Mutation: Immunotherapies in Gastrointestinal Stromal Tumors

Matthieu Roulleaux Dugage[1]*, *Robin Lewis Jones*[2], *Jonathan Trent*[3], *Stéphane Champiat*[4] and *Sarah Dumont*[1]

[1] Département d'Oncologie Médicale, Gustave Roussy, Université Paris Saclay, Villejuif, France, [2] Division of Clinical Studies, Institute of Cancer Research & Sarcoma Unit of the Royal Marsden NHS Foundation Trust, London, United Kingdom, [3] Department of Medicine, Division of Oncology, Sylvester Comprehensive Cancer Center, University of Miami Miller School of Medicine, Miami, FL, United States, [4] Département d'Innovation Thérapeutique et des Essais Précoces (DITEP), Gustave Roussy, Université Paris Saclay, Villejuif, France

OPEN ACCESS

Edited by:
Bo Qin,
Mayo Clinic, United States

Reviewed by:
Lixuan Wei,
Mayo Clinic, United States
Huanyao Gao,
Mayo Clinic, United States

***Correspondence:**
Matthieu Roulleaux Dugage
matthieu.roulleaux-dugage@gustaveroussy.fr

Specialty section:
This article was submitted to Cancer Immunity and Immunotherapy, a section of the journal Frontiers in Immunology

Received: 27 May 2021
Accepted: 04 August 2021
Published: 20 August 2021

Citation:
Roulleaux Dugage M, Jones RL, Trent J, Champiat S and Dumont S (2021) Beyond the Driver Mutation: Immunotherapies in Gastrointestinal Stromal Tumors. Front. Immunol. 12:715727. doi: 10.3389/fimmu.2021.715727

Gastrointestinal stromal tumors (GISTs) are a subtype of soft tissue sarcoma (STS), and have become a concept of oncogenic addiction and targeted therapies.The large majority of these tumors develop after a mutation in *KIT* or platelet derived growth factor receptor α (*PDGFRα*), resulting in uncontrolled proliferation. GISTs are highly sensitive to imatinib. GISTs are immune infiltrated tumors with a predominance of tumor-associated macrophages (TAMs) and T-cells, including many CD8+ T-cells, whose numbers are prognostic. The genomic expression profile is that of an inhibited Th1 response and the presence of tertiary lymphoid structures and B cell signatures, which are known as predictive to response to ICI. However, the microtumoral environment has immunosuppressive attributes, with immunosuppressive M2 macrophages, overexpression of indoleamine 2,3-dioxygenase (IDO) or PD-L1, and loss of major histocompatibility complex type 1. In addition to inhibiting the *KIT* oncogene, imatinib appears to act by promoting cytotoxic T-cell activity, interacting with natural killer cells, and inhibiting the expression of PD-L1. Paradoxically, imatinib also appears to induce M2 polarization of macrophages. There have been few immunotherapy trials with anti-CTLA-4 or anti-PD-L1drugs and available clinical data are not very promising. Based on this comprehensive analysis of TME, we believe three immunotherapeutic strategies must be underlined in GIST. First, patients included in clinical trials must be better selected, based on the identified driver mutation (such as *PDGFRα* D842V mutation), the presence of tertiary lymphoid structures (TLS) or PD-L1 expression. Moreover, innovative immunotherapeutic agents also provide great interest in GIST, and there is a strong rationale for exploring IDO targeting after disease progression during imatinib therapy. Finally and most importantly, there is a strong rationale to combine of *c-kit* inhibition with immune checkpoint inhibitors.

Keywords: GIST - gastro intestinal stromal tumor, immunotherapy, PD-L1, imatinib, IDO - indoleamine 2,3-dioxygenase, KIT, immunologic response, macrophages (M1/M2)

INTRODUCTION

Gastrointestinal stromal tumors (GISTs) represent a subtype of soft tissue sarcoma (STS) and are characterized by the malignant proliferation of Cajal cells in the bowel (1). Although rare with an annual rate of around 1 patients per 100.000 inhabitants, GISTs represent around 20% of STSs, making them the most frequent type of STS (2). Although they most frequently develop from the gastric stroma, GISTs can occur on every part of the digestive tract, and secondary locations are often liver and peritoneum (3). In most cases, the underlying mechanism is a mutation in the *KIT* gene (also known as *CD117*), coding for an activated transmembrane receptor c-kit and resulting in uncontrolled proliferation (4). Other cases are due to mutations in *platelet derived growth factor receptor* α (*PDGFR*α), *NF1*(coding for neurofibromin 1) or in the genes coding region for *succinate dehydrogenase* (SDH) (5). Treatment with imatinib results in deep (6) as well as sustained responses (7), but subsequent therapies offer a less durable clinical benefit. There is therefore an important need for new treatments for advanced GIST.

We conducted a literature review to describe the GIST microenvironment and current approaches to immunotherapy. The immune system seems to play a crucial role this controlling the disease, but the results of immunotherapy are disappointing to date. New molecular targets could be of interest.

GASTROINTESTINAL STROMAL TUMORS AS A SPECIFIC TUMOR MODEL

GISTs are a model of oncogenic addiction: its tumor cells are totally dependent on the activation of one molecular pathway, due to an identified mutation. Whereas some soft-tissue sarcomas are characterized by complex genomic variations (5) and are supposed to be more immunogenic, GIST oncogenesis is driven by a mutation in the *KIT* gene, coding for the transmembrane receptor c-kit (in 80% of all cases). This mutation occurs in exon 11 (coding for an intracellular domain), and more rarely, in exon 9 (coding for an extracellular domain). An activating *KIT* mutation leads to a signal for proliferation as well as the inhibition of apoptosis, through *phosphatidylinositol-3,4-bisphosphate kinase* (PIK3CA)/AKT/*mammalian target of rapamycin* (mTOR) and *mitogen activated proteins* (MAP) kinase pathways. *PDGFR*α is the second most frequent molecular alteration in GIST (in about 8% of cases), on various loci (such as D842V or V561D) and the D842V mutation is the most frequent alteration (8). The remaining 10-15% of tumors are *KIT*/*PDGFR*α wild-type, but several other mutations have been identified. SDH-deficient GISTs represent around 7% of all GISTs and are most frequent in young adults, occurring in around 50% of cases because of a loss-of-function germline mutation in one of the SDH complex genes (9). Mutations in the gene *NF1* can also be found, and autopsies of patients with Neurofibromatis 1 show undiagnosed GIST in one third of patients (10). *BRAF* V600E mutations have also been described in a small subset of patients, representing around 3.5% of all cases (11).

Advanced GIST is naturally chemoresistant with a response rate of about 7% to doxorubicin-based regimens (12). Prior to the introduction of imatinib and other tyrosine kinase inhibitors (TKIs), GISTs were associated with a very poor outcome with overall survival (OS) of only 12-19 months (13). However, the development of targeted therapy has revolutionized the prognosis of these patients. Imatinib is a multikinase inhibitor (multi-TKI) which was developed at the end of the 1990s and targets c-kit, PDGFRα, *Vascular endothelium growth factor* (VEGFR), *basic fibroblast growth factor* (b-FGF) among others kinases (14). Treatment with imatinib leads to progression-free survival (PFS) of around 30 months. The sensitivity of GISTs to imatinib mainly depends on the mutation locus and is higher in *KIT* exon 11 mutations (15). Unfortunately, not all GIST benefit from imatinib: SDH-deficient, NF1 and D842V-mutated GIST are imatinib resistant (5, 8, 9, 16). In imatinib-sensitive GIST, disease progression eventually occurs, mainly due to new oncogenic alterations. *KIT*-mutated GISTs can harbor secondary mutations in *KIT*, which most often occur in the imatinib target on c-kit, namely the *adenosine triphosphate* (ATP)-binding pocket (exon 13-14), or on the activation loop (exon 17-18) (5). In most cases, these mutations remain sensitive to sunitinib in a second-line setting or regorafenib in a third-line setting. Sunitinib is a multi-TKI targeting c-kit, PDGFRα and VEGFR, among others, which allows a meaningful median progression-free survival (median PFS) of around 6 months (17). After progression under sunitinib, regorafenib can be administrated, allowing a median PFS of around 5 months (18). Using all of these treatments sequentially results in a median OS of around 8 years in advanced GIST (15). More recently, ripretinib has been shown to result in median PFS of 6 months after three previous lines of treatments (19). This drug is currently being investigated as second-line *versus* sunitinib (20). The consensual strategy concerning advanced GIST is summarized in **Table 1**.

Drug development in advanced GIST mainly focuses on new multi-TKI, with interesting activity (19, 21, 22), especially with the FDA (*Food and Drug Administration*) approval of

TABLE 1 | Therapeutic options in the treatment of gastrointestinal stromal tumors (NCCN Guidelines, October 2020).

Phase	Setting	Treatment
Localized disease	(Neo-)Adjuvant	Imatinib
		PGFRα*-D842V:* Avapritinib
Advanced disease	First-line setting	Imatinib
		PGFRα*-D842V:* Avapritinib
	Second-line setting	Sunitinib
	Third-line setting	Regorafenib
	Fourth-line setting	Ripretinib
	Other options	Avapritinib
		Cabozantinb
		Dasatinib
		Nilotinib
		Pazopanib

avapritinib in D842V mutated GIST and ripretinib as fourth-line therapy. However, as in other tumor types, clinical benefit to systemic treatments decreases with the number of previous lines, and, in the very particular model of GIST, with the accumulation of resistance mutations. In the first-line setting, no TKI has improved outcome compared to imatinib. New treatment strategies are therefore needed.

Evidence is accumulating of an associated immune escape, leading to drug resistance and disease progression and this evidence opens up the field of immunotherapy for the treatment of advanced GIST.

A HIGHLY INFILTRATED TUMOR MICROENVIRONMENT

Despite an oncogenesis based on a single pathway alteration and a low tumor mutational burden (23) suggesting a poor immunogenicity, GIST commonly harbors a rich immune infiltrate, suggesting a recognition of tumor cells by the immune system.

The microenvironment of GISTs is characterized by a high density of immune cells, with two main cell populations: tumor-associated macrophages (TAMs) and T-cells (CD4+, CD8+ and FoxP3+) in both untreated and treated tumors (24). There also seems to be some natural killer cells (NK cells) and a few B-cells. This microenvironment plays a major role in disease control, and *Rusakiewicz et al.* demonstrated that CD3+ cell and NKp46 cell infiltrates were independently positively correlated with PFS in both imatinib-treated and untreated localized GISTs, contrary to FoxP3 infiltrate (25). The type of *KIT* mutation did not seem to play a role in PFS in multivariate analysis. The worst prognosis was found amongst patients with a high Miettinen score but a low CD3+ cell count, and a low NKp46+ cell infiltrate.

The most common cells found in this immune infiltrate are TAMs, around twice more as T cells. M1 macrophages are differentiated from monocytes when exposed to *Granulocyte-macrophage colony-stimulating factor* (GM-CSF), *Lipopolysaccharide* (LPS) or *Interferon gamma* (IFN-γ) and promote an inflammatory microenvironment through the expression of IL-1, IL-6, IL-12 or *Tumor necrosis factor α* (TNFα). In contrast, M2 macrophages differentiate from monocytes in the presence of *Macrophage colony-stimulating factor* (M-CSF), IL-4 or IL-10 and are known to promote immune escape through the high expression of *Programmed death ligand* 1(PD-L1), IL-10 or *Transforming growth factor β* (TGFβ) (26). The polarization of TAMs is still controversial: in a cohort of 31 GIST samples with a majority of untreated primary tumors, these macrophages were in a majority of cases M2-polarized (27), whereas Cavnar et al. described an important M1 contingent in 25 untreated GISTs (28). In this study, TAMs became M2-polarized after treatment by imatinib (*see infra*). Although the most common T-cells are CD4+ helper lymphocytes, CD8+ T-cells are highly represented in this dense immune infiltrate. Regulatory T-cells (CD4+, FoxP3+) are also present but in much lower numbers (24). CD8+ T-cells are the key lymphocytes for killing tumor cells, and it has been proven that their presence is necessary to achieve a response to a treatment with anti-PD-1 (*programmed cell death 1*) antibodies (29). Furthermore, their density has been shown to be positively correlated with a response to immune checkpoint inhibitors (ICIs) in advanced melanomas (30) and renal cell carcinomas (31).

B-cells are described in GIST, but they seem to be present in higher numbers in metastatic lesions, where they represent around 2% of all immune cells, than in the primary tumor in untreated GISTs (32). The interest is rising regarding their importance in the immune response against cancer, where they play a role in tertiary lymphoid structures (*see* infra). Moreover, tumor infiltrating B-cells are known to provide a humoral antitumor response, leading to antibody-dependent cellular cytotoxicity (ADCC) and complement-dependent cytotoxicity (CDC) (25, 27).

As in other tumor models, there also seems to be immune activity mediated through NK cells. NK cells are lymphocytes belonging to the innate immune system and are involved in the first line defense against infection or tumors. They recognize pathological cells through a sum of activatory or inhibitory signals on their surface. They particularly target cells with a reduced expression of *major histocompatibility complex 1* (MHC I), which is common in GISTs. NK cells are described in the GIST microenvironment, and their presence is associated with a lower proliferation index and a better prognosis in untreated metastatic GIST (32). NK cells are activated by dendritic cells *via* the NKp30 receptor. However, in the peripheral blood of patients with advanced GIST, the NKp30c isotype is overexpressed at diagnosis. This isotype is the result of a splice variant due to genetic polymorphism and is immunosuppressive, in contrast to NKp30a and NKp30b. This leads to a decrease in TNFα, CD107a and IFNγ secretion, and seems to be associated with poorer OS (33).

Overall, with a tumor microenvironment highly infiltrated with different immune cells, whose proportion has a prognostic impact, the immune response seems to be of interest in GIST. Some studies have investigated the immune signatures in GIST more closely.

AN INFLAMMATORY PROFILE SUGGESTING THE BENEFIT OF IMMUNOTHERAPY

In a study analyzing the immune infiltrate of 31 patients with a majority of primary untreated tumors by RNA sequencing, Pantaleo et al. demonstrated that their tumor microenvironment is similar to that of melanomas, which is the very paradigm for efficacy of immunotherapy (27). The TIS (*T-cell inflamed signature)* encompasses 18 genes related to antigen presenting cell abundance, T-cell/NK cell abundance, IFN activity and T cell exhaustion and has been shown to be predictive for response to immunotherapy in melanomas (34) and head and neck carcinomas (35). TIS score for GIST was between the 65th and 70th percentile of the Cancer Genome Atlas dataset, which shows that there is an inhibited T cell activity as found in lung or renal

carcinomas (27, 35). Interestingly, this signature was positively correlated with PD-L1 expression.

Based on the RNA-sequencing of 608 tumor samples of patients with STS, Petitprez et al. have recently investigated the role of tumor microenvironment (TME) in STS and its association with response to anti-PD1 immunotherapy. They created the Sarcoma Immune Classification (SIC), a classification that sorts STSs based on their tumor microenvironment, ranging from SIC-A (immune desert) to SIC-E (rich immune infiltrate).The main features of each group are described in **Table 2** (36). When applied to the pretherapeutic biopsies of 47 patients included in the SARC028 trial, SIC was found to be predictive of response to anti-PD-1 antibody therapy with around 50% of responders in the SIC E group. GIST is the most represented histologic subtype in this group, with around 25% of all 60 GISTs studied (*versus* around 20% in all sarcomas). This study highlights the role of B-cells in the immune response, with the importance of CXCL13 (an attractive TLS-associated B-cell chemokine) in the SIC-E group. As described above, B lymphocytes are part of the immune infiltrate in advanced GIST. Tertiary lymphoid structures (TLS) are ectopic lymphoid structures developing in non-lymphoid structures where intense and chronic inflammation takes place, including tumors. They are composed of a T-cell zone with mature dendritic cells and a B-cell follicle with a germinal center. More and more studies suggest their crucial involvement in antitumor immunity (37–41), where they seem to promote a T-cell response (42). Their clinical impact has also been shown in localized GIST, where they are very frequent (found in around 45% of patients) and seem to be positively correlated with a better OS and reduced risk of relapse (43).

The impact of the driver mutation on tumor microenvironment (TME) remains controversial. In *Pantaleo et al*, no relationship was found between the identified mutation and TME (27). In constrast, *Vitiello et al.* found in a cohort of 75 untreated GISTs that *PDGFRα*-mutated GISTs were more infiltrated with immune cells, especially CD8+ cells, expressed more neoepitopes as well as regulatory T cell indicators and harbored a higher expression of ICP such as *T cell immunoreceptor with Ig and ITIM domains* (TIGIT), CD48 or *B- and T-lymphocyte attenuator* (BTLA) than *KIT*-mutated GISTs (44). This difference was even more important in *D842V*-mutated GISTs, which was corroborated by the comparison of RNA sequencing between 5 *D842V- PDGFRα* and 5 *non-D842V-PDGFRα* tumors (45). Immune control could explain the relatively low aggressiveness of these tumors.

These data provide a strong basis for the evaluation of immunotherapy approaches in GISTs.

MECHANISMS OF IMMUNE ESCAPE IN GIST

Some micro-GISTs (0.2-1cm) remain asymptomatic and will not evolve even if driven by the same oncogenic mutations as described above (46). This suggests the presence of other mechanisms of tumor development and progression to aggressive disease. Among other mechanisms, immune escape might play a major role.

Immunosuppressive M2 Macrophages

As described previously, TAMs in GIST represent the most important immune cell subset in untreated GISTs and are often described as M2-polarized, thus promoting a rather immunosuppressive microenvironment (24, 27). Imatinib could accentuate this polarization (*see infra*) (2650).

Indoleamine 2,3-Dioxygenase (IDO) Overexpression

The constitutional activation of c-kit induces, *via* transcription factor Etv4, the expression of IDO (47) (see **Figure 1**). IDO metabolizes the essential amino acid tryptophan into kynurenin, which is known to change the microenvironment from immunogenic to tolerogenic. IDO induces the differentiation of CD4+ lymphocytes into regulatory T lymphocytes and directly inhibits CD8+ T cells (48–50). Moreover, in the presence of tryptophan metabolites, antigen presenting cells (such as macrophages) are more likely to polarize to an immunotolerant phenotype, secreting TGFβ or IL-10 (51). In a Phase 2 trial evaluating the combination of pembrolizumab and cyclophosphamide in STS, IDO was overexpressed in 63% of cases in imatinib pretreated GISTs (52). The decrease in this ratio has been shown to be a major factor in the immune escape (24).

Loss of MHC 1 Expression

Another crucial element of the immunosuppressive environment, described by Van Dongen et al, is the loss of

TABLE 2 | Tumor microenvironment features across the different groups in the Sarcoma Immune Classification (36).

SIC A Immune desert	SIC B Heterogeneous low	SIC C Vascularized	SIC D Heterogeneous high	SIC E Immune and TLS high
Low expression of immune cells-related genes	Heterogeneously low expression of immune cells-related genes	**High expression of endothelial-related cells**	High expression of T-cell, B-cell, and NK-cell related genes High T Cell activation High MHC I expression	High expression of T-cell, B-cell, and NK-cell related genes High T Cell activation High MHC I expression B cell chemokine)
Low vasculature Negligible CXCL13 expression	Moderate ICP expression Low CXCL13 expression	Moderate ICP expression Low CXCL13 expression	High ICP expression Moderate CXCL13 expression	High ICP expression **High CXCL13 expression and presence of TLS**

MHC I, Type I Major histocompatibility complex; TLS, Tertiary lymphoid structures; ICP, Immune checkpoint protein.

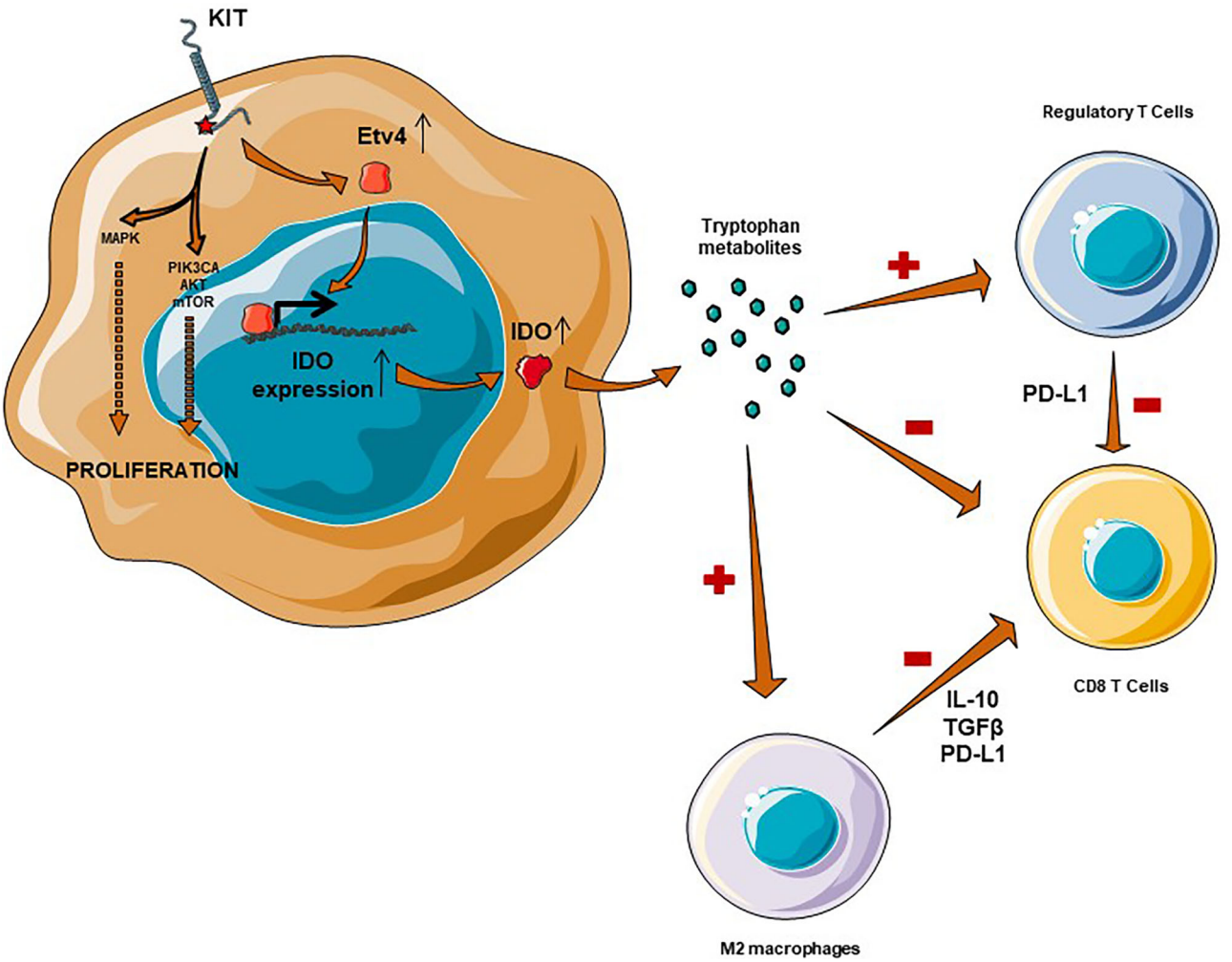

FIGURE 1 | Immunosuppressive microenvironment in GIST is mediated by IDO and M2 macrophages. IDO expression is mediated through Etv4 and KIT activation, which results in an overexpression of IDO. IDO is responsible for a recruitment of regulatory T cells, an inhibition of CD8+ T Cells complementary to a macrophage M2-polarization.

expression of the MHC I, described in 70% of GISTs, leading to a decrease in the recognition of tumor cells by cytotoxic T lymphocytes. MHC I presents antigens on the surface of the cell, leading to antigen recognition by T-cells and antitumor immunity. This MHC I lower expression is well described in the immune escape of cancers and is often due to a loss of β2-microglobulin by tumor cells (53). Loss of MHC I is also an identified mechanism of secondary resistance to immunotherapy in melanomas (54).

Immune Checkpoint Proteins Expression

Cytotoxic T-lymphocytes are inhibited by significant expression of immune checkpoint proteins (ICP). In comparison to circulating immune cells, tumor infiltrating lymphocytes (TILs) have a greater expression of PD1, *T-cell immunoglobulin and mucin containing protein-3* (TIM-3) or *Lymphocyte-Activation Gene 3* (LAG3) in imatinib-naive as well as imatinib-sensitive and resistant-tumors (55). This expression is independent of the type of mutation and seems to be increased in the case of resistance to imatinib. PD-L1 expression on tumor cells, described in about 70% of cases, has recently been identified as a poor prognostic factor in GIST and is inversely correlated with the presence of CD8+ T-lymphocytes (56, 57), suggesting a real lymphocyte anergy induced by PD-L1 expression on tumor cells. CD8+ T cells are also inhibited by regulatory T-cells and it has recently been shown that GISTs harbor a particularly high density of FoxP3+ T-cell-associated ICPs, such as *Glucocorticoid-Induced TNFR-Related protein* (GITR) or *Inducible T-cell costimulator* (ICOS). These ICPs are associated with a poorer outcome, underlining the role of regulatory T-cells in the immune escape of GIST (58).

IMMUNOLOGICAL EFFECT OF IMATINIB

Imatinib is a TKI that targets c-kit and PDGFRα by interacting with the ATP binding site. However, in addition to an oncogenic addiction inhibition mechanism, accumulating evidence seems to point to immunologic activity.

On the one hand, it appears that imatinib, through the activation of CCAT enhancer binding protein β (C/EBPβ), is responsible for a reversible M2 polarization of macrophages (28). This effect is supported by the study by Van Dongen et al. which describes that M1 macrophages secrete IL-10 during imatinib treatment (24), and also by data showing that TAMs express less CD40 (59). Moreover, another off-target effect of imatinib is to inhibit differentiation and function of normal dendritic cells, as shown in a murine model (60).

On the other hand, the inhibition of c-kit by imatinib has a meaningful immunologic benefit in GISTs. First, imatinib seems to interact with NK cells as c-kit is located on the surface of dendritic cells and inhibits the cross-activation of NK lymphocytes. Imatinib, by inhibiting c-kit, induces NK cell activation and an increase in the Th1 response, with an increased secretion of IFNγ (61). This off-target activity seems to be relevant in terms of mechanism of action since the increase in secretion of IFNγ after 2 months of treatment with imatinib, which defines a group of "good immunological responders", is a major prognostic factor (85% PFS at 2 years, *vs.* only 50% in non-responders) (62). It also appears that imatinib amplifies a pre-existing CD8+ immune response by inducing the influx of CD8+ T cells into the tumor and drainage node in a murine model, with decreased activity in the case of CD8 lymphodepletion (47). This influx is mainly related to the inhibition of tumor overexpression of IDO by imatinib, since a decrease in *IDO1* mRNA (independent of the decrease in the number of tumor cells) was mainly observed, leading to a depletion of intratumoral regulatory T cells and thus an increase in the CD8/Treg ratio. The decrease in this ratio has been shown to be a major factor in immune escape (24). This result is consistent with the analysis of human tumors, where imatinib-sensitive GISTs are enriched in CD8 T cells and have fewer regulatory T cells. The remaining question concerns resistance mutations and their implications for a recovery of IDO overexpression and eventually for imatinib escape. An additional mechanism suggested is the release of neoantigens by imatinib-induced lysis of tumor cells, with tumor cells in GISTs variably expressing peptides from the cancer testis antigens group (63). In addition, imatinib may decrease the immune escape by decreasing the expression of PD-L1 on tumor cells. The overexpression of PD-L1 induced by the presence of IFNγ is mediated by the *Janus kinase* (JAK)- *Signal Transducers and Activators of Transcription* (STAT) pathway and is blocked by the presence of imatinib (55). In models of chronic myeloid leukemia, imatinib has been shown to inhibit *vascular endothelial growth factor* (VEGF) transcription, through Sp1 and Sp3 transcription factors (64). VEGF is known to induce an immunosuppressive microenvironment, notably through a decrease in CD8/FoxP3+ T cell ratio and is a promising target in combination with immunotherapy (65). This inhibition probably has an important impact on the immunomodulatory microenvironment of GISTs by imatinib.

IMMUNOTHERAPY IN GIST: CLINICAL DATA

Immune Checkpoint Inhibitors in GIST

Immune checkpoint inhibitors have been poorly explored in the management of GIST although, as discussed previously, preclinical data suggest they may be effective.

Anti-PD(L)1 Antibodies

Anti-PD(L)1 antibodies have not shown any efficacy against GIST as a monotherapy (**Table 3**). The Pembrosarc trial was a multicentric phase II trial evaluating pembrolizumab in combination with metronomic cyclophosphamide in advanced STS (52). The results were not encouraging in GIST: out of nine

TABLE 3 | Results of clinical trials evaluating immunotherapeutic approaches in GIST.

Description	Phase	Number of GISTs	ORR (RECIST)	Median PFS	mOS	Notes	Reference
Peg-IFNα2b + imatinib followed by imatinib maintenance	II	8	100%	NR (> 3years)	NR	New PR achieved after reintroduction of peg-IFNα2 in a patient who progressed on imatinib maintenance therapy	Chen et al, 2012 (66)
Dasatinib + Ipilimumab in advanced GIST and other sarcomas	Ib	20	0%	2.8M	mOS: 13,5M	7/13 evaluable GISTs had PR by CHOI criteria	D'Angelo et al, 2017 (67)
Pembrolizumab + Cyclophosphamide in advanced STS	II	9	0%	6M-PFS: 11%	–	63% of GISTs showed a high IDO expression	Toulmonde et al, 2018 (52)
Nivolumab +/- ipilimumab in advanced GIST refractory to imatinib	II	N: 15 N+ I: 12	N: 0% N+I: 8.3%	N: 8.57w N+I: 9.1w	–	–	Singh AS et al, 2018 (68)
Nivolumab +/- Ipilimumab in advanced STS	II	N: 9 N + I: 9	N : 0% N+I : 0%	N : 1.5M N+I : 2.9M	N: 9.1M N +I :12.1M	-	Chen et al, 2020 (69)

ORR, objective response rate; median PFS, median progression-free survival; mOS, median overall survival; STS, soft-tissue sarcoma; 6M-PFS, 6 month progression-free survival; N, nivolumab; N+I, nivolumab+ipilimumab; M, months; w, weeks.

cases of GIST, there was no objective RECIST (*Response Evaluation Criteria in Solid Tumours*) response and 3 patients only had a stable disease as best overall response. PFS at 6 months was only 11%. In this study, the authors highlight the relevance of targeting IDO, as the tumor infiltrate was enriched in M2 macrophages overexpressing IDO in 63% of GISTs. In the preliminary results of a randomized phase II trial evaluating nivolumab or nivolumab and ipilimumab, 15 heavily pretreated patients with advanced GIST received nivolumab as a monotherapy: no partial responses were observed and the median PFS was 8.57 weeks (68). Seven patients had a stable disease as their best response, resulting in a clinical benefit rate of 46.7%. Alliance A091401 is a multicentric randomized phase II trial evaluating nivolumab alone or in combination with ipilimumab in advanced soft-tissue sarcomas. The results of the expansion cohorts were presented in 2020. In the 9 patients with GIST received nivolumab alone, the results were disappointing: no partial responses were observed as well, and the median PFS was 1.5 months.

Anti-CTLA-4 Antibodies

Anti-CTLA-4 (*cytotoxic T-lymphocyte-associated protein 4*) antibodies have not, to our knowledge, been studied as monotherapy in GIST.

In 2011, while describing the immunological effect of imatinib, Balachandran et al. suggested its synergy with anti-CTLA-4 antibodies (47). This synergy has not yet been observed in the clinic. In a phase Ib trial, the combination of dasatinib (multi-TKI with an anti-KIT activity) plus ipilimumab (anti-CTLA-4 antibody), 20 extensively pretreated patients with GIST were enrolled. This association did not demonstrate any efficacy (67): median PFS was 2.8 months and median OS was approximately 13 months. There appeared to be no response according to RECIST, but of the 13 evaluable cases, there were seven responses according to Choi criteria, which are known to have a better positive correlation to OS and PFS in GIST (70). Once again, one of the crucial elements of the immunosuppressive environment in GIST was IDO. Of 6 patients with evaluable biopsies, the only patient who had a loss of IDO expression following dasatinib and anti-CTLA-4 therapy had a stable disease for 19 weeks. Two patients without IDO suppression had progressive disease at first evaluation. One patient with SDH-deficient GIST had a stable disease for 47 weeks, without IDO suppression, but can reflect the natural history of this indolent subtype.

Association of Anti-PD-1 and Anti CTLA-4 Antibodies

The trials evaluating PD-1 and CTLA-4 antibodies coinhibition have also proven disappointing. In 2019, Singh AS et al. reported on 12 patients treated with nivolumab and ipilimumab after progression under imatinib in a phase II trial (68). One patient achieved a partial response, and 2 patients had a stable disease as best overall response. The median PFS was 9.1 weeks. Similarly, *Chen et al.* reported on the results of nivolumab in association with ipilimumab in the A091401 phase II trial (69). Nine patients received the combined therapy, and no objective response was observed. Median PFS was 2.9 months in this cohort, and median OS was 12.1 months. In comparison to the median overall survival of 9.1 months with nivolumab alone, the association seems to increase survival. However, the number of patients was not powered for overall survival, and the absence of objective response to both nivolumab and combination therapy did not support synergy. Once again the issue of the relevance of RECIST to evaluate PFS in GIST is apparent as is the importance of maintaining KIT inhibition when treating GIST with immunotherapy.

Other Immunologic Approaches

An interesting approach has been to combine imatinib with pegylated IFNα2b(*peg-IFNα2b*). In a non-comparative monocentric phase II trial, eight patients with advanced imatinib-naive (or who had progressed more than 10 months after the end of adjuvant imatinib) GIST were treated by *peg-IFNα2b* weekly for 22 cycles in combination with imatinib, followed by imatinib maintenance. The safety profile was acceptable. The combination therapy resulted in an increase in IFNγ-producing lymphocytes, both in peripheral blood and inside the tumor. This immunological shift was responsible for an impressive 100% response rate, and lasting responses. Median PFS was not reached but no patients had disease progression before 2 years of treatment. Interestingly, after 3.6 years of median follow-up, the only patient who had tumor progression on imatinib maintenance monotherapy achieved a new partial response after the re-introduction of peg-IFNα2b (66).

PERSPECTIVES AND PROMISING STUDY DESIGNS: THE NEED FOR COMBINATION THERAPIES

With the combination of a rich inflammatory infiltrate, an inhibited Th1 response, identified mechanisms of immune escape and the demonstration of an immunologic effect of the main systemic therapy, exciting perspectives are opening up in the world of immune-oncology of GIST, a disease with an unfavorable evolution after the development of resistance to TKIs.

In spite of this, clinical trials evaluating anti-PD-(L)1 antibodies alone or in combination with anti-CTLA-4 antibodies have failed to demonstrate any efficacy in GIST so far. However, some responses or sustained stable diseases were described and recent translational studies in the field should encourage us to persevere: closer characterization of the immune infiltrate, frequency of TLSs, and immunologic classification of sarcomas (*see* **Figure 2**). In 2019, Zhao et al. demonstrated *in vitro* that imatinib was less effective in patients with high PD-L1expression, but there was a benefit of adding an anti-PD-L1 antibody in this population (56). Moreover, data are accumulating in favor of the early introduction of immunotherapy in the tumor course (71). Future trials evaluating anti-PD(L)1 should therefore focus on the first- or second-line setting and on the biological approaches, for example an evaluation of anti-PD(L)1 antibodies by selecting patients with a better chance of benefiting from these drugs: higher PD-L1 expression on tumor cells, patients with *PDGFRα* D842V mutation or classified in the *SIC-E* group (36).

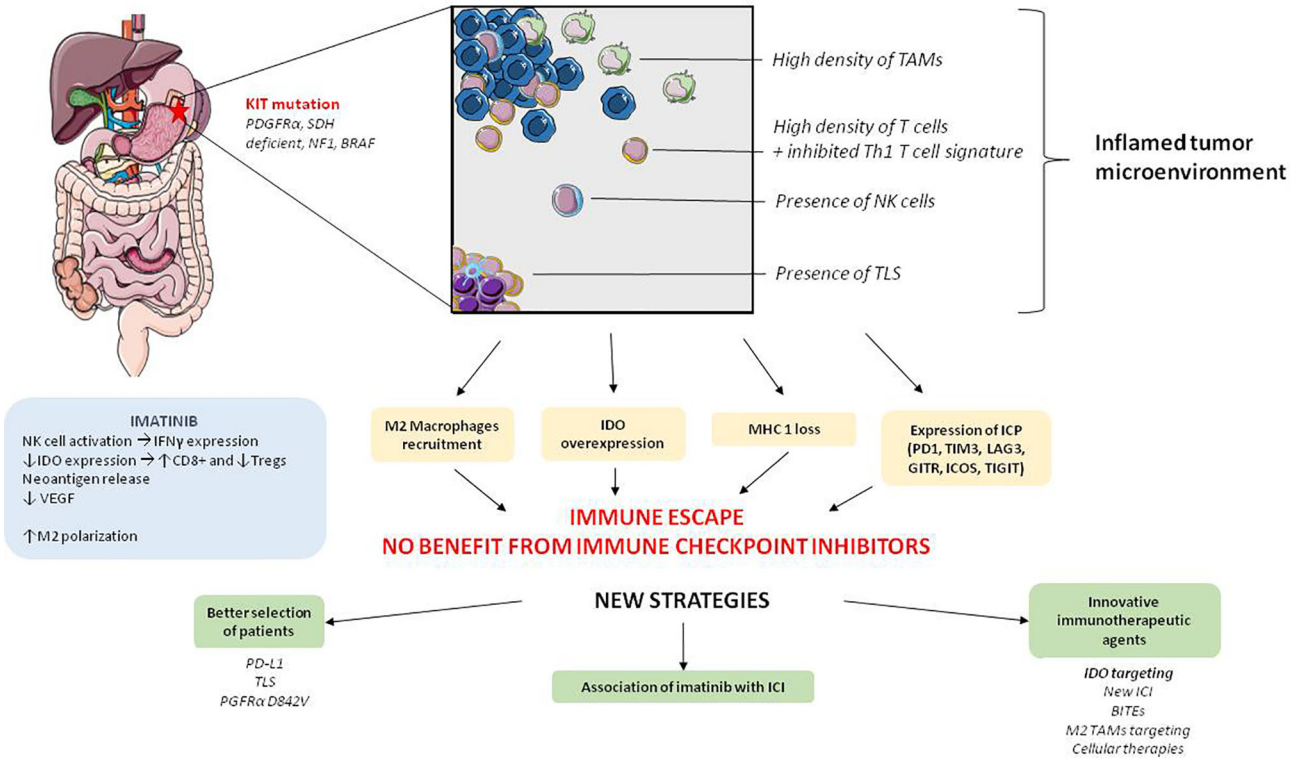

FIGURE 2 | Global characteristics of tumor microenvironment and immunotherapeutic perspectives in GIST. PGFRα: platelet derived growth factor receptor α, SDH, succinate dehydrogenase; NF1, Neurofibrimin 1; NK cell, Natural killer cells; IDO, Indoleamine 2,3-dioxygenase; MHC, Major histocompatibility complex; ICP, Immune checkpoint protein; VEGF, vascular endothelium growth factor; IFN- γ, Interferon- γ; TLS, Tertiary lymphoid structure; PD-1, programmed cell death 1; TIM-3, T-cell immunoglobulin and mucin containing protein-3; LAG-3, Lymphocyte-Activation Gene 3; GITR, Glucocorticoid-Induced TNFR-Related protein; ICOS, Inducible T-cell costimulatory; TIGIT, T cell immunoreceptor with Ig and ITIM domains); BITEs, Bispécific T cell Engager antibodies; ICI, immune checkpoint inhibitors.

Innovative immunotherapeutic approaches could also be of interest in GIST, and some are currently being investigated. One of them is to activate T cells in contact with tumor cells thanks to bispecific T-cell engager antibodies. A trial is currently evaluating XmAb18087, an antibody targeting CD3 and SSTR2, a surface antigen expressed by tumor cells in GIST (72). Moreover, even though the results of clinical trials evaluating IDO inhibitors have been disappointing to date in other tumors (73), targeting IDO in GISTs is of great interest considering its oncogenic overexpression. Epacadostat is currently being studied in combination with pembrolizumab in GIST (**Table 4**). We believe that the most promising strategy would be to study IDO inhibitors in combination with imatinib, following progression during imatinib monotherapy, in order to inhibit IDO-mediated immune escape. As discussed above, TAMs play a key role in the immunosuppressive TME and may be involved in tumor escape in GISTs. One strategy could be to promote their intratumor maturation and activation, and a CD-40 agonist antibody could allow better CD8+ T lymphocyte activation, while inhibiting imatinib-induced M2 polarization. In an *in vivo* model, the combination of imatinib with a CD-40 agonist provided better anti-tumor activity than imatinib alone, while there seemed to be effective activation of TAMs (59). In addition, a number of therapeutic approaches are currently being developed to target M2 macrophages such as STING (*Stimulator of Interferon Genes*) agonists (74), or anti-CLEVER-1 (*Common lymphatic endothelial and vascular endothelial receptor-1)* antibodies (75). Cellular therapies also seem interesting, but although Katz et al. succeeded in developing a 1st and a 2nd generation modified T-Cell with a KIT-ligand combined with an intracellular activation domain, no clinical study using such a strategy has been conducted so far (76).

Eventually, there are strong arguments pushing to evaluate anti-PD-(L)1 in combination with imatinib. Imatinib enhances IFN-γ secretion by NK cells, lowers VEGF and IDO expression in TME, thus resulting in an influx of CD8+ T cells and a decrease of regulatory T cells. Moreover, it seems unreasonable not to target KIT or PGFRα mutations in a disease in which oncogenic addiction plays such an important role. This supposition is corroborated by the work by Chen et al, and the impressive 100% response rate to imatinib combined with peg-IFNα2b (66). Based on these observations, it would be interesting to combine anti-PD(L)1 and imatinib treatment, before immunologic escape of the tumor, in a first-line setting. Therapeutic trials are currently exploring the relevance of inhibiting KIT and PD(L)1 pathways concomitantly (see **Table 4**), but to our knowledge, no association evaluates such an association with imatinib. With regard to the activity of anti-

TABLE 4 | Ongoing studies of immunotherapy in gastrointestinal stromal tumors.

Study number	Phase	Description
	Association of anti-PD(L)-1 and anti-CTLA-4 antibodies	
NCT02880020	Phase II	*Nivolumab +/-ipilimumab after progression under imatinib*
NCT02500797		
NCT02834013		
NCT02982486		
	Association of anti-PD-1 antibodies and IDO inhibitors	
NCT03291054	Phase II	*Pembrolizumab +/- epacadostat after progression under imatinib*
	Association of TKI and anti-PD(L)1 antibody	
NCT04258956	Phase II	*Axitinib + avelumab after progression under imatinib*
NCT01738139	Phase I	*Imatinib + ipilimumab in tumors with a c-kit mutation*
NCT03609424	Phase I/II	*Imatinib + PDR001*
	Bispecific T Cell Engagers antibodies (BITEs)	
NCT03411915	Phase I	*XmAb18087 (bispecific antibody against anti-SSTR2 et CD3)*

CTLA-4 antibodies, the synergy reported by *Balachandran et al.* has not been demonstrated clinically with the combination of dasatinib plus ipilimumab (67). However, dasatinib has been less studied for its immunological impact than imatinib. A phase 1 trial evaluating a combination of ipilimumab and imatinib is currently underway (see **Table 4**). Finally, as described above, some other ICP lead to T cell exhaustion and to immune escape in GIST, such as LAG-3 or TIM-3, and could be of interest in combination with imatinib. ICI targeting regulatory T cells, such as GITR agonists or ICOS, also seem promising in this setting.

Overall, this review summarizes the rationale to evaluate immunologic therapeutics in GIST, the paradigm for oncogenic driver mutation, and the limits of current investigative approaches. We believe three approaches must be highlighted: a better selection of patients included in clinical trials (presence of TLS, PD-L1 expression, *PDGFR*α-D842V mutation), the use of innovative immunotherapeutic drugs (especially IDO inhibitors), and most importantly the combination of *c-kit* inhibition with immune checkpoint inhibitors. One of the limits of this review is that we chose to focus on therapeutics which are developed specifically in GISTs and thus restricted the field of promising therapies. On the other hand, we think the comprehensive analysis of TME in GIST we provide and its correlation in terms of treatment strategies might help drug development in this very particular disease.

CONCLUSION

The GIST microenvironment is highly infiltrated with immune cells, with a large infiltrate of CD8+ T-cells (associated with a genomic signature of inhibited Th1 immune response), the presence of B-cells and TLSs, and NK cell activity. Despite this inflammatory infiltrate, however, an immune escape is observed, mediated primarily by the recruitment of immunosuppressive M2 macrophages, secretion of IDO by tumor cells, recruitment of regulatory T cells, loss of MHC type 1 and expression of ICPs.

Imatinib has demonstrated immunologic activity in the management of GIST and appears to promote a CD8+ T-cell response. However, the results of clinical trials of immunotherapy treatments (anti-PD(L)1 and anti-CTLA-4 antibodies) after progression during imatinib treatment have been disappointing to date.

Promising perspectives are based on a better selection of patients (presence of TLS, PD-L1 expression, *PDGFR*α-D842V mutation), innovative therapeutic agents (especially IDO inhibitors) and the association on immunotherapeutic agents with imatinib.

AUTHOR CONTRIBUTIONS

MRD, RLJ, SC and SD contributed to conception of this review. MRD wrote the first draft of the manuscript and designed the figures and tables. All authors contributed to the article and approved the submitted version.

ACKNOWLEDGMENTS

We thank Newmed for providing a language review of this work.

REFERENCES

1. Kindblom LG, Remotti HE, Aldenborg F, Meis-Kindblom JM. Gastrointestinal Pacemaker Cell Tumor (GIPACT): Gastrointestinal Stromal Tumors Show Phenotypic Characteristics of the Interstitial Cells of Cajal. *Am J Pathol* (1998) 152(5):1259–69.
2. Ducimetière F, Lurkin A, Ranchère-Vince D, Decouvelaere A-V, Péoc'h M, Istier L, et al. Incidence of Sarcoma Histotypes and Molecular Subtypes in a Prospective Epidemiological Study With Central Pathology Review and Molecular Testing. *PloS One* (2011) 6(8):e20294. doi: 10.1371/journal.pone.0020294
3. Miettinen M, Lasota J. Gastrointestinal Stromal Tumors–Definition, Clinical, Histological, Immunohistochemical, and Molecular Genetic Features and Differential Diagnosis. *Virchows Arch Int J Pathol* (2001) 438(1):1–12. doi: 10.1007/s004280000338
4. Hirota S, Isozaki K, Moriyama Y, Hashimoto K, Nishida T, Ishiguro S, et al. Gain-of-Function Mutations of C-Kit in Human Gastrointestinal Stromal Tumors. *Science* (1998) 279(5350):577–80. doi: 10.1126/science.279.5350.577

5. Corless CL, Barnett CM, Heinrich MC. Gastrointestinal Stromal Tumours: Origin and Molecular Oncology. *Nat Rev Cancer* (2011) 11(12):865–78. doi: 10.1038/nrc3143
6. Demetri GD, von Mehren M, Blanke CD, Van den Abbeele AD, Eisenberg B, Roberts PJ, et al. Efficacy and Safety of Imatinib Mesylate in Advanced Gastrointestinal Stromal Tumors. *N Engl J Med* (2002) 347(7):472–80. doi: 10.1056/NEJMoa020461
7. Blanke CD, Rankin C, Demetri GD, Ryan CW, von Mehren M, Benjamin RS, et al. Phase III Randomized, Intergroup Trial Assessing Imatinib Mesylate at Two Dose Levels in Patients With Unresectable or Metastatic Gastrointestinal Stromal Tumors Expressing the Kit Receptor Tyrosine Kinase: S0033. *J Clin Oncol Off J Am Soc Clin Oncol* (2008) 26(4):626–32. doi: 10.1200/JCO.2007.13.4452
8. Corless CL, Schroeder A, Griffith D, Town A, McGreevey L, Harrell P, et al. PDGFRA Mutations in Gastrointestinal Stromal Tumors: Frequency, Spectrum and *In Vitro* Sensitivity to Imatinib. *J Clin Oncol Off J Am Soc Clin Oncol* (2005) 23(23):5357–64. doi: 10.1200/JCO.2005.14.068
9. Miettinen M, Wang Z-F, Sarlomo-Rikala M, Osuch C, Rutkowski P, Lasota J. Succinate Dehydrogenase-Deficient GISTs: A Clinicopathologic, Immunohistochemical, and Molecular Genetic Study of 66 Gastric GISTs With Predilection to Young Age. *Am J Surg Pathol* (2011) 35(11):1712–21. doi: 10.1097/PAS.0b013e3182260752
10. Andersson J, Sihto H, Meis-Kindblom JM, Joensuu H, Nupponen N, Kindblom L-G. NF1-Associated Gastrointestinal Stromal Tumors Have Unique Clinical, Phenotypic, and Genotypic Characteristics. *Am J Surg Pathol* (2005) 29(9):1170–6. doi: 10.1097/01.pas.0000159775.77912.15
11. Daniels M, Lurkin I, Pauli R, Erbstösser E, Hildebrandt U, Hellwig K, et al. Spectrum of KIT/PDGFRA/BRAF Mutations and Phosphatidylinositol-3-Kinase Pathway Gene Alterations in Gastrointestinal Stromal Tumors (GIST). *Cancer Lett* (2011) 312(1):43–54. doi: 10.1016/j.canlet.2011.07.029
12. Zalupski M, Metch B, Balcerzak S, Fletcher WS, Chapman R, Bonnet JD, et al. Phase III Comparison of Doxorubicin and Dacarbazine Given by Bolus Versus Infusion in Patients With Soft-Tissue Sarcomas: A Southwest Oncology Group Study. *J Natl Cancer Inst* (1991) 83(13):926–32. doi: 10.1093/jnci/83.13.926
13. DeMatteo RP, Lewis JJ, Leung D, Mudan SS, Woodruff JM, Brennan MF. Two Hundred Gastrointestinal Stromal Tumors: Recurrence Patterns and Prognostic Factors for Survival. *Ann Surg* (2000) 231(1):51–8. doi: 10.1097/00000658-200001000-00008
14. Buchdunger E, O'Reilly T, Wood J. Pharmacology of Imatinib (STI571). *Eur J Cancer Oxf Engl 1990* (2002) 38 Suppl 5:S28–36. doi: 10.1016/s0959-8049(02)80600-1
15. Patrikidou A, Domont J, Chabaud S, Ray-Coquard I, Coindre J-M, Bui-Nguyen B, et al. Long-Term Outcome of Molecular Subgroups of GIST Patients Treated With Standard-Dose Imatinib in the BFR14 Trial of the French Sarcoma Group. *Eur J Cancer Oxf Engl 1990* (2016) 52:173–80. doi: 10.1016/j.ejca.2015.10.069
16. Nishida T, Blay J-Y, Hirota S, Kitagawa Y, Kang Y-K. The Standard Diagnosis, Treatment, and Follow-Up of Gastrointestinal Stromal Tumors Based on Guidelines. *Gastric Cancer* (2016) 19(1):3–14. doi: 10.1007/s10120-015-0526-8
17. Demetri GD, van Oosterom AT, Garrett CR, Blackstein ME, Shah MH, Verweij J, et al. Efficacy and Safety of Sunitinib in Patients With Advanced Gastrointestinal Stromal Tumour After Failure of Imatinib: A Randomised Controlled Trial. *Lancet Lond Engl* (2006) 368(9544):1329–38. doi: 10.1016/S0140-6736(06)69446-4
18. Demetri GD, Reichardt P, Kang Y-K, Blay J-Y, Rutkowski P, Gelderblom H, et al. Efficacy and Safety of Regorafenib for Advanced Gastrointestinal Stromal Tumours After Failure of Imatinib and Sunitinib (GRID): An International, Multicentre, Randomised, Placebo-Controlled, Phase 3 Trial. *Lancet Lond Engl* (9863) 2013:381. doi: 10.1016/S0140-6736(12)61857-1
19. Blay J-Y, Serrano C, Heinrich MC, Zalcberg J, Bauer S, Gelderblom H, et al. Ripretinib in Patients With Advanced Gastrointestinal Stromal Tumours (INVICTUS): A Double-Blind, Randomised, Placebo-Controlled, Phase 3 Trial. *Lancet Oncol* (2020) 21(7):923–34. doi: 10.1016/S1470-2045(20)30168-6
20. Nemunaitis J, Bauer S, Blay J-Y, Choucair K, Gelderblom H, George S, et al. Intrigue: Phase III Study of Ripretinib Versus Sunitinib in Advanced Gastrointestinal Stromal Tumor After Imatinib. *Future Oncol Lond Engl* (2020) 16(1):4251–64. doi: 10.2217/fon-2019-0633
21. Banks E, Grondine M, Bhavsar D, Barry E, Kettle JG, Reddy VP, et al. Discovery and Pharmacological Characterization of AZD3229, a Potent KIT/Pdgfrα Inhibitor for Treatment of Gastrointestinal Stromal Tumors. *Sci Transl Med* (2020) 12(541):eaaz2481. doi: 10.1126/scitranslmed.aaz2481
22. Heinrich MC, Jones RL, von Mehren M, Schöffski P, Serrano C, Kang Y-K, et al. Avapritinib in Advanced PDGFRA D842V-Mutant Gastrointestinal Stromal Tumour (NAVIGATOR): A Multicentre, Open-Label, Phase 1 Trial. *Lancet Oncol* (2020) 21(7):935–46. doi: 10.1016/S1470-2045(20)30269-2
23. Chalmers ZR, Connelly CF, Fabrizio D, Gay L, Ali SM, Ennis R, et al. Analysis of 100,000 Human Cancer Genomes Reveals the Landscape of Tumor Mutational Burden. *Genome Med* (2017) 9(1). doi: 10.1186/s13073-017-0424-2
24. van Dongen M, Savage NDL, Jordanova ES, Briaire-de Bruijn IH, Walburg KV, Ottenhoff THM, et al. Anti-Inflammatory M2 Type Macrophages Characterize Metastasized and Tyrosine Kinase Inhibitor-Treated Gastrointestinal Stromal Tumors. *Int J Cancer* (2010) NA–A. doi: 10.1002/ijc.25113
25. Rusakiewicz S, Semeraro M, Sarabi M, Desbois M, Locher C, Mendez R, et al. Immune Infiltrates Are Prognostic Factors in Localized Gastrointestinal Stromal Tumors. *Cancer Res* (2013) 73(12):3499–510. doi: 10.1158/0008-5472.CAN-13-0371
26. Tamura R, Tanaka T, Yamamoto Y, Akasaki Y, Sasaki H. Dual Role of Macrophage in Tumor Immunity. *Immunotherapy* (2018) 10(10):899–909. doi: 10.2217/imt-2018-0006
27. Pantaleo MA, Tarantino G, Agostinelli C, Urbini M, Nannini M, Saponara M, et al. Immune Microenvironment Profiling of Gastrointestinal Stromal Tumors (GIST) Shows Gene Expression Patterns Associated to Immune Checkpoint Inhibitors Response. *Oncoimmunology* (2019) 8(9):e1617588. doi: 10.1080/2162402X.2019.1617588
28. Cavnar MJ, Zeng S, Kim TS, Sorenson EC, Ocuin LM, Balachandran VP, et al. KIT Oncogene Inhibition Drives Intratumoral Macrophage M2 Polarization. *J Exp Med* (2013) 210(13):2873–86. doi: 10.1084/jem.20130875
29. Tumeh PC, Harview CL, Yearley JH, Shintaku IP, Taylor EJM, Robert L, et al. PD-1 Blockade Induces Responses by Inhibiting Adaptive Immune Resistance. *Nature* (2014) 515(7528):568–71. doi: 10.1038/nature13954
30. Loo K, Tsai KK, Mahuron K, Liu J, Pauli ML, Sandoval PM, et al. Partially Exhausted Tumor-Infiltrating Lymphocytes Predict Response to Combination Immunotherapy. *JCI Insight* (2017) 2(14). doi: 10.1172/jci.insight.93433
31. Motzer RJ, Robbins PB, Powles T, Albiges L, Haanen JB, Larkin J, et al. Avelumab Plus Axitinib Versus Sunitinib in Advanced Renal Cell Carcinoma: Biomarker Analysis of the Phase 3 JAVELIN Renal 101 Trial. *Nat Med* (2020). doi: 10.1038/s41591-020-1044-8
32. Cameron S, Gieselmann M, Blaschke M, Ramadori G, Füzesi L. Immune Cells in Primary and Metastatic Gastrointestinal Stromal Tumors (GIST). *Int J Clin Exp Pathol* (2014) 7(7):3563–79.
33. Delahaye NF, Rusakiewicz S, Martins I, Ménard C, Roux S, Lyonnet L, et al. Alternatively Spliced NKp30 Isoforms Affect the Prognosis of Gastrointestinal Stromal Tumors. *Nat Med* (2011) 17(6):700–7. doi: 10.1038/nm.2366
34. Ayers M, Lunceford J, Nebozhyn M, Murphy E, Loboda A, Kaufman DR, et al. IFN-γ–Related mRNA Profile Predicts Clinical Response to PD-1 Blockade. *J Clin Invest* (2020) 127(8):2930–40. doi: 10.1172/JCI91190
35. Danaher P, Warren S, Lu R, Samayoa J, Sullivan A, Pekker I, et al. Pan-Cancer Adaptive Immune Resistance as Defined by the Tumor Inflammation Signature (TIS): Results From The Cancer Genome Atlas (TCGA). *J Immunother Cancer* (2018) 6. doi: 10.1186/s40425-018-0367-1
36. Petitprez F, de Reyniès A, Keung EZ, Chen TW-W, Sun C-M, Calderaro J, et al. B Cells are Associated With Survival and Immunotherapy Response in Sarcoma. *Nature* (2020) 577(7791):556–60. doi: 10.1038/s41586-019-1906-8
37. Helmink BA, Reddy SM, Gao J, Zhang S, Basar R, Thakur R, et al. B Cells and Tertiary Lymphoid Structures Promote Immunotherapy Response. *Nature* (2020) 577(7791):549–55. doi: 10.1038/s41586-019-1922-8
38. Germain C, Gnjatic S, Tamzalit F, Knockaert S, Remark R, Goc J, et al. Presence of B Cells in Tertiary Lymphoid Structures is Associated With a Protective Immunity in Patients With Lung Cancer. *Am J Respir Crit Care Med* (2014) 189(7):832–44. doi: 10.1164/rccm.201309-1611OC

39. Hiraoka N, Ino Y, Yamazaki-Itoh R, Kanai Y, Kosuge T, Shimada K. Intratumoral Tertiary Lymphoid Organ is a Favourable Prognosticator in Patients With Pancreatic Cancer. *Br J Cancer* (2015) 112(11):1782–90. doi: 10.1038/bjc.2015.145
40. Martinet L, Garrido I, Filleron T, Le Guellec S, Bellard E, Fournie J-J, et al. Human Solid Tumors Contain High Endothelial Venules: Association With T- and B-Lymphocyte Infiltration and Favorable Prognosis in Breast Cancer. *Cancer Res* (2011) 71(17):5678–87. doi: 10.1158/0008-5472.CAN-11-0431
41. Wirsing AM, Ervik IK, Seppola M, Uhlin-Hansen L, Steigen SE, Hadler-Olsen E. Presence of High-Endothelial Venules Correlates With a Favorable Immune Microenvironment in Oral Squamous Cell Carcinoma. *Mod Pathol Off J U S Can Acad Pathol Inc* (2018) 31(6):910–22. doi: 10.1038/s41379-018-0019-5
42. Sautès-Fridman C, Petitprez F, Calderaro J, Fridman WH. Tertiary Lymphoid Structures in the Era of Cancer Immunotherapy. *Nat Rev Cancer* (2019) 19 (6):307–25. doi: 10.1038/s41568-019-0144-6
43. Lin Q, Tao P, Wang J, Ma L, Jiang Q, Li J, et al. Tumor-Associated Tertiary Lymphoid Structure Predicts Postoperative Outcomes in Patients With Primary Gastrointestinal Stromal Tumors. *Oncoimmunology* (2020) 9(1). doi: 10.1080/2162402X.2020.1747339
44. Vitiello GA, Bowler TG, Liu M, Medina BD, Zhang JQ, Param NJ, et al. Differential Immune Profiles Distinguish the Mutational Subtypes of Gastrointestinal Stromal Tumor. *J Clin Invest* (2019) 129(5):1863–77. doi: 10.1172/JCI124108
45. Indio V, Ravegnini G, Astolfi A, Urbini M, Saponara M, De Leo A, et al. Gene Expression Profiling of PDGFRA Mutant GIST Reveals Immune Signatures as a Specific Fingerprint of D842V Exon 18 Mutation. *Front Immunol* (2020) 11:851. doi: 10.3389/fimmu.2020.00851
46. Kawanowa K, Sakuma Y, Sakurai S, Hishima T, Iwasaki Y, Saito K, et al. High Incidence of Microscopic Gastrointestinal Stromal Tumors in the Stomach. *Hum Pathol* (2006) 37(12):1527–35. doi: 10.1016/j.humpath.2006.07.002
47. Balachandran VP, Cavnar MJ, Zeng S, Bamboat ZM, Ocuin LM, Obaid H, et al. Imatinib Potentiates Antitumor T Cell Responses in Gastrointestinal Stromal Tumor Through the Inhibition of Ido. *Nat Med* (2011) 17(9):1094–100. doi: 10.1038/nm.2438
48. Schafer CC, Wang Y, Hough KP, Sawant A, Grant SC, Thannickal VJ, et al. Indoleamine 2,3-Dioxygenase Regulates Anti-Tumor Immunity in Lung Cancer by Metabolic Reprogramming of Immune Cells in the Tumor Microenvironment. *Oncotarget* (2016) 7(46):75407–24. doi: 10.18632/oncotarget.12249
49. Mezrich JD, Fechner JH, Zhang X, Johnson BP, Burlingham WJ, Bradfield CA. An Interaction Between Kynurenine and the Aryl Hydrocarbon Receptor can Generate Regulatory T Cells. *J Immunol Baltim Md 1950* (2010) 185(6):3190–8. doi: 10.4049/jimmunol.0903670
50. Munn DH, Mellor AL. IDO in the Tumor Microenvironment: Inflammation, Counter-Regulation and Tolerance. *Trends Immunol* (2016) 37(3):193–207. doi: 10.1016/j.it.2016.01.002
51. Ravishankar B, Liu H, Shinde R, Chandler P, Baban B, Tanaka M, et al. Tolerance to Apoptotic Cells is Regulated by Indoleamine 2,3-Dioxygenase. *Proc Natl Acad Sci U S A* (2012) 109(10):3909–14. doi: 10.1073/pnas.1117736109
52. Toulmonde M, Penel N, Adam J, Chevreau C, Blay J-Y, Le Cesne A, et al. Use of PD-1 Targeting, Macrophage Infiltration, and IDO Pathway Activation in Sarcomas: A Phase 2 Clinical Trial. *JAMA Oncol* (2018) 4(1):93. doi: 10.1001/jamaoncol.2017.1617
53. Marincola FM, Jaffee EM, Hicklin DJ, Ferrone S. Escape of Human Solid Tumors From T-Cell Recognition: Molecular Mechanisms and Functional Significance. *Adv Immunol* (2000) 74:181–273. doi: 10.1016/s0065-2776(08)60911-6
54. Carretero R, Romero JM, Ruiz-Cabello F, Maleno I, Rodriguez F, Camacho FM, et al. Analysis of HLA Class I Expression in Progressing and Regressing Metastatic Melanoma Lesions After Immunotherapy. *Immunogenetics* (2008) 60(8):439–47. doi: 10.1007/s00251-008-0303-5
55. Seifert AM, Zeng S, Zhang JQ, Kim TS, Cohen NA, Beckman MJ, et al. PD-1/PD-L1 Blockade Enhances T-Cell Activity and Antitumor Efficacy of Imatinib in Gastrointestinal Stromal Tumors. *Clin Cancer Res Off J Am Assoc Cancer Res* (2017) 23(2):454–65. doi: 10.1158/1078-0432.CCR-16-1163
56. Zhao R, Song Y, Wang Y, Huang Y, Li Z, Cui Y, et al. PD-1/PD-L1 Blockade Rescue Exhausted CD8+ T Cells in Gastrointestinal Stromal Tumours *via* the PI3K/Akt/mTOR Signalling Pathway. *Cell Prolif* (2019) 52(3):e12571. doi: 10.1111/cpr.12571
57. Blakely AM, Matoso A, Patil PA, Taliano R, Machan JT, Miner TJ, et al. Role of Immune Microenvironment in Gastrointestinal Stromal Tumours. *Histopathology* (2018) 72(3):405–13. doi: 10.1111/his.13382
58. Dufresne A, Lesluyes T, Ménétrier-Caux C, Brahmi M, Darbo E, Toulmonde M, et al. Specific Immune Landscapes and Immune Checkpoint Expressions in Histotypes and Molecular Subtypes of Sarcoma. *Oncoimmunology* (2020) 9 (1):1792036. doi: 10.1080/2162402X.2020.1792036
59. Zhang JQ, Zeng S, Vitiello GA, Seifert AM, Medina BD, Beckman MJ, et al. Macrophages and CD8 $^{+}$ T Cells Mediate the Antitumor Efficacy of Combined CD40 Ligation and Imatinib Therapy in Gastrointestinal Stromal Tumors. *Cancer Immunol Res* (2018) 6(4):434–47. doi: 10.1158/2326-6066.CIR-17-0345
60. Appel S, Boehmler AM, Grünebach F, Müller MR, Rupf A, Weck MM, et al. Imatinib Mesylate Affects the Development and Function of Dendritic Cells Generated From CD34+ Peripheral Blood Progenitor Cells. *Blood* (2004) 103 (2):538–44. doi: 10.1182/blood-2003-03-0975
61. Borg C, Terme M, Taïeb J, Ménard C, Flament C, Robert C, et al. Novel Mode of Action of C-Kit Tyrosine Kinase Inhibitors Leading to NK Cell–Dependent Antitumor Effects. *J Clin Invest* (2004) 114(3):379–88. doi: 10.1172/JCI200421102
62. Ménard C, Blay J-Y, Borg C, Michiels S, Ghiringhelli F, Robert C, et al. Natural Killer Cell IFN-Gamma Levels Predict Long-Term Survival With Imatinib Mesylate Therapy in Gastrointestinal Stromal Tumor-Bearing Patients. *Cancer Res* (2009) 69(8):3563–9. doi: 10.1158/0008-5472.CAN-08-3807
63. Perez D, Herrmann T, Jungbluth AA, Samartzis P, Spagnoli G, Demartines N, et al. Cancer Testis Antigen Expression in Gastrointestinal Stromal Tumors: New Markers for Early Recurrence. *Int J Cancer* (2008) 123(7):1551–5. doi: 10.1002/ijc.23698
64. Legros L, Bourcier C, Jacquel A, Mahon F-X, Cassuto J-P, Auberger P, et al. Imatinib Mesylate (STI571) Decreases the Vascular Endothelial Growth Factor Plasma Concentration in Patients With Chronic Myeloid Leukemia. *Blood* (2004) 104(2):495–501. doi: 10.1182/blood-2003-08-2695
65. Yang J, Yan J, Liu B. Targeting VEGF/VEGFR to Modulate Antitumor Immunity. *Front Immunol* (2018) 9:978. doi: 10.3389/fimmu.2018.00978
66. Chen LL, Chen X, Choi H, Sang H, Chen LC, Zhang H, et al. Exploiting Antitumor Immunity to Overcome Relapse and Improve Remission Duration. *Cancer Immunol Immunother CII* (2012) 61(7):1113–24. doi: 10.1007/s00262-011-1185-1
67. D'Angelo SP, Shoushtari AN, Keohan ML, Dickson MA, Gounder MM, Chi P, et al. Combined KIT and CTLA-4 Blockade in Patients With Refractory GIST and Other Advanced Sarcomas: A Phase Ib Study of Dasatinib Plus Ipilimumab. *Clin Cancer Res Off J Am Assoc Cancer Res* (2017) 23 (12):2972–80. doi: 10.1158/1078-0432.CCR-16-2349
68. Singh AS, Chmielowski B, Hecht JR, Rosen LS, Chow WA, Wang X, et al. A Randomized Phase II Study of Nivolumab Monotherapy Versus Nivolumab Combined With Ipilimumab in Advanced Gastrointestinal Stromal Tumor (GIST). *J Clin Oncol* (2019). doi: 10.1200/JCO.2019.37.15_suppl.11017
69. Chen JL, Mahoney MR, George S, Antonescu CR, Liebner DA, Van Tine BA, et al. A Multicenter Phase II Study of Nivolumab +/- Ipilimumab for Patients With Metastatic Sarcoma (Alliance A091401): Results of Expansion Cohorts. *J Clin Oncol* (2020) 38(15_suppl):11511–1. doi: 10.1200/JCO.2020.38.15_suppl.11511
70. Choi H, Charnsangavej C, Faria SC, Macapinlac HA, Burgess MA, Patel SR, et al. Correlation of Computed Tomography and Positron Emission Tomography in Patients With Metastatic Gastrointestinal Stromal Tumor Treated at a Single Institution With Imatinib Mesylate: Proposal of New Computed Tomography Response Criteria. *J Clin Oncol Off J Am Soc Clin Oncol* (2007) 25(13):1753–9. doi: 10.1200/JCO.2006.07.3049
71. Topalian SL, Taube JM, Pardoll DM. Neoadjuvant Checkpoint Blockade for Cancer Immunotherapy. *Science* (2020) 367(6477):eaax0182. doi: 10.1126/science.aax0182
72. Arne G, Nilsson B, Dalmo J, Kristiansson E, Arvidsson Y, Forssell-Aronsson E, et al. Gastrointestinal Stromal Tumors (GISTs) Express Somatostatin Receptors and Bind Radiolabeled Somatostatin Analogs. *Acta Oncol Stockh Swed* (2013) 52(4):783–92. doi: 10.3109/0284186X.2012.733075

73. Long GV, Dummer R, Hamid O, Gajewski TF, Caglevic C, Dalle S, et al. Epacadostat Plus Pembrolizumab Versus Placebo Plus Pembrolizumab in Patients With Unresectable or Metastatic Melanoma (ECHO-301/KEYNOTE-252): A Phase 3, Randomised, Double-Blind Study. *Lancet Oncol* (2019) 20(8):1083–97. doi: 10.1016/S1470-2045(19)30274-8
74. Corrales L, Glickman LH, McWhirter SM, Kanne DB, Sivick KE, Katibah GE, et al. Direct Activation of STING in the Tumor Microenvironment Leads to Potent and Systemic Tumor Regression and Immunity. *Cell Rep* (2015) 11 (7):1018–30. doi: 10.1016/j.celrep.2015.04.031
75. Karikoski M, Marttila-Ichihara F, Elima K, Rantakari P, Hollmén M, Kelkka T, et al. Clever-1/Stabilin-1 Controls Cancer Growth and Metastasis. *Clin Cancer Res Off J Am Assoc Cancer Res* (2014) 20(24):6452–64. doi: 10.1158/1078-0432.CCR-14-1236
76. Katz SC, Burga RA, Naheed S, Licata LA, Thorn M, Osgood D, et al. Anti-KIT Designer T Cells for the Treatment of Gastrointestinal Stromal Tumor. *J Transl Med* (2013) 11:46. doi: 10.1186/1479-5876-11-46

Conflict of Interest: The authors declare that the research was conducted in the absence of any commercial or financial relationships that could be construed as a potential conflict of interest.

frontiers in Immunology

ORIGINAL RESEARCH
published: 17 September 2021
doi: 10.3389/fimmu.2021.719175

Construction of a Ferroptosis-Related Nine-lncRNA Signature for Predicting Prognosis and Immune Response in Hepatocellular Carcinoma

*Zhijie Xu[1], Bi Peng[1], Qiuju Liang[2,3], Xi Chen[2,3], Yuan Cai[1], Shuangshuang Zeng[2,3], Kewa Gao[1], Xiang Wang[2,3], Qiaoli Yi[2,3], Zhicheng Gong[2,3] and Yuanliang Yan[2,3]**

[1] Department of Pathology, Xiangya Hospital, Central South University, Changsha, China, [2] Department of Pharmacy, Xiangya Hospital, Central South University, Changsha, China, [3] National Clinical Research Center for Geriatric Disorders, Xiangya Hospital, Central South University, Changsha, China

OPEN ACCESS

Edited by:
Bo Qin,
Mayo Clinic, United States

Reviewed by:
Hou-Qun Ying,
Second Affiliated Hospital of Nanchang University, China
Zheqiong Tan,
Johns Hopkins Medicine, United States

***Correspondence:**
Yuanliang Yan
yanyuanliang@csu.edu.cn

Specialty section:
This article was submitted to Cancer Immunity and Immunotherapy, a section of the journal Frontiers in Immunology

Received: *02 June 2021*
Accepted: *26 August 2021*
Published: *17 September 2021*

Citation:
Xu Z, Peng B, Liang Q, Chen X, Cai Y, Zeng S, Gao K, Wang X, Yi Q, Gong Z and Yan Y (2021) Construction of a Ferroptosis-Related Nine-lncRNA Signature for Predicting Prognosis and Immune Response in Hepatocellular Carcinoma. Front. Immunol. 12:719175. doi: 10.3389/fimmu.2021.719175

Ferroptosis is an iron-dependent cell death process that plays important regulatory roles in the occurrence and development of cancers, including hepatocellular carcinoma (HCC). Moreover, the molecular events surrounding aberrantly expressed long non-coding RNAs (lncRNAs) that drive HCC initiation and progression have attracted increasing attention. However, research on ferroptosis-related lncRNA prognostic signature in patients with HCC is still lacking. In this study, the association between differentially expressed lncRNAs and ferroptosis-related genes, in 374 HCC and 50 normal hepatic samples obtained from The Cancer Genome Atlas (TCGA), was evaluated using Pearson's test, thereby identifying 24 ferroptosis-related differentially expressed lncRNAs. The least absolute shrinkage and selection operator (LASSO) algorithm and Cox regression model were used to construct and validate a prognostic risk score model from both TCGA training dataset and GEO testing dataset (GSE40144). A nine-lncRNA-based signature (CTD-2033A16.3, CTD-2116N20.1, CTD-2510F5.4, DDX11-AS1, LINC00942, LINC01224, LINC01231, LINC01508, and ZFPM2-AS1) was identified as the ferroptosis-related prognostic model for HCC, independent of multiple clinicopathological parameters. In addition, the HCC patients were divided into high-risk and low-risk groups according to the nine-lncRNA prognostic signature. The gene set enrichment analysis enrichment analysis revealed that the lncRNA-based signature might regulate the HCC immune microenvironment by interfering with tumor necrosis factor α/nuclear factor kappa-B, interleukin 2/signal transducers and activators of transcription 5, and cytokine/cytokine receptor signaling pathways. The infiltrating immune cell subtypes, such as resting memory CD4(+) T cells, follicular helper T cells, regulatory T cells, and M0 macrophages, were all significantly different between the high-risk group and the low-risk group as indicated in Spearman's correlation analysis. Moreover, a substantial increase in the expression of B7H3 immune checkpoint molecule was found in the high-risk group. Our findings provided a promising

insight into ferroptosis-related lncRNAs in HCC and a personalized prediction tool for prognosis and immune responses in patients.

Keywords: ferroptosis, immune cell infiltrate, lncRNA, hepatocellular carcinoma, survival analysis

INTRODUCTION

Hepatocellular carcinoma (HCC) is a heterogeneous tumor with increased incidence in the world (1, 2). As a common malignancy, many factors have been proven to be involved in its development, such as virus infection and cirrhosis (3). Currently, the effective treatment options for HCC predominantly include percutaneous approaches, liver transplantation, hepatic resection, *etc.* (4, 5). Even with advances in therapeutic management, the prognosis for patients with HCC remains unfavorable and poses a challenge to clinical therapists (6). Thus, uncovering novel and reliable screening methods is urgently needed to improve the diagnostic accuracy and therapeutic effect, facilitating the efforts to ameliorate the prognosis.

During the past few years, the literature suggested an increasing research progression in the area of tumor ferroptosis. Ferroptosis is a recently discovered form of reactive oxygen species (ROS)-mediated programmed cell death, which is dependent on iron metabolism and lipid peroxidation (7). The importance of ferroptosis has been demonstrated in the regulation of metabolism and redox biology, affecting the pathogenesis and treatment of cancers, including HCC. Shan and colleagues reported that ubiquitin-like modifier activating enzyme 1 promoted the development of HCC by upregulating the Nrf2 signaling pathway and downregulating Fe^{2+} levels, triggering ferroptosis inhibitory bioactivities (8). Sorafenib and sulfasalazine could synergistically inhibit the activation of branched-chain amino acid aminotransferase 2, a key enzyme participating in sulfur amino acid metabolism, resulting in ferroptosis in HCC HepG2 cells *in vitro* and *in vivo* (9). In addition, Liu et al. reported a ferroptosis- and immune-related signature and found that this prognostic signature could be used to screen the HCC patients for immunotherapies and targeted therapies (10). Therefore, understanding the underlying mechanisms and functions of ferroptosis-associated gene changes in HCC is of vital importance.

Long non-coding RNAs (lncRNAs) are non-coding transcripts of 200 nucleotides in length, which could regulate the expression of various cancer-associated genes. Recently, Zhu et al. comprehensively investigated the molecular profiles of lncRNAs in plasma samples from HCC patients and revealed that the differentially expressed lncRNAs were mainly enriched in the biological functions related to tumorigenesis, such as cell metastasis, immune response, and metabolism regulation (11). A high level of LINC00958 aggravated HCC lipogenesis and progression through sponging miR-3619-5p, further upregulating the hepatoma-derived growth factor expression (12). To date, emerging evidence have shown the potential of lncRNAs in regulating ferroptotic cell death for cancer biology. In HCC cells, a high level of lncRNA GABPB1 antisense RNA 1 enhanced erastin-induced ferroptosis by blocking GA-binding protein subunit beta-1 (GABPB1) translation and suppressing peroxiredoxin-5 peroxidase, leading to inhibition of cellular antioxidant capacity and cell viability (13). However, the application of ferroptosis–lncRNA combinations in prognostic prediction for patients with HCC remains to be elucidated.

Here a promising prognostic model for HCC was developed based on ferroptosis-associated differentially expressed lncRNAs that could be used for prognosis prediction and selection of patients for immunotherapies.

MATERIALS AND METHODS

Data Collection

Data from 424 samples, including 374 HCC tissues and 50 normal hepatic tissues, were downloaded from TCGA database up to April 1, 2021 (https://portal.gdc.cancer.gov/repository) as depicted in **Figure 1A**. The Data Transfer Tool of GDC Apps was utilized for downloading gene expression profiles and clinical information (https://tcga-data.nci.nih.gov/). The gene expression profiles were normalized using the scale method provided in the "limma" R package. Based on the set cutoff criteria of |fold-change| >2 and P <0.001, the differentially expressed genes (DEGs) between HCC and normal hepatic tissues were identified, and these included lncRNAs, protein-coding genes, miRNAs, *etc.* The lncRNA expression profiles and clinical information of another 59 tumor samples (GSE40144) were obtained from the GEO database (http://www.ncbi.nlm.nih.gov/geo) as testing cohort. The follow-up for the patients described in GSE40144 did not exceed 5 years.

Identification of Ferroptosis-Related lncRNAs

To identify ferroptosis-related lncRNAs, 60 ferroptosis-related genes were retrieved from the previous literature (**Supplementary Table S1**) (14), which contains an up-to-date list of ferroptosis-related genes. Pearson's test was performed to examine the correlation between ferroptosis-related DEGs and differentially expressed lncRNAs. Pearson's R >0.5 was considered to be statistically significant.

Cell Culture

The human embryonic hepatocyte—HHL-5—and HCC cells—MHCC97H and HUH-7—were cultured in Dulbecco's modified Eagle's medium, supplemented with 10% fetal bovine serum and 1% penicillin/streptomycin. The cultures were placed in a sterile incubator maintained at 37°C with 5% CO_2. The cells in logarithmic growth phase were collected for subsequent experiments.

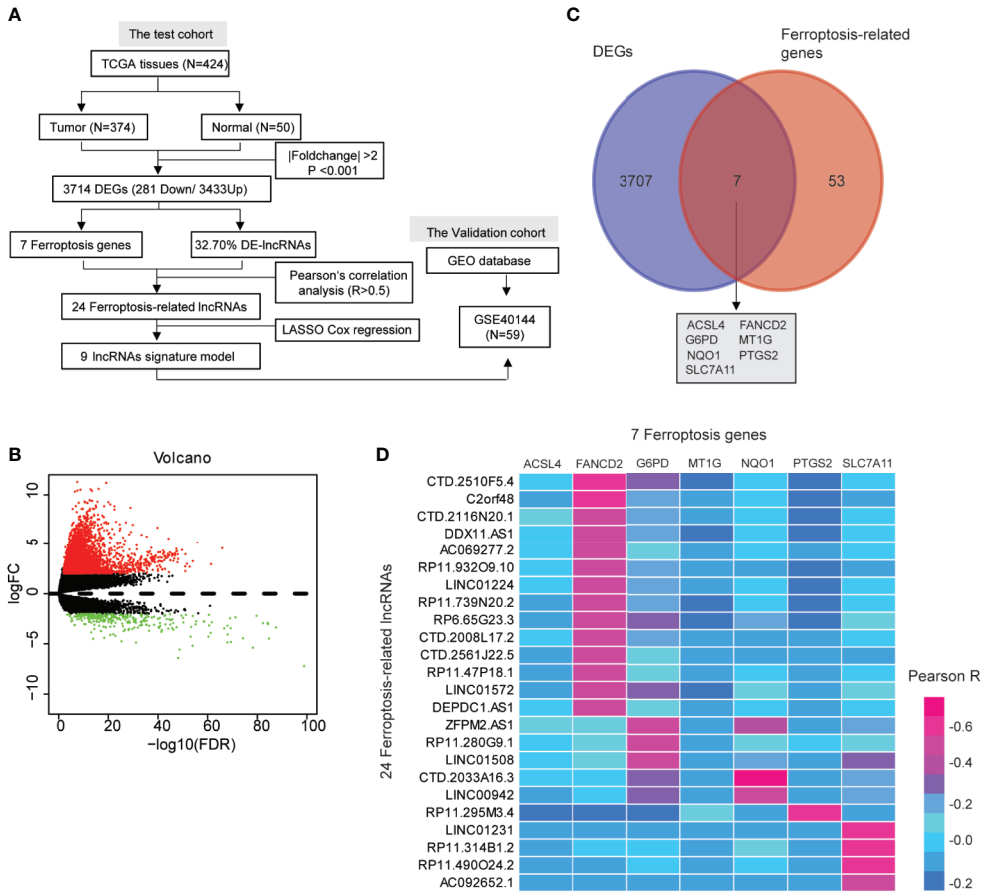

FIGURE 1 | A screen of the differentially expressed ferroptosis-associated lncRNAs in hepatocellular carcinoma (HCC). **(A)** Flow chart of the analytical process in this study. **(B)** Volcano plot representing the differentially expressed genes (DEGs) between the normal and the HCC groups. The upregulated and downregulated DEGs are highlighted in red and green, respectively. **(C)** Venn diagrams of the differentially expressed ferroptosis-related genes. **(D)** Heat map showing the Pearson's correlation between the differentially expressed-lncRNAs and the differentially expressed ferroptosis-associated genes.

RNA Extraction and Quantitative PCR

Total cellular RNA was extracted using the TRIzol reagent (Invitrogen, 15596-026) according to the protocol of the manufacturer. The cDNA synthesis was reverse-transcribed using the PrimeScript RT reagent kit (Takara, 6210, China). The qPCR assay was conducted with iTaq Universal SYBR green Supermix (Bio-Rad, 172-5850, USA). The gene expression levels of candidate lncRNAs were normalized to 18srRNA expression levels. The relative quantification of lncRNAs was calculated using the 2-ΔΔCT method (15–17). The sequences of all primers used in this study are provided in **Supplementary Table S2**.

Apoptosis Analysis

For apoptosis analysis, HUH-7 cells were transfected with the lncRNA-targeted siRNAs (GenePharma, China). The sequences of all siRNAs used in this study are provided in **Supplementary Table S2**. Afterward, the cell apoptosis rate was analyzed using Annexin V-fluorescein isothiocyanate (BD Biosciences, USA). The Dxp AthenaTM flow cytometer (Cytek, Fremont, CA, USA) was used to analyze the results of the flow cytometry.

Colony Forming Assay

The HUH-7 cells were transfected with lncRNA-targeted siRNAs for about 48 h. Afterward, 1,000 cells were plated in six-well culture plates and cultured for about 15 days. The cellular colonies were counted by staining with crystal violet.

Lipid Peroxidation Assay

Lipid peroxidation was analyzed using a lipid peroxidation assay kit (Sigma, MAK085) according to the protocol of the manufacturer. Upon oxidative stress, one of the end products, such as malondialdehyde (MDA), could act as a promising marker for lipid peroxidation. Then, the reaction of MDA with thiobarbituric acid results in a pink color with a maximum absorption at 532 nm. Therefore, the levels of cellular lipid peroxidation can be identified by measuring the absorbance at 532 nm.

Iron Assay

The concentration of ferrous (Fe^{2+}) and/or ferric (Fe^{3+}) iron in biological samples could be determined using an iron assay kit

(Abcam, ab83366). In brief, in the acid assay buffer, the ferric carrier proteins could dissociate ferric into the solution. Then, the reaction of free ferrous iron with Ferene S results in stable-colored complexes with absorbance at 593 nm. Therefore, the levels of intracellular iron can be identified by measuring the absorbance at 593 nm.

Construction and Validation of Ferroptosis-Related lncRNA Signature

Least absolute shrinkage and selection operator (LASSO) Cox regression of overall survival (OS) with a 10-fold cross-validation was performed to screen for ferroptosis-related lncRNAs with prognostic values. A total of 374 lncRNA-seq samples and the latest clinical follow-up information were downloaded from TCGA using GDC API (https://portal.gdc.cancer.gov/repository). Patients with unknown clinical information were excluded (n = 92), leaving 255 lncRNA-seq samples in the final cohort for analysis. The R package "glmnet" was used to identify the gene signature that contains the most helpful biomarkers for prognosis, and the risk score of each sample in all the datasets was calculated based on the signature (18). For the training group, the lncRNA-based prognosis risk score was established by linearly combining the following formula with the expression level-multiplied regression model (β): risk score = βlncRNA1 × lncRNA1 expression + βlncRNA2 × lncRNA2 expression + · ···· + βlncRNAn × lncRNAn expression. To evaluate the predictive power of the lncRNA-based prognosis risk classifier, receiver operating characteristic (ROC) of 10-year survival was analyzed using the R package "timeROC" in the training and testing datasets (19). For survival analysis, the samples were divided into high-risk group and low-risk group based on the optimal cutoff value of risk score as analyzed by the R package "survival" (20). Kaplan–Meier analysis was used to explore the prognostic significance of the ferroptosis-associated nine-lncRNA signature on HCC. Next, univariate and multivariate Cox regression analyses were conducted to assess whether this risk score model displayed good predictive ability for prognosis independent of other clinicopathological features, such as body mass index, age, gender, and pathologic staging. In addition, a prognostic nomogram was established based on the TCGA-HCC dataset. All independent prognostic parameters and relevant clinical parameters were included in the construction of a prognostic nomogram *via* a stepwise Cox regression model to predict the 3-, 5-, and 10-year OS of HCC patients in the TCGA dataset.

Immune Infiltrate Analysis

CIBERSORT (21) was used to analyze 22 types of tumor-infiltrating immune cells (TIICs) from each sample, such as naive CD4+ T cells, CD4+ resting memory T cells, CD4+ memory-activated T cells, naive B cells, memory B cells, plasma cells, CD8+ T cells, follicular helper T cells, regulatory T cells, gammadelta T cells, M0 macrophages, M1 macrophages, M2 macrophages, resting natural killer cells, activated natural killer cells, monocytes, resting dendritic cells, activated dendritic cells, resting mast cells, activated mast cells, eosinophils, and neutrophils. The original gene expression data downloaded from TCGA was normalized prior to the CIBERSORT analysis. The statistical significance of the deconvolution results was evaluated by a derived P-value ($P < 0.05$) to filter out the samples with less significant accuracy. The association between the risk score of the signature and immune cells was assessed using Spearman's correlation test. Pearson's test was used to assess the correlation between the risk score of the signature and the expression of the immune checkpoint genes, such as programmed cell death protein 1 (PD1), PD ligand 1 (PDL1), cytotoxic T-lymphocyte-associated protein 4 (CTLA4), V-set immunoregulatory receptor (VSIR) (22), and B7H3 (23).

Function Enrichment Analysis

Gene set enrichment analysis (GSEA) (24) was performed to identify the potential molecular mechanisms or potential functional pathways that involve the ferroptosis-related lncRNA signature. The TCGA samples were divided into a high-risk group and a low-risk group according to the optimal cutoff values. GSEA was performed in java GSEA v. 4.0.3 on the molecular signature dataset, h.all.v7.4 symbols.gmt [Hallmarks], and Kyoto Encyclopedia of Genes and Genomes (KEGG) dataset, c2.cp.kegg.v7.4.symbols.gmt, to identify enriched pathways between the high-risk group and the low-risk group. |NES| >1 and false discovery rate <0.05 were considered statistically significant.

Statistical Analysis

All statistical analyses were performed using RStudio and its appropriate packages. P-values <0.05 were regarded as statistically significant.

RESULTS

Identification of Differentially Expressed Ferroptosis-Associated lncRNAs

We identified 3,714 genes (3,433 upregulated and 281 downregulated) that were differentially expressed in the TCGA-HCC dataset (**Figures 1A, B** and **Supplementary Table S3**). Moreover, the pie chart exhibited that the differentially expressed lncRNAs (DE-lncRNAs) accounted for up to 32.70% of the DEGs (**Supplementary Figure S1** and **Supplementary Table S4**). Ferroptosis has been reported to be involved in the development of HCC (25, 26), so we wanted to explore whether ferroptosis-related genes existed in the DEGs. As shown in the Venn diagram (http://bioinformatics.psb.ugent.be/webtools/Venn/), seven ferroptosis-associated genes (ACSL4, FANCD2, G6PD, MT1G, NQO1, PTGS2, and SLC7A11) were identified among the 3,714 DEGs (**Figure 1C**). A total of 24 DE-lncRNAs were determined as the ferroptosis-related lncRNAs (**Supplementary Table S5**). Moreover, compared with normal hepatic tissues, 23 DE-lncRNAs were highly expressed in the HCC tissues, while only one DE-lncRNA (RP11-295M3.4) was lower in the HCC tissues (**Supplementary Table S6**). The heat map indicated a correlation between the 24 DE-lncRNAs and the seven ferroptosis-associated genes ($R > 0.5$, **Figure 1D**).

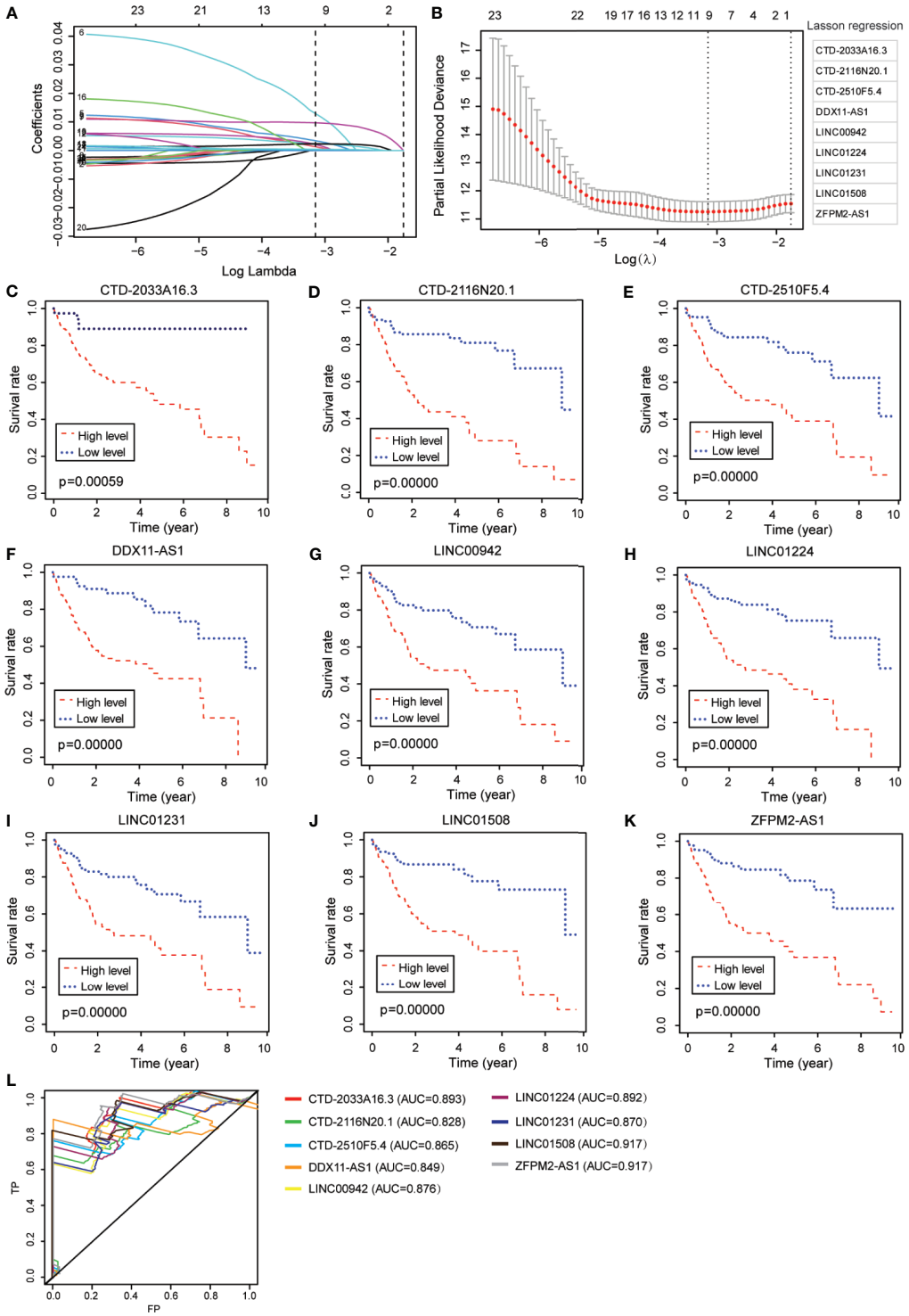

FIGURE 2 | Identification of ferroptosis-associated nine-lncRNAs with prognostic value in hepatocellular carcinoma (HCC) patients. **(A, B)** LASSO Cox regression with a 10-fold cross-validation for the prognostic value of the ferroptosis-associated nine-lncRNAs, including CTD-2033A16.3, CTD-2116N20.1, CTD-2510F5.4, DDX11-AS1, LINC00942, LINC01224, LINC01231, LINC01508, and ZFPM2-AS1. **(C–K)** Kaplan–Meier analytical evaluation of the prognostic values of the candidate lncRNAs. **(L)** Time-dependent receiver operating characteristic curves for the prognostic model based on the expression of nine-lncRNAs in The Cancer Genome Atlas–HCC cohort.

From the abovementioned 24 ferroptosis-associated lncRNAs, nine lncRNAs (CTD-2033A16.3, CTD-2116N20.1, CTD-2510F5.4, DDX11-AS1, LINC00942, LINC01224, LINC01231, LINC01508, and ZFPM2-AS1) were ultimately identified to be related to prognosis (**Figures 2A, B** and **Supplementary Table S7**). Kaplan–Meier survival analysis was further used to evaluate the significance of lncRNA expression on the prognosis of patients. As shown in **Figures 2C–K**, high levels of these candidate lncRNAs were all correlated with poor prognosis in patients with HCC. Furthermore, the time-dependent ROC analyses for the survival prediction of these key lncRNAs obtained area under the curve (AUC) values of 0.893 for CTD-2033A16.3, 0.828 for CTD-2116N20.1, 0.865 for CTD-2510F5.4, 0.849 for DDX11-AS1, 0.876 for LINC00942, 0.892 for LINC01224, 0.870 for LINC01231, 0.917 for LINC01508, and 0.917 for ZFPM2-AS1 (**Figure 2L**). In addition, qPCR showed that the expression levels of the nine candidate lncRNAs were significantly increased in two HCC cell lines—MHCC97H and HUH-7—compared to the normal liver cell line, HHL-5 (**Figure 3A**). Given that the roles of several lncRNAs, such as CTD-2033A16.3, LINC01231, and LINC01508, in HCC have not been reported, we wanted to explore whether these lncRNAs affect the apoptosis and proliferation of HCC cells. As expected, the knock-down of CTD-2033A16.3, LINC01231, and LINC01508 by siRNAs significantly promoted cell apoptosis and attenuated cell survival in the HCC cells HUH-7 (**Supplementary Figures S2A–E**). In addition, studies have indicated that intracellular iron and MDA are the characteristic features of ferroptosis (27). Next, we wanted to assess how these candidate lncRNAs regulate the cellular iron and MDA. As shown in **Figures 3B, C**, the knock-down of CTD-2033A16.3, LINC01231, and LINC01508 by siRNAs significantly improved the concentration of cellular iron and MDA in the HCC cells HUH-7, indicating their anti-ferroptosis effects. The

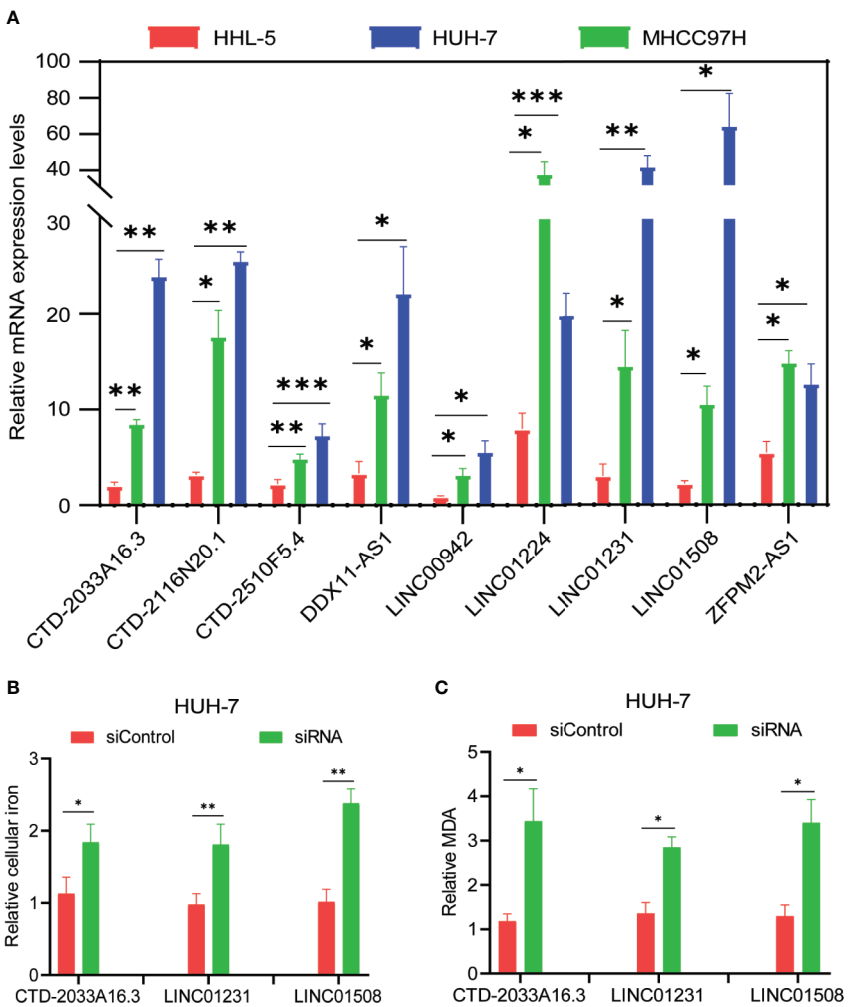

FIGURE 3 | Evaluation of candidate lncRNAs in the ferroptosis of hepatocellular carcinoma cells. **(A)** The levels of candidate lncRNAs were normalized to 18srRNA. **(B)** The intracellular iron was analyzed using an iron assay kit. **(C)** The cellular malondialdehyde concentration was analyzed using a lipid peroxidation assay kit. The values are displayed as mean ± SD for three independent replicates. *$p < 0.05$, **$p < 0.01$, ***$p < 0.001$.

results suggest that these ferroptosis-associated lncRNAs play important roles in HCC pathology.

Construction of the Prognostic Signature Based on Ferroptosis-Associated Nine-lncRNAs

The nine-lncRNA expression risk score (risk score = 2.677e-05 × CTD-2033A16.3 + 1.841e-02 × CTD-2116N20.1 + 9.499e-03 × CTD-2510F5.4 + 1.016e-02 × DDX11-AS1 + 1.779e-04 × LINC00942 + 3.657e-03 × LINC01224 + 4.413e-03 × LINC01231 + 1.673e-03 × LINC01508 + 9.253e-04 × ZFPM2-AS1) for each sample was calculated (**Supplementary Table S8**). Subsequently, an X-tile diagram was used to produce the optimal cutoff point for the risk score. According to this cutoff value of risk score, the TCGA-HCC patients were divided into a high-risk group and a low-risk group. A prognostic curve and a scatter plot were used to indicate the risk score and the survival status of each HCC patient (**Figures 4A, B**). Moreover, most of the death cases were mainly distributed in the high-risk group (**Figure 4B**). In addition, the heat map of the expression profiles of candidate lncRNAs demonstrated that CTD-2033A16.3, CTD-2116N20.1, CTD-2510F5.4, DDX11-AS1, LINC00942, LINC01224, LINC01231, LINC01508, and ZFPM2-AS1 were all highly expressed in the high-risk group (**Figure 4C** and **Supplementary Table S9**). Taken together, these findings presented the ferroptosis-associated nine-lncRNAs as the prognostic signature for HCC patients.

The Prognostic Value of Ferroptosis-Associated lncRNA Signature

Kaplan–Meier analysis validated that the HCC-TCGA patients in the high-risk group displayed a significantly worse survival than those in the low-risk group for the 3-, 5-, and 10-year survival times (**Figures 5A–C**). Furthermore, the time-dependent ROC analyses showed that the AUC of the risk score model was 0.812 at 3 years, 0.846 at 5 years, and 0.908 at 10 years (**Figures 5D–F**). To demonstrate its prognostic generality, we further verified this nine-lncRNA-based risk score model with a GEO dataset (GSE40144), which contains lncRNA expression profiling and clinical survival data from 59 HCC patients. Consistent with the results from the HCC-TCGA cohort, the Kaplan–Meier curves revealed that the survival of HCC cases in the high-risk group was significantly lower than those in the low-risk group (**Supplementary Figure S3A**), and the AUC of a time-dependent ROC curve for the survival prediction of risk score model was 0.635 at 3 years (**Supplementary Figure S3B**). All these data demonstrated the superior specificity and sensitivity of this ferroptosis-associated nine-lncRNA signature than other clinical parameters.

Next, univariate Cox analysis revealed that lncRNA-based signature (hazard ratio: 2.211, 95% confidence interval: 1.696–2.882) as well as T stage (hazard ratio: 1.483, 95% confidence interval: 1.919–1.847) were independent factors for the prognosis of HCC patients (**Figure 5G**). The multivariate Cox analysis revealed likewise that both the lncRNA-based signature (hazard

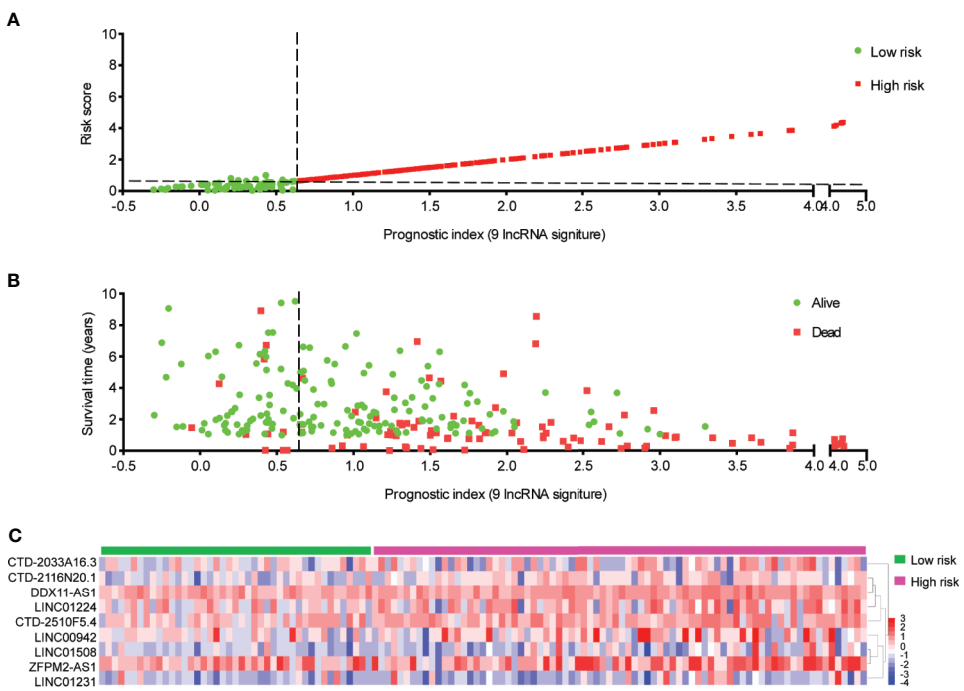

FIGURE 4 | Distribution of hepatocellular carcinoma (HCC) patients based on the risk score. **(A)** Risk curve and **(B)** scatter plot for the risk score and survival status of each HCC case. The red and green dots in **(B)** represent death and survival, respectively. **(C)** Heat map showing the expression profiles of ferroptosis-associated nine-lncRNAs in the high-risk group and the low-risk group.

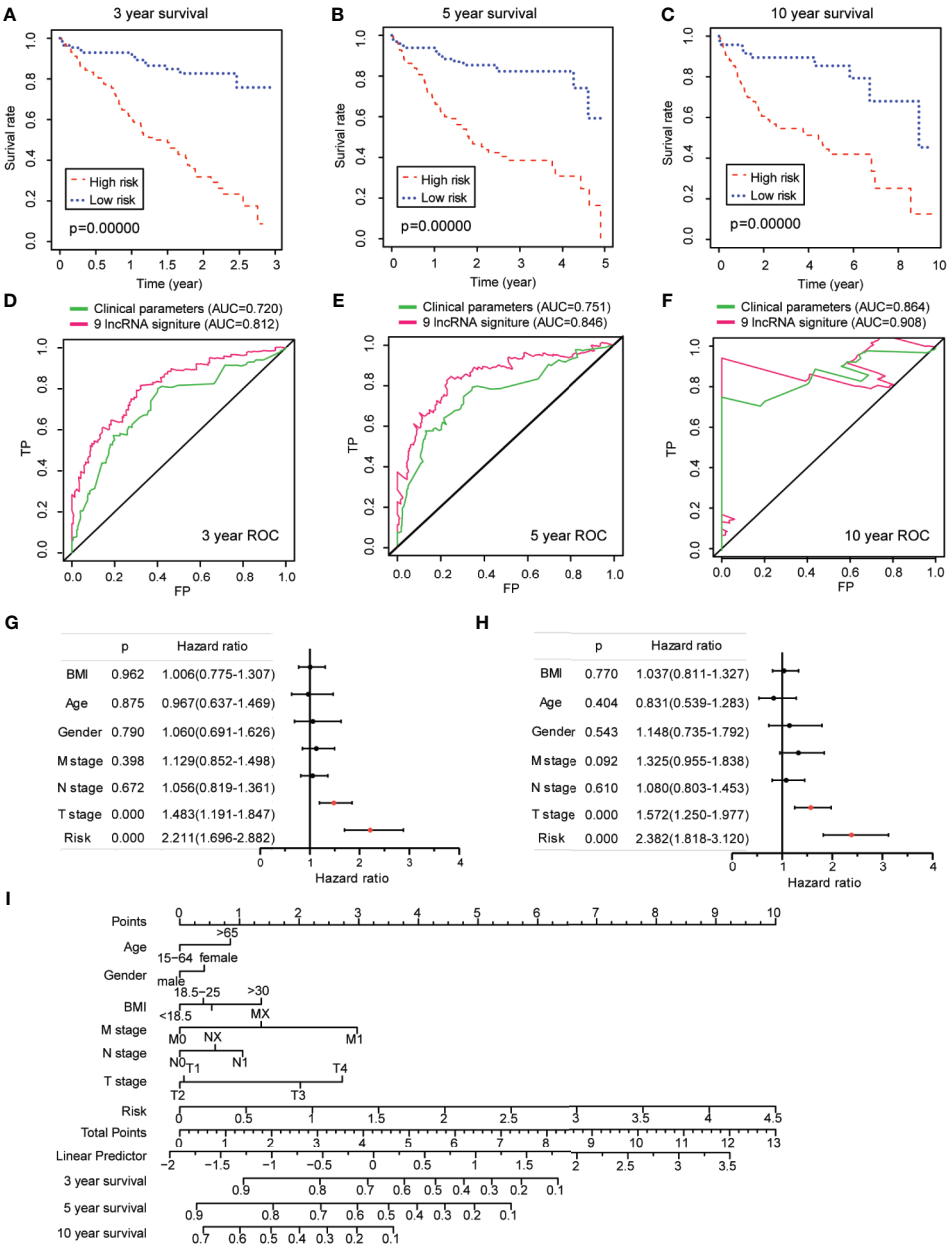

FIGURE 5 | Prognostic value of ferroptosis-associated lncRNA signature in The Cancer Genome Atlas–hepatocellular carcinoma cohort. **(A–C)** Kaplan–Meier analyses for the prognostic prediction of risk score model at 3-, 5-, and 10-year survival time, respectively. **(D–F)** Time-dependent receiver operating characteristic curves for the prognostic prediction of risk score model at 3-, 5-, and 10-year survival times, respectively. **(G, H)** Univariate and multivariate Cox regression analyses for the risk score model as an independent prognostic factor. **(I)** A combined nomogram for the risk score model and other clinicopathological factors.

ratio: 2.382, 95% confidence interval: 1.818–3.120) and the T stage (hazard ratio: 1.572, 95% confidence interval: 1.250–1.977) were independent prognostic risk factors for HCC patients (**Figure 5H**). To make the lncRNA-based signature more applicable in the clinic, a nomogram was established to explore the probability of the lncRNA signature in predicting the 3-, 5-, and 10-year survival in the TCGA-HCC cohort. As shown in **Figure 5I**, the predictive factors in the nomogram contained the novel risk score model and other clinicopathological features. In this combined nomogram, the risk score model was proven to exert the most excellent weight among all these clinically relevant covariates, which was similar to the findings from the multivariable Cox regression analysis. These studies collectively verified that this novel ferroptosis-associated lncRNA signature could reliably serve as an independent prognostic factor for patients with HCC.

GSEA Enrichment and Immunity Analysis of the Risk Score

The GSEA analysis indicated that the tumor hallmarks correlated with the low-risk group, which may be involved in the regulation of several immune-associated signaling pathways, such as tumor necrosis factor α (TNFα)/nuclear factor kappa-B (NFκB), interleukin 2 (IL2)/signal transducers and activators of transcription 5 (STAT5), *etc.* (**Figures 6A, B**). Moreover, the GSEA analysis, along with the KEGG pathways, further revealed that the pathways correlated with the low-risk group were mainly involved in the regulation of cytokine/cytokine receptor signaling pathways (**Figure 6C**). Previous studies reported that TNFα could promote NFκB activation through binding with TNF receptor, facilitating the production of elevated levels of T-helper 1/T-helper 17-related cytokines that drive proinflammatory signaling (28). Inhibition of the TNFα/NFκB-driven proinflammatory signaling resulted in the suppression of tumor growth and progression *in vivo* and *in vitro* (29). In addition, IL2 and its downstream target STAT5 have been proven to exert an effect on multiple aspects of immune responses, for example, the regulation of T cell development and function (30, 31). Thus, GSEA enrichment confirmed the biological significance of the ferroptosis-associated lncRNA signature in immune regulation.

To determine whether this nine-lncRNA signature was related to tumor immunity, we next evaluated the association between the risk score and the 22 types of TIICs in HCC from the CIBERSORT algorithm (**Supplementary Figure S4**). As shown in **Figure 7A** and **Supplementary Table S10**, the heat map of immune responses based on CIBERSORT displayed that M0 macrophages and T cell functions, including follicular helper T cells, regulatory T cells, and resting memory CD4(+) T cells, were all significantly different between the high-risk group and the low-risk group. We observed significantly higher proportions of resting memory CD4(+) T cell and lower proportions of follicular helper T cells, regulatory T cells, and M0 macrophages in the high-risk group (**Figures 7B–E**). These observations implied that the infiltration of these immune cell subtypes might exert an important influence on the prognosis of HCC patients. Given the clinical importance of therapeutic strategies based on immune checkpoint blockade in HCC (32, 33), we then explore the association between the risk score and several immune checkpoints, such as PD1, PDL1, CTLA4, VSIR, and B7H3. As shown in **Figure 7F**, the heat map showed the positive relations between risk score and these immune checkpoints. Moreover, a substantial increase in the expression of B7H3 was found in the high-risk group (**Figure 7G**). Taken together, these data suggested that the ferroptosis-associated lncRNA signature might affect the response to immunotherapy in HCC patients.

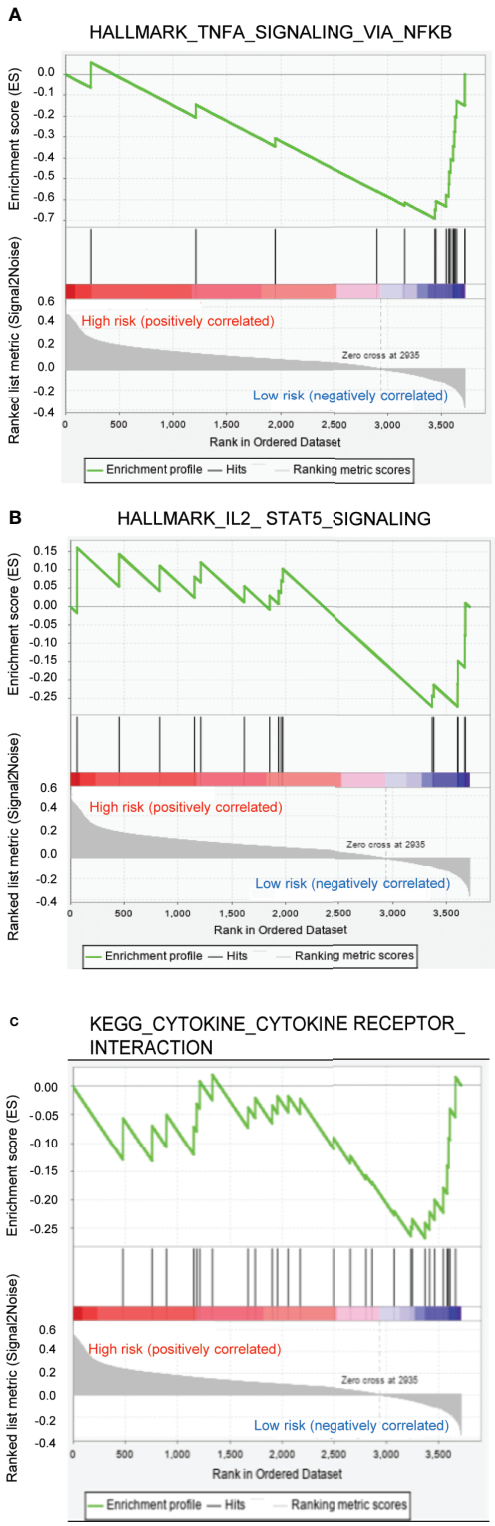

FIGURE 6 | Gene set enrichment analysis enrichment analysis for ferroptosis-associated lncRNA signature. **(A, B)** Two remarkably enriched immune-associated HALLMARK pathways in low-risk patients. **(C)** Two remarkably enriched immune-associated Kyoto Encyclopedia of Genes and Genomes pathways in low-risk patients.

DISCUSSION

HCC is one of the most common malignancies with a high mortality in the world. Identifying reliable and effective

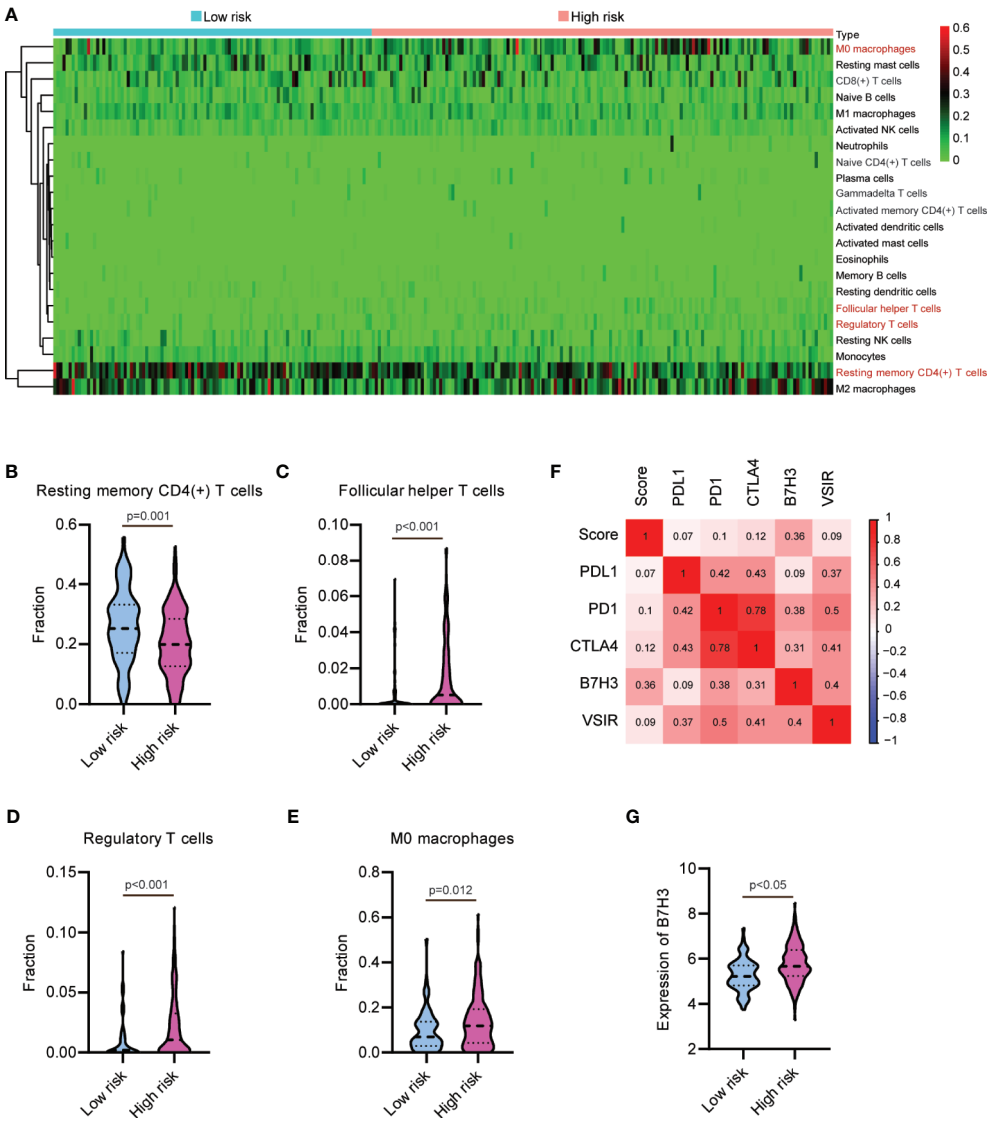

FIGURE 7 | Relationship between the lncRNA-based signature and immune responses in hepatocellular carcinoma. **(A)** Heat map of immune responses based on CIBERSORT in the low-risk group and the high-risk group. The proportion of **(B)** resting memory CD4(+) T cell, **(C)** follicular helper T cells, **(D)** regulatory T cells, and **(E)** M0 macrophages in the low-risk group and the high-risk group. **(F)** Heat map showing the positive relations between risk score and several immune checkpoints. **(G)** B7H3 is upregulated in the high-risk group.

biomarkers for HCC prognosis is of great importance. Here we identified a novel ferroptosis-related nine-lncRNA signature in a large-scale HCC cohort, including a testing dataset and a validation dataset, demonstrating its sensitivity and specificity.

In previous investigations, the lncRNA signatures for prognostic prediction have been described in many kinds of cancers, such as breast cancer (34), gastric cancer (35), *etc.* Similarly, based on the differentially expressed lncRNAs and disease pathogenesis, several lncRNA-associated signatures have also been developed to predict the outcome of HCC patients. A six-lncRNA signature (MSC-AS1, POLR2J4, EIF3J-AS1, SERHL, RMST, and PVT1) could be used to effectively predict the HCC recurrence risk (36). Another autophagy-related four-lncRNA signature (LUCAT1, AC099850.3, ZFPM2-AS1, and AC009005.1) has been developed to evaluate the autophagy-related regulatory mechanisms of identified lncRNAs in HCC outcome (37). However, the ferroptosis–lncRNA interaction in the HCC prognostic model remains to be clarified. Here we report for the first time the ferroptosis-related lncRNA signature for prognosis and immune response of HCC populations, providing a promising strategy with an important clinical implication for guiding individual therapy and improving outcome prediction. In addition, the biological functions of candidate lncRNAs in the pathology of human cancers have been proven in several independent reports, for example, the high-level expression of CTD-2510F5.4 strengthened the

malignant phenotype in gastric cancer (38). Knockdown of DDX11-AS1 significantly inhibited cell proliferation and migration in HCC *in vitro* and *in vivo* (39). LINC01224 silently repressed the HCC progression through sponging of microRNA-330-5p (40).

To date, ferroptosis has been recognized as a form of regulated cell death (41), which displays functional roles in HCC tumorigenesis and immune regulation. A newly identified circular RNA, Circ0097009, could upregulate the expression of SLC7A11, a key ferroptosis-associated regulator, by sponging miR-1261 in multiple HCC cell lines (42). O-GlcNAcylation-mediated YAP stabilization enhanced the sensitivity of HCC cells to RSL3-induced ferroptosis *in vitro* and *in vivo* (43). Recent studies have reported the direct crosstalk between ferroptosis and anti-tumor immunity. Tumor-infiltrating lymphocyte-mediated ferroptosis can effectively enhance the efficacy of immune checkpoint inhibitors. Iron overload in cancer cells is considered to boost the immune checkpoint blockade in HCC therapy *via* stimulating ROS accumulation and sensitizing cancer cells to ferroptosis (44, 45). Thus, explorations focusing on the detailed mechanisms and functions of ferroptosis in HCC will help pave the way to identify ferroptosis induction as a promising therapeutic method.

Through strengthening the immune system of patients, immunotherapy has been shown to be successful in making cancer a curable disease in various malignancies. A considerable body of preclinical and clinical literatures highlight that immune-based therapeutic strategies offer survival benefits for HCC. Moreover, a combination of immunotherapy and other therapeutic methods is likely to become an alternative option in HCC treatment (46, 47). Wen et al. synthetized a double-stranded polyinosinic-polycytidylic acid (polyIC) and demonstrated that the combination of polyIC with checkpoint inhibitors could distinctly activate the anti-tumor immune, thus effectively preventing liver tumorigenesis (48). In addition, emerging studies have proven the importance of tumor-infiltrating lymphocytes in driving immune evasion during HCC progression, including regulatory T cells, tumor-associated macrophages, *etc.* (49). The exhaustion of follicular helper T cells induced by intra-tumoral PDL1 resulted in the defective B cell function, facilitating the progression of advanced HCC (50). In this study, high levels of follicular helper T cells, regulatory T cells, and M0 macrophages were found in the high-risk group, indicating immune tolerance in the high-risk HCC patients. Thus, the ferroptosis-related lncRNA signature could provide potential cues for the patient selection for more effective anti-tumor immunotherapies. However, additional validation is required to understand the roles of our signature in the prediction of immunotherapeutic response in HCC patients.

However, there are several limitations in our study. Our report is mainly based on integrative bioinformatics, and effective experimental validation for these findings is currently lacking. Furthermore, the accuracy of ferroptosis-related lncRNA signature for the prognosis and immune regulation of HCC patients will remain an important issue in the clinic. In particular, the guidelines for the clinical use of this prognostic risk score model needs to be further defined.

CONCLUSION

In conclusion, a novel ferroptosis-related nine-lncRNA signature was constructed as an efficient computational technique for predicting the prognosis and immune response of patients with HCC. This signature was robustly connected to the risk scores, survival time, and tumor clinical parameters. Immune analysis supported the association between the risk value of this signature and specific immune cell populations. Thus, our findings suggested a promising insight into ferroptosis-related lncRNAs in the HCC population and provided a personalized prediction tool for prognosis and immune responses.

DATA AVAILABILITY STATEMENT

The original contributions presented in the study are included in the article/**Supplementary Material**. Further inquiries can be directed to the corresponding author.

AUTHOR CONTRIBUTIONS

ZX, ZG, and YY contributed to the conception and design of the study. BP, QL, XC, YC, and SZ contributed to the writing, review, and/or revision of the manuscript. KG, XW, and QY provided administrative, technical, or material support. All authors contributed to the article and approved the submitted version.

FUNDING

This study is supported by grants from the China Postdoctoral Science Foundation (grant numbers 2021T140754 and 2020M672521), the National Natural Science Foundation of China (grant number 81803035), the Natural Science Foundation of Hunan Province (grant numbers 2019JJ50932 and 2020JJ5934), and the Postdoctoral Science Foundation of Central South University (grant number 248485).

SUPPLEMENTARY MATERIAL

The Supplementary Material for this article can be found online at: https://www.frontiersin.org/articles/10.3389/fimmu.2021.719175/full#supplementary-material

Supplementary Figure 1 | Pie chart for the composition of differentially expressed genes (DEGs). The DEGs consisted of 53.28% protein-coding genes, 32.70% lncRNAs, 0.44% miRNAs, *etc.*

Supplementary Figure 2 | Effects of CTD-2033A16.3, LINC01231, and LINC01508 on the apoptosis and proliferation of hepatocellular carcinoma (HCC) cells HUH-7. **(A)** qPCR analysis of lncRNA expression after transfection with the lncRNA-targeted siRNAs. **(B, C)** The inhibition of CTD-2033A16.3, LINC01231, and LINC01508 by siRNAs leads to the promotion of cell apoptosis rate. **(D, E)** The inhibition of CTD-2033A16.3, LINC01231, and LINC01508 by siRNAs leads to the inhibition of the cell colony forming rate. Values are displayed as mean ± SD for three independent replicates. $^{*}p < 0.05$, $^{**}p < 0.01$.

Supplementary Figure 3 | Prognostic value of ferroptosis-associated lncRNA signature in GSE40144. **(A)** Kaplan–Meier analysis was used to verify the prognostic values of novel lncRNA-based signature in hepatocellular carcinoma patients from GSE40144. **(B)** Time-dependent receiver operating characteristic curve for the survival prediction of the risk score model in the GSE40144 cohort.

Supplementary Figure 4 | Spearman's correlation on the association between the risk score of the signature and immune cells.

REFERENCES

1. Liu P, Tang Q, Chen M, Chen W, Lu Y, Liu Z, et al. Hepatocellular Senescence: Immunosurveillance and Future Senescence-Induced Therapy in Hepatocellular Carcinoma. *Front Oncol* (2020) 10:589908. doi: 10.3389/fonc.2020.589908
2. Huang X, Qin F, Meng Q, Dong M. Protein Tyrosine Phosphatase Receptor Type D (PTPRD)-Mediated Signaling Pathways for the Potential Treatment of Hepatocellular Carcinoma: A Narrative Review. *Ann Trans Med* (2020) 8 (18):1192. doi: 10.21037/atm-20-4733
3. Cheng CW, Tse E. Targeting PIN1 as a Therapeutic Approach for Hepatocellular Carcinoma. *Front Cell Dev Biol* (2019) 7:369. doi: 10.3389/fcell.2019.00369
4. Li J, Zhu Y. Recent Advances in Liver Cancer Stem Cells: Non-Coding RNAs, Oncogenes and Oncoproteins. *Front Cell Dev Biol* (2020) 8:548335. doi: 10.3389/fcell.2020.548335
5. Feng D, Wang M, Hu J, Li S, Zhao S, Li H, et al. Prognostic Value of the Albumin-Bilirubin Grade in Patients With Hepatocellular Carcinoma and Other Liver Diseases. *Ann Trans Med* (2020) 8(8):553. doi: 10.21037/atm.2020.02.116
6. Li W, Chen QF, Huang T, Wu P, Shen L, Huang ZL. Identification and Validation of a Prognostic lncRNA Signature for Hepatocellular Carcinoma. *Front Oncol* (2020) 10:780. doi: 10.3389/fonc.2020.00780
7. Tang R, Hua J, Xu J, Liang C, Meng Q, Liu J, et al. The Role of Ferroptosis Regulators in the Prognosis, Immune Activity and Gemcitabine Resistance of Pancreatic Cancer. *Ann Trans Med* (2020) 8(21):1347. doi: 10.21037/atm-20-2554a
8. Shan Y, Yang G, Huang H, Zhou Y, Hu X, Lu Q, et al. Ubiquitin-Like Modifier Activating Enzyme 1 as a Novel Diagnostic and Prognostic Indicator That Correlates With Ferroptosis and the Malignant Phenotypes of Liver Cancer Cells. *Front Oncol* (2020) 10:592413. doi: 10.3389/fonc.2020.592413
9. Wang K, Zhang Z, Tsai HI, Liu Y, Gao J, Wang M, et al. Branched-Chain Amino Acid Aminotransferase 2 Regulates Ferroptotic Cell Death in Cancer Cells. *Cell Death Differ* (2021) 28(4):1222–36. doi: 10.1038/s41418-020-00644-4
10. Liu Y, Zhang X, Zhang J, Tan J, Li J, Song Z. Development and Validation of a Combined Ferroptosis and Immune Prognostic Classifier for Hepatocellular Carcinoma. *Front Cell Dev Biol* (2020) 8:596679. doi: 10.3389/fcell.2020.596679
11. Zhu Y, Wang S, Xi X, Zhang M, Liu X, Tang W, et al. Integrative Analysis of Long Extracellular RNAs Reveals a Detection Panel of Noncoding RNAs for Liver Cancer. *Theranostics* (2021) 11(1):181–93. doi: 10.7150/thno.48206
12. Zuo X, Chen Z, Gao W, Zhang Y, Wang J, Wang J, et al. M6A-Mediated Upregulation of LINC00958 Increases Lipogenesis and Acts as a Nanotherapeutic Target in Hepatocellular Carcinoma. *J Hematol Oncol* (2020) 13(1):5. doi: 10.1186/s13045-019-0839-x
13. Qi W, Li Z, Xia L, Dai J, Zhang Q, Wu C, et al. LncRNA GABPB1-AS1 and GABPB1 Regulate Oxidative Stress During Erastin-Induced Ferroptosis in HepG2 Hepatocellular Carcinoma Cells. *Sci Rep* (2019) 9(1):16185. doi: 10.1038/s41598-019-52837-8
14. Liang JY, Wang DS, Lin HC, Chen XX, Yang H, Zheng Y, et al. A Novel Ferroptosis-Related Gene Signature for Overall Survival Prediction in Patients With Hepatocellular Carcinoma. *Int J Biol Sci* (2020) 16(13):2430–41. doi: 10.7150/ijbs.45050
15. Pandelides Z, Thornton C, Faruque AS, Whitehead AP, Willett KL, Ashpole NM. Developmental Exposure to Cannabidiol (CBD) Alters Longevity and Health Span of Zebrafish (Danio Rerio). *GeroScience* (2020) 42(2):785–800. doi: 10.1007/s11357-020-00182-4
16. Buford TW, Sun Y, Roberts LM, Banerjee A, Peramsetty S, Knighton A, et al. Angiotensin (1-7) Delivered Orally *via* Probiotic, But Not Subcutaneously, Benefits the Gut-Brain Axis in Older Rats. *GeroScience* (2020) 42(5):1307–21. doi: 10.1007/s11357-020-00196-y
17. Kiss T, Giles CB, Tarantini S, Yabluchanskiy A, Balasubramanian P, Gautam T, et al. Nicotinamide Mononucleotide (NMN) Supplementation Promotes Anti-Aging miRNA Expression Profile in the Aorta of Aged Mice, Predicting Epigenetic Rejuvenation and Anti-Atherogenic Effects. *GeroScience* (2019) 41 (4):419–39. doi: 10.1007/s11357-019-00095-x
18. Friedman J, Hastie T, Tibshirani R. Regularization Paths for Generalized Linear Models *via* Coordinate Descent. *J Stat Softw* (2010) 33(1):1–22.
19. Blanche P, Dartigues JF, Jacqmin-Gadda H. Estimating and Comparing Time-Dependent Areas Under Receiver Operating Characteristic Curves for Censored Event Times With Competing Risks. *Stat Med* (2013) 32 (30):5381–97. doi: 10.1002/sim.5958
20. Eaton A, Therneau T, Le-Rademacher J. Designing Clinical Trials With (Restricted) Mean Survival Time Endpoint: Practical Considerations. *Clin Trials* (2020) 17(3):285–94. doi: 10.1177/1740774520905563
21. Newman AM, Liu CL, Green MR, Gentles AJ, Feng W, Xu Y, et al. Robust Enumeration of Cell Subsets From Tissue Expression Profiles. *Nat Methods* (2015) 12(5):453–7. doi: 10.1038/nmeth.3337
22. Pilones KA, Hensler M, Daviaud C, Kraynak J, Fucikova J, Galluzzi L, et al. Converging Focal Radiation and Immunotherapy in a Preclinical Model of Triple Negative Breast Cancer: Contribution of VISTA Blockade. *Oncoimmunology* (2020) 9(1):1830524. doi: 10.1080/2162402X.2020.1830524
23. Picarda E, Ohaegbulam KC, Zang X. Molecular Pathways: Targeting B7-H3 (CD276) for Human Cancer Immunotherapy. *Clin Cancer Res* (2016) 22 (14):3425–31. doi: 10.1158/1078-0432.CCR-15-2428
24. Subramanian A, Tamayo P, Mootha VK, Mukherjee S, Ebert BL, Gillette MA, et al. Gene Set Enrichment Analysis: A Knowledge-Based Approach for Interpreting Genome-Wide Expression Profiles. *Proc Natl Acad Sci USA* (2005) 102(43):15545–50. doi: 10.1073/pnas.0506580102
25. Jin M, Shi C, Li T, Wu Y, Hu C, Huang G. Solasonine Promotes Ferroptosis of Hepatoma Carcinoma Cells *via* Glutathione Peroxidase 4-Induced Destruction of the Glutathione Redox System. *Biomed Pharmacother = Biomed Pharmacother* (2020) 129:110282. doi: 10.1016/j.biopha.2020.110282
26. Sun J, Zhou C, Zhao Y, Zhang X, Chen W, Zhou Q, et al. Quiescin Sulfhydryl Oxidase 1 Promotes Sorafenib-Induced Ferroptosis in Hepatocellular Carcinoma by Driving EGFR Endosomal Trafficking and Inhibiting NRF2 Activation. *Redox Biol* (2021) 41:101942. doi: 10.1016/j.redox.2021.101942
27. Mancuso RI, Foglio MA, Olalla Saad ST. Artemisinin-Type Drugs for the Treatment of Hematological Malignancies. *Cancer Chemother Pharmacol* (2021) 87(1):1–22. doi: 10.1007/s00280-020-04170-5
28. Lin WJ, Su YW, Lu YC, Hao Z, Chio II, Chen NJ, et al. Crucial Role for TNF Receptor-Associated Factor 2 (TRAF2) in Regulating NFkappaB2 Signaling That Contributes to Autoimmunity. *Proc Natl Acad Sci USA* (2011) 108 (45):18354–9. doi: 10.1073/pnas.1109427108
29. Pollard BS, Suckow MA, Wolter WR, Starr JM, Eidelman O, Dalgard CL, et al. Digitoxin Inhibits Epithelial-To-Mesenchymal-Transition in Hereditary Castration Resistant Prostate Cancer. *Front Oncol* (2019) 9:630. doi: 10.3389/fonc.2019.00630
30. Czerwinska P, Rucinski M, Wlodarczyk N, Jaworska A, Grzadzielewska I, Gryska K, et al. Therapeutic Melanoma Vaccine With Cancer Stem Cell Phenotype Represses Exhaustion and Maintains Antigen-Specific T Cell Stemness by Up-Regulating BCL6. *Oncoimmunology* (2020) 9(1):1710063. doi: 10.1080/2162402X.2019.1710063
31. Mahmud SA, Manlove LS, Farrar MA. Interleukin-2 and STAT5 in Regulatory T Cell Development and Function. *Jak-Stat* (2013) 2(1):e23154. doi: 10.4161/jkst.23154

32. Wing-Sum Cheu J, Chak-Lui Wong C. Mechanistic Rationales Guiding Combination Hepatocellular Carcinoma Therapies Involving Immune Checkpoint Inhibitors. *Hepatology* (2021). doi: 10.1002/hep.31840
33. Yang W, Feng Y, Zhou J, Cheung OK, Cao J, Wang J, et al. A Selective HDAC8 Inhibitor Potentiates Antitumor Immunity and Efficacy of Immune Checkpoint Blockade in Hepatocellular Carcinoma. *Sci Trans Med* (2021) 13(588):eaaz6804. doi: 10.1126/scitranslmed.aaz6804
34. Sun M, Liu X, Xia L, Chen Y, Kuang L, Gu X, et al. A nine-lncRNA Signature Predicts Distant Relapse-Free Survival of HER2-Negative Breast Cancer Patients Receiving Taxane and Anthracycline-Based Neoadjuvant Chemotherapy. *Biochem Pharmacol* (2020) 189:114285. doi: 10.1016/j.bcp.2020.114285
35. He Y, Wang X. Identification of Molecular Features Correlating With Tumor Immunity in Gastric Cancer by Multi-Omics Data Analysis. *Ann Trans Med* (2020) 8(17):1050. doi: 10.21037/atm-20-922
36. Gu JX, Zhang X, Miao RC, Xiang XH, Fu YN, Zhang JY, et al. Six-Long non-Coding RNA Signature Predicts Recurrence-Free Survival in Hepatocellular Carcinoma. *World J Gastroenterol* (2019) 25(2):220–32. doi: 10.3748/wjg.v25.i2.220
37. Zhang Y, Zhang L, Xu Y, Wu X, Zhou Y, Mo J. Immune-Related Long Noncoding RNA Signature for Predicting Survival and Immune Checkpoint Blockade in Hepatocellular Carcinoma. *J Cell Physiol* (2020) 235(12):9304–16. doi: 10.1002/jcp.29730
38. Wang Z, Qin B. Prognostic and Clinicopathological Significance of Long Noncoding RNA CTD-2510F5.4 in Gastric Cancer. *Gastric Cancer* (2019) 22 (4):692–704. doi: 10.1007/s10120-018-00911-x
39. Li Y, Zhuang W, Huang M, Li X. Long Noncoding RNA DDX11-AS1 Epigenetically Represses LATS2 by Interacting With EZH2 and DNMT1 in Hepatocellular Carcinoma. *Biochem Biophys Res Commun* (2019) 514 (4):1051–7. doi: 10.1016/j.bbrc.2019.05.042
40. Gong D, Feng PC, Ke XF, Kuang HL, Pan LL, Ye Q, et al. Silencing Long Non-Coding RNA LINC01224 Inhibits Hepatocellular Carcinoma Progression *via* MicroRNA-330-5p-Induced Inhibition of CHEK1. *Mol Ther Nucleic Acids* (2020) 19:482–97. doi: 10.1016/j.omtn.2019.10.007
41. Wei R, Qiu H, Xu J, Mo J, Liu Y, Gui Y, et al. Expression and Prognostic Potential of GPX1 in Human Cancers Based on Data Mining. *Ann Trans Med* (2020) 8(4):124. doi: 10.21037/atm.2020.02.36
42. Lyu N, Zeng Y, Kong Y, Chen Q, Deng H, Ou S, et al. Ferroptosis Is Involved in the Progression of Hepatocellular Carcinoma Through the Circ0097009/miR-1261/SLC7A11 Axis. *Ann Trans Med* (2021) 9(8):675. doi: 10.21037/atm-21-997
43. Zhu G, Murshed A, Li H, Ma J, Zhen N, Ding M, et al. O-GlcNAcylation Enhances Sensitivity to RSL3-Induced Ferroptosis *via* the YAP/TFRC Pathway in Liver Cancer. *Cell Death Discov* (2021) 7(1):83. doi: 10.1038/s41420-021-00468-2
44. Zhang W, Wang F, Hu C, Zhou Y, Gao H, Hu J. The Progress and Perspective of Nanoparticle-Enabled Tumor Metastasis Treatment. *Acta Pharm Sin B* (2020) 10(11):2037–53. doi: 10.1016/j.apsb.2020.07.013
45. Alu A, Han X, Ma X, Wu M, Wei Y, Wei X. The Role of Lysosome in Regulated Necrosis. *Acta Pharm Sin B* (2020) 10(10):1880–903. doi: 10.1016/j.apsb.2020.07.003
46. Obi S, Sato T, Sato S. Immune Checkpoint Inhibitor in Liver Cancer-Unique Regional Differences. *Ann Trans Med* (2020) 8(21):1336. doi: 10.21037/atm-20-3378
47. Tang X, Shu Z, Zhang W, Cheng L, Yu J, Zhang M, et al. Clinical Significance of the Immune Cell Landscape in Hepatocellular Carcinoma Patients With Different Degrees of Fibrosis. *Ann Trans Med* (2019) 7(20):528. doi: 10.21037/atm.2019.09.122
48. Wen L, Xin B, Wu P, Lin CH, Peng C, Wang G, et al. An Efficient Combination Immunotherapy for Primary Liver Cancer by Harmonized Activation of Innate and Adaptive Immunity in Mice. *Hepatology* (2019) 69 (6):2518–32. doi: 10.1002/hep.30528
49. Lurje I, Werner W, Mohr R, Roderburg C, Tacke F, Hammerich L. *In Situ* Vaccination as a Strategy to Modulate the Immune Microenvironment of Hepatocellular Carcinoma. *Front Immunol* (2021) 12:650486. doi: 10.3389/fimmu.2021.650486
50. Zhou ZQ, Tong DN, Guan J, Tan HW, Zhao LD, Zhu Y, et al. Follicular Helper T Cell Exhaustion Induced by PD-L1 Expression in Hepatocellular Carcinoma Results in Impaired Cytokine Expression and B Cell Help, and Is Associated With Advanced Tumor Stages. *Am J Trans Res* (2016) 8(7):2926–36.

Conflict of Interest: The authors declare that the research was conducted in the absence of any commercial or financial relationships that could be construed as a potential conflict of interest.

Publisher's Note: All claims expressed in this article are solely those of the authors and do not necessarily represent those of their affiliated organizations, or those of the publisher, the editors and the reviewers. Any product that may be evaluated in this article, or claim that may be made by its manufacturer, is not guaranteed or endorsed by the publisher.

frontiers in Immunology

ORIGINAL RESEARCH
published: 30 September 2021
doi: 10.3389/fimmu.2021.760747

Elevated N6-Methyladenosine RNA Levels in Peripheral Blood Immune Cells: A Novel Predictive Biomarker and Therapeutic Target for Colorectal Cancer

Jinye Xie[1†], Zhijian Huang[2†], Ping Jiang[3†], Runan Wu[4], Hongbo Jiang[4], Chuanghua Luo[5], Honghai Hong[6*] and Haofan Yin[2,4*]*

[1] Department of Clinical Laboratory, Zhongshan City People's Hospital, The Affiliated Zhongshan Hospital of Sun Yat-Sen University, Zhongshan, China, [2] Digestive Medicine Center, The Seventh Affiliated Hospital of Sun Yat-sen University, Shenzhen, China, [3] Department of Clinical Medical Laboratory, Guangzhou First People Hospital, School of Medicine, South China University of Technology, Guangzhou, China, [4] Department of Clinical Laboratory, The Seventh Affiliated Hospital of Sun Yat-sen University, Shenzhen, China, [5] State Key Laboratory of Oncology in South China, Collaborative Innovation Center for Cancer Medicine, Sun Yat-sen University Cancer Center, Guangzhou, China, [6] Department of Clinical Laboratory, The Third Affiliated Hospital of Guangzhou Medical University, Guangzhou, China

Effective biomarkers for the diagnosis of colorectal cancer (CRC) are essential for improving prognosis. Imbalance in regulation of N6-methyladenosine (m^6A) RNA has been associated with a variety of cancers. However, whether the m^6A RNA levels of peripheral blood can serve as a diagnostic biomarker for CRC is still unclear. In this research, we found that the m^6A RNA levels of peripheral blood immune cells were apparently elevated in the CRC group compared with those in the normal controls (NCs) group. Furthermore, the m^6A levels arose as CRC progressed and metastasized, while these levels decreased after treatment. The area under the curve (AUC) of the m^6A levels was 0.946, which was significantly higher than the AUCs for carcinoembryonic antigen (CEA; 0.817), carbohydrate antigen 125 (CA125; 0.732), and carbohydrate antigen 19-9 (CA19-9; 0.771). Moreover, the combination of CEA, CA125, and CA19-9 with m^6A levels improved the AUC to 0.977. Bioinformatics and qRT-PCR analysis further confirmed that the expression of m^6A modifying regulator IGF2BP2 was markedly elevated in peripheral blood of CRC patients. Gene set variation analysis (GSVA) implied that monocyte was the most abundant m^6A-modified immune cell type in CRC patients' peripheral blood. Additionally, m^6A modifications were negatively related to the immune response of monocytes. In conclusion, our results revealed that m^6A RNA of peripheral blood immune cells was a prospective non-invasive diagnostic biomarker for CRC patients and might provide a valuable therapeutic target.

Keywords: N6-methyladenosine, colorectal cancer, biomarker, therapeutic target, peripheral blood

OPEN ACCESS

Edited by:
Bo Qin,
Mayo Clinic, United States

Reviewed by:
Wen-Wei Sung,
Chung Shan Medical University Hospital, Taiwan
Ting Deng,
Tianjin Medical University Cancer Institute and Hospital, China

***Correspondence:**
Chuanghua Luo
luoch3@sysucc.org.cn
Honghai Hong
gaolaosao@126.com
Haofan Yin
yinhf@mail2.sysu.edu.cn

†These authors have contributed equally to this work

Specialty section:
This article was submitted to Cancer Immunity and Immunotherapy, a section of the journal Frontiers in Immunology

Received: *18 August 2021*
Accepted: *09 September 2021*
Published: *30 September 2021*

Citation:
Xie J, Huang Z, Jiang P, Wu R, Jiang H, Luo C, Hong H and Yin H (2021) Elevated N6-Methyladenosine RNA Levels in Peripheral Blood Immune Cells: A Novel Predictive Biomarker and Therapeutic Target for Colorectal Cancer. Front. Immunol. 12:760747. doi: 10.3389/fimmu.2021.760747

INTRODUCTION

Colorectal cancer (CRC) is a common malignancy and the fourth leading cause of cancer-related deaths globally (1). If diagnosed in the early stage, the 5-year survival rate of CRC patients is as high as 70%–90% (2). Nevertheless, CRC patients with tumor metastases present a worse prognosis, with a 5-year survival rate of only approximately 20% (3). Furthermore, due to changes in people's dietary and lifestyle habits, a growing number of patients with CRC are diagnosed at an advanced stage, which leads to challenging therapeutic resection of primary tumors and metastases (4).

Consequently, improving the prognosis of CRC patients largely depends on early and accurate diagnosis. At present, colonoscopy and tissue biopsy are the most efficient methods for CRC screening (5). Nonetheless, colonoscopy is an invasive procedure that can be traumatic for subjects, and the whole operation is occasionally hard to complete due to poor compliance of patients with CRC (2). Additionally, considering the invasiveness and cost of these operations, it is impractical to perform comprehensive screening as part of a general physical examination. Therefore, there is an urgent demand for more noninvasive and efficacious biomarkers for clinical diagnosis. Over recent years, the identification of blood biomarkers has become an important issue because of the pain-free operation of blood biomarkers testing (6). Blood biomarkers such as carbohydrate antigen 19-9 (CA19-9), carbohydrate antigen 125 (CA125), and carcinoembryonic antigen (CEA) are broadly applied for CRC detection (7, 8). Yet, these three biomarkers, alone or in combination, are not sufficient for diagnosing CRC due to their poor specificity and sensitivity (8, 9). Hence, there is an urgent need to optimize the diagnosis of CRC by other efficient blood biomarkers.

N6-methyladenosine (m^6A) modification, which was encoded by the methyltransferase complex consisting of "writers", "erasers", and "readers", has emerged as a critical regulator in a multitude of diseases (10, 11). The modification of m^6A is enriched close to the 3′ untranslated terminal region (UTR) and the stop codon, thus influencing RNA transcription, processing, and translation (12, 13). Over recent years, activation of m^6A modification has been reported in CRC tumor cells (10, 13). Upregulated m^6A modification contributes to tumor progression by maintaining SOX2 expression in CRC cells through IGF2 mRNA binding proteins 2 (IGF2BP2)-dependent mechanisms (14, 15). Moreover, activating the glycolytic pathway by m^6A methylation promotes CRC tumorigenesis, indicating that m^6A modification of CRC tumor cells might become a therapeutic target (16, 17). Besides, the m^6A-modified status of peripheral blood has been recently reported as a new promising hallmark in diabetes and gastric cancer (18, 19). Nevertheless, whether the m^6A modification of peripheral blood RNA may act as a new diagnostic biomarker or therapeutic target for CRC remains unclear.

In this study, we examined the levels of m^6A in peripheral blood RNA of CRC patients and NCs to assess its value as a diagnostic biomarker. We also used bioinformatics, which revealed that elevated m^6A levels were mainly associated with monocytes and suppressed their immune response, indicating that m^6A modifications of peripheral blood immune cells might become a therapeutic target for CRC.

MATERIALS AND METHODS

Human Samples

The Institutional Review Board of Zhongshan People's Hospital approved this retrospective study (IRB number: K2020-20) on March 20, 2020. Between March 2020 and June 2021, peripheral blood samples from 105 CRC patients and 64 NCs who had no history of basic or chronic diseases were collected from the Zhongshan People's Hospital, using EDTA anticoagulation tubes. Whole blood (0.5 ml) and 1 ml of red blood cell lysate (TIANGEN, Beijing, China) were mixed and centrifuged. The precipitate was taken and dissolved with 1 ml TRIzol to stabilize RNA, after which the mixed samples were stored at −80°C for no longer than 6 months. All CRC patients were diagnosed on the basis of the histopathology by biopsy or endoscopic examination, and informed consent was obtained for all participants. A total of 105 CRC patients' peripheral blood samples were collected at the time of diagnosis before surgery or radiochemotherapy. Of these, peripheral blood was collected for the first time on admission and for the second time 14 days after surgery in 33 CRC patients. Ethics approval was obtained from the Ethics Committee of the Zhongshan People's Hospital. The clinical and biological characteristics of the patients are described in **Table 1**.

RNA Isolation and qRT-PCR

Total RNA was extracted using TRIzol (Thermo Scientific, MA, USA) according to the manufacturer's protocol. First-strand cDNA synthesis was performed using 500 ng of total RNA, and the qRT-PCR analysis system was performed using iQ SYBR Green Supermix (Accurate Biology, Changsha, China) and the iCycler Real-time PCR Detection System (Bio-Rad, California, USA). β-actin was used for normalization. Primers of targeted genes are listed in **Supplementary Table S1**.

Monocyte Isolation

Peripheral blood mononuclear cells (PBMCs) were isolated from peripheral blood samples from CRC patients and normal subjects *via* density gradient centrifugation. Whole blood was collected in EDTA tubes. The blood was diluted 1:1 with PBS free of calcium and magnesium. PBMCs were obtained by Ficoll density gradient isolation (Stemcell Technologies, Cologne, Germany). From the freshly isolated PBMCs, $CD14^+$ monocytes were isolated using the EasySep Human Monocyte Isolation Kit (Stemcell Technologies, Cologne, Germany).

RNA m^6A Quantification

The m^6A levels in total RNA were measured using EpiQuik m^6A RNA Methylation Quantification Kit (Colorimetric) (Epigentek, New York, USA) according to the manufacturer's protocol. RNA (200 ng) was added to assay wells covered with binding solution. Capture antibody solution, detection antibody solution, and

TABLE 1 | Correlation between the levels of m^6A and clinicopathological characteristics in CRC.

Characteristics	No. of patients	Peripheral blood m^6A levels % (mean ± SD)	*p*-value
Age			
≤60	57	0.268 ± 0.057	0.649
>60	48	0.273 ± 0.040	
Gender			
Female	36	0.276 ± 0.064	0.386
Male	69	0.267 ± 0.043	
Clinical stage			
I	6	0.243 ± 0.031	0.682
II	20	0.263 ± 0.031	
III	31	0.260 ± 0.048	
IV	26	0.302 ± 0.063	
T classification			
T1–T2	15	0.268 ± 0.040	0.739
T3–T4	64	0.274 ± 0.056	
N classification			
N0	29	0.273 ± 0.066	0.933
N1–N2	50	0.272 ± 0.046	
N classification			
N0–N1	57	0.269 ± 0.056	0.291
N2	22	0.283 ± 0.047	
M classification			
M0	57	0.260 ± 0.041	<0.001
M1	26	0.302 ± 0.063	
Differentiation			
Poor	14	0.273 ± 0.030	0.975
Moderate/Well	70	0.273 ± 0.056	
Tumor budding			
Bd1–Bd2	12	0.262 ± 0.043	0.861
Bd3	16	0.259 ± 0.042	
HER2 expression			
Negative	26	0.256 ± 0.040	0.368
Positive	26	0.267 ± 0.044	
KRAS genotyping			
Wild type	10	0.277 ± 0.042	0.360
Mutation type	7	0.299 ± 0.053	
BRAF genotyping			
Wild type	17	0.279 ± 0.049	0.600
Mutation type	3	0.295 ± 0.031	
CEA (ng/ml)			
<5	44	0.265 ± 0.040	0.202
≥5	54	0.278 ± 0.057	
CA125 (ng/ml)			
<35	68	0.269 ± 0.043	0.298
≥35	30	0.280 ± 0.063	
CA19-9 (ng/ml)			
<35	66	0.271 ± 0.054	0.742
≥35	32	0.275 ± 0.041	

enhancer solution were sequentially added to assay wells with diluted concentration, as specified in the manufacturer's instructions. Developer solution and stop solution were added to the color reaction, after which the absorbance of each well at a wavelength of 450 nm was measured. The m^6A levels were calculated based on the standard curve.

Bioinformatics Analysis

The RNA-seq data and clinical data of the peripheral blood of CRC and NCs were obtained from GEO (Gene Expression Omnibus) databases (GSE164191). Differential expression analysis was conducted by "limma" package of R studio (3.6.1) software. Gene set variation analysis (GSVA) was performed to estimate m6A modified pathways based on GO molecular function N6 methyladenosine containing RNA binding gene set and **Figure 4B** listed genes. Immune infiltrates of peripheral blood were estimated *via* MCP-counter method. Gene Set Enrichment Analysis (GSEA) was manipulated to predict the GO biological process gene sets of the Molecular Signature Database v7.4 (http://www.broadinstitute.org/gsea/msigdb) based on IGF2BP1/IGF2BP2/IGF2BP3 high and low expressed phenotype. A leading edge analysis was performed by GSEA 4.1.0 to elucidate key genes related to selected genes sets. EnrichmentMap plugin in Cytoscape 3.8.2 software was utilized with the following parameters: *p*-value cutoff = 0.05; similarity coefficient cutoff = 0.5. The protein–protein interaction (PPI) networks were constructed using The Search Tool for the Retrieval of Interacting Genes (STRING), which is a publicly available software for assessing the interaction between proteins and proteins (https://string-db.org/).

Statistical Analysis

The variability of the data, which was presented as the SD (mean ± SD), was assessed with unpaired Student's *t* test between two groups for normally distributed data. Otherwise, the data were analyzed by nonparametric Mann–Whitney test. Paired *t*-tests were used to analyze the effects of treatment on m^6A levels. For multiple groups, significant differences were determined using one-way ANOVA. Pearson correlation analysis was conducted to determine the correlation between GSVA scores and immune infiltrates. Forest plot of multivariate logistic regression analysis was performed to access risk indicators associated with CRC diagnosis. Statistical significance was defined at $p < 0.05$.

RESULTS

The m^6A RNA Levels of Peripheral Blood Immune Cells in CRC Patients and NCs

First, we analyzed the m6A levels of total RNA in NCs ($n = 64$) and CRC patients ($n = 105$) so as to evaluate the status of m6A modification in peripheral blood immune cells. The m^6A levels in peripheral blood immune cells were remarkably increased in patients with CRC (0.271 ± 0.051) than in NCs (0.185 ± 0.038; **Figure 1A**). Furthermore, statistical analyses of the relationship between the m^6A levels and clinicopathological features of CRC are performed in **Table 1**. Our data indicated that the m^6A levels correlated with M classification ($p < 0.001$), but not with clinical

stage, T classification, N classification, differentiation, tumor budding, as well as other common CRC tumor markers, including CEA, CA125, and CA19-9 (**Table 1**). As shown in **Figure 1B**, the levels of m^6A were dramatically elevated in the stage IV group (n = 26, 0.302 ± 0.063) than in stage I (n = 6, 0.243 ± 0.031), II (n = 20, 0.263 ± 0.031), or III groups (n = 31, 0.260 ± 0.048). In addition, CRC patients with distant tumor metastasis (n = 26, 0.302 ± 0.063) had apparently increased m^6A levels compared to those without distant metastasis (n = 57, 0.259 ± 0.041; **Figure 1C**). These results suggested that peripheral blood m^6A RNA levels could partially distinguish the various pathological stages in patients with CRC.

To elucidate whether m^6A could be used to assess treatment status in CRC patients, we compared the m^6A levels of peripheral blood between the pre-treatment group and post-treatment group. The obtained results demonstrated that m^6A levels were markedly reduced in the post-treatment group (**Figure 1D**). We also observed significant changes in m^6A levels before and after surgery (14 days) in 33 CRC patients, indicating that m^6A RNA levels of peripheral blood immune cells could be used as a promising indicator for post-treatment follow-up (**Figure 1E**).

Clinical Utility for CEA, CA125, CA19-9, and the m^6A RNA Levels of Peripheral Blood Immune Cells to Diagnose CRC Patients

We plotted ROC curves to further assess the diagnostic capability of m^6A RNA levels of peripheral blood immune cells for CRC. The area under the curve (AUC) of m^6A was up to 0.946 (95% CI, 0.914–0.977), indicating that m^6A levels could differentiate CRC patients from NCs (**Figure 2A**). Also, the optimum m^6A cutoff value was 0.235 (specificity, 0.953; sensitivity, 0.800; **Figure 2B**). Impressively, the diagnostic ability of m^6A was superior to the usual CRC blood biomarkers, such as CEA, CA125, and CA19-9, with AUCs of 0.817, 0.732, and 0.771, respectively (**Figure 2C** and **Table 2**). Moreover, the ROC curve for the multivariate combination of m^6A, CEA, CA125, and CA19-9 increased the AUC to 0.977 (95% CI, 0.961–0.994; **Figure 2C**). Furthermore, the forest plot of multivariate logistic regression analysis demonstrated that the m^6A levels were an independent factor associated with CRC diagnosis (**Figure 2D**). Taken together, these results clarified that the m^6A RNA levels of peripheral blood immune cells presented satisfactory diagnostic utility for CRC patients.

Expressions and Diagnostic Values of IGF2BP1, IGF2BP2, and IGF2BP3 in Peripheral Blood Immune Cells of CRC Patients

To screen for core molecules that regulate m^6A modifications in peripheral blood immune cells RNA, we analyzed the GSE164191 dataset, containing RNA-seq data on peripheral blood leukocytes of CRC patients and normal subjects. Surprisingly, members of the IGF2BP family (IGF2BP1, IGF2BP2, and IGF2BP3) were the most dramatically altered molecules in the methyltransferase complex consisting of "writers", "erasers", and "readers" (**Figures 3A, B**). Meanwhile, the strongest increase in IGF2BP2 was observed in CRC patients, suggesting a potentially vital role in m^6A modification of peripheral blood immune cells (**Figures 3A, B**). qRT-PCR analysis also proved significantly higher expression of IGF2BP1, IGF2BP2, and IGF2BP3 in CRC patients compared to normal subjects (**Figures 3C–E**). We further discovered a relationship between the levels of m^6A and the expressions of IGF2BP2, but no correlation with the expressions of IGF2BP1 and IGF2BP3 (**Figures 3F, G** and **Supplementary Figure 1**). The AUCs of IGF2BP1, IGF2BP2, and IGF2BP3 were 0.710, 0.795, and 0.710, respectively (**Figure 3H**). Their AUCs were similar to common CRC blood biomarkers CEA, CA125, and CA19-9 but still smaller than the AUC of m^6A. Collectively, IGF2BP2 in peripheral blood immune cells was a potentially valuable diagnostic biomarker for CRC associated with m^6A modification.

Correlation Between Immune Infiltrating Cell Types and m^6A Modification in Peripheral Blood Immune Cells of CRC Patients

To further elucidate the specific immune cells associated with elevated m^6A levels of peripheral blood in CRC patients, we analyzed the GSE164191 database by GSVA. The obtained results suggested that the methyltransferase complexes, consisting of "writer", "eraser", and "reader", all exhibited the strongest positive correlation with monocytes infiltrating (**Figure 4A**). Detection of monocytes isolated from peripheral blood of CRC patients and normal subjects also revealed that monocytes from CRC patients possessed higher levels of m^6A (**Supplementary Figure 2**). Meanwhile, infiltration of monocytes was also markedly correlated with IGF2BP2 expression, consistent with the results in **Figure 3** regarding the importance of IGF2BP2 in m^6A modifications (**Figure 4B**). In conclusion, monocytes resulted as the specific immune cells most strongly associated with upregulated m^6A levels of peripheral blood immune cells in CRC patients.

IGF2BP2 Involved in the Immune Response of Monocytes in Peripheral Blood of CRC Patients

The function of IGF2BP2 in the monocytes of the peripheral blood of CRC patients was investigated using the EnrichmentMap plugin in Cytoscape 3.8.2 software. The corresponding association network showed that the IGF2BP2 high-expression phenotype presented a robust positive association between several monocyte immune response pathways (**Figure 5A**). GSEA was applied to predict the biological processes of monocytes in peripheral blood based on IGF2BP2 expression. Likewise, high IGF2BP2 expression was mainly enriched in the immune response pathways, such as "Negative regulation of immune effector process", "Regulation of monocyte chemotaxis", and "Cytokine production" (**Figures 5B, C**). Additionally, the results of leading edge analysis identified the intersection of important genes associated with the immune response pathways (**Figure 5D**). Meanwhile, the PPI networks structured by the STRING database suggested that IGF2BP2 may interact with the above vital genes (**Figure 5E**). IGF2BP1 and IGF2BP3 also performed approximately the same immune

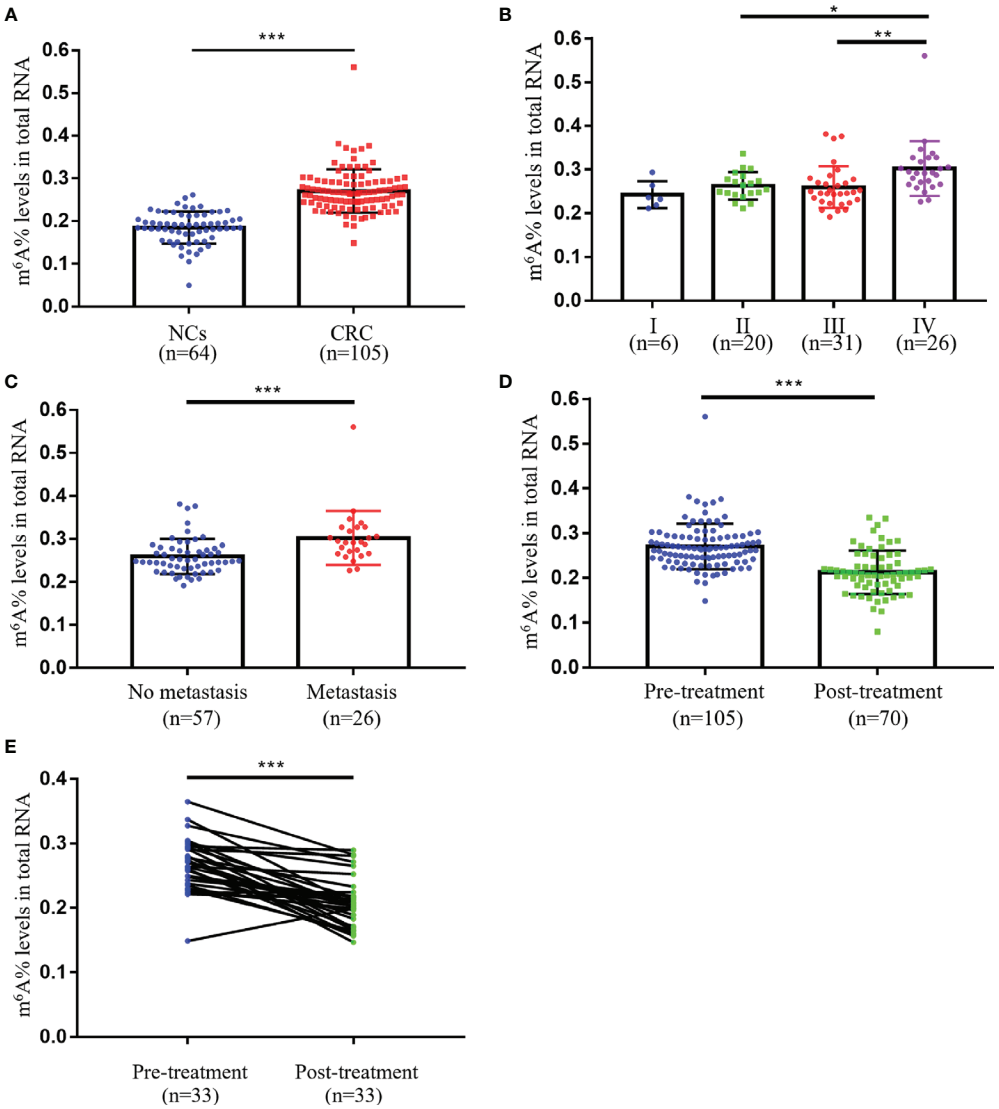

FIGURE 1 | The m^{6}A RNA levels of peripheral blood immune cells in CRC patients and NCs. **(A)** The m^{6}A levels of peripheral blood RNA in NCs (n = 64) and CRC patients (n = 105). **(B)** The m^{6}A levels of peripheral blood RNA at different clinical stages of CRC patients (stage I, n = 6; stage II, n = 20; stage III, n = 31; stage IV, n = 26). **(C)** Comparison of m^{6}A levels of peripheral blood RNA between CRC patients with (n = 26) and without (n = 57) metastasis. **(D)** Comparison of m^{6}A levels of peripheral blood RNA between CRC patients with (n = 70) and without (n = 105) treatment. **(E)** The m^{6}A levels of peripheral blood RNA in CRC patients (n = 33) before and after 14 days of treatment. Bars represent the mean ± SD of the results from replicate measurements; *p < 0.05, **p < 0.01 and ***p < 0.001.

functions as IGF2BP2 in monocytes (**Supplementary Figure 3**). Taken together, IGF2BP2 exerted an essential role in the immune response of peripheral blood monocytes of CRC patients.

DISCUSSION

Most patients are already at an advanced stage by the time they are diagnosed with CRC, which substantially contributes to the poor prognosis (4). Hence, improving the prognosis of CRC patients depends on an early and accurate diagnosis. However, the currently used clinical tumor biomarkers for CRC such as CEA, CA125, and CA19-9 are not specific or sensitive enough to detect CRC patients (7, 9). Therefore, optimizing the diagnosis of CRC with other validated biomarkers is of urgent importance. The present study identified the m^{6}A status of peripheral blood immune cells as a novel marker for CRC screening. In addition, it might also serve as a new target for CRC treatment.

Despite a growing body of reports that have linked m^{6}A dysregulation to various cancers, the role of m^{6}A modifications in CRC tumor tissues remained controversial (10, 20). Stimulating m^{6}A modification promotes β-catenin translation to drive the epithelial–mesenchymal transition of CRC cells, while some studies found that m6A regulation suppresses

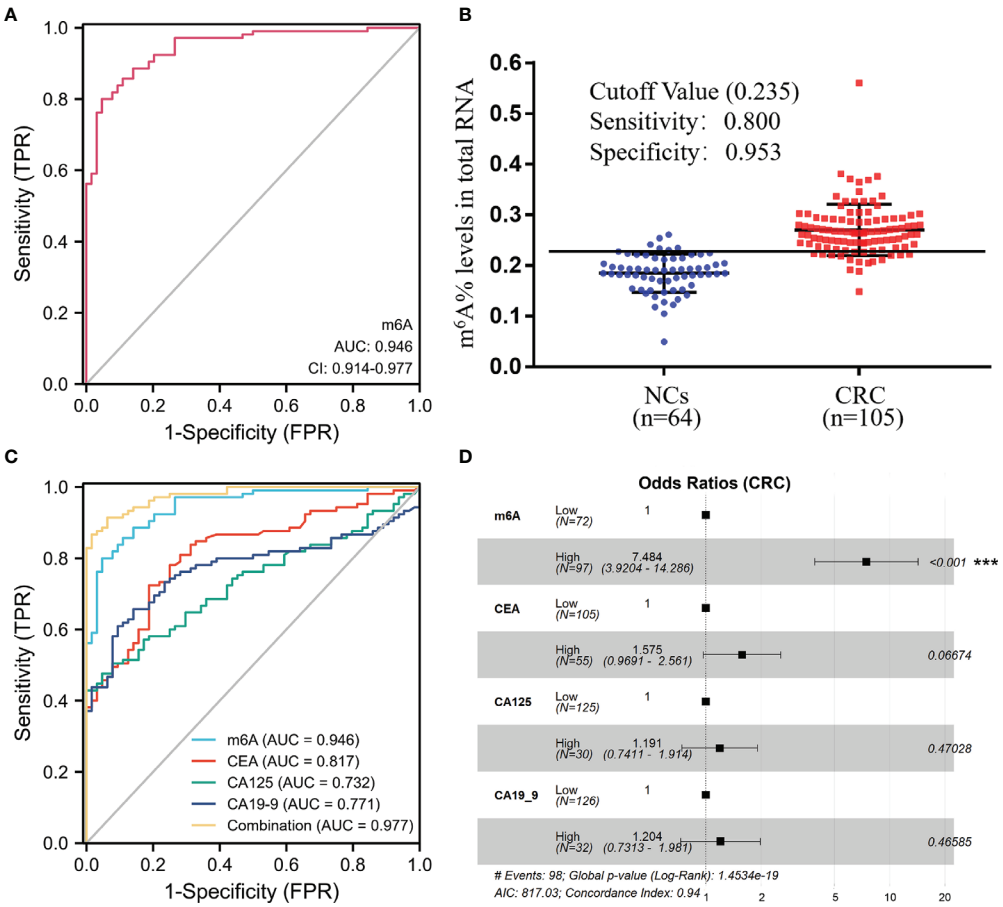

FIGURE 2 | Clinical utility for CEA, CA125, CA19-9, and the m^{6}A RNA levels of peripheral blood immune cells to diagnose CRC patients. **(A, B)** ROC curve **(A)** and cutoff value **(B)** of the m^{6}A levels of peripheral blood RNA in NCs (n = 64) and CRC patients (n = 105). **(C)** ROC curve of the m^{6}A levels of peripheral blood RNA compared and combined diagnosis with CEA, CA125, and CA19-9. **(D)** Forest plot of multivariate logistic regression analysis demonstrated that the m6A levels were an independent factor associated with CRC diagnosis; ***$p < 0.001$.

proliferation and metastasis (15, 21, 22). Our research revealed for the first time that the m^{6}A RNA levels of peripheral blood immune cells were dramatically higher in patients with CRC than in healthy subjects (**Figure 1A**). Our results demonstrated that m^{6}A RNA was more strongly modified in peripheral blood immune cells of CRC, yet m^{6}A modification in CRC tumor tissue needs to be further explored. Additionally, the m^{6}A status of peripheral blood immune cells was substantially elevated in CRC patients with distant metastases compared to those without metastases, implying that it could also discriminate if the tumor had metastasized (**Figures 1B, C**). Although the m^{6}A levels were reduced in treated CRC patients, more clinical samples were requested to determine whether they could be used as an indicator of oncologic efficacy, such as relapse and drug resistance (**Figures 1D, E**). It has been discussed that the m^{6}A levels might be applied as a biomarker for gastric cancer, but the regulation of m^{6}A modification in different tumors varied significantly (18, 23). Therefore, it is worthwhile to investigate further whether the m^{6}A levels had diagnostic value in other tumors.

TABLE 2 | Sensitivity and specificity of the diagnostic value of various markers alone and in combination.

Marker	Sensitivity	Specificity	AUC	95% CI
m^{6}A	0.800	0.953	0.946	0.914–0.977
CEA	0.724	0.812	0.817	0.754–0.881
CA125	0.476	0.953	0.732	0.659–0.806
CA19-9	0.657	0.859	0.771	0.700–0.842
m^{6}A+CEA+CA125+CA19-9	0.914	0.938	0.977	0.961–0.994

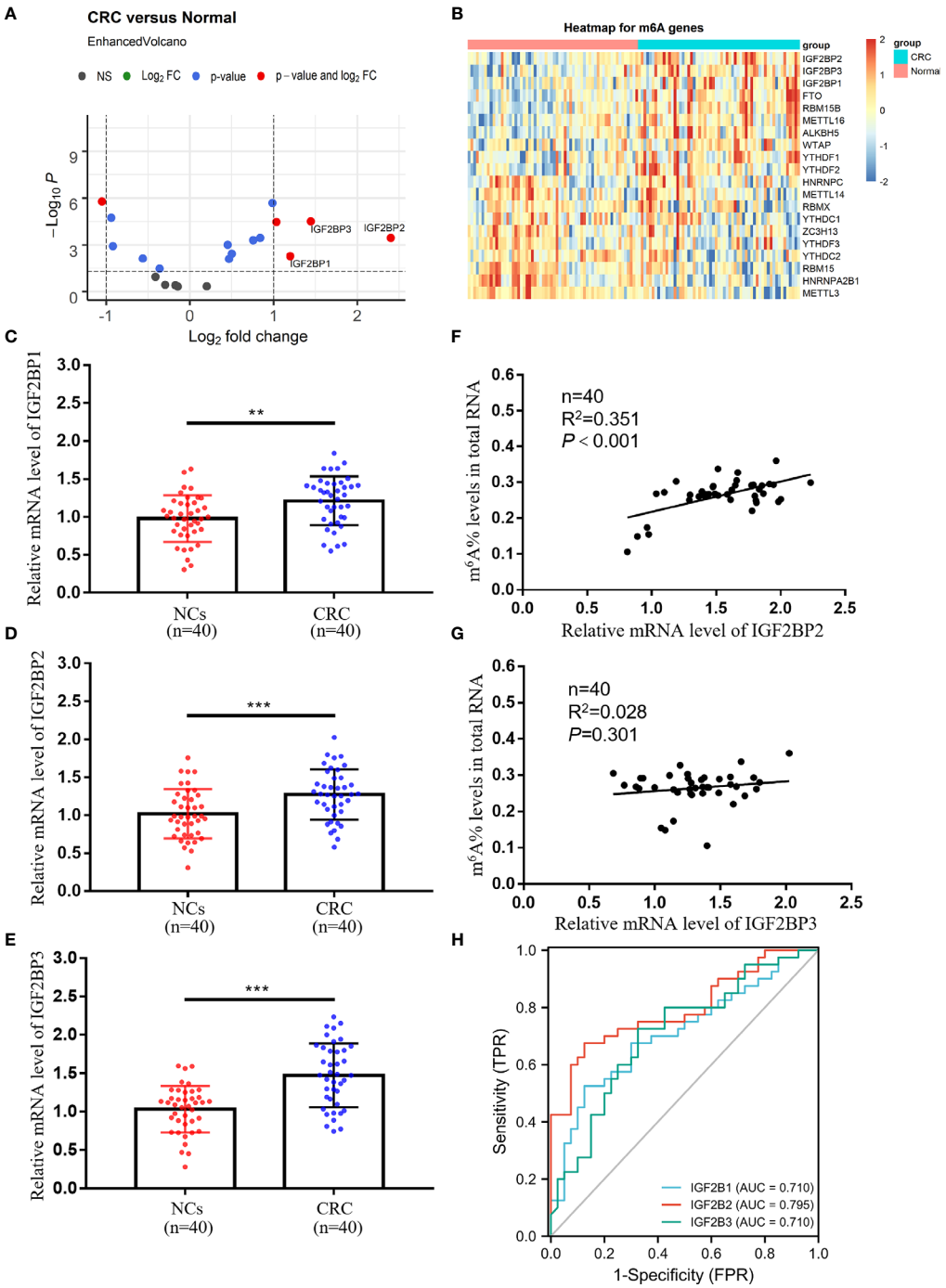

FIGURE 3 | Expressions and diagnostic values of IGF2BP1, IGF2BP2, and IGF2BP3 in peripheral blood immune cells of CRC patients. **(A)** Screening key molecules related to m^{6}A modification in peripheral blood of CRC patients (n = 59) compared to normal subjects (n = 62) by limma differential analysis. **(B)** Heatmap of key molecules related to m6A modification in peripheral blood of CRC patients. **(C–E)** qRT-PCR analysis of IGF2BP1 **(C)**, IGF2BP2 **(D)**, and IGF2BP3 **(E)** mRNA expression levels in peripheral blood of NCs and CRC patients. **(F, G)** Correlation between the levels of IGF2BP2/IGF2BP3 and m^{6}A in peripheral blood of CRC patients. **(H)** ROC curves of the IGF2BP1, IGF2BP2, and IGF2BP3 mRNA expression levels in peripheral blood of CRC patients. Bars represent the mean ± SD of the results from replicate measurements; $^{**}p < 0.01$, $^{***}p < 0.001$.

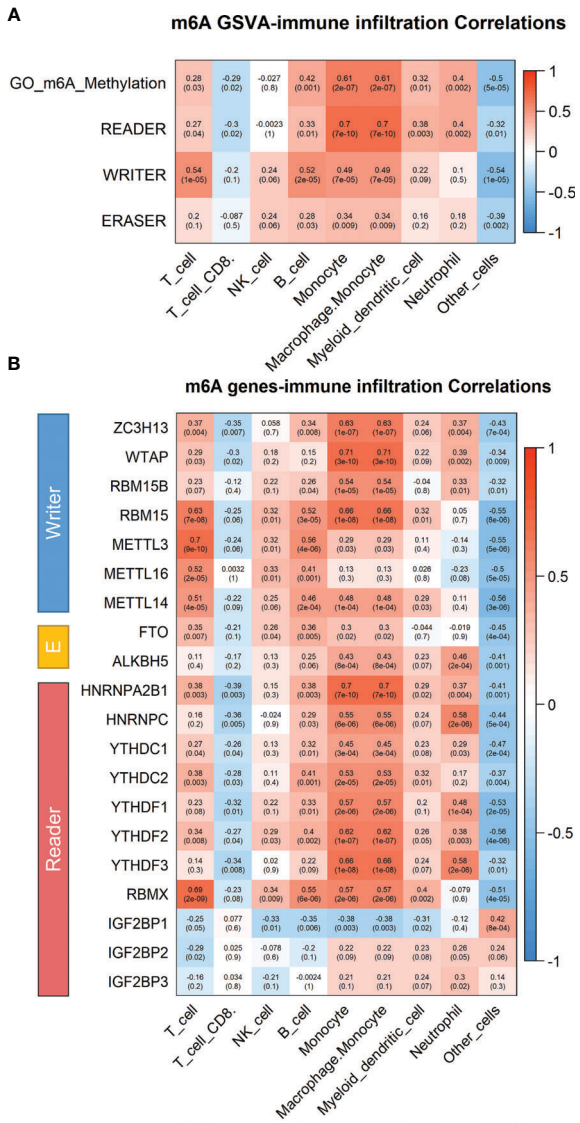

FIGURE 4 | Correlation between immune infiltrating cell types and m^{6}A modification in peripheral blood immune cells of CRC patients. **(A)** Heatmap of correlation between immune infiltrating cell types and m^{6}A modification pathways in peripheral blood of CRC patients by Gene set variation analysis by GSVA (n = 59). **(B)** Heatmap of correlation between immune infiltrating cell types and m^{6}A modification related gene in peripheral blood of CRC patients by GSVA.

CEA, CA125, and CA19-9 are widely used in physical screening for CRC (9). Nevertheless, due to their poor specificity and sensitivity, these three biomarkers alone or in combination are not sufficient to diagnose CRC (7). As shown in **Figure 2**, the AUC for m^{6}A to differentiate CRC patients from healthy subjects was 0.946 (95% CI, 0.914–0.977), which was significantly higher than the AUC for CEA (0.817; 95% CI, 0.754–0.881), CA125 (0.732; 95% CI, 0.659–0.806), and CA19-9 (0.771; 95% CI, 0.700–0.842). The combination of CEA, CA125, and CA19-9 with m^{6}A further increased the AUC to 0.977 (95% CI, 0.961–0.994). Besides, forest plots from multiple logistic regression analysis showed that the m^{6}A levels were an independent risk factor associated with the diagnosis of CRC compared to these common tumor biomarkers (**Figure 2D**). Our study presented a considerable challenge to the value of these tumor biomarkers.

"Writers", "erasers", and "readers" together formed the methyltransferase complex responsible for m^{6}A modification. Wilms tumor 1-associated protein (WTAP), Methyltransferase-like 3 (METTL3), and METTL14 were classified as "writers" catalyzing the formation of m^{6}A (24–26). AlkB homolog 5 (ALKBH5) and Fat mass and obesity-associated protein (FTO) represented "erasers", meaning they could induce selective removal of methylation code from the target mRNA (27, 28). "Readers" were able to decode m^{6}A modification, comprising YT521-B homology domain-containing protein (YTHDF) as well as IGF2BP families (16, 29). m^{6}A modifications altered the expression of target genes and changed the consequent biological features (30). To further understand the role of the elevated m^{6}A levels in CRC tumor progression, we screened for the most variable "writers", "erasers", and "readers" in CRC peripheral blood immune cells by limma differential analysis. Members of the IGF2BP family (IGF2BP1, IGF2BP2, and IGF2BP3), which belonged to "readers", were the most markedly changed molecules in the methyltransferase complex (**Figure 3**). Simultaneously, IGF2BP2 revealed the greatest increase, thus suggesting a potentially crucial role in peripheral blood immune cell m^{6}A modification (**Figure 3**). Unlike other readers, IGF2BPs acted as a unique family of m^{6}A readers that target a multitude of mRNA transcripts and enhance the conservation and stability of their candidate mRNAs in an m^{6}A-dependent way (14, 15, 31). Our study further demonstrated that elevated IGF2BP2 might interact with several essential genes to negatively regulate immunity, such as cytokine production and chemotaxis (**Figure 5** and **Supplementary Figure 3**). Although we found that increased IGF2BPs expression combined with elevated m^{6}A levels affected cancer immunity in CRC, we have not yet clarified the mechanism of increased IGF2BPs, which is also the biggest limitation of the current study. Taken together, m^{6}A modification and IGF2BPs expression were likely to be novel targets for CRC treatment, but further *in vivo* experimental studies are required.

Previous studies reported that elevated m^{6}A levels of peripheral blood in patients with gastric cancer might be due to downregulation of FTO and ALKBH5, which belonged to "erasers" (18). Our qRT-PCR results also revealed a slight downregulation of FTO and ALKBH5 in peripheral blood cells of CRC patients, partially explaining the increased m^{6}A levels (**Supplementary Figure 4**). Other unknown methylases and demethylases may also be involved in the changes of m^{6}A levels that deserved further exploration (32). Additionally, monocytes were identified as the immune cells most strongly associated with the increased regulation of upregulated m^{6}A levels in peripheral blood of CRC patients (**Figure 4**). It has been noted that the presence of a large number of m^{6}A-modified infiltrating immune

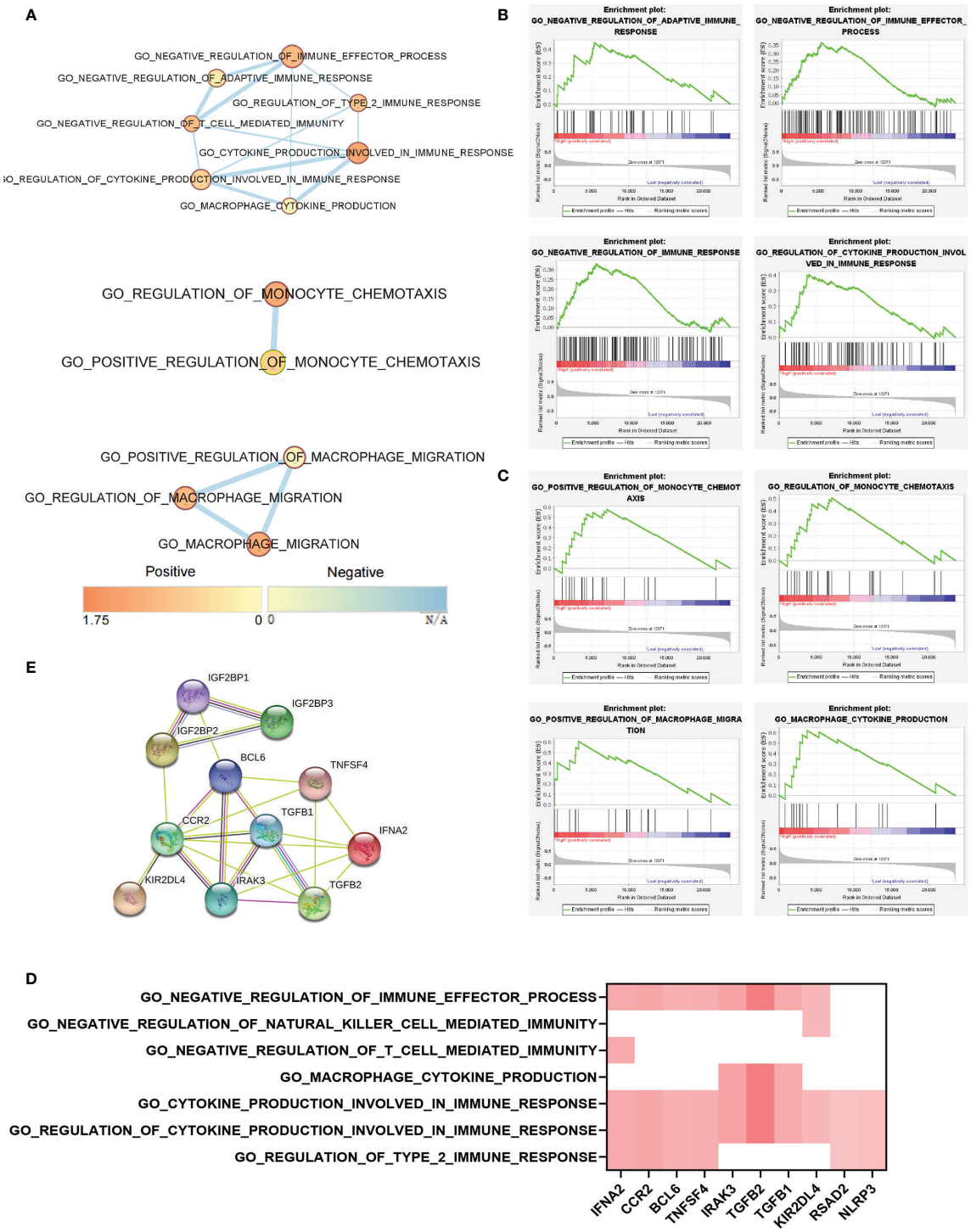

FIGURE 5 | IGF2BP2 involved in the immune response of monocytes in peripheral blood of CRC patients. **(A)** EnrichmentMap pathways network revealed overlaps among IGF2BP2 high-expressed phenotype enriched pathways relating to immunity in peripheral blood of CRC patients. Nodes are colored by Enrichment Score, and edges are sized on the basis of the number of genes shared by the connected pathways. **(B)** GSEA indicated that IGF2BP2 was negatively correlated with the immune response of monocytes. **(C)** GSEA indicated that IGF2BP2 was positively correlated with monocyte chemotaxis and cytokine production. **(D)** Leading edge analysis of their intersection genes indicates the vital genes shared by the IGF2BP2 high-expressed phenotype associated with the immune response of monocytes. **(E)** STRING database analysis revealed that IGF2BP2 interacted with the above vital genes related to the immune response of monocytes.

cells in the tumor tissue microenvironment promotes tumor progression (33, 34). Furthermore, imbalanced m^6A regulation strongly conferred immune disruption and tumor evasion, primarily by affecting immune cell migration, rather than apoptosis or survival (35). These observations were generally consistent with our findings in peripheral blood immune cells. Moreover, the number of monocytes in the $CD14^+CD16^+HLA\text{-}DR^{hi}$ subpopulation of patient's peripheral blood was found to be the most accurate predictor of progression-free survival and overall survival after receiving PD-1 inhibitor therapy (36). Whether the subset of monocytes with elevated m^6A levels had a similar role in tumor immunotherapy to the $CD14^+CD16^+HLA\text{-}DR^{hi}$ subset deserves further investigation.

In conclusion, the highlights of our research were the first identification of m^6A RNA levels in peripheral blood immune cells as a novel biomarker for the diagnosis of CRC and the provision of a new strategy for the treatment of CRC by targeting m^6A levels or IGF2BPs expression in peripheral blood immune cells.

DATA AVAILABILITY STATEMENT

The original contributions presented in the study are included in the article/**Supplementary Material**. Further inquiries can be directed to the corresponding authors.

ETHICS STATEMENT

The studies involving human participants were reviewed and approved by the Ethics Committee of the Zhongshan People's Hospital. The patients/participants provided their written informed consent to participate in this study.

AUTHOR CONTRIBUTIONS

HY, HH, and CL conceived and designed this study. JX, ZH, and PJ performed the experiments and analyzed the data. RW and HJ contributed to the data analysis and discussion. All authors contributed to the article and approved the submitted version.

FUNDING

This study was supported by the fund from the National Nature Science Foundation of China (81900775; 81902693); Educational Commission of Guangdong Province (2017KTSCX155); Guangdong Basic and Applied Basic Research Foundation (2019A1515011318); Natural Science Foundation of Guangdong Province (2018A030310298); the Science Foundation of Guangzhou First People's Hospital (Q2019004; KYQD0046); China Postdoctoral Science Foundation (2019M662991); Key Medical and Health Projects of Zhongshan City (2020K0012); Guangzhou Science and Technology Planning Project (202102020142).

SUPPLEMENTARY MATERIAL

The Supplementary Material for this article can be found online at: https://www.frontiersin.org/articles/10.3389/fimmu.2021.760747/full#supplementary-material

Supplementary Figure 1 | Correlation between the levels of IGF2BP1 and m^6A in peripheral blood of CRC patients. Absence of correlation between the m^6A levels and IGF2BP1 expression.

Supplementary Figure 2 | The m^6A levels of monocytes isolated from peripheral blood of CRC patients and normal subjects. The m^6A levels of monocytes isolated from CRC patients was higher than those in monocytes from normal subjects.

Supplementary Figure 3 | IGF2BP1 and IGF2BP3 expression are negatively associated with several immune response pathways. **(A, B)** EnrichmentMap pathways network exhibited connectivity among IGF2BP1 **(A)** and IGF2BP3 **(B)** high-expressed phenotype enriched pathways relating to immunity response in peripheral blood of CRC patients. **(C, D)** GSEA indicated that IGF2BP1 **(C)** and IGF2BP3 **(D)** were negatively correlated with the immune response of monocytes.

Supplementary Figure 4 | Expressions of FTO and ALKBH5 in peripheral blood RNA of CRC patients. **(A, B)** Q-PCR analysis of FTO **(A)** and ALKBH5 **(B)** mRNA expression levels in peripheral blood of NCs and CRC patients.

REFERENCES

1. Jacobs D, Zhu R, Luo J, Grisotti G, Heller DR, Kurbatov V, et al. Defining Early-Onset Colon and Rectal Cancers. *Front Oncol* (2018) 8:504. doi: 10.3389/fonc.2018.00504
2. Tong GJ, Zhang GY, Liu J, Zheng ZZ, Chen Y, Niu PP, et al. Comparison of the Eighth Version of the American Joint Committee on Cancer Manual to the Seventh Version for Colorectal Cancer: A Retrospective Review of Our Data. *World J Clin Oncol* (2018) 9(7):148–61. doi: 10.5306/wjco.v9.i7.148
3. Cespedes Feliciano EM, Kroenke CH, Meyerhardt JA, Prado CM, Bradshaw PT, Dannenberg AJ, et al. Metabolic Dysfunction, Obesity, and Survival Among Patients With Early-Stage Colorectal Cancer. *J Clin Oncol* (2016) 34 (30):3664–71. doi: 10.1200/JCO.2016.67.4473
4. Baars JE, Kuipers EJ, van Haastert M, Nicolai JJ, Poen AC, van der Woude CJ. Age at Diagnosis of Inflammatory Bowel Disease Influences Early Development of Colorectal Cancer in Inflammatory Bowel Disease Patients: A Nationwide, Long-Term Survey. *J Gastroenterol* (2012) 47(12):1308–22. doi: 10.1007/s00535-012-0603-2
5. Tfaily MA, Naamani D, Kassir A, Sleiman S, Ouattara M, Moacdieh MP, et al. Awareness of Colorectal Cancer and Attitudes Towards Its Screening Guidelines in Lebanon. *Ann Glob Health* (2019) 85(1):75. doi: 10.5334/aogh.2437
6. Wagner IC, Guimaraes MJ, da Silva LK, de Melo FM, Muniz MT. Evaluation of Serum and Pleural Levels of the Tumor Markers CEA, CYFRA21-1 and CA 15-3 in Patients With Pleural Effusion. *J Bras Pneumol* (2007) 33(2):185–91. doi: 10.1590/s1806-37132007000200013
7. Li L, Zhang L, Tian Y, Zhang T, Duan G, Liu Y, et al. Serum Chemokine CXCL7 as a Diagnostic Biomarker for Colorectal Cancer. *Front Oncol* (2019) 9:921. doi: 10.3389/fonc.2019.00921
8. Bagaria B, Sood S, Sharma R, Lalwani S. Comparative Study of CEA and CA19-9 in Esophageal, Gastric and Colon Cancers Individually and in Combination (ROC Curve Analysis). *Cancer Biol Med* (2013) 10(3):148–57. doi: 10.7497/j.issn.2095-3941.2013.03.005
9. Thomas DS, Fourkala EO, Apostolidou S, Gunu R, Ryan A, Jacobs I, et al. Evaluation of Serum CEA, CYFRA21-1 and CA125 for the Early Detection of Colorectal Cancer Using Longitudinal Preclinical Samples. *Br J Cancer* (2015) 113(2):268–74. doi: 10.1038/bjc.2015.202

10. Chen XY, Zhang J, Zhu JS. The Role of M^6a RNA Methylation in Human Cancer. *Mol Cancer* (2019) 18(1):103. doi: 10.1186/s12943-019-1033-z
11. Zhao BS, He C. Fate by RNA Methylation: M6a Steers Stem Cell Pluripotency. *Genome Biol* (2015) 16:43. doi: 10.1186/s13059-015-0609-1
12. Ke S, Alemu EA, Mertens C, Gantman EC, Fak JJ, Mele A, et al. A Majority of M6a Residues are in the Last Exons, Allowing the Potential for 3' UTR Regulation. *Genes Dev* (2015) 29(19):2037–53. doi: 10.1101/gad.269415.115
13. Li T, Hu PS, Zuo Z, Lin JF, Li X, Wu QN, et al. METTL3 Facilitates Tumor Progression *via* an M(6)a-IGF2BP2-Dependent Mechanism in Colorectal Carcinoma. *Mol Cancer* (2019) 18(1):112. doi: 10.1186/s12943-019-1038-7
14. Hu X, Peng WX, Zhou H, Jiang J, Zhou X, Huang D, et al. IGF2BP2 Regulates DANCR by Serving as an N6-Methyladenosine Reader. *Cell Death Differ* (2020) 27(6):1782–94. doi: 10.1038/s41418-019-0461-z
15. Hu BB, Wang XY, Gu XY, Zou C, Gao ZJ, Zhang H, et al. N(6)-Methyladenosine (M(6)a) RNA Modification in Gastrointestinal Tract Cancers: Roles, Mechanisms, and Applications. *Mol Cancer* (2019) 18 (1):178. doi: 10.1186/s12943-019-1099-7
16. Wang Y, Lu JH, Wu QN, Jin Y, Wang DS, Chen YX, et al. Lncrna LINRIS Stabilizes IGF2BP2 and Promotes the Aerobic Glycolysis in Colorectal Cancer. *Mol Cancer* (2019) 18(1):174. doi: 10.1186/s12943-019-1105-0
17. Shen C, Xuan B, Yan T, Ma Y, Xu P, Tian X, et al. M(6)a-Dependent Glycolysis Enhances Colorectal Cancer Progression. *Mol Cancer* (2020) 19 (1):72. doi: 10.1186/s12943-020-01190-w
18. Ge L, Zhang N, Chen Z, Song J, Wu Y, Li Z, et al. Level of N6-Methyladenosine in Peripheral Blood RNA: A Novel Predictive Biomarker for Gastric Cancer. *Clin Chem* (2020) 66(2):342–51. doi: 10.1093/clinchem/hvz004
19. Shen F, Huang W, Huang JT, Xiong J, Yang Y, Wu K, et al. Decreased N(6)-Methyladenosine in Peripheral Blood RNA From Diabetic Patients is Associated With FTO Expression Rather Than ALKBH5. *J Clin Endocrinol Metab* (2015) 100(1):E148–54. doi: 10.1210/jc.2014-1893
20. Linder B, Grozhik AV, Olarerin-George AO, Meydan C, Mason CE, Jaffrey SR. Single-Nucleotide-Resolution Mapping of M6a and m6Am Throughout the Transcriptome. *Nat Methods* (2015) 12(8):767–72. doi: 10.1038/nmeth.3453
21. Song P, Feng L, Li J, Dai D, Zhu L, Wang C, et al. Beta-Catenin Represses Mir455-3p to Stimulate M6a Modification of HSF1 mRNA and Promote its Translation in Colorectal Cancer. *Mol Cancer* (2020) 19(1):129. doi: 10.1186/s12943-020-01244-z
22. Chen X, Xu M, Xu X, Zeng K, Liu X, Pan B, et al. METTL14-Mediated N6-Methyladenosine Modification of SOX4 mRNA Inhibits Tumor Metastasis in Colorectal Cancer. *Mol Cancer* (2020) 19(1):106. doi: 10.1186/s12943-020-01220-7
23. Li F, Kennedy S, Hajian T, Gibson E, Seitova A, Xu C, et al. A Radioactivity-Based Assay for Screening Human M6a-RNA Methyltransferase, METTL3-METTL14 Complex, and Demethylase ALKBH5. *J Biomol Screen* (2016) 21 (3):290–7. doi: 10.1177/1087057115623264
24. Schumann U, Shafik A, Preiss T. METTL3 Gains R/W Access to the Epitranscriptome. *Mol Cell* (2016) 62(3):323–4. doi: 10.1016/j.molcel.2016.04.024
25. Liu J, Yue Y, Han D, Wang X, Fu Y, Zhang L, et al. A METTL3-METTL14 Complex Mediates Mammalian Nuclear RNA N6-Adenosine Methylation. *Nat Chem Biol* (2014) 10(2):93–5. doi: 10.1038/nchembio.1432
26. Ping XL, Sun BF, Wang L, Xiao W, Yang X, Wang WJ, et al. Mammalian WTAP is a Regulatory Subunit of the RNA N6-Methyladenosine Methyltransferase. *Cell Res* (2014) 24(2):177–89. doi: 10.1038/cr.2014.3
27. Jia G, Fu Y, Zhao X, Dai Q, Zheng G, Yang Y, et al. N6-Methyladenosine in Nuclear RNA Is a Major Substrate of the Obesity-Associated FTO. *Nat Chem Biol* (2011) 7(12):885–7. doi: 10.1038/nchembio.687
28. Zheng G, Dahl JA, Niu Y, Fedorcsak P, Huang CM, Li CJ, et al. ALKBH5 is a Mammalian RNA Demethylase That Impacts RNA Metabolism and Mouse Fertility. *Mol Cell* (2013) 49(1):18–29. doi: 10.1016/j.molcel.2012.10.015
29. Haussmann IU, Bodi Z, Sanchez-Moran E, Mongan NP, Archer N, Fray RG, et al. M(6)a Potentiates Sxl Alternative Pre-mRNA Splicing for Robust Drosophila Sex Determination. *Nature* (2016) 540(7632):301–4. doi: 10.1038/nature20577
30. Lan Q, Liu PY, Haase J, Bell JL, Huttelmaier S, Liu T. The Critical Role of RNA M(6)a Methylation in Cancer. *Cancer Res* (2019) 79(7):1285–92. doi: 10.1158/0008-5472.CAN-18-2965
31. Muller S, Glass M, Singh AK, Haase J, Bley N, Fuchs T, et al. IGF2BP1 Promotes SRF-Dependent Transcription in Cancer in a M6a- and Mirna-Dependent Manner. *Nucleic Acids Res* (2019) 47(1):375–90. doi: 10.1093/nar/gky1012
32. Ben-Haim MS, Moshitch-Moshkovitz S, Rechavi G. FTO: Linking M6a Demethylation to Adipogenesis. *Cell Res* (2015) 25(1):3–4. doi: 10.1038/cr.2014.162
33. Zhang B, Wu Q, Li B, Wang D, Wang L, Zhou YL. M(6)a Regulator-Mediated Methylation Modification Patterns and Tumor Microenvironment Infiltration Characterization in Gastric Cancer. *Mol Cancer* (2020) 19(1):53. doi: 10.1186/s12943-020-01170-0
34. Zhang X, Zhang S, Yan X, Shan Y, Liu L, Zhou J, et al. M6a Regulator-Mediated RNA Methylation Modification Patterns are Involved in Immune Microenvironment Regulation of Periodontitis. *J Cell Mol Med* (2021) 25 (7):3634–45. doi: 10.1111/jcmm.16469
35. Li M, Zha X, Wang S. The Role of N6-Methyladenosine mRNA in the Tumor Microenvironment. *Biochim Biophys Acta Rev Cancer* (2021) 1875(2):188522. doi: 10.1016/j.bbcan.2021.188522
36. Krieg C, Nowicka M, Guglietta S, Schindler S, Hartmann FJ, Weber LM, et al. High-Dimensional Single-Cell Analysis Predicts Response to Anti-PD-1 Immunotherapy. *Nat Med* (2018) 24(2):144–53. doi: 10.1038/nm.4466

Conflict of Interest: The authors declare that the research was conducted in the absence of any commercial or financial relationships that could be construed as a potential conflict of interest.

frontiers in Immunology

REVIEW
published: 29 October 2021
doi: 10.3389/fimmu.2021.768957

Mechanisms of Immune Checkpoint Inhibitor-Mediated Colitis

Harm Westdorp[1,2], Mark W. D. Sweep[1,2†], Mark A. J. Gorris[1,3†], Frank Hoentjen[4,5], Marye J. Boers-Sonderen[2], Rachel S. van der Post[6], Michel M. van den Heuvel[7], Berber Piet[1,7], Annemarie Boleij[6], Haiko J. Bloemendal[2] and I. Jolanda M. de Vries[1]*

[1] Department of Tumor Immunology, Radboud Institute for Molecular Life Sciences, Radboud University Medical Centre, Nijmegen, Netherlands, [2] Department of Medical Oncology, Radboud University Medical Centre, Nijmegen, Netherlands, [3] Oncode Institute, Nijmegen, Netherlands, [4] Department of Gastroenterology, Radboud University Medical Centre, Nijmegen, Netherlands, [5] Division of Gastroenterology, University of Alberta, Edmonton, AB, Canada, [6] Department of Pathology, Radboud Institute for Molecular Life Sciences, Radboud University Medical Centre, Nijmegen, Netherlands, [7] Department of Pulmonary Diseases, Radboud University Medical Centre, Nijmegen, Netherlands

OPEN ACCESS

Edited by:
Ti Wen,
The First Affiliated Hospital of China Medical University, China

Reviewed by:
Evelien Smits,
University of Antwerp, Belgium
Shomyseh Sanjabi,
Genentech, Inc., United States

***Correspondence:**
Harm Westdorp
Harm.Westdorp@radboudumc.nl

†These authors have contributed equally to this work

Specialty section:
This article was submitted to Cancer Immunity and Immunotherapy, a section of the journal Frontiers in Immunology

Received: *01 September 2021*
Accepted: *11 October 2021*
Published: *29 October 2021*

Citation:
Westdorp H, Sweep MWD, Gorris MAJ, Hoentjen F, Boers-Sonderen MJ, Post RSvd, Heuvel MMvd, Piet B, Boleij A, Bloemendal HJ and de Vries IJM (2021) Mechanisms of Immune Checkpoint Inhibitor-Mediated Colitis. Front. Immunol. 12:768957. doi: 10.3389/fimmu.2021.768957

Immune checkpoint inhibitors (ICIs) have provided tremendous clinical benefit in several cancer types. However, systemic activation of the immune system also leads to several immune-related adverse events. Of these, ICI-mediated colitis (IMC) occurs frequently and is the one with the highest absolute fatality. To improve current treatment strategies, it is important to understand the cellular mechanisms that induce this form of colitis. In this review, we discuss important pathways that are altered in IMC in mouse models and in human colon biopsy samples. This reveals a complex interplay between several types of immune cells and the gut microbiome. In addition to a mechanistic understanding, patients at risk should be identifiable before ICI therapy. Here we propose to focus on T-cell subsets that interact with bacteria after inducing epithelial damage. Especially, intestinal resident immune cells are of interest. This may lead to a better understanding of IMC and provides opportunities for prevention and management.

Keywords: immune checkpoint inhibitor (ICI), immune-related adverse events, colitis, mechanisms, treatment

INTRODUCTION

Immune checkpoint inhibitors (ICIs), such as anti-programmed cell death-1 (PD-1), anti-programmed cell death ligand-1 (PD-L1), and anti-cytotoxic T-lymphocyte antigen-4 (CTLA-4), have revolutionized the treatment of cancer in the past decades. ICI therapy resulted in overall survival benefit for patients with advanced stage cancer, shifting standard clinical practice (1). ICIs are now often administered instead of or along with conventional therapies, such as chemotherapy and radiation therapy, in several advanced cancer types (2).

ICIs release the brake of the immune system during priming of naive T-cells [anti-CTLA-4, but more recently also shown for anti-PD-(L)1 (3, 4)] and during reactivation of memory anti-cancer T-cell responses (anti-PD-(L)1), rather than inducing direct tumor cell death as conventional therapies. However, one may argue that ICIs work by normalization rather than enhancement of the immune system (5). This means that an immune defect, in this case inactivation of T-cells, is normalized. Naive T-cell activation needs three signals: I) T-cell receptor binding to an antigen presented in the context of MHC; II) a signal mostly generated by binding of costimulatory

molecules CD80 and/or CD86 on antigen presenting cells (APCs) to receptors of the B7 family (6), and III) cytokine-derived signals mediating T-cell differentiation and expansion (7).

ICI antibodies interfere during different time points of T-cell activation. CTLA-4 is a costimulatory molecule that negatively regulates activation of T-cells. It is a direct antagonist of CD28 (8). CTLA-4 is frequently expressed on regulatory T-cells (Tregs) (9). In mouse models the important role of CTLA-4 expression by Tregs is demonstrated: CTLA-4 deficiency leads to fatal auto-immunity (10). Blocking of the CTLA-4 receptor with ipilimumab, a clinically approved monoclonal IgG1 antibody (11), increases the number of $CD4^+$ and $CD8^+$ T-cells (12). It was debated for a long time whether anti-CTLA-4 therapy causes depletion of Tregs. In a prospective study in humans, the ratio of $CD8^+$ T-cell/Treg increased due to anti-CTLA-4 treatment. However, the density of Tregs in the tumor increased upon anti-CTLA-4 treatment in most cancer types studied (13). Increased levels of Tregs are also observed in patients with autosomal dominant immune dysregulation syndrome due to *CTLA4* mutations. The Tregs in these patients were not functional, most likely related to the inability of the CTLA-4 protein to bind and antagonize the T-cell costimulatory molecule CD80. In contrast to healthy controls, Tregs from these patients were not able to inhibit proliferation of $CD4^+$ T-cells (14). Although patients with germline *CTLA4* gene variants and response of cancer patients to ICI therapy are fundamentally very different, both result in an impairment of CTLA-4 binding, impacting the function of Tregs.

PD-1 and the known PD-1 ligands, PD-L1 and PD-L2, are immune checkpoint proteins involved in cell-cell interaction and downstream signal transduction. PD-1 expression has been well characterized on T-cells. Upon binding to PD-L1, T-cell proliferation is inhibited or T-cells are inactivated by inducing a state of anergy (15, 16). PD-L1 is expressed on almost all tumors, as well as on T-cells, B-cells, DCs, and macrophages. In some tumor types PD-L1 expression has proven utility as a predictive response biomarker, whereas certain PD-L1 positive patients do not respond to anti-PD-(L)1 therapies (17). Nevertheless, assessment of PD-L1 expression on protein level on tumor tissue has become clinical practice even though its predictive value is moderate at best. Methods to detect and quantify tumor PD-L1 expression vary greatly (18). The expression and function of PD-L2 is rather similar to PD-L1 (19). PD-L2 is mainly expressed on DCs and macrophages (20). Its expression is also observed in several solid tumors and in hematologic malignancies (21). PD-1 is blocked with FDA- and EMA-approved antibodies nivolumab, pembrolizumab, and cemiplimab, and PD-L1 with atezolizumab, avelumab, and durvalumab (22–27). There are no approved drugs that target PD-L2 directly. Blocking the PD-(L)1 axis leads to increased numbers of $CD8^+$ cells, predominantly near the tumor site, with high expression of the cytotoxic granzyme B pathway (28).

Taken together, described anti-CTLA-4 and anti-PD-(L)1 antibodies restore the ability of the immune system to attack the tumor. However, this systemic activation of immune cells and induction of potentially self-reactive T-cells also leads to off-target activity.

IMMUNE-RELATED ADVERSE EVENTS (irAEs)

Dual ICI therapy with anti-CTLA-4 and anti-PD-1 antibodies frequently leads to severe irAEs in more than half of the patients (29, 30). All-grade irAEs have been reported in up to 90% of patients receiving both ICIs (30, 31). IrAEs range from mild (50-90%) to severe (10-50%) according to Common Terminology Criteria for Adverse Events (CTCAE). Common immunotoxicity includes dermatitis, rash, endocrinopathy, diarrhea, colitis, hepatitis, and pneumonitis (32, 33). Of these, ICI-mediated colitis (IMC) most frequently requires discontinuation of ICI therapy and is also responsible for at least 3 out of 10 fatal irAEs (33, 34). This particular inflammation in the colon is often characterized by excessive, watery diarrhea, possibly with blood or mucus in the stool, or abdominal pain (35). As discussed, anti-CTLA-4 therapy leads to more naïve T-cell priming, hence expected to be more frequently accompanied with systemic adverse events, such as IMC. Indeed, a higher occurrence of high-grade ICI-mediated diarrhea (IMD) or IMC is observed after ipilimumab monotherapy (15%) compared to anti-PD-1 monotherapy (3%) in patients with metastatic melanoma and non-small cell lung cancer. In combination therapy with anti-CTLA-4 and anti-PD-1 severe IMD/IMC was observed in 17% of treated patients (30).

Ideally, one would like to be able to restore homeostasis in irAE tissues while maintaining an antitumor response, or to be able to predict which patients are at risk of severe irAE development. To do so, understanding the origin and mechanisms of action of irAEs is essential. In this review, we discuss the current knowledge on mechanisms, biomarkers, and risk factors of IMC. Based on our review of the existing literature, we make recommendations for future research aimed at enhancing fundamental knowledge of the mechanisms and risks of IMC development.

MECHANISMS OF IMC DEVELOPMENT

While the antitumor mechanisms of ICIs have been carefully studied, large studies trying to unravel the mechanisms involved in irAEs are still lacking. The clinical picture of IMC is often considered comparable to inflammatory bowel diseases (IBD), but there are also many differences. Normal colonic mucosa consists of a normocellular inflammatory infiltrate, which is a mixture of lymphocytes, plasma cells, eosinophilic granulocytes, and histiocytes. In IBD there is an increase in cells, predominantly more plasma cells and neutrophilic granulocytes. In patients with IMC, an increase in cell numbers, intraepithelial lymphocytes, and neutrophilic granulocytes is observed (36). For a better understanding of IMC, and to gain insight in possible differences

between ICI therapies in IMC, it is imperative to understand the mechanisms by which IMC is developed in these patients.

Immune Cell Profile

A CTLA-4 deficiency downregulates Treg functionality in mice, leading to resistance to the inhibitory effects of Tregs on $CD4^+$ and $CD8^+$ T-cell induction (10). Accordingly, an increased frequency of activated $CD4^+$ and $CD8^+$ T-cells with a concomitant decrease in naive T-cell populations was seen in blood of ipilimumab-treated patients (12, 13). Histopathologic features of IMC patients treated with ipilimumab showed mainly neutrophilic inflammation, but also increased $CD4^+$ cells in the lamina propria and increased $CD8^+$ cells within the crypt epithelium were observed (36). A recent study by Luoma et al. has shown that in particular the numbers of cytotoxic T-lymphocytes (CTLs) and proliferating T-cells ($Ki\text{-}67^+$) were increased in IMC biopsies following ipilimumab monotherapy or ICI combination therapy (37). In contrast, tissue-resident memory (Trm) T-cells, a T-cell subset that does not recirculate (38), were reduced in IMC patients as a fraction of total T cells. Interestingly, ICI treated patients who did not develop IMC did not show changes in colonic Trm cells. In IMC patients only, T-cell receptor clonotypes overlapped between $CD8^+$ Trm cells and CTLs, suggesting differentiation from the former to the latter (37). This might indicate that there is a shift from $CD8^+$ Trm cells towards CTLs in patients with IMC specifically. In non-small cell lung carcinoma, Trm cells have indeed shown to be capable of becoming cytotoxic (39). These potentially Trm-derived CTLs of IMC patients exhibited a genetic profile strongly related to an interferon gamma (IFNγ)-mediated T-helper 1 (Th1) response (37). If IFNγ is indeed abundantly secreted by CTLs in IMC, this could cause disruption of the epithelial barrier function or even apoptosis of human colonic epithelial cells, as shown in *in vitro* models (40, 41). This might explain colonic inflammation and damage that is seen in colonoscopies.

Under normal circumstances, Tregs are able to suppress intestinal inflammation (42), which is evidently compromised in IMC. Similarly to intratumoral Tregs (13), in colonic biopsies of patients with IMC, ipilimumab treatment tends to increase the number of Tregs, defined as $FOXP3^+$ cells (43, 44). In a study with IMC patients who received combination therapy, an altered genetic Treg expression profile was seen. These alterations were considered beneficial for suppressing an IFNγ-mediated Th1 response (37). Likewise, elevated mRNA expression of interleukin-10 (IL-10) has been reported in colonic mucosa of IMC patients after anti-CTLA-4 treatment (44). This cytokine is typically secreted by Tregs to dampen inflammation and is an important mediator to suppress colon inflammation (45). However, IL-10 is regulated by various factors on the posttranscriptional level, and its mRNA stability and degradation may vary immensely based on extrinsic signals (46, 47). Thus, while Tregs of IMC patients show expression of Th1-suppressive mechanisms, it may very well be attenuated at the translational or protein level, thereby limiting Treg functionality.

In the context of reduced Treg-mediated immune suppression, Th17 cells may become more pronounced in IMC. Th17 cells are capable of developing colitis in mouse models when the IL-10 receptor (IL-10R) is deleted in Tregs (48), highlighting the importance of IL-10 in maintaining intestinal homeostasis. In addition to IL-10, CTLA-4 is required for Tregs to suppress Th17 cells (48, 49). Inability to suppress Th17 cells possibly explains why CTLA-4 blockade leads to increased mucosal IL-10 mRNA in IMC biopsies without successfully resolving IMC (44). Th17 cells, which are potent secretors of IL-17, are present in IMC. Serum IL-17 levels correlated strongly with ipilimumab-induced IMC, from onset to resolution, while the other examined cytokines did not express such a pattern (50). Parallel to serum levels, in ipilimumab-induced IMC IL-17A mRNA is significantly increased in colonic biopsies, as is similar to IBD (44). Together, these findings indicate an important role for Th17 cells in IMC.

The Th17/IL-17 axis is, amongst others, responsible for production of the chemokines CXCL8 and GM-CSF by intestinal epithelial cells (51). These chemokines attract neutrophils and prevent their apoptosis, employing them as a mucosal barrier defense (52–54). Neutrophil infiltration in the epithelial layers is indeed a characteristic of human IMC biopsies after both anti-CTLA-4 (36) and anti-PD-1 therapy (55). Th17-mediated neutrophil recruitment may thus be an important mechanism of inflammation in IMC. Furthermore, the mouse equivalent of human CXCL1, an important chemokine for neutrophil recruitment (56, 57), was found in serum following ICI therapy in colitis mouse models (58, 59). The same mouse models showed high serum levels of IL-6, which has a significant role in the balance between Tregs and Th17 cells, after ICI treatment. IL-6 skews transforming growth factor-beta-mediated differentiation of naïve $CD4^+$ cells into Tregs towards Th17 differentiation, even by reprogramming Tregs into Th17 cells (60, 61). The serum levels of CXCL1 and IL-6 thus indicate that neutrophil recruitment and the Treg/Th17 balance are important mechanisms in IMC.

In IBD, CXCL1 and IL-6 are secreted by activated macrophages. This cell type may play a significant role in neutrophil recruitment and the skewed Th17 balance in IMC (62, 63). Indeed, in human IMC biopsies macrophages have been reported to upregulate CXCL9/10 expression, alongside their ligand CXCR3 on T-cells (37), and are therefore responsible for recruiting T-cells to a site of Th1-type inflammation (64). CXCR3 deficient mice have shown to be resistant to dextran sulfate sodium-induced colitis (65), highlighting the role of this pathway in the development of colitis. Moreover, macrophage-derived CXCL9 and CXCL10 is also required for T-cell infiltration in tumor sites, indicating the importance of this pathway (66). However, macrophages form a heterogeneous cell population, which has been studied to a limited extent in the context of IMC. Taken together, these data suggest that macrophages potentially have a significant role in T-cell recruitment in IMC. It is therefore to be expected that macrophages are important in more aspects of IMC.

Anti-Microbial Immunity

The lumen of the colon contains a multitude of mostly bacteria, together referred to as the microbiome. Under certain conditions, some bacteria may become pathogenic. Epithelial

tight-junctions, mucus covering the mucosa, and tissue resident macrophages are the first line of defense against such intestinal pathogens. Macrophages detect these pathogens through recognition of exogenous pathogen-associated molecular patterns (67). As a response, macrophages secrete many pro-inflammatory cytokines, such as TNFα, IL-1 and IL-6, but also the anti-inflammatory cytokine IL-10 (68). In ulcerative colitis (UC) and Crohn's disease (CD), both IBDs, an abnormal reaction to commensal bacteria leads to mucosal inflammation. Several bacteria in IBD stimulate a pathogenic Th1/Th17 response while other bacteria are associated with regulation of Tregs and regulatory B-cells (69). Whether this also applies to IMC is yet to be investigated.

Next to macrophages, Th17 cells are prominent actors in resistance against intestinal pathogens. Interestingly, the composition of commensal bacteria in the gut can skew differentiation of Tregs into Th17 cells (60), a phenomenon that is important in IMC, as discussed above. Noteworthily, a knockout of IL-10R leads to Th17-mediated colitis in regular mice (48), but not in germfree mice (70). This strengthens the idea of a significant role for the microbiome in the onset of UC, and probably also IMC. It is evident that active UC, and most probably also IMC, share a shift toward a Th1/Th17-mediated immune response to the commensal and/or pathogenic microbiota.

Another cell type that leads us to the importance of the microbiome is mucosal-associated invariant T (MAIT) cells. These cells are elevated in gut biopsies of patients with IMC after ipilimumab and nivolumab combination therapy, but not in patients that remained free of adverse events or in patients with UC (71). MAIT-cells are activated indirectly upon bacterial infection and exert antimicrobial properties on bacterial-infected cells (72, 73). The fact that these cells were specifically enhanced in IMC patients, provides a link between the microbiome and IMC that is not seen in similar pathologies. Antimicrobial activity of MAIT-cells against epithelial cells may lead to an impaired barrier function and immune regulation towards intestinal bacteria in patients with IMC.

Bacterial Strains

The importance of intestinal bacteria has been especially highlighted in mouse models of IMC, induced by oral administration of dextran sulfate sodium prior to anti-CTLA-4 therapy. Treatment with vancomycin, an antibiotic agent that depletes Gram-positive bacteria, reportedly exacerbated severity of IMC histologically and clinically (58, 74). Interestingly, re-introduction of a genus of Gram-positive anaerobic bacteria, *Bifidobacterium* (74) or *Lactobacillus* (58), after vancomycin treatment caused significant amelioration of IMC, both clinically and histologically. Specific strains of these genera, at least *Lactobacillus reuteri, Lactobacillus rhamnosum* and *Bifidobacterium breve*, have shown to be responsible for this positive effect in mice (58, 59).

In humans, Abu-Sbeih and colleagues tested the effect of antibiotic treatment on IMC, including IMD, in a cohort of 826 patients (75). Whereas the use of antibiotics strongly correlated with a lower occurrence of total IMC and IMD, it caused more severe IMC and more hospitalizations. More specifically, anaerobic antibiotics were clinically more detrimental than aerobic antibiotics. This is in accordance with the observations in aforementioned mouse models that Gram-positive anaerobic bacteria were required for IMC resolution (58, 59, 74). The importance of the anaerobic bacterial strains used in those mouse studies is possibly enhanced by it being Gram-positive bacteria that are capable of inducing anti-inflammatory cytokines, rather than induction of only a Th1 secretome by Gram-negative bacteria (76). Nevertheless, the lower overall occurrence of total IMC and IMD following antibiotic therapy in humans, but on the other hand a clinically more severe IMC phenotype, could indicate that IMD and IMC are mechanistically different. Data supporting this hypothesis are currently lacking.

In mouse models of IMC, aiming to get more insight in the underlying bacterial-related mechanisms has yielded various important observations. Anti-CTLA-4 treatment induced a decline in the relative abundance of *Lactobacillus* in stool samples (58). Probiotic *Bifidobacterium* treatment, however, increased the relative abundance of *Lactobacillus*, thereby showing a relation between the two genera (59). These strains may be important to protect the colon against IFNγ-induced epithelial barrier disruption, as shown in human organoid models *in vitro* (40). Any protective function of *Bifidobacterium* is Treg-mediated, since depletion of Tregs abrogated beneficial effects of *Bifidobacterium* in IMC mouse models (59). This bacterial strain caused a genetic upregulation of IL-17R in Tregs of the colonic lamina propria, suggesting Treg behavior in response to IL-17, and thus Th17 cells, may be altered. To date, the effect of IL-17R activation in Tregs remains unknown, but an increase in the receptor for IL-17 might indicate increased sensitivity to Th17 cytokines, allowing Tregs to regulate these cells properly. Tregs may indeed reduce Th17 differentiation and neutrophil infiltration following either *Bifidobacterium* or *Lactobacillus* treatment, since those treatments lead to a decrease in serum levels of IL-6 and keratinocyte-derived chemokine (58, 59).

Another indication for Tregs suppressing inflammation following *Bifidobacterium* administration is the upregulation of the IL-10R on these cells. Interestingly, not only IL-10 was required for attenuation of IMC, but IL-22, a key modulator of epithelial homeostasis (77), also showed to be important (59). This fits with an observation by Wang et al. in mice treated with *Lactobacillus reuteri* (58). They reported that the presence of type 3 innate lymphoid cells (ILC3s), a lymphoid line innate immune cell type known to secrete IL-22 (78), is strongly related to IMC severity. Beneficial probiotic treatment reduced ILC3 cell numbers and improved inflammation in these mice. However, ILC3 cell numbers may be a consequence of IMC, rather than a cause, since crosstalk between ILC3s, macrophages, and the microbiome is reported to be essential for maintaining intestinal homeostasis (79). In addition, a recent study showed that IL-22 producing ILC3s were able to protect against colitis in mice, even when the mice were modified to express abnormal pro-inflammatory secretion profiles (80). However, ILCs, among

which those of group 3, are also known for secretion of IL-17 (81, 82), indicating that there could be an ambivalent role for ILCs in IMC.

In general, mouse studies have shed light on the importance of certain genera for protection against IMC. However, fundamental data are limited and thus many other genera or species could be beneficial or detrimental for IMC. Probiotic treatment has not been tested in humans in the context of IMC. Nevertheless, in two out of the three patients who received fecal microbiota transplantation (FMT), a quick reduction of inflammation, as observed by colonoscopy, was noticed (83, 84). Following FMT, *Bifidobacterium* was elevated, even though the patients had a distinct taxonomy from each other prior to FMT (83). This finding might indicate that this particular genus is as important in IMC in humans, as it is in mice.

Anti-CTLA-4 vs Anti-PD-1

Most studies regarding IMC focus on ipilimumab-induced IMC, either through monotherapy or combination therapy. Several differences in T-cell behavior in IMC between ipilimumab and nivolumab or pembrolizumab treatment are shown (85, 86). In anti-PD-1 treated patients, mucosal infiltration of T-cells was dominated by $CD8^+$ T-cells, whereas $CD4^+$ dominated after ipilimumab (85). Additionally, ipilimumab led to more epithelial infiltration of lymphocytes and significantly higher levels of mucosal TNFα compared to anti-PD-1 treatment (85, 86). This suggests that mechanisms by which IMC is induced are, to some extent, different between ICI therapies. Furthermore, endoscopic evaluation following anti-PD-1 treatment often does not show aberrations, as opposed to ipilimumab-induced IMC (87). Other than that, mechanistic understanding of IMC and the differences between ICI therapies are mostly suggestive, such as CTLA-4 blockade increasing the numbers of Th17 cells (88), while PD-1 blockade leading to a Th1 dominancy as described in a case report of two IMC patients (89). However, in-depth, head-to-head comparisons are still lacking.

Any additional functional discrepancies between ICI treatments in IMC might be hypothesized by the role of each receptor in colonic homeostasis. In mice, the PD-1/PD-L1 axis is important to maintain tolerance against self-antigens in peripheral tissues, including the gut, by limiting expansion of $CD4^+$ and $CD8^+$ T-cells (90, 91). That seems to indicate that anti-PD-1 therapy predisposes to intestinal toxicity. However, it has been suggested that PD-L1 can also affect T-cells in the absence of PD-1 (92), thereby possibly remaining functional to some extent after anti-PD-1 blockade. CTLA-4 affects Treg accumulation in the intestinal lamina propria, but not in the thymus, spleen, and mesenteric lymph nodes (93), highlighting its importance in the gut in particular. Considering the difference in frequency of IMC between ICI treatment strategies, CTLA-4 indeed appears to have a more pronounced role in maintaining intestinal homeostasis. The evidence for this difference is mostly suggestive, as data is difficult to compare across studies and different ICI regimens were not studied head-to-head. Hence, it is not yet clear why blockade of CTLA-4 causes IMC more frequently than anti-PD-1 therapy in humans, even though it is clear that both CTLA-4 and PD-1/PD-L1 are important for maintaining mucosal homeostasis in mice.

Overall, more evidence is emerging suggesting that some immune cells are predominantly responsible for IMC. As described, in IMC the functional balance between Tregs and Th17s is skewed towards Th17s, leading to increased neutrophil infiltration. Moreover, there is a Th1-dependent inflammatory state, in which in particular IFNγ is suggested to disrupt the epithelial barrier (**Figure 1**). Epithelial permeability leads to interaction between the microbiome and immune cells, although potentially pathogenic microbes and/or commensal microbes that trigger an uncontrolled inflammatory response have not been identified in IMC. However, there are also some subsets for which it is not clear what their exact role is, such as MAIT-cells, ILC3s, and macrophages. In addition, it is not understood why these pathways are induced in some patients and not in others. Answers to these uncertainties may explain the occurrence of immune-related toxicities in certain patients, whereas others remain free of adverse events.

BIOMARKERS

In-depth understanding of the mechanisms underlying IMC development is critical to select appropriate immunosuppressive treatments, or to prevent the development of IMC. Another way to reduce the incidence and severity of IMC is to identify markers which predict patients at risk of developing IMC, either all grade or specifically high-grade toxicity. Being able to predict the risk of IMC for patients allows closer monitoring of those that are likely to develop high-grade toxicities, or enables selection of an alternative anti-cancer treatment.

Cellular Indicators

Several cell types are involved in or correlate with IMC. Cellular products or even the mere presence of cells are potential candidates for biomarkers of IMC development.

As already discussed, IL-17 secreting Th17s are important mediators. While baseline IL-17 serum levels do not correlate with all grade ipilimumab-induced IMC occurrence (50), it significantly correlated with grade 3 IMC in a cohort of 33 patients (94). Baseline serum IL-17 is therefore a potential marker for high-grade colitis, although it remains to be confirmed in larger cohorts.

Another cell type that is abundantly present in IMC is neutrophils. A high neutrophil to lymphocyte ratio (NLR) in serum is known to correlate with worsened ICI clinical outcome (95–97). Although its predictive correlation with all irAEs is mostly weak, NLR distinguishes grade 3 and higher irAEs from low grade irAEs after pembrolizumab therapy and it can be used to monitor the onset of irAEs (98, 99). For IMC in particular, a baseline NLR higher than 5 correlated with development of IMC (100). However, in the same study, a validation cohort failed to show a significant correlation between NLR and IMC. Another interesting marker related to neutrophils is the genetic expression of *CD177*, a modulator of neutrophil migration

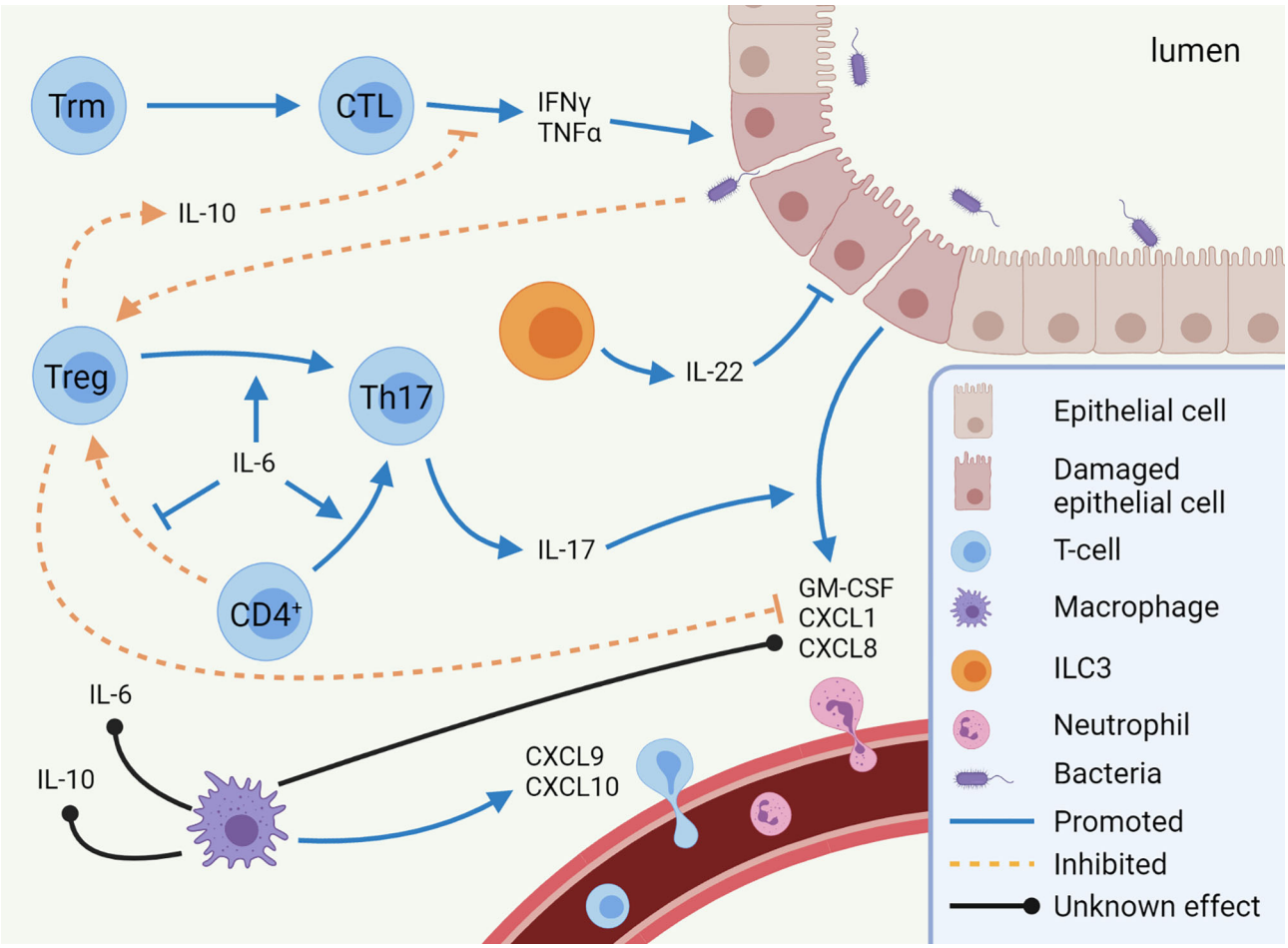

FIGURE 1 | Mechanisms of immune checkpoint inhibitor-mediated colitis (IMC). Pro-inflammatory pathways (CTL, Th17 cells, and neutrophils) are predominantly enhanced in IMC, while anti-inflammatory pathways (Treg differentiation and IL-10 secretion) are inhibited. Other cell types, such as macrophages and ILC3s, are expected to play a role in IMC, but to which extent is unknown. This image was created with BioRender.com. CTL, Cytotoxic T-lymphocyte; CXCL, C-X-C motif chemokine ligand; GM-CSF, Granulocyte-macrophage colony-stimulating factor; IFN, Interferon; IL, Interleukin; ILC, innate lymphoid cell; Th17, T helper 17 cell; TNF, Tumor necrosis factor; Treg, regulatory T-cell; Trm, tissue-resident memory T-cell.

(101), in circulating cells. At week 3 after the first ipilimumab treatment, this marker showed high specificity for predicting patients who later developed gastrointestinal adverse events (102). However, the sensitivity was low in this study, meaning *CD177* is unable to capture all patients at risk of IMC on its own.

Other potential neutrophil-related biomarkers are based on similarities with IBD. Fecal calprotectin and lactoferrin are established markers for active inflammation in IBD (103). Calprotectin is abundantly present in the cytoplasm of phagocytes and has pro-inflammatory functions upon secretion (104). A major source of calprotectin release is cell death of neutrophils (105). Lactoferrin is, amongst others, released in granules by activated neutrophils (106). Neutrophil infiltration is often observed in IMC biopsies. Accordingly, levels of fecal calprotectin and lactoferrin correlate with endoscopic findings of ulceration and histological signs of IMC (107). Furthermore, fecal calprotectin is increased upon the onset of diarrhea and reduced when clinical remission is observed (108, 109). This could therefore be a promising marker to monitor disease activity and relapse in patients, as already suggested in American Society of Clinical Oncology guidelines (110). The predictive value of fecal calprotectin and lactoferrin has not yet been investigated. However, since these are both markers for neutrophil infiltration, distinguishing IMC from an IBD exacerbation will not be possible for IBD patients who underwent ICI therapy (111, 112).

Microbiota

At a bacterial level, some potential biomarkers have been reported. In two patient cohorts of 34 and 55 patients, microbiota composition analysis was performed on feces of patients prior to the start of ICI therapy for metastatic melanoma. In feces of patients later developing IMC, several families of the *Bacteroidetes* phylum were underrepresented

(113, 114). The same observation was made for IMD in a cohort of 26 patients with lung cancer, which may suggest a gut protective role of this phylum (115). The *Firmicutes* phylum, on the other hand, was increased at baseline for patients later developing IMC (114, 115). Thus, a high ratio of *Firmicutes* to *Bacteroidetes* at baseline measurements of feces may provide predictive insight in which patients are likely to develop IMC, although these observations should be validated in larger patient cohorts to test clinical applicability. Whereas IMC has overlapping characteristics with several IBDs, a low *Firmicutes* to *Bacteroidetes* ratio is actually seen in CD (116). This indicates a different role of these bacterial families in IMC and CD.

Looking at resistance to IMC development rather than risk of development, polyamine transport units in bacteria may be beneficial. A prediction model using molecular levels of these polyamine transport units showed a sensitivity of 70% and a specificity of 100% for resistance to IMC development, indicating all patients that were predicted to develop IMC indeed did so, however, 30% of patients were false negatively assigned to remain free of IMC (113). Interestingly, blocking polyamine reduces the number of tumor-infiltrating immune suppressor cells, such as myeloid-derived suppressor cells, Tregs and M2 macrophages, thereby boosting the antitumor response in mouse models (117, 118). Hence, the microbiome might exert a suppressive function in the immune response through polyamine transport, which could explain its correlation with resistance to IMC.

Other Markers

While most of the potential biomarkers reported so far focused on neutrophils, Th17 cells, or the microbiome, there are also some markers that are less specific. In IBD, vitamin D intake has been reported to improve clinical outcomes (119). The importance of vitamin D is underscored in mice: immune cells from vitamin D deprived mice do show increased IL-17 and IFNγ secretion, failure to develop essential anti-inflammatory T-cell subsets, and disruption of the epithelial barrier, all of which are important mechanisms of IMC (120, 121). Indeed, vitamin D intake during ICI treatment was found to be strongly correlated with reduced risk of IMC development in a cohort of 213 patients, which was additionally validated on an independent cohort of 169 patients (100). Although this does not necessarily mean that vitamin D has a predictive value in this context, it is interesting to take vitamin D into account in the clinic, particularly in case of an insufficiency.

For irAEs in general, a wide range of predictive markers is studied. For instance, a large multi-omics study showed that a bivariate model using ADPGK and LCP1, which are both related to T-cell activation, is a promising prediction tool (122). Since such markers are not specific for IMC, we would like to refer the reader to some reviews on this topic (123, 124). While some of these markers provide a decent predictive value, it is mostly unclear whether these are applicable for IMC specifically. Such general markers, however, are definitely of interest to investigate in prospective studies regarding IMC.

MECHANISM-BASED FUTURE RESEARCH AND APPROACHES TO MANAGEMENT

It is well established that Th17 cells, derived from Tregs or naïve T-cells, are important actors in IMC. Also, CTLs are thought to be pathogenic in IMC by disrupting the epithelial barrier and creating a state of inflammation. However, many questions still remain. It is often unclear which signals induce these cell developments, or why this signaling is evoked in certain patients. Is it directly or indirectly related to ICI therapy? In other words, does ICI treatment lead to attraction of macrophages and skewing towards Th17 cells, or is it secondary to e.g., activation of autoreactive B or T-cells? Moreover, there is still a lot to be elucidated about tissue-resident T-cells. For instance, CTLs appear to be to be partly derived from Trms, although its mechanism is unknown. In addition, several resident T-cell types involved in interactions with the microbiome, ILC3s, MAIT-cells, and macrophages, are indicated to be affected. While macrophages are suggested to promote T-cell recruitment, it is likely that their role in IMC is larger. Their secretome has strong overlap with several cytokines and chemokines that are expressed in IMC. Yet, many studies have focused on the role of T-cells in IMC. ILC3s and MAIT-cells may have more protective, antimicrobial roles. Knowledge on how these cell types are behaving in IMC is important for understanding the role of potentially pathogenic bacteria.

To answer these remaining questions, future research should focus on specific mechanisms of IMC development. Cellular composition and involved cytokines and chemokines in baseline and on-treatment sigmoid biopsies should be compared in ICI-treated patients who developed IMC. With the use of several advanced techniques, such as RNA-sequencing, multiplex immunohistochemistry, and flow cytometry, cellular and molecular data can be readily harvested from these biopsies. The microbiome should also be taken into account in prospective studies, considering its significant role. Especially those microbes in close contact with the mucosal tissue should be examined and differences in host-microbe interactions in the mucosa of patients with IMC versus patients remaining free of IMC should be explored. In future IMC-focused trials, blood, colon biopsies, and stool should be collected at standardized points in time, e.g., at baseline and during ICI cycles. Understanding the interactions between all key players in IMC is of utmost importance to improve the current clinical treatments. This research may lead to additional targets for treatment, as well as biomarkers that could identify patients at risk of high-grade IMC.

Currently, several guidelines suggest that patients diagnosed with high-grade IMC are to be treated with first-line systemic corticosteroids (110, 125, 126). In case of steroid-refractory IMC, anti-TNFα treatment with infliximab is often initiated. However, both treatments are unspecific for IMC and therefore come with several drawbacks, such as risk of infection and drug-induced comorbidities (127, 128). Infliximab has even been observed to compromise the long-term anti-tumor response in steroid refractory patients (129).

Recently, the use of immunosuppressants targeting specifically the gut in IMC has been investigated, primarily vedolizumab. This antibody blocks the α4β7 integrin, which is involved in homing of T-cells to the gut (130). Vedolizumab has adequately replaced infliximab in steroid-refractory patients, and administration within 10 days of IMC onset leads to better management and clinical remission (131, 132). However, histologic remission is often not seen six months after clinical remission, indicating that there is room for improvement (131). Prospective studies interfering with alternative pathways may provide more options for IMC-specific treatments.

Several potential targets for IMC are already in clinical trials (**Figure 2**). For instance, blocking IL-6 with tocilizumab could reduce Th17 differentiation, thereby restoring the dysfunctional balance between Tregs and Th17 cells (NCT03601611). Additionally, cytokine secretion by Th17 cells could be targeted using secukinumab, an anti-IL-17A monoclonal antibody. Secukinumab has already shown a beneficial therapeutic effect in patients suffering from ICI-induced psoriasis, without affecting their anti-tumor response (133). Caution is required when using this antibody to treat IMC, since secukinumab is ineffective in CD, risking fungal infections along the way (134). In UC, an antagonist of the p40 subunit of IL-12 and IL-23, called ustekinumab, showed to induce and maintain disease remission (135). It has not been studied in the context of IMC and the cytokines IL-12 and IL-23 have not been

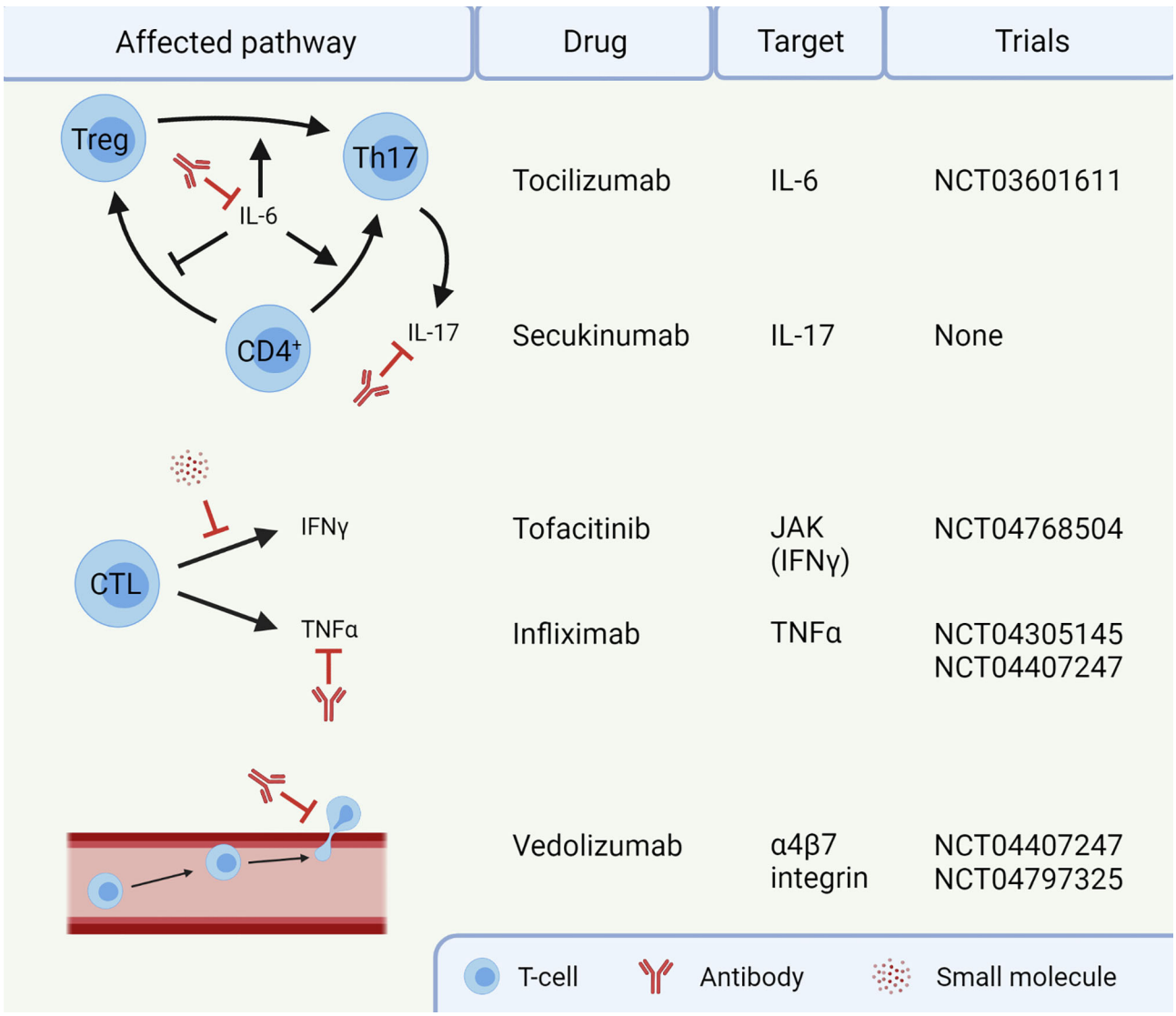

FIGURE 2 | Targets for treatment of immune checkpoint inhibitor-mediated colitis (IMC). Infliximab and vedolizumab are already standard of care in steroid-refractory IMC. The other agents are currently not routinely given to patients. This image was created with BioRender.com. CTL, Cytotoxic T-lymphocyte; IFN, Interferon; IL, Interleukin; JAK, Janus kinase; Th17, T helper 17 cell; TNF, Tumor necrosis factor; Treg, regulatory T-cell.

reported to be important in IMC yet. IFNγ, on the other hand, does have an important role in IMC, causing a pro-inflammatory response and epithelial damage. The function of IFNγ can be inhibited by targeting the JAK signaling pathway with tofacitinib. Tofacitinib has shown efficacy against IMC in five patients (136, 137) and will be investigated in a clinical trial with ten patients (NCT04768504). Tofacitinib has also shown efficacy in treatment of IBD (138). However, JAK signaling is reported to be important for an anti-tumor response upon ICI therapy (139), so caution with inhibition of this pathway in IMC is necessary. Future IMC trials should focus on mechanism-based approaches for selection of first-line immunomodulating agents. Such agents should interfere with IMC, without compromising the efficacy of ICI antibodies.

In addition to interfering with pathways of the immune system, targeting the microbiome is also an option for treatment of IMC. For instance, an experimental FMT immediately showed alleviation of IMC symptoms in patients refractory to corticosteroids, infliximab, and vedolizumab (83, 84). FMT has already shown promising therapeutic effects in *Clostridoides difficile* infections (140). Recently, a large clinical trial, 800 patients with any stage melanoma, non-small cell lung cancer or genitourinary cancer, has been set up to study potential biomarkers in the microbiome and the safety and efficacy of FMT in IMC (NCT03819296). An alternative to FMT would be the use of probiotics. Probiotics are effective in mouse models of IMC, and successfully used against necrotizing enterocolitis in human preterm infants (141). Since FMT and probiotics aim to normalize the gut microbiome, it is an attractive strategy to treat IMC without affecting the efficacy of ICI therapy. The composition of the gut microbiome can affect the antitumor response negatively or positively (142, 143). Promising is the observation in mouse models that probiotic treatment with two different bacterial genera attenuates IMC without compromising the antitumor response (58, 74). Therefore, IMC treatment with specific bacterial strains might be more suitable than unspecific FMT treatment with the risk of lowering the anticancer activity of the immune system.

All in all, it is expected that ICI therapy becomes available for more types of cancer in upcoming years (144, 145). To reduce physical harm and loss of quality of life due to irAEs, the balance between efficacy and toxicity requires optimization. Results of mechanism-based IMC research may lead to optimization of treatments and predictions of IMC. In addition, it may provide new insights concerning non-intestinal irAEs. We envision direct clinical relevance for future patients undergoing ICI therapy, in which severe irAEs with quality-of-life deterioration can be treated or even be prevented.

AUTHOR CONTRIBUTIONS

HW and IV conceptualized this review. HW, MS, and MG were responsible for writing the manuscript. All authors contributed to the article and approved the submitted version.

FUNDING

This work was supported by NWO-Vici grant (918.14.655) to IV and EU grant 825410 (Oncobiome).

REFERENCES

1. Pennock GK, Chow LQM. New Drug Development and Clinical Pharmacology the Evolving Role of Immune Checkpoint Inhibitors in Cancer Treatment. *Oncologist* (2015) 20:812–22. doi: 10.1634/theoncologist.2014-
2. Yan Y, Kumar AB, Finnes H, Markovic SN, Park S, Dronca RS, et al. Combining Immune Checkpoint Inhibitors With Conventional Cancer Therapy. *Front Immunol* (2018) 9:1739. doi: 10.3389/fimmu.2018.01739
3. Sugiura D, Maruhashi T, Okazaki I, Shimizu K, Maeda TK, Takemoto T, et al. Restriction of PD-1 Function by Cis -PD-L1/CD80 Interactions Is Required for Optimal T Cell Responses. *Science* (2019) 364:558–66. doi: 10.1126/science.aav7062
4. van Pul KM, Fransen MF, van de Ven R, de Gruijl TD. Immunotherapy Goes Local: The Central Role of Lymph Nodes in Driving Tumor Infiltration and Efficacy. *Front Immunol* (2021) 12:643291. doi: 10.3389/fimmu.2021.643291
5. Sanmamed MF, Chen L. A Paradigm Shift in Cancer Immunotherapy: From Enhancement to Normalization. *Cell* (2018) 175:313–26. doi: 10.1016/j.cell.2018.09.035
6. Bakdash G, Simone P, Dijk TV, Figdor CG, De Vries IJM. The Nature of Activatory and Tolerogenic Dendritic Cell-Derived Signal II. *Front Immunol* (2013) 4:53. doi: 10.3389/fimmu.2013.00053
7. Sckisel GD, Bouchlaka MN, Monjazeb AM, Crittenden M, Curti BD, Wilkins DEC, et al. Out-of-Sequence Signal 3 Paralyzes Primary CD4+ T-Cell-Dependent Immunity. *Immunity* (2015) 43:240–50. doi: 10.1016/j.immuni.2015.06.023
8. Zenke S, Palm MM, Braun J, Gavrilov A, Meiser P, Böttcher JP, et al. Quorum Regulation *via* Nested Antagonistic Feedback Circuits Mediated by the Receptors CD28 and CTLA-4 Confers Robustness to T Cell Population Dynamics. *Immunity* (2020) 52:313–27.e7. doi: 10.1016/j.immuni.2020.01.018
9. Jago CB, Yates J, Saraiva Câmara NO, Lechler RI, Lombardi G. Differential Expression of CTLA-4 Among T Cell Subsets. *Clin Exp Immunol* (2004) 136:463–71. doi: 10.1111/j.1365-2249.2004.02478.x
10. Wing K, Onishi Y, Prieto-Martin P, Yamaguchi T, Miyara M, Fehervari Z, et al. CTLA-4 Control Over Foxp3+ Regulatory T Cell Function. *Science* (2008) 322:271–5. doi: 10.1126/science.1160062
11. Graziani G, Tentori L, Navarra P. Ipilimumab: A Novel Immunostimulatory Monoclonal Antibody for the Treatment of Cancer. *Pharmacol Res* (2012) 65:9–22. doi: 10.1016/j.phrs.2011.09.002
12. Weber JS, Hamid O, Chasalow SD, Wu DY, Parker SM, Galbraith S, et al. Ipilimumab Increases Activated T Cells and Enhances Humoral Immunity in Patients With Advanced Melanoma. *J Immunother* (2012) 35:89–97. doi: 10.1097/CJI.0b013e31823aa41c
13. Sharma A, Subudhi SK, Blando J, Scutti J, Vence L, Allison JP, et al. Anti-CTLA-4 Immunotherapy Does Not Deplete FOXP3+ Regulatory T Cells (Tregs) in Human Cancers. *Clin Cancer Res* (2019) 25:1233–8. doi: 10.1158/1078-0432.CCR-18-0762.Anti
14. Schubert D, Bode C, Kenefeck R, Hou TZ, Wing JB, Kennedy A, et al. Autosomal Dominant Immune Dysregulation Syndrome in Humans With CTLA4 Mutations. *Nat Med* (2014) 20:1410–6. doi: 10.1038/nm.3746
15. Keir ME, Liang SC, Guleria I, Latchman YE, Qipo A, Albacker LA, et al. Tissue Expression of PD-L1 Mediates Peripheral T Cell Tolerance. *J Exp Med* (2006) 203:883–95. doi: 10.1084/jem.20051776
16. Song S, Yuan P, Wu H, Chen J, Fu J, Li P, et al. Dendritic Cells With an Increased PD-L1 by TGF-β Induce T Cell Anergy for the Cytotoxicity of

Hepatocellular Carcinoma Cells. *Int Immunopharmacol* (2014) 20:117–23. doi: 10.1016/j.intimp.2014.02.027
17. Patel SP, Kurzrock R. PD-L1 Expression as a Predictive Biomarker in Cancer Immunotherapy. *Mol Cancer Ther* (2015) 14:847–56. doi: 10.1158/1535-7163.MCT-14-0983
18. Kluger HM, Zito CR, Turcu G, Baine MK, Zhang H, Adeniran A, et al. PD-L1 Studies Across Tumor Types, Its Differential Expression and Predictive Value in Patients Treated With Immune Checkpoint Inhibitors. *Clin Cancer Res* (2017) 23:4270–9. doi: 10.1158/1078-0432.CCR-16-3146
19. Latchman Y, Wood CR, Chernova T, Chaudhary D, Borde M, Chernova I, et al. PD-L2 Is a Second Ligand for PD-1 and Inhibits T Cell Activation. *Nat Immunol* (2001) 2:261–8. doi: 10.1038/85330
20. Keir ME, Butte MJ, Freeman GJ, Sharpe AH. PD-1 and Its Ligands in Tolerance and Immunity. *Annu Rev Immunol* (2008) 26:677–704. doi: 10.1146/annurev.immunol.26.021607.090331
21. Yearley JH, Gibson C, Yu N, Moon C, Murphy E, Juco J, et al. PD-L2 Expression in Human Tumors: Relevance to Anti-PD-1 Therapy in Cancer. *Clin Cancer Res* (2017) 23:3158–67. doi: 10.1158/1078-0432.CCR-16-1761
22. Brahmer JR, Hammers H, Lipson EJ. Nivolumab: Targeting PD-1 to Bolster Antitumor Immunity. *Futur Oncol* (2015) 11:1307–26. doi: 10.2217/fon.15.52
23. Pai-Scherf L, Blumenthal GM, Li H, Subramaniam S, Mishra-Kalyani PS, He K, et al. FDA Approval Summary: Pembrolizumab for Treatment of Metastatic Non-Small Cell Lung Cancer: First-Line Therapy and Beyond. *Oncologist* (2017) 22:1392–9. doi: 10.1634/theoncologist.2017-0078
24. Markham A, Duggan S. Cemiplimab: First Global Approval. *Drugs* (2018) 78:1841–6. doi: 10.1007/s40265-018-1012-5
25. Weinstock C, Khozin S, Suzman D, Zhang L, Tang S, Wahby S, et al. Food and Drug Administration Approval Summary: Atezolizumab for Metastatic non–Small Cell Lung Cancer. *Clin Cancer Res* (2017) 23:4534–9. doi: 10.1158/1078-0432.CCR-17-0540
26. Kim ES. Avelumab: First Global Approval. *Drugs* (2017) 77:929–37. doi: 10.1007/s40265-017-0749-6
27. Syed YY. Durvalumab: First Global Approval. *Drugs* (2017) 77:1369–76. doi: 10.1007/s40265-017-0782-5
28. Tumeh PC, Harview CL, Yearley JH, Shintaku IP, Taylor EJM, Robert L, et al. PD-1 Blockade Induces Responses by Inhibiting Adaptive Immune Resistance. *Nature* (2014) 515:568–71. doi: 10.1038/nature13954
29. Postow MA, Sidlow R, Hellmann MD. Immune-Related Adverse Events Associated With Immune Checkpoint Blockade. *N Engl J Med* (2018) 378:158–68. doi: 10.1056/nejmra1703481
30. Larkin J, Chiarion-Sileni V, Gonzalez R, Grob JJ, Cowey CL, Lao CD, et al. Combined Nivolumab and Ipilimumab or Monotherapy in Untreated Melanoma. *N Engl J Med* (2015) 373:23–34. doi: 10.1056/nejmoa1504030
31. Xu C, Chen YP, Du XJ, Liu JQ, Huang CL, Chen L, et al. Comparative Safety of Immune Checkpoint Inhibitors in Cancer: Systematic Review and Network Meta-Analysis. *BMJ* (2018) 363:k4226. doi: 10.1136/bmj.k4226
32. Cameron F, Whiteside G, Perry C. Ipilimumab: First Global Approval. *Drugs* (2011) 71:1093–104. doi: 10.2165/11595310-000000000-00000
33. Khoja L, Day D, Wei-Wu Chen T, Siu LL, Hansen AR. Tumour- and Class-Specific Patterns of Immune-Related Adverse Events of Immune Checkpoint Inhibitors: A Systematic Review. *Ann Oncol* (2017) 28:2377–85. doi: 10.1093/annonc/mdx286
34. Wang DY, Salem JE, Cohen JV, Chandra S, Menzer C, Ye F, et al. Fatal Toxic Effects Associated With Immune Checkpoint Inhibitors: A Systematic Review and Meta-Analysis. *JAMA Oncol* (2018) 4:1721–8. doi: 10.1001/jamaoncol.2018.3923
35. Marthey L, Mateus C, Mussini C, Nachury M, Nancey S, Grange F, et al. Cancer Immunotherapy With Anti-CTLA-4 Monoclonal Antibodies Induces an Inflammatory Bowel Disease. *J Crohn's Colitis* (2016) 10:395–401. doi: 10.1093/ecco-jcc/jjv227
36. Beck KE, Blansfield JA, Tran KQ, Feldman AL, Marybeth S, Royal RE, et al. Enterocolitis in Patients With Cancer After Antibody Blockade of Cytotoxic T-Lymphocyte-Associated Antigen 4. *J Clin Oncol* (2006) 24:2283–9. doi: 10.1200/JCO.2005.04.5716
37. Luoma AM, Suo S, Williams HL, Sharova T, Sullivan K, Manos M, et al. Molecular Pathways of Colon Inflammation Induced by Cancer Immunotherapy. *Cell* (2020) 182:655–71.e22. doi: 10.1016/j.cell.2020.06.001
38. Mami-Chouaib F, Tartour E. Editorial: Tissue Resident Memory T Cells. *Front Immunol* (2019) 10:1018. doi: 10.3389/fimmu.2019.01018
39. Corgnac S, Boutet M, Kfoury M, Naltet C, Mami-Chouaib F. The Emerging Role of CD8+ Tissue Resident Memory T (TRM) Cells in Antitumor Immunity: A Unique Functional Contribution of the CD103 Integrin. *Front Immunol* (2018) 9:1904. doi: 10.3389/fimmu.2018.01904
40. Han X, Lee A, Huang S, Gao J, Spence JR, Owyang C. Lactobacillus Rhamnosus GG Prevents Epithelial Barrier Dysfunction Induced by Interferon-Gamma and Fecal Supernatants From Irritable Bowel Syndrome Patients in Human Intestinal Enteroids and Colonoids. *Gut Microbes* (2019) 10:59–76. doi: 10.1080/19490976.2018.1479625
41. Deem RL, Shanahan F, Targan SR. Triggered Human Mucosal T Cells Release Tumour Necrosis Factor-Alpha and Interferon-Gamma Which Kill Human Colonic Epithelial Cells. *Clin Exp Immunol* (1991) 83:79–84. doi: 10.1111/j.1365-2249.1991.tb05592.x
42. Izcue A, Coombes JL, Powrie F. Regulatory T Cells Suppress Systemic and Mucosal Immune Activation to Control Intestinal Inflammation. *Immunol Rev* (2006) 212:256–71. doi: 10.1111/j.0105-2896.2006.00423.x
43. Lord JD, Hackman RC, Moklebust A, Thompson JA, Higano CS, Chielens D, et al. Refractory Colitis Following Anti-CTLA4 Antibody Therapy: Analysis of Mucosal FOXP3+ T Cells. *Dig Dis Sci* (2010) 55:1396–405. doi: 10.1007/s10620-009-0839-8
44. Bamias G, Delladetsima I, Perdiki M, Siakavellas SI, Goukos D, Papatheodoridis GV, et al. Immunological Characteristics of Colitis Associated With Anti-CTLA-4 Antibody Therapy. *Cancer Invest* (2017) 35:443–55. doi: 10.1080/07357907.2017.1324032
45. Yu L, Yang F, Zhang F, Guo D, Li L, Wang X, et al. CD69 Enhances Immunosuppressive Function of Regulatory T-Cells and Attenuates Colitis by Prompting IL-10 Production. *Cell Death Dis* (2018) 9(9):905. doi: 10.1038/s41419-018-0927-9
46. Teixeira-Coelho M, Guedes J, Ferreirinha P, Howes A, Pedrosa J, Rodrigues F, et al. Differential Post-Transcriptional Regulation of IL-10 by TLR2 and TLR4-Activated Macrophages. *Eur J Immunol* (2014) 44:856–66. doi: 10.1002/eji.201343734
47. Ma F, Liu X, Li D, Wang P, Li N, Lu L, et al. Microrna-466l Upregulates IL-10 Expression in TLR-Triggered Macrophages by Antagonizing RNA-Binding Protein Tristetraprolin-Mediated IL-10 Mrna Degradation. *J Immunol* (2010) 184:6053–9. doi: 10.4049/jimmunol.0902308
48. Chaudhry A, Samstein RM, Treuting P, Liang Y, Pils MC, Heinrich JM, et al. Interleukin-10 Signaling in Regulatory T Cells Is Required for Suppression of Th17 Cell-Mediated Inflammation. *Immunity* (2011) 34:566–78. doi: 10.1016/j.immuni.2011.03.018
49. Ying H, Yang L, Qiao G, Li Z, Zhang L, Yin F, et al. Cutting Edge: Ctla-4–B7 Interaction Suppresses Th17 Cell Differentiation. *J Immunol* (2010) 185:1375–8. doi: 10.4049/jimmunol.0903369
50. Callahan MK, Yang A, Tandon S, Xu Y, Subudhi SK, Roman RA, et al. Evaluation of Serum IL-17 Levels During Ipilimumab Therapy: Correlation With Colitis. *J Clin Oncol* (2011) 29:2505–5. doi: 10.1200/jco.2011.29.15_suppl.2505
51. Blaschitz C, Raffatellu M. Th17 Cytokines and the Gut Mucosal Barrier. *J Clin Immunol* (2010) 30:196–203. doi: 10.1007/s10875-010-9368-7
52. Ina K, Kusugami K, Hosokawa T, Imada A, Shimizu T, Yamaguchi T, et al. Increased Mucosal Production of Granulocyte Colony-Stimulating Factor Is Related to a Delay in Neutrophil Apoptosis in Inflammatory Bowel Disease. *J Gastroenterol Hepatol* (1999) 14:46–53. doi: 10.1046/j.1440-1746.1999.01807.x
53. Metzemaekers M, Vandendriessche S, Berghmans N, Gouwy M, Proost P. Truncation of CXCL8 to CXCL8(9-77) Enhances Actin Polymerization and *In Vivo* Migration of Neutrophils. *J Leukoc Biol* (2020) 107:1167–73. doi: 10.1002/JLB.3AB0220-470R
54. Pelletier M, Maggi L, Micheletti A, Lazzeri E, Tamassia N, Costantini C, et al. Evidence for a Cross-Talk Between Human Neutrophils and Th17 Cells. *Blood* (2010) 115:335–43. doi: 10.1182/blood-2009-04-216085
55. Chen JH, Pezhouh MK, Lauwers GY, Masia R. Histopathologic Features of Colitis Due to Immunotherapy With Anti-PD-1 Antibodies. *Am J Surg Pathol* (2017) 41:643–54. doi: 10.1097/PAS.0000000000000829
56. Ritzman AM, Hughes-Hanks JM, Blaho VA, Wax LE, Mitchell WJ, Brown CR. The Chemokine Receptor CXCR2 Ligand KC (CXCL1) Mediates

Neutrophil Recruitment and Is Critical for Development of Experimental Lyme Arthritis and Carditis. *Infect Immun* (2010) 78:4593–600. doi: 10.1128/IAI.00798-10
57. De Filippo K, Dudeck A, Hasenberg M, Nye E, Van Rooijen N, Hartmann K, et al. Mast Cell and Macrophage Chemokines CXCL1/CXCL2 Control the Early Stage of Neutrophil Recruitment During Tissue Inflammation. *Blood* (2013) 121:4930–7. doi: 10.1182/blood-2013-02-486217
58. Wang T, Zheng N, Luo Q, Jiang L, He B, Yuan X, et al. Probiotics Lactobacillus Reuteri Abrogates Immune Checkpoint Blockade-Associated Colitis by Inhibiting Group 3 Innate Lymphoid Cells. *Front Immunol* (2019) 10:1235. doi: 10.3389/fimmu.2019.01235
59. Sun S, Luo L, Liang W, Yin Q, Guo J, Rush AM, et al. Bifidobacterium Alters the Gut Microbiota and Modulates the Functional Metabolism of T Regulatory Cells in the Context of Immune Checkpoint Blockade. *Proc Natl Acad Sci* (2020) 117:2–8. doi: 10.1073/pnas.1921223117
60. Omenetti S, Pizarro TT. The Treg/Th17 Axis: A Dynamic Balance Regulated by the Gut Microbiome. *Front Immunol* (2015) 6:639. doi: 10.3389/fimmu.2015.00639
61. Kimura A, Kishimoto T. IL-6: Regulator of Treg/Th17 Balance. *Eur J Immunol* (2010) 40:1830–5. doi: 10.1002/eji.201040391
62. Reinecker HC, Steffen M, Witthoeft T, Pflueger I, Schreiber S, MacDermott RP, et al. Enhanced Secretion of Tumour Necrosis Factor-Alpha, IL-6, and IL-1β by Isolated Lamina Propria Mononuclear Cells From Patients With Ulcerative Colitis and Crohn's Disease. *Clin Exp Immunol* (1993) 94:174–81. doi: 10.1111/j.1365-2249.1993.tb05997.x
63. Jones GR, Bain CC, Fenton TM, Kelly A, Brown SL, Ivens AC, et al. Dynamics of Colon Monocyte and Macrophage Activation During Colitis. *Front Immunol* (2018) 9:2764. doi: 10.3389/fimmu.2018.02764
64. Groom JR, Luster AD. CXCR3 in T Cell Function. *Exp Cell Res* (2011) 317:620–31. doi: 10.1016/j.yexcr.2010.12.017
65. Chami B, Yeung AWS, Van Vreden C, King NJC, Bao S. The Role of CXCR3 in DSS-Induced Colitis. *PLoS One* (2014) 9(7):e101622. doi: 10.1371/journal.pone.0101622
66. House IG, Savas P, Lai J, Chen AXY, Oliver AJ, Teo ZL, et al. Macrophage-Derived CXCL9 and CXCL10 Are Required for Antitumor Immune Responses Following Immune Checkpoint Blockade. *Clin Cancer Res* (2020) 26:487–504. doi: 10.1158/1078-0432.CCR-19-1868
67. Han X, Ding S, Jiang H, Liu G. Roles of Macrophages in the Development and Treatment of Gut Inflammation. *Front Cell Dev Biol* (2021) 9:625423. doi: 10.3389/fcell.2021.625423
68. Bain CC, Mowat AM. Macrophages in Intestinal Homeostasis and Inflammation. *Immunol Rev* (2014) 260:102–17. doi: 10.1111/imr.12192
69. Mishima Y, Sartor RB. Manipulating Resident Microbiota to Enhance Regulatory Immune Function to Treat Inflammatory Bowel Diseases. *J Gastroenterol* (2020) 55:4–14. doi: 10.1007/s00535-019-01618-1
70. Stehr M, Greweling MC, Tischer S, Singh M, Blöcker H, Monner DA, et al. Charles River Altered Schaedler Flora (CRASF®) Remained Stable for Four Years in a Mouse Colony Housed in Individually Ventilated Cages. *Lab Anim* (2009) 43:362–70. doi: 10.1258/la.2009.0080075
71. Sasson SC, Zaunders JJ, Nahar K, Munier CML, Fairfax BP, Olsson-Brown A, et al. Mucosal-Associated Invariant T (MAIT) Cells Are Activated in the Gastrointestinal Tissue of Patients With Combination Ipilimumab and Nivolumab Therapy-Related Colitis in a Pathology Distinct From Ulcerative Colitis. *Clin Exp Immunol* (2020) 202:335–52. doi: 10.1111/cei.13502
72. Gold MC, Cerri S, Smyk-Pearson S, Cansler ME, Vogt TM, Delepine J, et al. Human Mucosal Associated Invariant T Cells Detect Bacterially Infected Cells. *PloS Biol* (2010) 8:1–14. doi: 10.1371/journal.pbio.1000407
73. Le Bourhis L, Martin E, Péguillet I, Guihot A, Froux N, Coré M, et al. Antimicrobial Activity of Mucosal-Associated Invariant T Cells. *Nat Immunol* (2010) 11:701–8. doi: 10.1038/ni.1890
74. Wang F, Yin Q, Chen L, Davis MM. Bifidobacterium can Mitigate Intestinal Immunopathology in the Context of CTLA-4 Blockade. *Proc Natl Acad Sci USA* (2018) 115:157–61. doi: 10.1073/pnas.1712901115
75. Abu-Sbeih H, Herrera LN, Tang T, Altan M, Chaftari AM, Okhuysen PC, et al. Impact of Antibiotic Therapy on the Development and Response to Treatment of Immune Checkpoint Inhibitor-Mediated Diarrhea and Colitis. *J Immunother Cancer* (2019) 7:1–11. doi: 10.1186/s40425-019-0832-5
76. Cross ML, Ganner A, Teilab D, Fray LM. Patterns of Cytokine Induction by Gram-Positive and Gram-Negative Probiotic Bacteria. *FEMS Immunol Med Microbiol* (2004) 42:173–80. doi: 10.1016/j.femsim.2004.04.001
77. Martin JC, Bériou G, Heslan M, Bossard C, Jarry A, Abidi A, et al. IL-22BP Is Produced by Eosinophils in Human Gut and Blocks IL-22 Protective Actions During Colitis. *Mucosal Immunol* (2016) 9:539–49. doi: 10.1038/mi.2015.83
78. Victor AR, Nalin AP, Dong W, McClory S, Wei M, Mao C, et al. IL-18 Drives ILC3 Proliferation and Promotes IL-22 Production *via* NF-κb. *J Immunol* (2017) 199:2333–42. doi: 10.4049/jimmunol.1601554
79. Mortha A, Chudnovskiy A, Hashimoto D, Bogunovic M, Spencer SP, Belkaid Y, et al. Microbiota-Dependent Crosstalk Between Macrophages and ILC3 Promotes Intestinal Homeostasis. *Science* (2014) 343 (6178):1249288. doi: 10.1126/science.1252785
80. Park HJ, Lee SW, Van Kaer L, Hong S. Cd1d-Dependent Inkt Cells Control Dss-Induced Colitis in a Mouse Model of Ifnγ-Mediated Hyperinflammation by Increasing Il22-Secreting Ilc3 Cells. *Int J Mol Sci* (2021) 22:1–11. doi: 10.3390/ijms22031250
81. Takatori H, Kanno Y, Watford WT, Tato CM, Weiss G, Ivanov II, et al. Lymphoid Tissue Inducer-Like Cells Are an Innate Source of IL-17 and IL-22. *J Exp Med* (2009) 206:35–41. doi: 10.1084/jem.20072713
82. Ciccia F, Guggino G, Rizzo A, Saieva L, Peralta S, Giardina A, et al. Type 3 Innate Lymphoid Cells Producing IL-17 and IL-22 Are Expanded in the Gut, in the Peripheral Blood, Synovial Fluid and Bone Marrow of Patients With Ankylosing Spondylitis. *Ann Rheum Dis* (2015) 74:1739–47. doi: 10.1136/annrheumdis-2014-206323
83. Wang Y, Wiesnoski DH, Helmink BA, Gopalakrishnan V, Choi K, DuPont HL, et al. Fecal Microbiota Transplantation for Refractory Immune Checkpoint Inhibitor-Associated Colitis. *Nat Med* (2018) 24:1804–8. doi: 10.1038/s41591-018-0238-9
84. Fasanello MK, Robillard KT, Boland PM, Bain AJ, Kanehira K. Use of Fecal Microbial Transplantation for Immune Checkpoint Inhibitor Colitis. *ACG Case Rep J* (2020) 7:e00360. doi: 10.14309/crj.0000000000000360
85. Coutzac C, Adam J, Soularue E, Collins M, Racine A, Mussini C, et al. Colon Immune-Related Adverse Events: Anti-CTLA-4 and Anti-PD-1 Blockade Induce Distinct Immunopathological Entities. *J Crohn's Colitis* (2017) 11:1238–46. doi: 10.1093/ecco-jcc/jjx081
86. Gonzalez RS, Salaria SN, Bohannon CD, Huber AR, Feely MM, Shi C. PD-1 Inhibitor Gastroenterocolitis: Case Series and Appraisal of 'Immunomodulatory Gastroenterocolitis. *Histopathology* (2017) 70:558–67. doi: 10.1111/his.13118
87. Dougan M. Checkpoint Blockade Toxicity and Immune Homeostasis in the Gastrointestinal Tract. *Front Immunol* (2017) 8:1547. doi: 10.3389/fimmu.2017.01547
88. von Euw E, Chodon T, Attar N, Jalil J, Koya RC, Comin-Anduix B, et al. CTLA4 Blockade Increases Th17 Cells in Patients With Metastatic Melanoma. *J Transl Med* (2009) 7:1–13. doi: 10.1186/1479-5876-7-35
89. Yoshino K, Nakayama T, Ito A, Sato E, Kitano S. Severe Colitis After PD-1 Blockade With Nivolumab in Advanced Melanoma Patients: Potential Role of Th1-Dominant Immune Response in Immune-Related Adverse Events: Two Case Reports. *BMC Cancer* (2019) 19:1–7. doi: 10.1186/s12885-019-6138-7
90. Reynoso ED, Elpek KG, Francisco L, Bronson R, Bellemare-Pelletier A, Sharpe AH, et al. Intestinal Tolerance Is Converted to Autoimmune Enteritis Upon PD-1 Ligand Blockade. *J Immunol* (2009) 182:2102–12. doi: 10.4049/jimmunol.0802769
91. Beswick EJ, Johnson JR, Saada JI, Humen M, House J, Dann S, et al. TLR4 Activation Enhances the PD-L1–Mediated Tolerogenic Capacity of Colonic CD90 + Stromal Cells. *J Immunol* (2014) 193:2218–29. doi: 10.4049/jimmunol.1203441
92. Zamani MR, Aslani S, Salmaninejad A, Javan MR, Rezaei N. PD-1/PD-L and Autoimmunity: A Growing Relationship. *Cell Immunol* (2016) 310:27–41. doi: 10.1016/j.cellimm.2016.09.009
93. Barnes MJ, Griseri T, Johnson AMF, Young W, Powrie F, Izcue A. CTLA-4 Promotes Foxp3 Induction and Regulatory T Cell Accumulation in the Intestinal Lamina Propria. *Mucosal Immunol* (2013) 6:324–34. doi: 10.1038/mi.2012.75
94. Tarhini AA, Zahoor H, Lin Y, Malhotra U, Sander C, Butterfield LH, et al. Baseline Circulating IL-17 Predicts Toxicity While TGF-β1 and IL-10 Are

Prognostic of Relapse in Ipilimumab Neoadjuvant Therapy of Melanoma. *J Immunother Cancer* (2015) 3:15–20. doi: 10.1186/s40425-015-0081-1
95. Bagley SJ, Kothari S, Aggarwal C, Bauml JM, Alley EW, Evans TL, et al. Pretreatment Neutrophil-to-Lymphocyte Ratio as a Marker of Outcomes in Nivolumab-Treated Patients With Advanced Non-Small-Cell Lung Cancer. *Lung Cancer* (2017) 106:1–7. doi: 10.1016/j.lungcan.2017.01.013
96. Ferrucci PF, Gandini S, Battaglia A, Alfieri S, Di Giacomo AM, Giannarelli D, et al. Baseline Neutrophil-to-Lymphocyte Ratio Is Associated With Outcome of Ipilimumab-Treated Metastatic Melanoma Patients. *Br J Cancer* (2015) 112:1904–10. doi: 10.1038/bjc.2015.180
97. Ferrucci PF, Ascierto PA, Pigozzo J, Del Vecchio M, Maio M, Antonini Cappellini GC, et al. Baseline Neutrophils and Derived Neutrophilto-Lymphocyte Ratio: Prognostic Relevance in Metastatic Melanoma Patients Receiving Ipilimumab. *Ann Oncol* (2016) 27:732–8. doi: 10.1093/annonc/mdw016
98. Matsukane R, Watanabe H, Minami H, Hata K, Suetsugu K, Tsuji T, et al. Continuous Monitoring of Neutrophils to Lymphocytes Ratio for Estimating the Onset, Severity, and Subsequent Prognosis of Immune Related Adverse Events. *Sci Rep* (2021) 11:1–11. doi: 10.1038/s41598-020-79397-6
99. Ksienski D, Wai ES, Alex D, Croteau NS, Freeman AT, Chan A, et al. Prognostic Significance of the Neutrophil-to-Lymphocyte Ratio and Platelet-to-Lymphocyte Ratio for Advanced Non-Small Cell Lung Cancer Patients With High PD-L1 Tumor Expression Receiving Pembrolizumab. *Transl Lung Cancer Res* (2021) 10:355–67. doi: 10.21037/tlcr-20-541
100. Grover S, Dougan M, Tyan K, Giobbie-Hurder A, Blum SM, Ishizuka J, et al. Vitamin D Intake Is Associated With Decreased Risk of Immune Checkpoint Inhibitor-Induced Colitis. *Cancer* (2020) 126:3758–67. doi: 10.1002/cncr.32966
101. Bai M, Grieshaber-Bouyer R, Wang J, Schmider AB, Wilson ZS, Zeng L, et al. CD177 Modulates Human Neutrophil Migration Through Activation-Mediated Integrin and Chemoreceptor Regulation. *Blood* (2017) 130:2092–100. doi: 10.1182/blood-2017-03-768507
102. Shahabi V, Berman D, Chasalow SD, Wang L, Tsuchihashi Z, Hu B, et al. Gene Expression Profiling of Whole Blood in Ipilimumab-Treated Patients for Identification of Potential Biomarkers of Immune-Related Gastrointestinal Adverse Events. *J Transl Med* (2013) 11:1–11. doi: 10.1186/1479-5876-11-75
103. Sipponen T. Diagnostics and Prognostics of Inflammatory Bowel Disease With Fecal Neutrophil-Derived Biomarkers Calprotectin and Lactoferrin. *Dig Dis* (2013) 31:336–44. doi: 10.1159/000354689
104. Vogl T, Tenbrock K, Ludwig S, Leukert N, Ehrhardt C, Van Zoelen MAD, et al. Mrp8 and Mrp14 Are Endogenous Activators of Toll-Like Receptor 4, Promoting Lethal, Endotoxin-Induced Shock. *Nat Med* (2007) 13:1042–9. doi: 10.1038/nm1638
105. Voganatsi A, Panyutich A, Miyasaki K, Murthy R. Mechanism of Extracellular Release of Human Neutrophil Calprotectin Complex Abstract : Calprotectin Is an Abundant Cytosolic Protein Complex of Human Neutrophils With *In Vitro* Extracellular Antimicrobial Activity. Studies Suggest Particulate Stimuli. *J Leukoc Biol* (2001) 70:130–4. doi: 10.1189/jlb.70.1.130
106. Anderson MC, Chaze T, Coïc YM, Injarabian L, Jonsson F, Lombion N, et al. MUB 40 Binds to Lactoferrin and Stands as a Specific Neutrophil Marker. *Cell Chem Biol* (2018) 25:483–93.e9. doi: 10.1016/j.chembiol.2018.01.014
107. Abu-Sbeih H, Ali FS, Luo W, Qiao W, Raju GS, Wang Y. Importance of Endoscopic and Histological Evaluation in the Management of Immune Checkpoint Inhibitor-Induced Colitis 11 Medical and Health Sciences 1103 Clinical Sciences. *J Immunother Cancer* (2018) 6:1–11. doi: 10.1186/s40425-018-0411-1
108. Bergqvist V, Hertervig E, Gedeon P, Kopljar M, Griph H, Kinhult S, et al. Vedolizumab Treatment for Immune Checkpoint Inhibitor-Induced Enterocolitis. *Cancer Immunol Immunother* (2017) 66:581–92. doi: 10.1007/s00262-017-1962-6
109. Zou F, Wang X, Glitza IC, Mcquade JL, Wang J, Zhang HC, et al. Fecal Calprotectin Concentration to Assess Endoscopic and Histologic Remission in Patients With Cancer With Immune-Mediated Diarrhea and Colitis. *J Immunother Cancer* (2021) 9:1–8. doi: 10.1136/jitc-2020-002058
110. Brahmer JR, Lacchetti C, Schneider BJ, Atkins MB, Brassil KJ, Caterino JM, et al. Management of Immune-Related Adverse Events in Patients Treated With Immune Checkpoint Inhibitor Therapy: American Society of Clinical Oncology Clinical Practice Guidelines. *J Clin Oncol* (2018) 17:3246–58. doi: 10.1200/JCO.2017.77.6385.Corresponding
111. Theede K, Holck S, Ibsen P, Kallemose T, Nordgaard-Lassen I, Nielsen AM. Fecal Calprotectin Predicts Relapse and Histological Mucosal Healing in Ulcerative Colitis. *Inflamm Bowel Dis* (2016) 22:1042–8. doi: 10.1097/MIB.0000000000000736
112. Kayazawa M, Saitoh O, Kojima K, Nakagawa K, Tanaka S, Tabata K, et al. Lactoferrin in Whole Gut Lavage Fluid as a Marker for Disease Activity in Inflammatory Bowel Disease: Comparison With Other Neutrophil-Derived Proteins. *Am J Gastroenterol* (2002) 97:360–9. doi: 10.1016/S0002-9270(01)04032-1
113. Dubin K, Callahan MK, Ren B, Khanin R, Viale A, Ling L, et al. Intestinal Microbiome Analyses Identify Melanoma Patients at Risk for Checkpoint-Blockade-Induced Colitis. *Nat Commun* (2016) 7:10391. doi: 10.1038/ncomms10391
114. Chaput N, Lepage P, Coutzac C, Soularue E, Le Roux K, Monot C, et al. Baseline Gut Microbiota Predicts Clinical Response and Colitis in Metastatic Melanoma Patients Treated With Ipilimumab. *Ann Oncol* (2017) 28:1368–79. doi: 10.1093/annonc/mdx108
115. Liu T, Xiong Q, Li L, Hu Y. Intestinal Microbiota Predicts Lung Cancer Patients at Risk of Immune-Related Diarrhea. *Immunotherapy* (2019) 11:385–96. doi: 10.2217/imt-2018-0144
116. Tastan C, Karhan E, Zhou W, Fleming E, Voigt AY, Yao X, et al. Tuning of Human MAIT Cell Activation by Commensal Bacteria Species and MR1-Dependent T-Cell Presentation. *Mucosal Immunol* (2018) 11:1591–605. doi: 10.1038/s41385-018-0072-x
117. Alexander ET, Minton A, Peters MC, Phanstiel O, Gilmour SK. A Novel Polyamine Blockade Therapy Activates an Anti-Tumor Immune Response. *Oncotarget* (2017) 8:84140–52. doi: 10.18632/oncotarget.20493
118. Hayes CS, Shicora AC, Keough MP, Snook AE, Burns MR, Gilmour SK. Polyamine-Blocking Therapy Reverses Immunosuppression in the Tumor Microenvironment. *Cancer Immunol Res* (2014) 2:274–85. doi: 10.1158/2326-6066.CIR-13-0120-T
119. Reich KM, Fedorak RN, Madsen K, Kroeker KI. Vitamin D Improves Inflammatory Bowel Disease Outcomes: Basic Science and Clinical Review. *World J Gastroenterol* (2014) 20:4934–47. doi: 10.3748/wjg.v20.i17.4934
120. Meeker S, Seamons A, Maggio-Price L, Paik J. Protective Links Between Vitamin D, Inflammatory Bowel Disease and Colon Cancer. *World J Gastroenterol* (2016) 22:933–48. doi: 10.3748/wjg.v22.i3.933
121. Fletcher J, Cooper SC, Ghosh S, Hewison M. The Role of Vitamin D in Inflammatory Bowel Disease: Mechanism to Management. *Nutrients* (2019) 11(5):1019. doi: 10.3390/nu11051019
122. Jing Y, Liu J, Ye Y, Pan L, Deng H, Wang Y, et al. Multi-Omics Prediction of Immune-Related Adverse Events During Checkpoint Immunotherapy. *Nat Commun* (2020) 11:1–7. doi: 10.1038/s41467-020-18742-9
123. von Itzstein MS, Khan S, Gerber DE. Investigational Biomarkers for Checkpoint Inhibitor Immune-Related Adverse Event Prediction and Diagnosis. *Clin Chem* (2020) 66:779–93. doi: 10.1093/clinchem/hvaa081
124. Hommes JW, Verheijden RJ, Suijkerbuijk KPM, Hamann D. Biomarkers of Checkpoint Inhibitor Induced Immune-Related Adverse Events—a Comprehensive Review. *Front Oncol* (2021) 10:585311. doi: 10.3389/fonc.2020.585311
125. Haanen JBAG, Carbonnel F, Robert C, Kerr KM, Peters S, Larkin J, et al. Management of Toxicities From Immunotherapy: ESMO Clinical Practice Guidelines for Diagnosis, Treatment and Follow-Up. *Ann Oncol* (2017) 28:iv119–42. doi: 10.1093/annonc/mdx225
126. Thompson JA, Schneider BJ, Brahmer J, Andrews S, Armand P, Bhatia S, et al. Management of Immunotherapy-Related Toxicities, Version 1.2019. *JNCCN J Natl Compr Cancer Netw* (2019) 17:255–89. doi: 10.6004/jnccn.2019.0013
127. Youssef J, Novosad SA, Winthrop KL. Infection Risk and Safety of Corticosteroid Use. *Rheum Dis Clin North Am* (2016) 42:157–76. doi: 10.1016/j.rdc.2015.08.004
128. Siegel CA, Hur C, Korzenik JR, Gazelle GS, Sands BE. Risks and Benefits of Infliximab for the Treatment of Crohn's Disease. *Clin Gastroenterol Hepatol* (2006) 4:1017–24. doi: 10.1016/j.cgh.2006.05.020
129. Verheijden RJ, May AM, Blank CU, Aarts MJB, Berkmortel FWPJVD, Eertwegh AJMVD, et al. Association of Anti-TNF With Decreased

Survival in Steroid Refractory Ipilimumab and Anti-PD1-Treated Patients in the Dutch Melanoma Treatment Registry. *Clin Cancer Res* (2020) 26:2268–74. doi: 10.1158/1078-0432.CCR-19-3322

130. Danylesko I, Bukauskas A, Paulson M, Peceliunas V, Gedde-Dahl d.y T, Shimoni A, et al. Anti-α4β7 Integrin Monoclonal Antibody (Vedolizumab) for the Treatment of Steroid-Resistant Severe Intestinal Acute Graft-Versus-Host Disease. *Bone Marrow Transplant* (2019) 54:987–93. doi: 10.1038/s41409-018-0364-5
131. Abu-Sbeih H, Ali FS, Wang X, Mallepally N, Chen E, Altan M, et al. Early Introduction of Selective Immunosuppressive Therapy Associated With Favorable Clinical Outcomes in Patients With Immune Checkpoint Inhibitor-Induced Colitis. *J Immunother Cancer* (2019) 7:1–11. doi: 10.1186/s40425-019-0577-1
132. Zou F, Shah AY, Glitza IC, Richards D, Thomas AS, Wang Y. S0137 Comparative Study of Vedolizumab and Infliximab Treatment in Patients With Immune-Mediated Diarrhea and Colitis. *Am J Gastroenterol* (2020) 115:S68. doi: 10.14309/ajg.0000000000000848
133. Johnson D, Patel AB, Uemura MI, Trinh VA, Jackson N, Zobniw CM, et al. IL17A Blockade Successfully Treated Psoriasiform Dermatologic Toxicity From Immunotherapy. *Cancer Immunol Res* (2019) 7:860–5. doi: 10.1158/2326-6066.CIR-18-0682
134. Hueber W, Sands BE, Lewitzky S, Vandemeulebroecke M, Reinisch W, Higgins PDR, et al. Secukinumab, a Human Anti-IL-17A Monoclonal Antibody, for Moderate to Severe Crohn's Disease: Unexpected Results of a Randomised, Double-Blindplacebo- Controlled Trial. *Gut* (2012) 61:1693–700. doi: 10.1136/gutjnl-2011-301668
135. Sands BE, Sandborn WJ, Panaccione R, O'Brien CD, Zhang H, Johanns J, et al. Ustekinumab as Induction and Maintenance Therapy for Ulcerative Colitis. *N Engl J Med* (2019) 381:1201–14. doi: 10.1056/nejmoa1900750
136. Bishu S, Melia J, Sharfman W, Lao CD, Fecher LA, Higgins PDR. Efficacy and Outcome of Tofacitinib in Immune Checkpoint Inhibitor Colitis. *Gastroenterology* (2021) 160:932–34.e3. doi: 10.1053/j.gastro.2020.10.029
137. Esfahani K, Hudson M, Batist G. Tofacitinib for Refractory Immune-Related Colitis From PD-1 Therapy. *N Engl J Med* (2020) 382:2374–5. doi: 10.1056/nejmc2010419
138. Fernández-Clotet A, Castro-Poceiro J, Panés J. Tofacitinib for the Treatment of Ulcerative Colitis. *Expert Rev Clin Immunol* (2018) 14:881–92. doi: 10.1080/1744666X.2018.1532291
139. Nguyen TT, Ramsay L, Ahanfeshar-Adams M, Lajoie M, Schadendorf D, Alain T, et al. Mutations in the IFNγ-JAK-STAT Pathway Causing Resistance to Immune Checkpoint Inhibitors in Melanoma Increase Sensitivity to Oncolytic Virus Treatment. *Clin Cancer Res* (2021) 27(12):3432–42. doi: 10.1158/1078-0432.ccr-20-3365. clincanres.3365.2020.
140. Voth E, Khanna S. Fecal Microbiota Transplantation for Treatment of Patients With Recurrent Clostridioides Difficile Infection. *Expert Rev Anti Infect Ther* (2020) 18:669–76. doi: 10.1080/14787210.2020.1752192
141. Alfaleh K, Anabrees J. Probiotics for Prevention of Necrotizing Enterocolitis in Preterm Infants. *Evidence-Based Child Heal* (2014) 9:584–671. doi: 10.1002/ebch.1976
142. Vétizou M, Pitt JM, Daillère R, Lepage P, Waldschmitt N, Flament C, et al. Anticancer Immunotherapy by CTLA-4 Blockade Relies on the Gut Microbiota. *Science* (2015) 350:1079–84. doi: 10.1126/science.aad1329
143. Routy B, Le Chatelier E, Derosa L, Duong CPM, Alou MT, Daillère R, et al. Gut Microbiome Influences Efficacy of PD-1-Based Immunotherapy Against Epithelial Tumors. *Science* (2018) 359:91–7. doi: 10.1126/science.aan3706
144. van Dijk N, Gil-Jimenez A, Silina K, Hendricksen K, Smit LA, de Feijter JM, et al. Preoperative Ipilimumab Plus Nivolumab in Locoregionally Advanced Urothelial Cancer: The NABUCCO Trial. *Nat Med* (2020) 26:1839–44. doi: 10.1038/s41591-020-1085-z
145. Rozeman EA, Hoefsmit EP, Reijers ILM, Saw RPM, Versluis JM, Krijgsman O, et al. Survival and Biomarker Analyses From the Opacin-Neo and Opacin Neoadjuvant Immunotherapy Trials in Stage III Melanoma. *Nat Med* (2021) 27:256–63. doi: 10.1038/s41591-020-01211-7

Conflict of Interest: FH has served on advisory boards, as speaker, or consultant for AbbVie, Celgene, Janssen-Cilag, Merck Sharp & Dohme, Takeda, Celltrion, Teva, Sandoz, and Dr Falk, and has received unrestricted grants from Dr Falk, Janssen-Cilag, and AbbVie. MH received research grants from Merck and AstraZeneca. BP received fees from advisory boards of Takeda, Bristol-Myers Squibb, Janssen, and Pfizer. BP received lecturing fees from AstraZeneca and Pfizer.

The remaining authors declare that the research was conducted in the absence of any commercial or financial relationships that could be construed as a potential conflict of interest.

Publisher's Note: All claims expressed in this article are solely those of the authors and do not necessarily represent those of their affiliated organizations, or those of the publisher, the editors and the reviewers. Any product that may be evaluated in this article, or claim that may be made by its manufacturer, is not guaranteed or endorsed by the publisher.

frontiers in Immunology

ORIGINAL RESEARCH
published: 24 November 2021
doi: 10.3389/fimmu.2021.723293

Exploring the Prognostic Value, Immune Implication and Biological Function of *H2AFY* Gene in Hepatocellular Carcinoma

*Yongbiao Huang†, Shanshan Huang†, Li Ma, Yali Wang, Xi Wang, Lingyan Xiao, Wan Qin, Long Li and Xianglin Yuan**

Department of Oncology, Tongji Hospital, Tongji Medical College, Huazhong University of Science and Technology, Wuhan, China

Background: Hepatocellular carcinoma (HCC) is an extremely malignant cancer with poor survival. *H2AFY* gene encodes for a variant of H2A histone, and it has been found to be dysregulated in various tumors. However, the clinical value, biological functions and correlations with immune infiltration of *H2AFY* in HCC remain unclear.

Methods: We analyzed the expression and clinical significance of *H2AFY* in HCC using multiple databases, including Oncomine, HCCDB, TCGA, ICGC, and so on. The genetic alterations of *H2AFY* were analyzed by cBioPortal and COSMIC databases. Co-expression networks of *H2AFY* and its regulators were investigated by LinkedOmics. The correlations between *H2AFY* and tumor immune infiltration were explored using TIMER, TISIDB databases, and CIBERSORT method. Finally, *H2AFY* was knocked down with shRNA lentiviruses in HCC cell lines for functional assays *in vitro*.

Results: *H2AFY* expression was upregulated in the HCC tissues and cells. Kaplan–Meier and Cox regression analyses revealed that high *H2AFY* expression was an independent prognostic factor for poor survival in HCC patients. Functional network analysis indicated that *H2AFY* and its co-expressed genes regulates cell cycle, mitosis, spliceosome and chromatin assembly through pathways involving many cancer-related kinases and E2F family. Furthermore, we observed significant correlations between *H2AFY* expression and immune infiltration in HCC. *H2AFY* knockdown suppressed the cell proliferation and migration, promoted cycle arrest, and apoptosis of HCC cells *in vitro*.

Conclusion: Our study revealed that *H2AFY* is a potential biomarker for unfavorable prognosis and correlates with immune infiltration in HCC.

Keywords: hepatocellular carcinoma, *H2AFY*, prognosis, immune infiltration, biomarker

OPEN ACCESS

Edited by:
Yanhong Deng,
The Sixth Affiliated Hospital of Sun Yat-sen University, China

Reviewed by:
Shin-ichiro Fujii,
RIKEN Center for Integrative Medical Sciences (IMS), Japan
Yi Liao,
Affiliated Hospital of Southwest Medical University, China
Shushan Li,
University of Regensburg, Germany

***Correspondence:**
Xianglin Yuan
yuanxianglin@hust.edu.cn

†These authors have contributed equally to this work

Specialty section:
This article was submitted to Cancer Immunity and Immunotherapy, a section of the journal Frontiers in Immunology

Received: *10 June 2021*
Accepted: *02 November 2021*
Published: *24 November 2021*

Citation:
Huang Y, Huang S, Ma L, Wang Y, Wang X, Xiao L, Qin W, Li L and Yuan X (2021) Exploring the Prognostic Value, Immune Implication and Biological Function of H2AFY Gene in Hepatocellular Carcinoma. Front. Immunol. 12:723293. doi: 10.3389/fimmu.2021.723293

INTRODUCTION

Hepatocellular carcinoma (HCC) is the major pathological type of primary liver cancer, which is an extremely malignant and aggressive cancer with poor clinical outcome and high mortality rate (1, 2). Due to the abuse of alcohol, hepatitis virus infection, and nonalcoholic fatty liver disease, the morbidity of HCC is increasing, and it has gradually become one of the leading causes of cancer-related death worldwide (3, 4). Nowadays, the common treatment methods for HCC include curative surgical resection, liver transplantation, radiation therapy, chemotherapy, immune and molecular-targeted therapy, curative resection is still considered the preferred treatment choice for early HCC (5, 6). On account of lacking the early specific symptoms and effective biomarkers, most HCC patients were usually at an advanced stage when they were first diagnosed, and lost the opportunity for curative resection. Therefore, it is urgent to identify a novel and reliable biomarker which could be helpful for early diagnosis and prognosis prediction of HCC and even serve as a therapeutic target.

In recent years, a growing body of studies suggest that epigenetics regulation mechanisms such as DNA methylation, m6A modification, and histone variants are involved in initiation and development of various human diseases, especially tumorigenesis (7–9). Histone variants can replace their corresponding canonical histones within the nucleosome and alter the composition and structure of chromatin, thereby regulating various fundamental cellular biological processes, and, their dysregulation may lead to cancer initiation and progression (10–12). There are plenty of histone variants, but most of the histone variants are from the H2A histone family. The *H2AFY* gene encodes for H2A variants family member macroH2A1, which has two splicing variant isoforms, macroH2A1.1 and macroH2A1.2 respectively (13). Currently, the role for *H2AFY* in the tumorigenesis and progression of various solid tumors has drawn considerable attention, such as lung cancer, melanoma, breast cancer, colorectal carcinoma, bladder cancer, and gastric cancer, and it has been found to be dysregulated in these tumors (14–19).

Although *H2AFY* has been reported to be highly expressed in HCC which may lead to a lower survival and a poorer prognosis (20, 21), the biological function of *H2AFY* and its relationship with clinicopathological characteristics and tumor immune infiltrates in HCC remain largely unclear. In this study, we comprehensively investigated the expression level, mutations, diagnostic and prognostic significance of *H2AFY* in patients with HCC in various public databases, including Oncomine, HCCDB, The Cancer Genome Atlas (TCGA), International Cancer Genome Consortium (ICGC) and others. Furthermore, through a range of bioinformatics analyses, we explored the potential biological functions and gene regulatory networks correlated with *H2AFY* in HCC, and analyzed the correlation between *H2AFY* and infiltrating immune cells in tumor microenvironment. Additionally, we performed a series of functional assays to further evaluated the effects of *H2AFY* knockdown on HCC cell proliferation, migration, apoptosis, and cell cycle *in vitro*, and our results revealed that *H2AFY* regulates HCC development may in part through the regulation of STAT3 signaling.

MATERIALS AND METHODS

Data Acquisition and Processing

The RNA-seq data, corresponding clinical data, and survival information of HCC patients were obtained from the TCGA database (22), and the details were shown in **Table 1**.

Differential Expression Analysis of *H2AFY*

We used the Oncomine database to examine the expression of *H2AFY* in liver cancers and normal tissues, set the threshold as: *P*-value as 0.001, fold change (FC) as 1.5, and gene rank as top 10% (23). Besides, we also analyzed the *H2AFY* gene expression level in HCC *via* TIMER database based on TCGA data (24). The HCCDB database contains 15 public HCC datasets which were from the Gene Expression Omnibus (GEO), TCGA, and ICGC, and it was further used for verifying the differential expression of *H2AFY* between HCC and normal tissues (25).

Genetic Alteration and Survival Analysis

The cBioPortal database and the Catalogue of Somatic Mutations in Cancer (COSMIC) database were utilized to evaluate the alteration frequency and types of *H2AFY* in HCC (26, 27). In the TCGA-LIHC cohort, patients with complete follow-up information were included in survival analyses, Kaplan–Meier curves, receiver operating characteristic (ROC) curves, and Cox regression models were applied to determine the prognostic significance of *H2AFY*. Additionally, the impacts of *H2AFY* expression on overall survival of HCC patients were further validated in the ICGC dataset (LIRI-JP project), Kaplan–Meier Plotter, and GEPIA2 database (28, 29). GeneMANIA was applied to visualize the interaction network of *H2AFY* and predict their function (30).

Coexpression Analysis in LinkedOmics

LinkedOmics is an online analysis platform that contains multi-dimensional data of 32 TCGA cancer types (31). *H2AFY* co-expression statistical analysis was performed using Spearman correlation test in the "LinkFinder" module, the results were presented in volcano plot and heat maps. The survival heatmaps of top 50 co-expressed genes were plotted by GEPIA2 database. The GO annotation, KEGG pathways, kinase-target enrichment, miRNA-target enrichment, and transcription factor-target enrichment analyses were conducted by gene set enrichment analysis (GSEA) in the "LinkInterpreter" module. The simulations of 500 and the rank criterion was set as false discovery rate (FDR) <0.05.

GSEA Between *H2AFY* High- and Low-Expression Groups

GSEA analysis was carried out to detect different functional phenotypes between *H2AFY* high- and low-expression groups by

TABLE 1 | The clinical characteristics of patients in the TCGA-LIHC cohort.

Characteristic		Total (371)	Percentage (%)
Status			
	Dead	130	35.04%
	Live	241	64.96%
Age at diagnosis			
	≤65	232	62.53%
	>60	138	37.20%
	Unknown	1	0.27%
Gender			
	Female	121	32.61%
	Male	250	67.39%
Tumor stage			
	Stage I	171	46.09%
	Stage II	86	23.18%
	Stage III	85	22.91%
	Stage IV	5	1.35%
	Unknown	24	6.47%
T classification			
	T1	181	48.79%
	T2	94	25.34%
	T3	80	21.56%
	T4	13	3.50%
	Unknown	3	0.81%
Grade			
	G1	55	14.82%
	G2	177	47.72%
	G3	122	32.88%
	G4	12	3.23
	Unknown	5	1.35%

using GSEA software (v.4.0.3) based on the expression profile of the TCGA-LIHC dataset (32). KEGG gene set (c2.cp.kegg.v7.4.symbols.gmt) and GO_BP gene set (c5.go.bp.v7.4.symbols.gmt were) were used as the reference gene sets, and 1,000 random permutations were performed per analysis. Nominal *P*-value <0.05 and FDR <0.05 were regarded significant.

Immune Infiltration Analysis

We used the TIMER database to investigate the correlations between *H2AFY* expression, copy number alterations and the abundance of six major tumor-infiltrating immune cells in HCC. Besides, the correlations between *H2AFY* and immune cell marker genes and several key immune checkpoint genes were also analyzed through the "Correlation" module of TIMER and GEPIA2. Then, we compared the expression of these immune checkpoint genes between patients with high- and low-*H2AFY* expression. The distribution of *H2AFY* expression across immune subtypes were further explored in TISIDB database (33). The relative fractions of 22 immune cell types of patients in TCGA-LIHC cohort were calculated through CIBERSORT algorithm, presenting in bar graphs, heatmap, and violin plot (34, 35).

Cell Culture and Transfection

The human normal liver cell line L02 and HCC cell lines MHCC-97H, Hep3B, Huh7 and HepG2 were gifts from gastroenterology laboratory and hepatic surgery laboratory of the Tongji Hospital, Wuhan, China. Jurkat cell line was stored in oncology laboratory of the Tongji Hospital, Wuhan, China. L02 cells and Jurkat cells were cultured in RPMI 1640 medium (HyClone, USA) and other hepatoma cells was in DMEM medium (HyClone, USA), with 10% fetal bovine serum (FBS, Gibco, USA), at 37°C in 5% CO2 incubator. The lentiviral *H2AFY*-specific shRNA vectors and negative control (NC) were obtained from OBiO (Shanghai, China). Transfection was carried out with polybrene (OBiO, China). The sequences of H2AFY-shRNAs were listed: *H2AFY*-sh1, 5′-GGATGCTGCGGTACATCAA-3′; *H2AFY*-sh2, 5′-GCTGAAATCCATTGCATTT-3′; *H2AFY*-sh3, 5′-GCGAGAGTATAGGCATCTA-3′; and NC, 5′-TTCTCCGAACGTGTCACGT-3′.

qRT-PCR

Total RNA from cells was extracted using TRIzol reagent (TaKaRa, Japan) and reverse transcribed by Hi Script II QRT SuperMix (Vazyme, China). The qRT-PCR was carried out using ChamQ Universal SYBR qPCR Master Mix (Vazyme, China). All primers were listed as follows: H2AFY, Forward: CGGATGCTGCGGTACATCAA, Reverse: CTCCGCTGTCAGGTATTCCAG. GAPDH, Forward: GACAGTCAGCCGCATCTTCT, and Reverse: GCGCCCAATACGACCAAATC. GAPDH was utilized as internal control.

CCK8 Viability Assay

Cells (3,000 cells/well) were seeded in 96-well plates, after overnight attachment, the medium was changed to 100 µl FBS-free medium with 10% CCK8 (MCE, USA) in each well and incubated for 2 h at 37°C, then the OD values at 450 nm were detected through microplate reader (BioTek, USA). These steps were repeated at 0, 24, 48, and 72 h, and the relative absorbance was calculated based on the OD values at 0 h.

Clone Formation Assay

Cells (2,000 cells/well) were seeded in 6-well plates and cultured until visible clones appeared. Then we used methanol to fix clones 15 min, 1% crystal violet to stain clones 20 min, and counted the number of clones (>50 cells).

Cell Apoptosis and Cell Cycle Assays

For cell apoptosis assay, cells were collected by EDTA-free trypsin, washed with PBS for three times, and resuspended in binding buffer. After incubation with PI and Annexin V-APC (BD Biosciences, USA) in dark for 15 min, the cell apoptosis was examined through flow cytometer (BD, Biosciences, USA) and analyzed by FlowJo 10.6.2. For cell cycle assay, cells were collected and fixed in 70% ethanol at 4°C overnight, then stained as the protocol of the cell cycle staining kit (MultiSciences, China). The cell cycle was examined using flow cytometer and analyzed by Modfit LT software.

Wound Healing Assay

Cells were seeded in 6-well plates with serum-free DMEM and cultured to 100% density, and then the scratch wounds were created using 10 µl pipette tips. Images of wounds were captured at 0, 24, and 48 h, the area of wounds was quantified by ImageJ software (40×).

Transwell For Migration Assay

For transwell migration assay, 4×10^4 cells were seeded on the upper transwell chambers in 200 µl serum-free culture medium, and 600 µl medium containing 20% FBS was added to the lower chambers. After 40 h incubation, the cells that migrated through membranes were fixed with methanol, stained with 1% crystal violet and counted under light microscope (200×).

Western Blot

Total cellular protein was extracted with RIPA lysis buffer (Servicebio, China), denatured by mixing 5× loading buffer and boiling for 5 min. Then the denatured protein was subjected to SDS/polyacrylamide-gel electrophoresis and transferred to 0.45 µm polyvinylidene fluoride membranes. The membranes were blocked in 5% nonfat milk for 1 h at room temperature, and subsequently incubated with the following primary antibodies: H2AFY (Abcam, CAT# ab183041, 1:10,000), Cyclin B1 (Proteintech, CAT# 28603-1-AP, 1:1,000), Cyclin D1 (Proteintech, CAT# 26939-1-AP, 1:1,000), E-Cadherin (Cell Signaling Technology, CAT# 3195, 1:1,000), Vimentin (Cell Signaling Technology, CAT# 5741, 1:1,000), Bcl-2 (Cell Signaling Technology, CAT# 4223, 1:1,000), STAT3 (Cell Signaling Technology, CAT# 9139, 1:1,000), p-STAT3 (Cell Signaling Technology, CAT# 9145, 1:1,000), and α-Tublin (Proteintech, CAT# 11224-1-AP, 1:5,000) at 4°C overnight. Next, the membranes were washed with TBST three times, each for 10 min and incubated with secondary antibodies at room temperature for 1 h. Finally, the indicated proteins were visualized by West Pico plus Chemiluminescent Substrate (Thermo Fisher Scientific, USA).

Statistical Analysis

All data of this study were statistically analyzed by R software 3.6.1 and Prism 8.0. The Wilcoxon test or Kruskal–Wallis test were used to examine the mRNA expression levels of *H2AFY* in different clinical subgroups, logistic regression was conducted to analyze the association of the *H2AFY* expression and clinicopathological characteristics. The Kaplan–Meier method and log-rank test were applied for comparing overall survival. Correlation analyses were performed by Spearman correlation test. For experimental data, Student's t-test was used to determine the differences between two groups. P <0.05 was regarded statistically significant.

RESULTS

High *H2AFY* Expression in HCC

We initially analyzed *H2AFY* mRNA expression levels in multiple public databases to examine *H2AFY* expression in HCC. Data from the Oncomine database revealed that *H2AFY* expression was dramatically higher in HCC tissues than normal tissues (FC >1.5, P <0.01), and ranked within the top 10% (**Figure 1A** and **Figure S1**). Meanwhile, the upregulation of *H2AFY* in HCC compared with normal tissues was also observed in TIMER database (**Figure 1B**). In the HCCDB database, analysis of ten HCC cohorts further verified that *H2AFY* was significantly upregulated in HCC (**Figure 1C**).

Association With *H2AFY* Expression and Clinical Variables

Based on the *H2AFY* expression data and clinical information from TCGA, a total of 371 HCC patients were analyzed. The *H2AFY* expression in younger patients (≤65 years) was significantly higher than patients older than 65 years (P = 0.031, **Figure 2A**). Dead patients presented increased *H2AFY* expression compared to alive patients (P = 0.004). *H2AFY* expression was increased in dead patients compared to alive patients (P = 0.004, **Figure 2B**), increased in female compared to male (P = 0.004, **Figure 2C**).

Besides, *H2AFY* expression increased with the histological grade (P = 6.562e−08, **Figure 2D**) and T classification (P = 0.016, **Figure 2F**). As shown in **Figure 2E**, the *H2AFY* expression levels were significant different in the subgroups of clinical stage (P = 0.01). In logistic regression analysis, *H2AFY* expression as a dependent categorical variable (according to the median value), the results indicated that increased *H2AFY* expression in HCC was prominently associated with age (OR = 1.669 for ≤65 *vs.* >65, P = 0.018), survival status (OR = 1.624 for dead *vs.* alive, P = 0.027), histological grade (OR = 3.394 for G3–G4 *vs.* G1–G2, P <0.0001), T classification (OR = 1.590 for T2–T3 *vs.* T1, P = 0.030; OR = 4.304 for T4 *vs.* T1, P = 0.031), clinical stage (OR = 1.638 for stages II–III *vs.* stage I, P = 0.024; OR = 1.784 for stage III *vs.* stage I, P <0.031) (**Table 2**).

Genetic Alterations of *H2AFY* in HCC

In the cBioPortal database, we evaluated the alteration (copy-number alteration and mutation) types and frequency of *H2AFY* in HCC. The TCGA–Firehose Legacy dataset was selected for analysis, which included 360 samples with complete DNA sequencing data. The alteration frequency of *H2AFY* was 1.1% in HCC, which include amplification in two cases, missense mutation in two cases (**Figure 3A**). The detailed mutation landscapes were showed in **Figure 3B**. Since the alteration frequency was relatively low, we failed to explore the association between *H2AFY* genetic alteration and the survival of HCC patients. In addition, we further evaluated the mutation types of *H2AFY* in another database, COSMIC. The mutation types of *H2AFY* were clearly displayed in two pie charts (**Figures 3C, D**). Approximately seven (10.29%) of the 68 samples had missense substitutions, two (2.94%) of the 68 samples had synonymous substitutions, and seven (8.82%) of the 68 samples had other mutations (**Figure 3C**). The substitution mutations mainly included A > C (22.22%), C > A (22.22%), G > A (22.22%), followed by A > G (11.11%), C > T (11.11%), and G > T (11.11%) (**Figure 3D**).

Prognostic Significance of *H2AFY* in HCC

Then, we explore the role of *H2AFY* in HCC patients' survival outcomes in multiple databases. Based on the median *H2AFY* expression value, the HCC patients were split into high- and low-*H2AFY* expression groups. In the TCGA-LIHC cohort, Kaplan–Meier survival curves indicated that patients with high

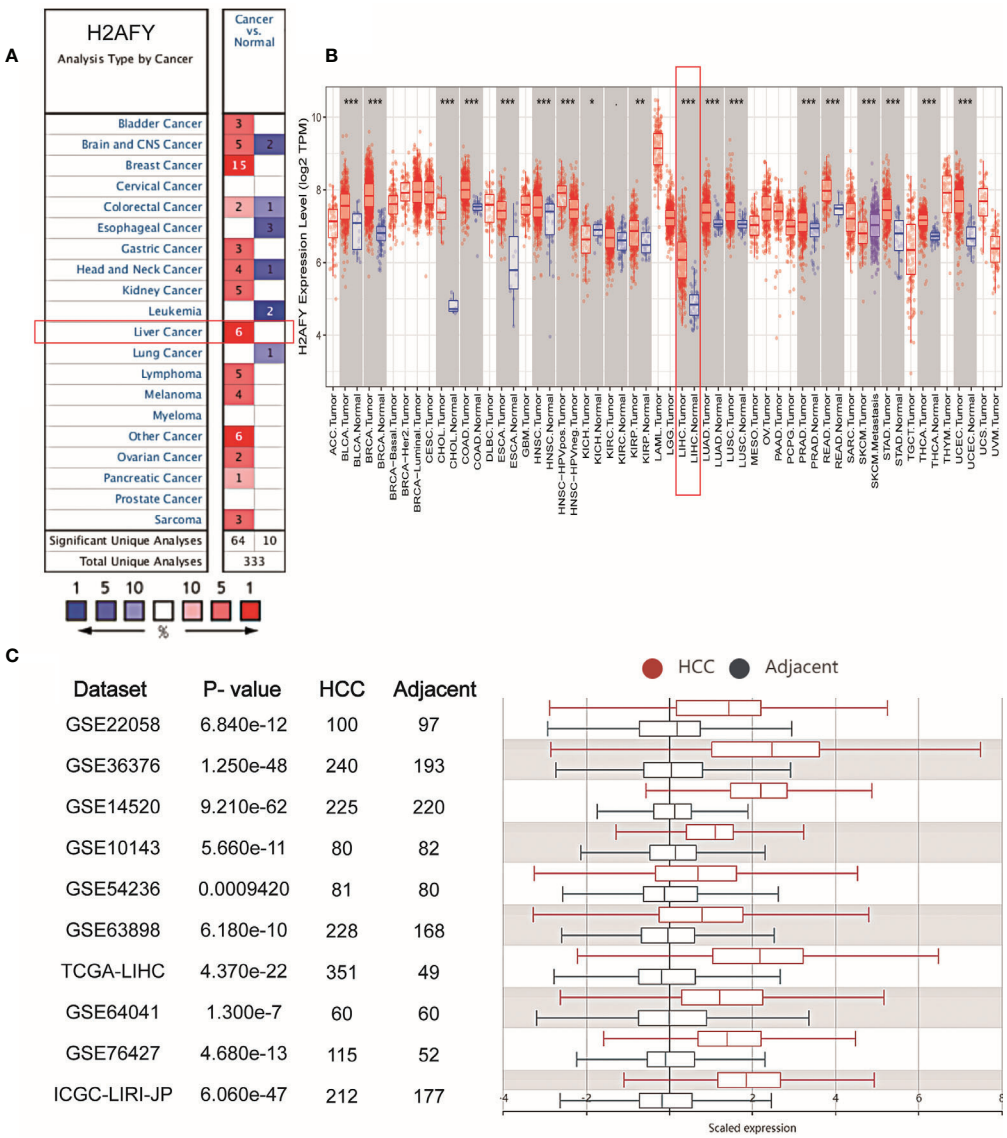

Dataset	P- value	HCC	Adjacent
GSE22058	6.840e-12	100	97
GSE36376	1.250e-48	240	193
GSE14520	9.210e-62	225	220
GSE10143	5.660e-11	80	82
GSE54236	0.0009420	81	80
GSE63898	6.180e-10	228	168
TCGA-LIHC	4.370e-22	351	49
GSE64041	1.300e-7	60	60
GSE76427	4.680e-13	115	52
ICGC-LIRI-JP	6.060e-47	212	177

FIGURE 1 | The elevated *H2AFY* expression in HCC. **(A)** Upregulated or downregulated *H2AFY* expression in different cancer types (Oncomine database, red color—upregulation, blue color—downregulation). **(B)** *H2AFY* expression levels in different tumor tissues and normal tissues (TIMER database). **(C)** Comparing the *H2AFY* expression between HCC and adjacent tissues in ten HCC cohorts (HCCDB database) $^{*}P < 0.05$; $^{**}P < 0.01$; $^{***}P < 0.001$.

H2AFY expression tended to have poor overall survival (log-rank P <0.001, **Figure 4A**), time-dependent ROC curves indicated that *H2AFY* had moderate sensitivity and specificity for predicting survival (**Figure 4B**). Further univariate and multivariate Cox regression analyses revealed that *H2AFY* could function as a prognostic indicator independent of other clinical parameters for HCC patients (**Figures 4C, D**). In the ICGC cohort, the similar results were observed (**Figures 4E, F**). Besides, we verified the prognostic significance of *H2AFY* through K–M plotter and GEPIA online databases, the results also indicated that high *H2AFY* expression was associated poor survival (log-rank P <0.001, **Figures 4G, H**).

H2AFY Co-Expression Networks in HCC

The co-expression pattern of *H2AFY* was explored in TCGA-LIHC cohort through LinkedOmics (Table S1). As presented in **Figure 5A**, a total of 7,201 genes positively correlated with *H2AFY* and 2,928 genes negatively correlated with *H2AFY* were identified (FDR <0.01). The top 50 positively and negatively correlated genes were presented in heat maps (**Figure 5B**). *H2AFY* expression exhibited a strong positive correlation with the expression of *CEP55* (positive rank #1, r = 0.663, FDR = 2.14E−44), *CCNB1* (r = 0.659, FDR = 7.55E−44) and *DEPDC1B* (r = 0.637, FDR = 6.98E−40), etc. Remarkably, the top 50 positively correlated genes had high probability of being

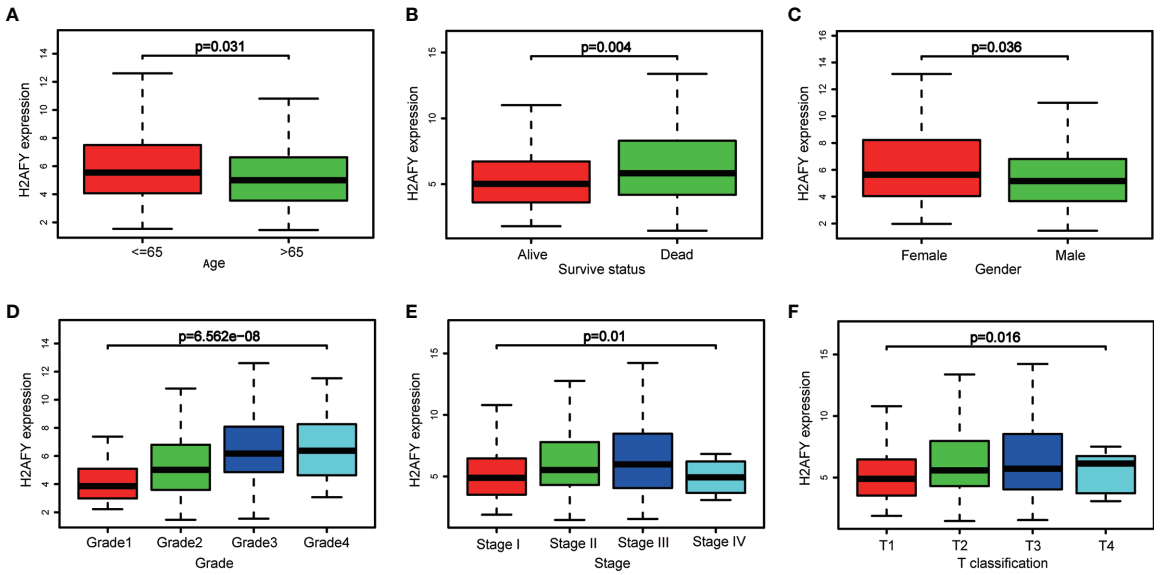

FIGURE 2 | *H2AFY* expression in sub-groups of different clinical characteristics. Subgroup analyses of *H2AFY* expression based on **(A)** age, **(B)** survive status, **(C)** gender, **(D)** histological grade, **(E)** tumor stage, and **(F)** T classification.

high-risk markers in HCC, of which 45/50 genes owned high hazard ratio (HR, P <0.05). Conversely, 23/50 genes were with low HR (P <0.05) in the top 50 negatively correlated genes (**Figure 5C**). The results of GO enrichment analysis by GSEA suggested that *H2AFY* co-expressed genes participate mainly in microtubule cytoskeleton organization involved in mitosis, organelle fission, kinetochore organization, chromosome segregation, cell cycle G2/M phase transition and regulation of cell cycle phase transition. (**Figure 5D** and **Table S2**). KEGG pathway analysis revealed enrichment in the cell cycle, homologous recombination, DNA replication, spliceosome, and mRNA surveillance pathway. (**Figure 5D** and **Table S3**). All these findings indicated the important roles of *H2AFY* and its co-expressed genes in cell cycle regulation for HCC progression.

Regulators of *H2AFY* Networks in HCC

To determine the regulatory factors of *H2AFY* in HCC, we further analyzed the kinase, miRNA, and transcription factor targets' enrichment of *H2AFY* co-expressed genes using GSEA. The top five most significant kinase-target networks were related mainly to *PLK1*, *CDK1*, *CHEK1*, *AURKB*, and *CDK2* (**Table 3** and **Table S4**). Interestingly, no significant miRNA targets were

TABLE 2 | Correlations between H2AFY expression and clinicopathological parameters by logistic regression.

Clinicopathological parameters	Total	Odds ratio in H2AFY expression	P-value
Age			
≤65 *vs* >65	370	1.669 (1.092–2.564)	**0.018**
Gender			
Female *vs* Male	371	1.198 (0.775–1.852)	0.417
Survival status			
Dead *vs* Alive	371	1.624 (1.058–2.505)	**0.027**
Histological grade			
G3–G4 *vs* G1–G2	366	3.394 (2.176–5.361)	**<0.001**
T classification			
T2 *vs* T1	275	1.531 (0.929–2.535)	0.095
T3 *vs* T1	261	1.578 (0.931–2.690)	0.091
T4 *vs* T1	194	4.304 (1.268–19.669)	**0.031**
T2–T3 *vs* T1	355	1.590 (1.047–2.423)	**0.030**
TNM stage			
II *vs* I	257	1.580 (0.939–2.670)	0.085
III *vs* I	256	1.784 (1.057–3.034)	**0.031**
IV *vs* I	176	1.966 (0.318–15.213)	0.465
II-III *vs* I	342	1.638 (1.070–2.517)	**0.023**

Bold values indicates P-value < 0.05.

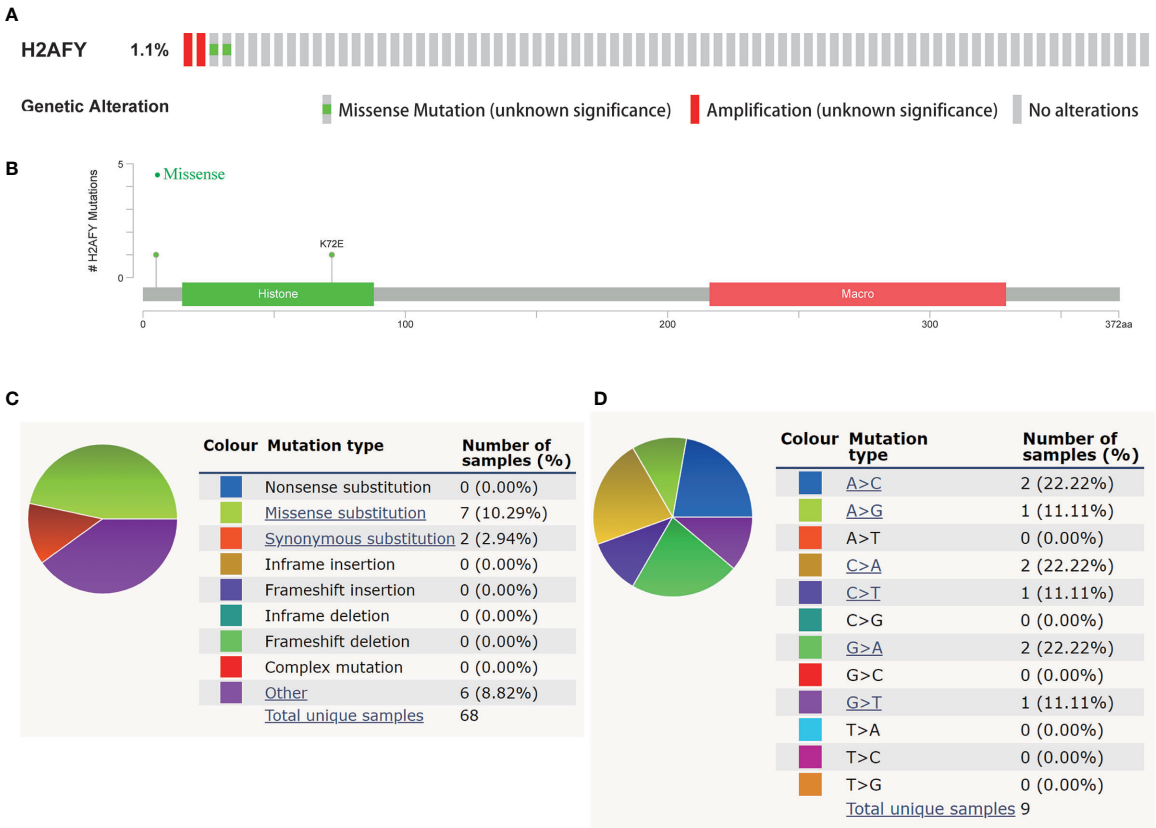

FIGURE 3 | Genetic alterations of *H2AFY* in HCC. **(A)** OncoPrint of *H2AFY* alterations in TCGA-LIHC cohort (cBioPortal). **(B)** Schematic presentation of *H2AFY* mutations in TCGA-LIHC cohort (cBioPortal). **(C, D)** The mutation types of *H2AFY* in HCC (Catalogue of Somatic Mutations in Cancer (COSMIC) database).

enriched for *H2AFY* co-expressed genes (**Table 3** and **Table S5**). The significantly enriched transcription factor-targets were associated primarily with E2F transcription factor family (**Table 3** and **Table S6**), including V$E2F_Q4, V$E2F_Q6, V$E2F_02, V$E2F1DP1_01, and V$E2F1DP2_01.

GSEA Between High- and Low-*H2AFY* Expression Groups

To explore the biological processes and signaling pathways that *H2AFY* may regulate, GSEA was performed between high- and low-*H2AFY* expression groups using TCGA-LIHC transcriptome data. We found some immune-related and cancer-related processes and pathways were significantly gathered in high-*H2AFY* expression group (**Figures 6A, C**), such as activation of innate immune response, innate immune response activating cell surface receptor signaling pathway, T-cell activation involved in immune response, B-cell activation involved in immune response, T-cell differentiation involved in immune response, lymphocyte activation of immune response, pathways in cancer, cell cycle, apoptosis and T-cell receptor signaling pathway, these results implied that *H2AFY* might be involved in immune response and impact immune infiltration. However, multiple metabolic processes like drug catabolic process, fatty acid catabolic process, lipid oxidation, drug metabolism cytochrome P450, and fatty acid metabolism were activated in low-*H2AFY* expression group (**Figures 6B, D**).

Association Between *H2AFY* Expression and Immune Infiltration

Then, we investigate the correlation between *H2AFY* expression and immune infiltration levels in HCC through TIMER database. The results revealed that a significant positive correlation between *H2AFY* expression and infiltration level of B cells (r = 0.441, P = 8.99e−18), CD8+ T cells (r = 0.292, P = 3.85e−08), CD4+ T cells (r = 0.442, P = 7.57e−18), Macrophages (r = 0.554, P = 8.38e−29), Neutrophils (r = 0.455, P = 4.84e−19), and Dendritic cells (r = 0.462, P = 2.34e−19) in HCC (**Figure 7A**). Moreover, the copy number alterations of *H2AFY* could affect the infiltration level of six dominant immune cells, especially high amplification (**Figure 7B**). Next, we comprehensively explored the correlation between *H2AFY* expression and related marker genes of various tumor-infiltrating immune cells in HCC tissues. Correlation analysis was adjusted by tumor purity. In line with the above results, the *H2AFY* expression was significantly correlated with most selected immune cell marker genes (**Table 4**).

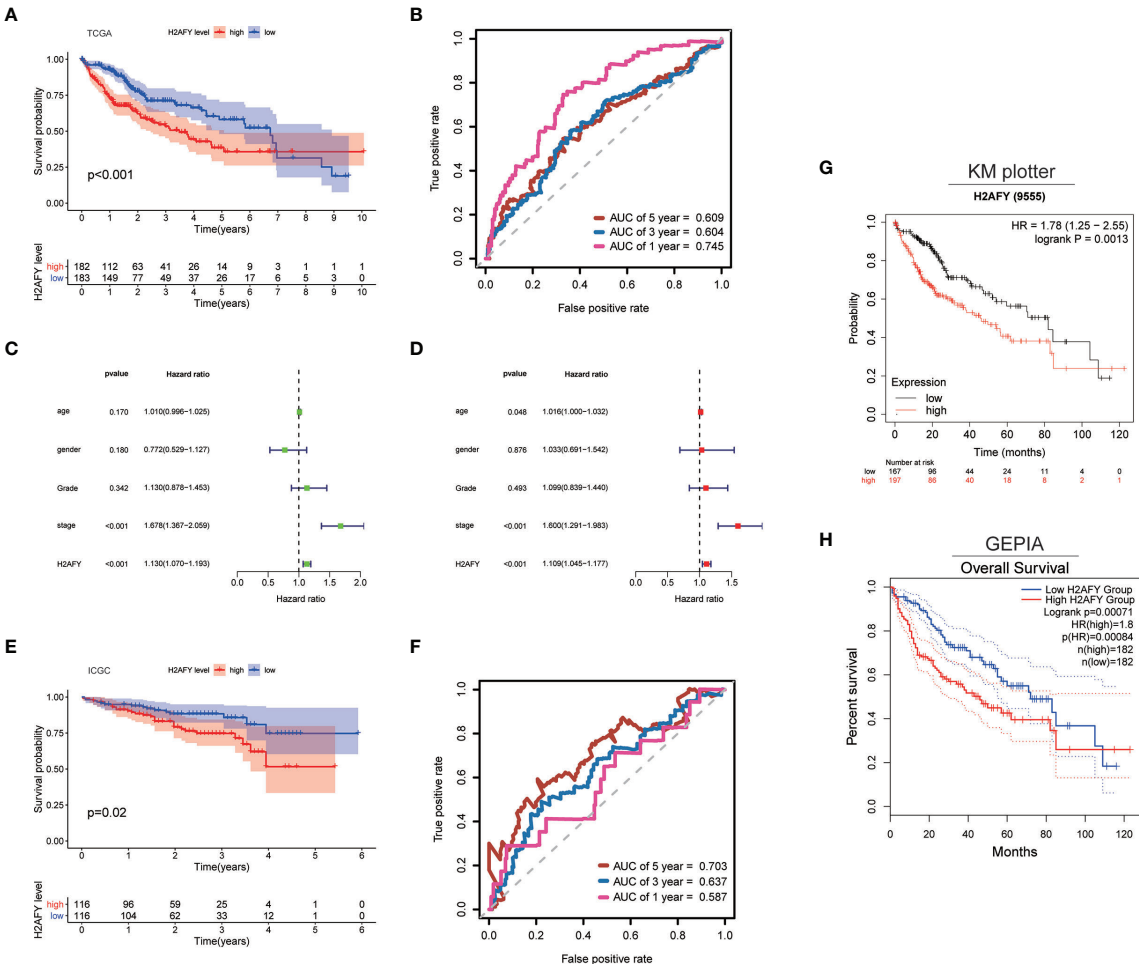

FIGURE 4 | *H2AFY* is associated with overall survival of HCC patients. **(A)** Kaplan–Meier survival curves and **(B)** time-dependent ROC curves of *H2AFY* in TCGA-LIHC cohort. **(C)** univariate Cox analysis and **(D)** multivariate Cox analysis in TCGA-LIHC cohort. **(E)** Kaplan–Meier survival curves and **(F)** time-dependent ROC curves of *H2AFY* in ICGC cohort (LIRI-JP project). **(G)** Kaplan–Meier survival analyses of *H2AFY* in Kaplan–Meier Plotter and **(H)** GEPIA2.

Based on reported studies, immune checkpoint molecules expression level might be tightly linked to the efficacy of immune checkpoint inhibitors. Therefore, we further investigated the correlation of *H2AFY* and seven key immune checkpoint molecules to clarify the role of *H2AFY* in immune checkpoint blockade therapy for HCC patients. The results in TIMER database pointed out that *H2AFY* had a close correlation with CD274 (PD-L1), CTLA4, HAVCR2, LAG3, PDCD1, PDCD1LG2, and TIGIT (P <0.001, **Figure 7C**), and the correlation was validated in GEPIA2 database (**Figure S3**). Additionally, compared with low-*H2AFY* expression group, these immune checkpoint genes expression levels were also higher in high-*H2AFY* expression group (P <0.001, **Figure 7D**). We further explored the relationship of *H2AFY* expression and immune subtypes, as displayed in **Figure 7E**, *H2AFY* expression was significantly differently distributed between six immune subtypes.

The CIBERSORT method was further employed to understand the association between *H2AFY* expression with 22 immune cell types in TCGA-LIHC cohort. **Figure 8A** summarized the relative fraction of these immune cells in each HCC patient. Within and between groups, the relative fraction of each immune cell type varied in HCC (**Figure 8B**). We found that high-*H2AFY* expression patients presented significantly higher B cell memory, T cells CD4 memory active, T cells regulatory (Tregs), T cells follicular helper, T cells gamma delta, macrophages M0 and Dendritic cells resting proportions (P <0.05), and lower B cell naive, NK cell resting, NK cell active, Monocytes, macrophages M2, Mast cells resting (P <0.05, **Figure 8C**). All these findings suggested that *H2AFY* was closely related to immune infiltration, and *H2AFY* might be able to predict the response of HCC patients to immune checkpoint blockade therapy.

Effects of *H2AFY* Knockdown on Cell Proliferation and Apoptosis in HCC Cells *In Vitro*

The qRT-PCR assay was applied to detect *H2AFY* mRNA expression in different HCC cell lines. We found that *H2AFY*

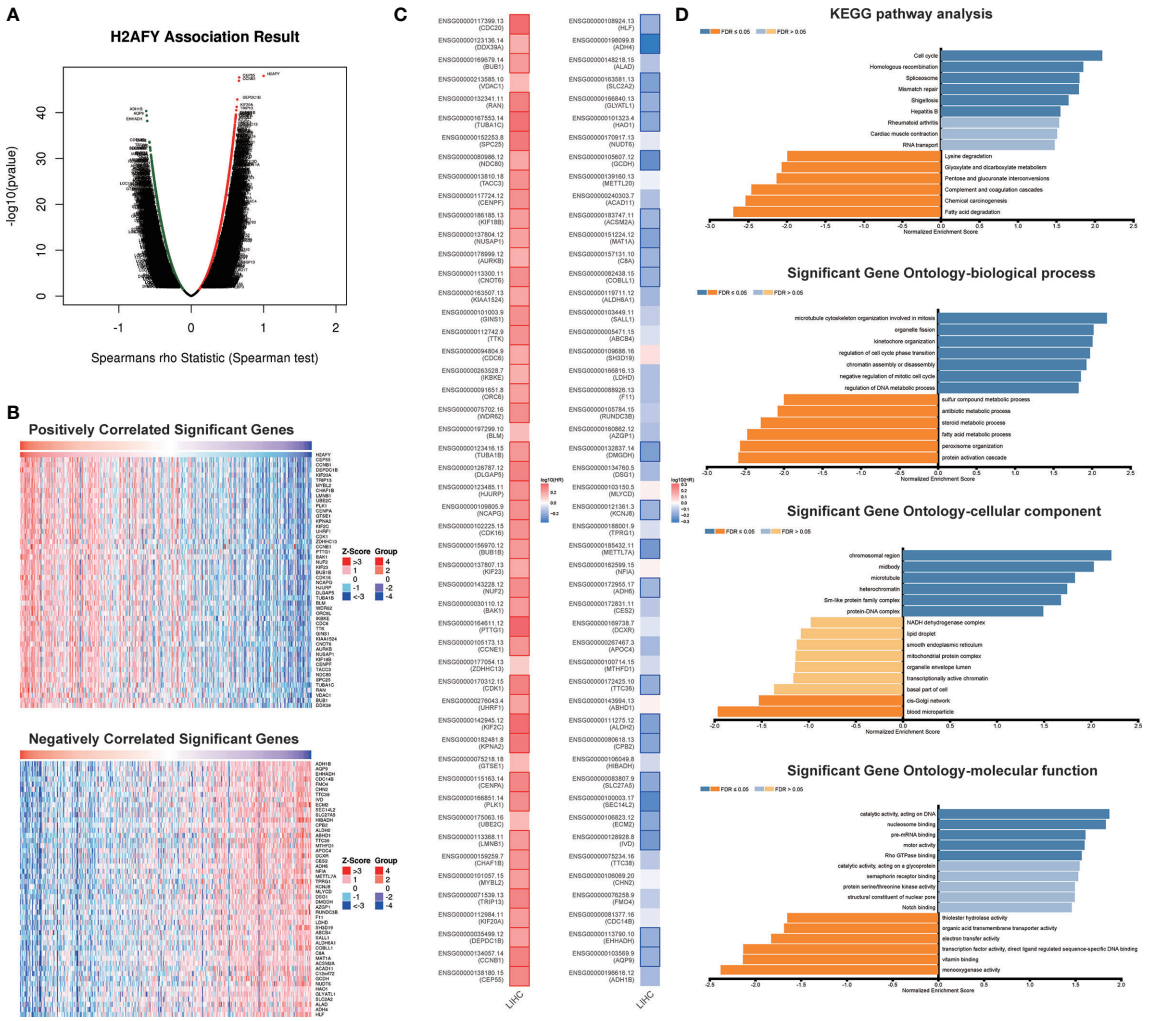

FIGURE 5 | *H2AFY* co-expression networks in HCC (LinkedOmics). **(A)** Volcano plot of the global *H2AFY* highly correlated genes identified by Spearman test. **(B)** Heat maps of top 50 genes positively and negatively correlated with *H2AFY*. **(C)** Survival heatmaps of top 50 genes positively and negatively correlated with *H2AFY*. **(D)** Significantly enriched GO terms and KEGG pathways related to *H2AFY*.

was also significantly overexpressed in HCC cell lines than normal liver cell line (**Figure 9A**), and selected HepG2 and Hep3B cell lines with relative higher *H2AFY* expression levels for subsequent experiments *in vitro*. *H2AFY* was knockdown in HepG2 and Hep3B cells by lentivirus transfection with shRNAs. Western blot assay examined the knockdown efficiency of shRNAs, the results showed that both shRNAs effectively inhibited H2AFY protein expression compared with negative control (NC) shRNA (**Figure 9B**). ShRNA-2 targeting *H2AFY* was used for the subsequent investigation.

The CCK8 assays were performed to explore the effect of *H2AFY* knockdown HCC cell proliferation, and the results revealed that the proliferation of HepG2 and Hep3B cells was significantly decreased after *H2AFY* knockdown (**Figure 9C**). Further colony formation assays suggested that *H2AFY* downregulation dramatically suppressed colony formation in both HepG2 and Hep3B cell lines (P <0.05, **Figure 9D**). In addition, the cell apoptosis was detected by flow cytometry, and *H2AFY* knockdown markedly enhanced the cell apoptosis in HepG2 and Hep3B cells (**Figure 9E**).

Effects of *H2AFY* Knockdown on Cell Cycle, Migration and anti-T-Cells Killing Ability in HCC Cells *In Vitro*

The preceding results indicated that *H2AFY* may be involved in the cell cycle process, we therefore performed cell cycle analysis using flow cytometry. As showcased in **Figure 10A**, the *H2AFY* downregulation resulted in G1/S phase arrest, the percentage of cells in G1 phase significantly increased and the proportion of cells in S phase decreased in both HepG2 and Hep3B cells (P <0.05). Subsequently, to investigate the impacts of the *H2AFY* knockdown on HCC cell migration ability, wound-healing and transwell assays was performed to measure the migration ability following *H2AFY* knockdown. These assays revealed that *H2AFY*

TABLE 3 | The kinase, miRNA and transcription factor-target networks of H2AFY in HCC (LinkedOmics).

Enriched Category	Enriched Geneset	LeadingEdgeNum	FDR
Kinase Target	Kinase_PLK1	32	0.00E+00
	Kinase_CDK1	77	0.00E+00
	Kinase_CHEK1	34	0.00E+00
	Kinase_AURKB	24	2.65E−04
	Kinase_CDK2	90	5.31E−04
miRNA Target	GAGCCAG, MIR-149	43	2.56E−01
	TAGGTCA, MIR-192, MIR-215	7	3.79E−01
	GCAAGAC, MIR-431	15	4.35E−01
	ACACTCC, MIR-122A	22	4.73E−01
	GGGGCCC, MIR-296	12	4.75E−01
Transcription Factor Target	V$E2F_Q4	75	0.00E+00
	V$E2F_Q6	75	0.00E+00
	V$E2F_02	82	0.00E+00
	V$E2F1DP1_01	82	0.00E+00
	V$E2F1DP2_01	82	0.00E+00

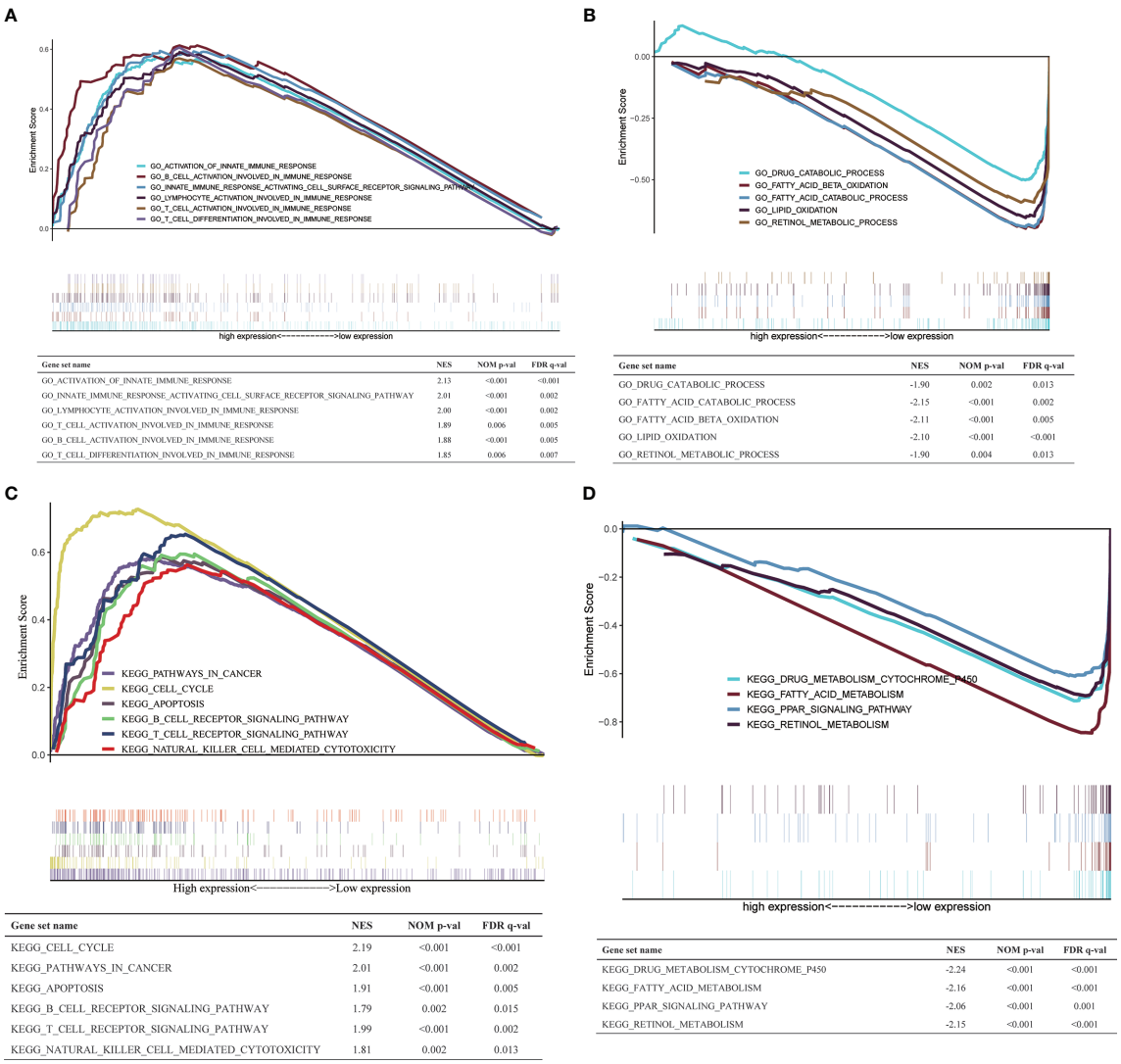

Gene set name	NES	NOM p-val	FDR q-val
GO_ACTIVATION_OF_INNATE_IMMUNE_RESPONSE	2.13	<0.001	<0.001
GO_INNATE_IMMUNE_RESPONSE_ACTIVATING_CELL_SURFACE_RECEPTOR_SIGNALING_PATHWAY	2.01	<0.001	0.002
GO_LYMPHOCYTE_ACTIVATION_INVOLVED_IN_IMMUNE_RESPONSE	2.00	<0.001	0.002
GO_T_CELL_ACTIVATION_INVOLVED_IN_IMMUNE_RESPONSE	1.89	0.006	0.005
GO_B_CELL_ACTIVATION_INVOLVED_IN_IMMUNE_RESPONSE	1.88	<0.001	0.005
GO_T_CELL_DIFFERENTIATION_INVOLVED_IN_IMMUNE_RESPONSE	1.85	0.006	0.007

Gene set name	NES	NOM p-val	FDR q-val
GO_DRUG_CATABOLIC_PROCESS	-1.90	0.002	0.013
GO_FATTY_ACID_CATABOLIC_PROCESS	-2.15	<0.001	0.002
GO_FATTY_ACID_BETA_OXIDATION	-2.11	<0.001	0.005
GO_LIPID_OXIDATION	-2.10	<0.001	<0.001
GO_RETINOL_METABOLIC_PROCESS	-1.90	0.004	0.013

Gene set name	NES	NOM p-val	FDR q-val
KEGG_CELL_CYCLE	2.19	<0.001	<0.001
KEGG_PATHWAYS_IN_CANCER	2.01	<0.001	0.002
KEGG_APOPTOSIS	1.91	<0.001	0.005
KEGG_B_CELL_RECEPTOR_SIGNALING_PATHWAY	1.79	0.002	0.015
KEGG_T_CELL_RECEPTOR_SIGNALING_PATHWAY	1.99	<0.001	0.002
KEGG_NATURAL_KILLER_CELL_MEDIATED_CYTOTOXICITY	1.81	0.002	0.013

Gene set name	NES	NOM p-val	FDR q-val
KEGG_DRUG_METABOLISM_CYTOCHROME_P450	-2.24	<0.001	<0.001
KEGG_FATTY_ACID_METABOLISM	-2.16	<0.001	<0.001
KEGG_PPAR_SIGNALING_PATHWAY	-2.06	<0.001	0.001
KEGG_RETINOL_METABOLISM	-2.15	<0.001	<0.001

FIGURE 6 | GSEA in TCGA-LIHC cohort. **(A, B)** The GO_BP annotations enriched in HCC patients with high/low *H2AFY* expression. **(C, D)** The KEGG pathways enriched in HCC patients with high/low *H2AFY* expression.

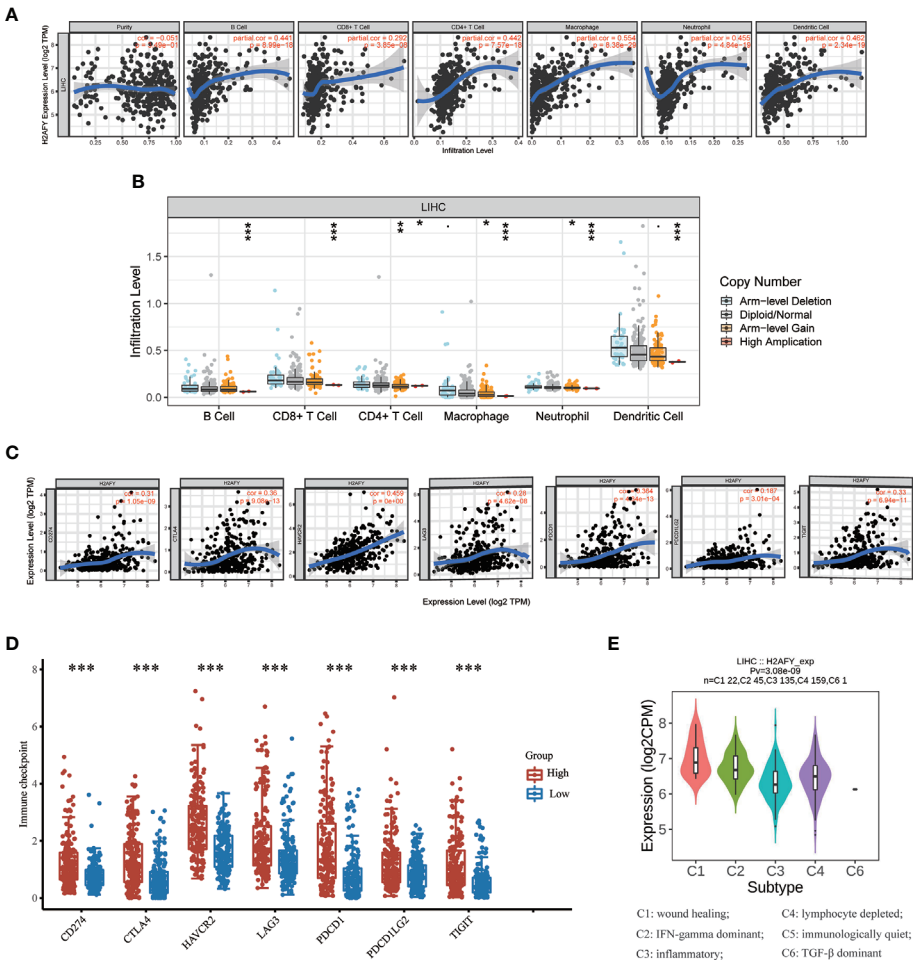

FIGURE 7 | Correlations of *H2AFY* expression with immune infiltration in HCC. **(A)** Correlation analysis of *H2AFY* expression and abundance of immune cells in TIMER. **(B)** *H2AFY* copy number alterations affects the immune infiltration levels. **(C)** Correlations between the expression of *H2AFY* and several immune checkpoint genes. **(D)** The expression of several immune checkpoint genes between high- and low-*H2AFY* expression patients. **(E)** *H2AFY* expression in different immune subtypes of HCC (TISIDB database) *$P < 0.05$; **$P < 0.01$; ***$P < 0.001$.

knockdown drastically decreased the migration ability of HepG2 and Hep3B cells, compared to NC group (**Figures 10B–D**). We next conducted T-cells-mediated cancer killing assay to detect the effect of *H2AFY* knockdown in HCC cells on anti-T-cells killing ability (36). We found that *H2AFY* knockdown significantly reduced the survival of HCC cells than those with NC after co-culturing with activated Jurkat cells (**Figure S4**). Besides, we also detected the expression of cell cycle, apoptosis and EMT related molecular markers in HCC cells with *H2AFY* knockdown. As expected, we observed that the expression levels of Cyclin B1, Cyclin D1, Bcl-2, and Vimentin showed significantly downward trends after suppressing *H2AFY* in HepG2 and Hep3B cells. Conversely, the expression of E-cadherin was significantly upregulated in HCC cells transfected with *H2AFY*-shRNA (**Figure 10E**).

Moreover, we noticed that *H2AFY* expression was positively correlated with STAT3 signaling pathway among the various pathways revealed by GSEA (**Figure 10F**). Some previous studies have demonstrated that the STAT3 signaling pathway was activated in HCC and associated with multiple malignant biological behaviors of HCC (37, 38). Therefore, we examined whether *H2AFY* might affect STAT3 signaling pathway activation in HCC cells. Western blot results indicated that *H2AFY* knockdown decreased the expression of phosphorylated STAT3 and inhibited STAT3 signaling pathway activation (**Figure 10G**). Overall, these results illustrated that *H2AFY* knockdown inhibited HCC progression at least partly *via* regulating STAT3 signaling.

DISCUSSION

The *H2AFY* gene encodes for macroH2A1, a histone variant of the histone H2A that have been reported to be dysregulated in various human cancers (39, 40). Several prior published studies

TABLE 4 | Correlations between H2AFY and markers of immune infiltrates for HCC in TIMER.

Description	Gene markers	H2AFY			
		None		Purity	
		Cor	*P*	Cor	*P*
CD8+ T cell	CD8A	0.242	***	0.232	***
	CD8B	0.184	**	0.169	*
T cell (general)	CD3D	0.314	***	0.316	***
	CD3E	0.298	***	0.311	***
	CD2	0.305	***	0.32	***
B cell	CD19	0.323	***	0.311	***
	CD20 (MS4A1)	0.183	**	0.17	*
	CD79A	0.236	***	0.226	***
Monocyte	CD86	0.448	***	0.487	***
	CD16 (FCGR3A)	0.36	***	0.367	***
	CD115 (CSF1R)	0.339	***	0.366	***
TAM	CCL2	0.266	***	0.27	***
	CD68	0.37	***	0.369	***
	IL10	0.345	***	0.353	***
M1 Macrophage	NOS2	0.14	*	0.135	0.0121
	CXCL10	0.165	*	0.161	*
	IRF5	0.522	***	0.516	***
	COX2 (PTGS2)	0.326	***	0.356	***
M2 Macrophage	CD163	0.206	***	0.205	**
	ARG1	–0.16	*	-0.172	*
	MRC1	0.045	0.389	0.037	0.493
Neutrophils	CD11b (ITGAM)	0.441	***	0.468	***
	CD66b (CEACAM8)	0.076	0.147	0.081	0.132
	CCR7	0.216	***	0.223	***
	CD15(FUT4)	0.602	***	0.59	***
Natural killer cell	KIR2DL1	–0.008	0.872	–0.054	0.317
	KIR2DL3	0.15	*	0.144	*
	KIR2DL4	0.182	**	0.164	*
	KIR3DL1	0.037	0.476	0.02	0.708
	KIR3DL2	0.085	0.104	0.067	0.212
	KIR3DL3	0.033	0.539	0.061	0.241
	KIR2DS4	0.052	0.317	0.044	0.419
Dendritic cell	HLA-DPB1	0.33	***	0.337	***
	HLA-DQB1	0.264	***	0.255	***
	HLA-DRA	0.351	***	0.365	***
	HLA-DPA1	0.328	***	0.348	***
	BDCA-1 (CD1C)	0.285	***	0.284	***
	BDCA-4 (NRP1)	0.363	***	0.358	***
	CD11c (ITGAX)	0.492	***	0.529	***
Th1	T-bet (TBX21)	0.132	0.011	0.118	0.0279
	STAT4	0.377	***	0.377	***
	STAT1	0.468	***	0.458	***
	IFNG (IFN-γ)	0.234	***	0.241	***
	TNF(TNF-α)	0.343	***	0.37	***
Th2	GATA3	0.333	***	0.361	***
	STAT6	0.255	***	0.237	***
	STAT5A	0.339	***	0.339	***
	IL13	0.116	0.0253	0.103	0.0558
Tfh	BCL6	0.174	**	0.185	**
	IL21	0.115	0.0271	0.131	0.0152
	CD278 (ICOS)	0.339	***	0.35	***
	CXCL13	0.206	***	0.211	***
Th17	STAT3	0.319	***	0.318	***
	IL17A	0.09	0.0834	0.1	0.064
Treg	FOXP3	0.204	***	0.224	***
	CCR8	0.467	***	0.489	***
	STAT5B	0.281	***	0.303	***
	TGFB1	0.435	***	0.446	***
T cell exhaustion	PDCD1	0.364	***	0.358	***
	CTLA4	0.36	***	0.369	***

(Continued)

TABLE 4 | Continued

Description	Gene markers	H2AFY			
		None		Purity	
		Cor	*P*	Cor	*P*
	LAG3	0.28	***	0.255	***
	HAVCR2 (TIM3)	0.459	***	0.503	***
	GZMB	0.091	0.0801	0.068	0.206

*TAM, tumor-associated macrophage; Th, T helper cell; Tfh, Follicular helper T cell; Treg, regulatory T cell; None, correlation without adjustment. Purity, correlation adjusted by purity; Cor, R value of Spearman's correlation. *P < 0.01; **P < 0.001; ***P < 0.0001.*

indicate that the decreased expression level of *H2AFY* was inversely correlated with cell proliferation and function as a marker for poor prognosis in lung cancer and colon cancer (14, 41). By contrast, *H2AFY* promoted cancer cell proliferation by interacting with HER2 and higher expression of *H2AFY* was associated with worse prognosis in triple-negative breast cancer (18, 19). Additionally, the expression *H2AFY* was reduced in metastatic cutaneous melanomas compared to benign nevi, and the loss of *H2AFY* promoted proliferation and migration of cutaneous melanoma cells through regulation of *CDK8* (17, 42). Interestingly, however, contrary to cutaneous melanoma, the metastatic uveal melanoma has been reported to have a higher *H2AFY* expression level than non-metastatic uveal melanoma, and *H2AFY* silencing decreases the invasiveness of uveal melanoma cells by reducing mitochondrial metabolism (43). These proofs of evidence suggest that *H2AFY* exhibits either oncogenic function or tumor suppressor function in different tumor types, which seems to depend on the context and genetic background of the specific tumor studied. To understand more details about the potential functions and regulatory network of *H2AFY* in HCC, we conducted a series of bioinformatics analyses and experiments *in vitro* to provide new insights for HCC.

In this study, we first investigated the expression of *H2AFY* in HCC, and found that *H2AFY* mRNA expression was prominently

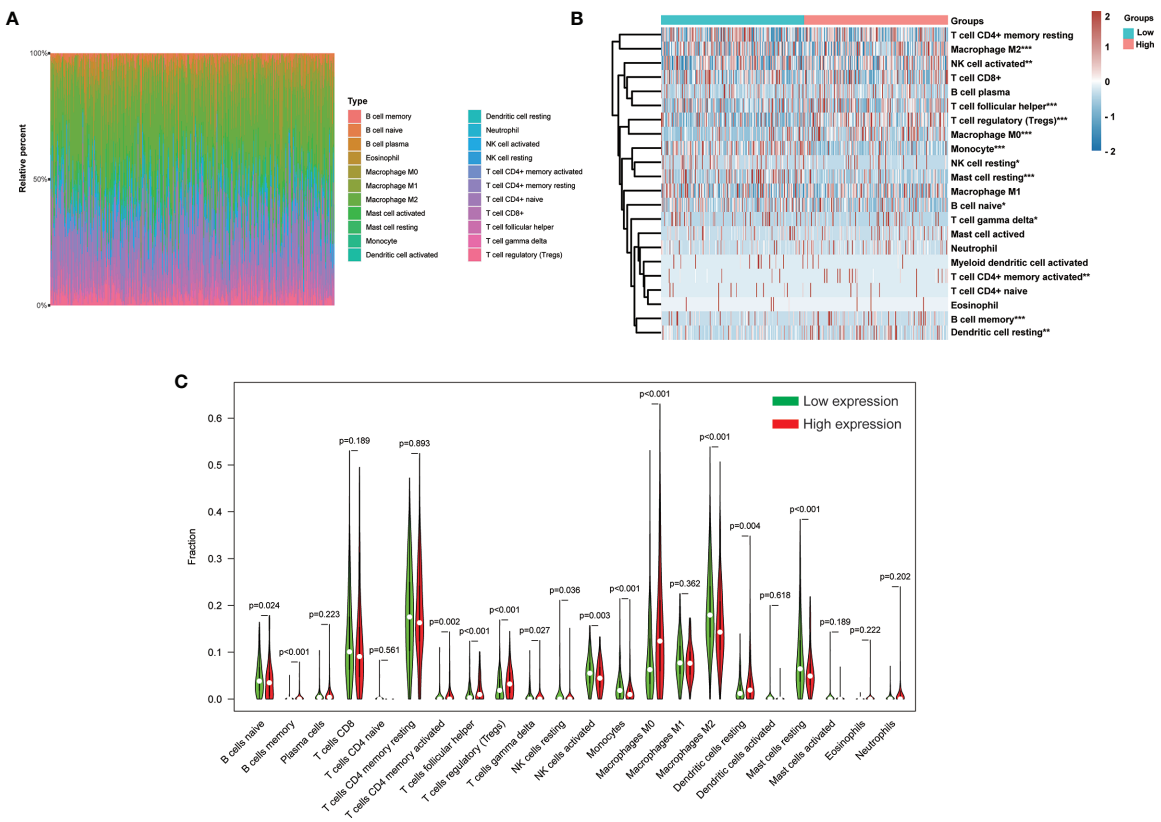

FIGURE 8 | Correlation of *H2AFY* expression and 22 immune cell types in HCC based on CIBERSORT. **(A)** The relative fraction of 22 immune cell types in TCGA-LIHC cohort. **(B)** The heat map showing relative immune cell fraction of HCC patients **(C)** Violin plots showing the difference of 22 immune cell types between high- and low-*H2AFY* expression patients *$P < 0.05$; **$P < 0.01$; ***$P < 0.001$.

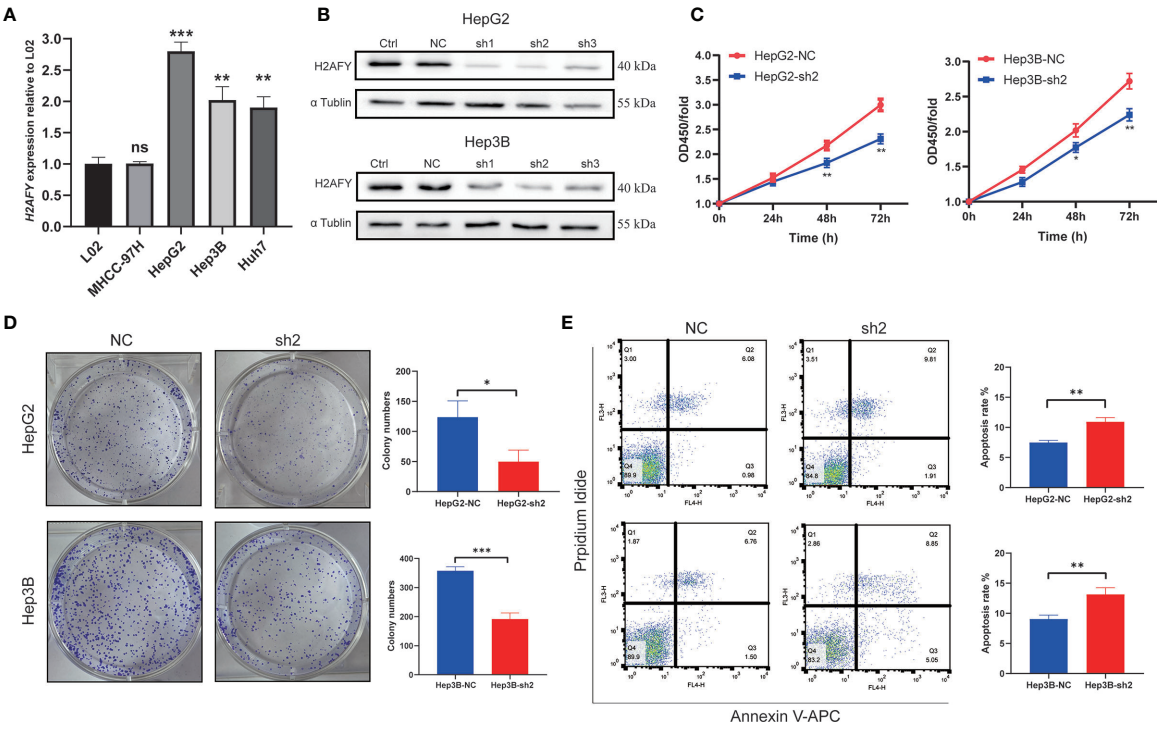

FIGURE 9 | Effects of H2AFY knockdown on cell proliferation and apoptosis in HCC cells. **(A)** *H2AFY* mRNA expression in normal liver cell line (L02) and several HCC cell lines. **(B)** Evaluation of *H2AFY* expression in HepG2 and Hep3B cells after shRNA transfection. **(C)** The effect of *H2AFY* knockdown on cell proliferation in HepG2 and Hep3B cells examined by CCK8 assay and **(D)** colony formation assay. **(E)** The effect of *H2AFY* knockdown on cell apoptosis in HepG2 and Hep3B cells examined by flow cytometry ns, no significance; $^{*}P < 0.05$; $^{**}P < 0.01$; $^{***}P < 0.001$.

upregulated in HCC compared to normal tissues across various public databases. Clinical association analyses demonstrated that increased *H2AFY* expression was correlated with higher histological grade, more advanced clinical stage and larger tumor size. Besides, we also found several genetic alterations of *H2AFY* in HCC, mainly amplification and missense mutation. Kaplan–Meier and Cox regression analyses further revealed that high *H2AFY* expression was an independent risk factor to predict poor OS for HCC patients. Therefore, our findings demonstrated that *H2AFY* could act as a potential diagnostic or prognostic biomarker for HCC and deserves further clinical verification.

Next, we explored the co-expression network of *H2AFY* and identified multiple genes co-expressed with *H2AFY*, which were further used for GO and KEGG enrichment analyses. The result displayed that the enrichment primarily associated with cell cycle, chromatin, mitosis, and spliceosome, and *H2AFY* may affect cell cycle and mitosis progression through these factors. The regulators responsible for *H2AFY* dysregulation were explored in HCC, and the kinase networks related to *H2AFY* were found, namely, *PLK1*, *CDK1*, *CHEK1*, *AURKB*, and *CDK2*. These kinases could regulate mitosis, cell cycle, and genome stability. All these kinase genes, except *CDK2*, were found to be significantly highly expressed in HCC and related to the poor OS of patients with HCC. *PKL1* is a key regulator for the cell cycle progression, the main function of *PLK1* is to control mitotic entry and maintain genomic stability in mitosis and DNA damage response (44). Studies have revealed the role of *PLK1* in most human cancers, and established a causal association between *PLK1* and hepatocarcinogenesis (45). The activity of *CDK1* is often enhanced in cancer cells, it therefore has been considered as an appealing specific anti-cancer target (46). Multiple inhibitors targeting *CDK1* have been developed and have entered early clinical trials for some malignancies (47). *AURKB* plays a crucial role for the cell cycle transition from G2 to M phase (48). In HCC, *H2AFY* may regulate cell cycle progression, mitosis and chromatin assembly *via* these interacted kinases. We also identified that the main transcription factor targets of *H2AFY* were E2F family members. E2F transcription factors are involved in cell cycle regulation and DNA synthesis, and the oncogenic role of the E2Fs has been reported in previous studies (49, 50). However, no miRNA targets significantly associated with *H2AFY* were identified, possibly because *H2AFY* participates in mRNA splicesome. Our results demonstrated that E2F1 is a pivotal regulator of *H2AFY*, and *H2AFY* might regulate the cell cycle and proliferation of HCC through this factor.

Furthermore, we observed many immune-related pathways significantly gathered in high-*H2AFY* expression phenotype, such as activation of innate immune response, lymphocyte activation of immune response, B-cell receptor signaling pathway, and T-cell receptor signaling pathway. Previous studies have manifested that infiltrating immune cells in tumor microenvironment play a major role in tumor development and metastasis, thus affecting the prognosis of cancer patients (51, 52). Recently, immunotherapeutic strategies especially immune checkpoint blockade therapy, have been

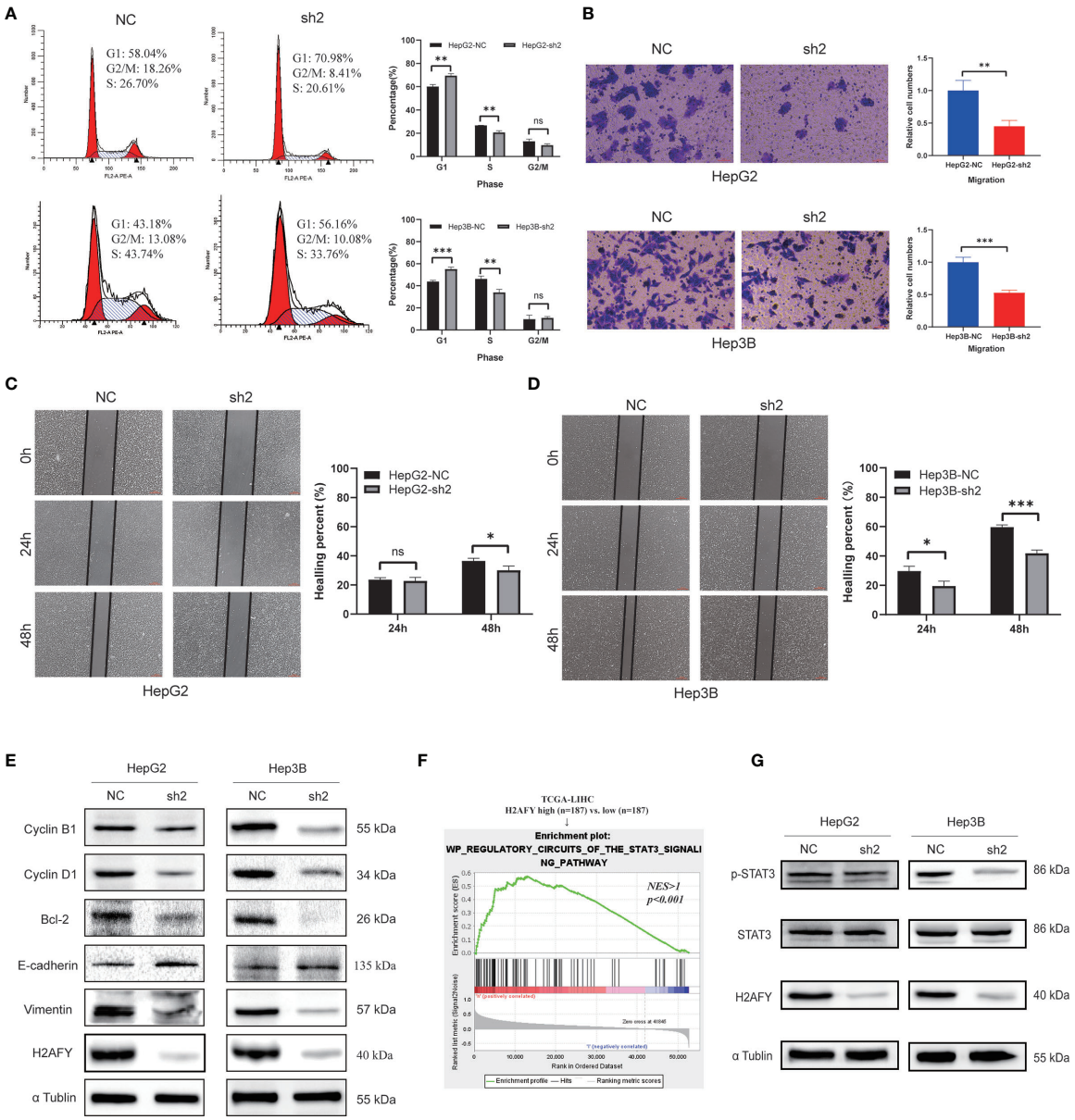

FIGURE 10 | Effects of *H2AFY* knockdown on cell cycle and migration in HCC cells. **(A)** Cell cycle detected by flow cytometry in HepG2 and Hep3B cells after *H2AFY* knockdown. **(B–D)** Representative images of transwell (200×) and wound healing assays (40×) in HepG2 and Hep3B cells, and the quantitative result following *H2AFY* knockdown. **(E)** Western blot analysis of cell cycle, apoptosis, EMT related molecular markers in HepG2 and Hep3B cells transfected with *H2AFY*-shRNA or the negative control. **(F)** STAT3 signaling pathway was significantly enriched in high-*H2AFY* expression patients. **(G)** Evaluation of p-STAT3 and STAT3 expression in HepG2 and Hep3B cells after transfecting *H2AFY*-shRNA ns, no significance; $^{*}P < 0.05$; $^{**}P < 0.01$; $^{***}P < 0.001$.

considered as promising options for the treatment of various malignancies, including HCC (53, 54). Therefore, the exploration of novel immune biomarkers or immunotherapeutic targets for HCC is clinically significant. Here, we revealed a correlation between *H2AFY* expression and immune infiltration in HCC. *H2AFY* expression showed significantly positive correlations with the expression of various immune cell marker genes and immune checkpoint molecules such as PD-L1 and CTLA4. Additionally, the high-*H2AFY* expression patients have higher expression of these immune checkpoint genes than low-*H2AFY* expression patients. The upregulated PD-L1 expression is found to be associated with poor prognosis of patients with HCC, and it was an appealing immunotherapeutic target for HCC. Together, these results suggested that *H2AFY* may exert a vital role in modulating tumor immunity, and serve as a potential biomarker related to immune infiltration in HCC.

Furthermore, a series of functional assays *in vitro* verified the role of *H2AFY* in HCC by downregulating the *H2AFY* expression. The

results showed that *H2AFY* knockdown suppressed the cell proliferation, migration and promoted apoptosis of HCC cells *in vitro*. In addition, we observed an increased proportion of HCC cells in G1 phase and a decreased proportion in S phase after *H2AFY* knockdown. The STAT3 signaling was activated in many cancers, its activation has been found to promote HCC progression (55–57). *H2AFY* knockdown also downregulated the phosphorylated STAT3 expression in HCC cells, and the result showed that *H2AFY* knockdown inhibited HCC malignant progression at least partly *via* regulating STAT3 signaling.

Nonetheless, several limitations in our study should be recognized. First, our finding is based on retrospective data from public databases, more prospective data and larger HCC cohorts were required to confirm its clinical suitability. Second, the role of *H2AFY* in tumor immune infiltration needs to be further validated *in vitro or in vivo*. Finally, we have demonstrated that *H2AFY* could regulate STAT3 signaling in HCC, but the detailed regulatory mechanism requires more functional studies to elucidate in future. Our findings should be taken with these limitations for interpretation.

In general, our study provided multi-level evidence for *H2AFY* as a potential biomarker and prognostic predictor for HCC. These results revealed that *H2AFY* was upregulated in HCC and its high expression was associated with poor prognosis of HCC patients. Moreover, *H2AFY* has a significantly positive correlation with immune infiltration in HCC.

DATA AVAILABILITY STATEMENT

The original contributions presented in the study are included in the article/**Supplementary Material**. Further inquiries can be directed to the corresponding author.

AUTHOR CONTRIBUTIONS

YH designed the study and wrote the manuscript. SH, LM, XW, LX, WQ, LL, and YW participated in data preparation and figure preparation. SH revised the manuscript. XY reviewed the manuscript. All authors contributed to the article and approved the submitted version.

FUNDING

This study was supported by National Natural Science Foundation of China (2018, 81773360).

ACKNOWLEDGMENTS

We acknowledge the following databases, TCGA (https://portal.gdc.cancer.gov/), ICGC (https://icgc.org/), Oncomine (www.oncomine.org), TIMER (https://cistrome.shinyapps.io/timer/), HCCDB (http://lifeome.net/database/hccdb/home.html), cBioPortal (http://www.cbioportal.org/), COSMIC (https://cancer.sanger.ac.uk/cosmic), GEPIA2 (http://gepia2.cancer-pku.cn/), Kaplan–Meier Plotter (http://kmplot.com), GeneMANIA (https://genemania.org/), LinkedOmics (http://linkedomics.org/login.php), and TISIDB (http://cis.hku.hk/TISIDB/index.php).

SUPPLEMENTARY MATERIAL

The Supplementary Material for this article can be found online at: https://www.frontiersin.org/articles/10.3389/fimmu.2021.723293/full#supplementary-material

REFERENCES

1. Llovet JM, Zucman-Rossi J, Pikarsky E, Sangro B, Schwartz M, Sherman M, et al. Hepatocellular Carcinoma. *Nat Rev Dis Primers* (2016) 2:16018. doi: 10.1038/nrdp.2016.18
2. Bray F, Ferlay J, Soerjomataram I, Siegel RL, Torre LA, Jemal A. Global Cancer Statistics 2018: GLOBOCAN Estimates of Incidence and Mortality Worldwide for 36 Cancers in 185 Countries. *CA Cancer J Clin* (2018) 68:394–424. doi: 10.3322/caac.21492
3. Forner A, Reig M, Bruix J. Hepatocellular Carcinoma. *Lancet* (2018) 391:1301–14. doi: 10.1016/S0140-6736(18)30010-2
4. Bruix J, Gores GJ, Mazzaferro V. Hepatocellular Carcinoma: Clinical Frontiers and Perspectives. *Gut.* (2014) 63:844–55. doi: 10.1136/gutjnl-2013-306627
5. Zhu ZX, Huang JW, Liao MH, Zeng Y. Treatment Strategy for Hepatocellular Carcinoma in China: Radiofrequency Ablation *Versus* Liver Resection. *Jpn J Clin Oncol* (2016) 46:1075–80. doi: 10.1093/jjco/hyw134
6. Schlachterman A, Craft WJ, Hilgenfeldt E, Mitra A, Cabrera R. Current and Future Treatments for Hepatocellular Carcinoma. *World J Gastroenterol* (2015) 21:8478–91. doi: 10.3748/wjg.v21.i28.8478
7. Koch A, Joosten SC, Feng Z, de Ruijter TC, Draht MX, Melotte V, et al. Analysis of DNA Methylation in Cancer: Location Revisited. *Nat Rev Clin Oncol* (2018) 15:459–66. doi: 10.1038/s41571-018-0004-4
8. He L, Li H, Wu A, Peng Y, Shu G, Yin G. Functions of N6-Methyladenosine and its Role in Cancer. *Mol Cancer* (2019) 18:176. doi: 10.1186/s12943-019-1109-9
9. Vardabasso C, Hasson D, Ratnakumar K, Chung CY, Duarte LF, Bernstein E. Histone Variants: Emerging Players in Cancer Biology. *Cell Mol Life Sci* (2014) 71:379–404. doi: 10.1007/s00018-013-1343-z
10. Hammond CM, Stromme CB, Huang H, Patel DJ, Groth A. Histone Chaperone Networks Shaping Chromatin Function. *Nat Rev Mol Cell Biol* (2017) 18:141–58. doi: 10.1038/nrm.2016.159
11. Buschbeck M, Hake SB. Variants of Core Histones and Their Roles in Cell Fate Decisions, Development and Cancer. *Nat Rev Mol Cell Biol* (2017) 18:299–314. doi: 10.1038/nrm.2016.166
12. Martire S, Banaszynski LA. The Roles of Histone Variants in Fine-Tuning Chromatin Organization and Function. *Nat Rev Mol Cell Biol* (2020) 21:522–41. doi: 10.1038/s41580-020-0262-8
13. Kozlowski M, Corujo D, Hothorn M, Guberovic I, Mandemaker IK, Blessing C, et al. MacroH2A Histone Variants Limit Chromatin Plasticity Through Two Distinct Mechanisms. *EMBO Rep* (2018) 19:e44445. doi: 10.15252/embr.201744445
14. Sporn JC, Kustatscher G, Hothorn T, Collado M, Serrano M, Muley T, et al. Histone Macroh2a Isoforms Predict the Risk of Lung Cancer Recurrence. *Oncogene* (2009) 28:3423–8. doi: 10.1038/onc.2009.26
15. Park SJ, Shim JW, Park HS, Eum DY, Park MT, Mi YJ, et al. MacroH2A1 Downregulation Enhances the Stem-Like Properties of Bladder Cancer Cells by Transactivation of Lin28B. *Oncogene* (2016) 35:1292–301. doi: 10.1038/onc.2015.187
16. Novikov L, Park JW, Chen H, Klerman H, Jalloh AS, Gamble MJ. QKI-Mediated Alternative Splicing of the Histone Variant MacroH2A1 Regulates Cancer Cell Proliferation. *Mol Cell Biol* (2011) 31:4244–55. doi: 10.1128/MCB.05244-11
17. Kapoor A, Goldberg MS, Cumberland LK, Ratnakumar K, Segura MF, Emanuel PO, et al. The Histone Variant Macroh2a Suppresses Melanoma Progression Through Regulation of CDK8. *Nature* (2010) 468:1105–9. doi: 10.1038/nature09590
18. Broggi G, Filetti V, Ieni A, Rapisarda V, Ledda C, Vitale E, et al. MacroH2A1 Immunoexpression in Breast Cancer. *Front Oncol* (2020) 10:1519. doi: 10.3389/fonc.2020.01519

19. Li X, Kuang J, Shen Y, Majer MM, Nelson CC, Parsawar K, et al. The Atypical Histone Macroh2a1.2 Interacts With HER-2 Protein in Cancer Cells. *J Biol Chem* (2012) 287:23171–83. doi: 10.1074/jbc.M112.379412
20. Rappa F, Greco A, Podrini C, Cappello F, Foti M, Bourgoin L, et al. Immunopositivity for Histone Macroh2a1 Isoforms Marks Steatosis-Associated Hepatocellular Carcinoma. *PloS One* (2013) 8:e54458. doi: 10.1371/journal.pone.0054458
21. Ma X, Ding Y, Zeng L. The Diagnostic and Prognostic Value of H2AFY in Hepatocellular Carcinoma. *BMC Cancer* (2021) 21:418. doi: 10.1186/s12885-021-08161-4
22. Chen J, Liao Y, Fan X. Prognostic and Clinicopathological Value of BUB1B Expression in Patients With Lung Adenocarcinoma: A Meta-Analysis. *Expert Rev Anticancer Ther* (2021) 21:795–803. doi: 10.1080/14737140.2021.1908132
23. Rhodes DR, Yu J, Shanker K, Deshpande N, Varambally R, Ghosh D, et al. ONCOMINE: A Cancer Microarray Database and Integrated Data-Mining Platform. *Neoplasia* (2004) 6:1–6. doi: 10.1016/s1476-5586(04)80047-2
24. Li T, Fan J, Wang B, Traugh N, Chen Q, Liu JS, et al. TIMER: A Web Server for Comprehensive Analysis of Tumor-Infiltrating Immune Cells. *Cancer Res* (2017) 77:e108–10. doi: 10.1158/0008-5472.CAN-17-0307
25. Lian Q, Wang S, Zhang G, Wang D, Luo G, Tang J, et al. HCCDB: A Database of Hepatocellular Carcinoma Expression Atlas. *Genomics Proteomics Bioinf* (2018) 16:269–75. doi: 10.1016/j.gpb.2018.07.003
26. Gao J, Aksoy BA, Dogrusoz U, Dresdner G, Gross B, Sumer SO, et al. Integrative Analysis of Complex Cancer Genomics and Clinical Profiles Using the Cbioportal. *Sci Signal* (2013) 6:pl1. doi: 10.1126/scisignal.2004088
27. Forbes SA, Beare D, Gunasekaran P, Leung K, Bindal N, Boutselakis H, et al. COSMIC: Exploring the World's Knowledge of Somatic Mutations in Human Cancer. *Nucleic Acids Res* (2015) 43:D805–11. doi: 10.1093/nar/gku1075
28. Nagy A, Munkacsy G, Gyorffy B. Pancancer Survival Analysis of Cancer Hallmark Genes. *Sci Rep* (2021) 11:6047. doi: 10.1038/s41598-021-84787-5
29. Tang Z, Kang B, Li C, Chen T, Zhang Z. GEPIA2: An Enhanced Web Server for Large-Scale Expression Profiling and Interactive Analysis. *Nucleic Acids Res* (2019) 47:W556–60. doi: 10.1093/nar/gkz430
30. Franz M, Rodriguez H, Lopes C, Zuberi K, Montojo J, Bader GD, et al. GeneMANIA Update 2018. *Nucleic Acids Res* (2018) 46:W60–4. doi: 10.1093/nar/gky311
31. Vasaikar SV, Straub P, Wang J, Zhang B. LinkedOmics: Analyzing Multi-Omics Data Within and Across 32 Cancer Types. *Nucleic Acids Res* (2018) 46: D956–63. doi: 10.1093/nar/gkx1090
32. Subramanian A, Tamayo P, Mootha VK, Mukherjee S, Ebert BL, Gillette MA, et al. Gene Set Enrichment Analysis: A Knowledge-Based Approach for Interpreting Genome-Wide Expression Profiles. *Proc Natl Acad Sci USA* (2005) 102:15545–50. doi: 10.1073/pnas.0506580102
33. Ru B, Wong CN, Tong Y, Zhong JY, Zhong S, Wu WC, et al. TISIDB: An Integrated Repository Portal for Tumor-Immune System Interactions. *Bioinformatics* (2019) 35:4200–2. doi: 10.1093/bioinformatics/btz210
34. Newman AM, Liu CL, Green MR, Gentles AJ, Feng W, Xu Y, et al. Robust Enumeration of Cell Subsets From Tissue Expression Profiles. *Nat Methods* (2015) 12:453–7. doi: 10.1038/nmeth.3337
35. Liao Y, He D, Wen F. Analyzing the Characteristics of Immune Cell Infiltration in Lung Adenocarcinoma *via* Bioinformatics to Predict the Effect of Immunotherapy. *Immunogenetics* (2021) 73:369–80. doi: 10.1007/s00251-021-01223-8
36. Liu Y, Liu X, Zhang N, Yin M, Dong J, Zeng Q, et al. Berberine Diminishes Cancer Cell PD-L1 Expression and Facilitates Antitumor Immunity *via* Inhibiting the Deubiquitination Activity of CSN5. *Acta Pharm Sin B* (2020) 10:2299–312. doi: 10.1016/j.apsb.2020.06.014
37. Zhou Q, Tian W, Jiang Z, Huang T, Ge C, Liu T, et al. A Positive Feedback Loop of AKR1C3-Mediated Activation of NF-kappaB and STAT3 Facilitates Proliferation and Metastasis in Hepatocellular Carcinoma. *Cancer Res* (2021) 81:1361–74. doi: 10.1158/0008-5472.CAN-20-2480
38. Liu Y, Liu L, Zhou Y, Zhou P, Yan Q, Chen X, et al. CKLF1 Enhances Inflammation-Mediated Carcinogenesis and Prevents Doxorubicin-Induced Apoptosis *via* IL6/STAT3 Signaling in HCC. *Clin Cancer Res* (2019) 25:4141–54. doi: 10.1158/1078-0432.CCR-18-3510
39. Cantarino N, Douet J, Buschbeck M. MacroH2A–an Epigenetic Regulator of Cancer. *Cancer Lett* (2013) 336:247–52. doi: 10.1016/j.canlet.2013.03.022
40. Corujo D, Buschbeck M. Post-Translational Modifications of H2A Histone Variants and Their Role in Cancer. *Cancers (Basel)* (2018) 10:59. doi: 10.3390/cancers10030059
41. Sporn JC, Jung B. Differential Regulation and Predictive Potential of MacroH2A1 Isoforms in Colon Cancer. *Am J Pathol* (2012) 180:2516–26. doi: 10.1016/j.ajpath.2012.02.027
42. Lei S, Long J, Li J. MacroH2A Suppresses the Proliferation of the B16 Melanoma Cell Line. *Mol Med Rep* (2014) 10:1845–50. doi: 10.3892/mmr.2014.2482
43. Giallongo S, Di Rosa M, Caltabiano R, Longhitano L, Reibaldi M, Distefano A, et al. Loss of Macroh2a1 Decreases Mitochondrial Metabolism and Reduces the Aggressiveness of Uveal Melanoma Cells. *Aging (Albany NY)* (2020) 12:9745–60. doi: 10.18632/aging.103241
44. Lens SM, Voest EE, Medema RH. Shared and Separate Functions of Polo-Like Kinases and Aurora Kinases in Cancer. *Nat Rev Cancer* (2010) 10:825–41. doi: 10.1038/nrc2964
45. Chaisaingmongkol J, Budhu A, Dang H, Rabibhadana S, Pupacdi B, Kwon SM, et al. Common Molecular Subtypes Among Asian Hepatocellular Carcinoma and Cholangiocarcinoma. *Cancer Cell* (2017) 32:57–70.e3. doi: 10.1016/j.ccell.2017.05.009
46. Prevo R, Pirovano G, Puliyadi R, Herbert KJ, Rodriguez-Berriguete G, O'Docherty A, et al. CDK1 Inhibition Sensitizes Normal Cells to DNA Damage in a Cell Cycle Dependent Manner. *Cell Cycle* (2018) 17:1513–23. doi: 10.1080/15384101.2018.1491236
47. Wang Q, Su L, Liu N, Zhang L, Xu W, Fang H. Cyclin Dependent Kinase 1 Inhibitors: A Review of Recent Progress. *Curr Med Chem* (2011) 18:2025–43. doi: 10.2174/092986711795590110
48. Yan M, Wang C, He B, Yang M, Tong M, Long Z, et al. Aurora-A Kinase: A Potent Oncogene and Target for Cancer Therapy. *Med Res Rev* (2016) 36:1036–79. doi: 10.1002/med.21399
49. Kent LN, Leone G. The Broken Cycle: E2F Dysfunction in Cancer. *Nat Rev Cancer* (2019) 19:326–38. doi: 10.1038/s41568-019-0143-7
50. Polager S, Ginsberg D. E2F - at the Crossroads of Life and Death. *Trends Cell Biol* (2008) 18:528–35. doi: 10.1016/j.tcb.2008.08.003
51. Bindea G, Mlecnik B, Tosolini M, Kirilovsky A, Waldner M, Obenauf AC, et al. Spatiotemporal Dynamics of Intratumoral Immune Cells Reveal the Immune Landscape in Human Cancer. *Immunity* (2013) 39:782–95. doi: 10.1016/j.immuni.2013.10.003
52. Bremnes RM, Busund LT, Kilvaer TL, Andersen S, Richardsen E, Paulsen EE, et al. The Role of Tumor-Infiltrating Lymphocytes in Development, Progression, and Prognosis of Non-Small Cell Lung Cancer. *J Thorac Oncol* (2016) 11:789–800. doi: 10.1016/j.jtho.2016.01.015
53. Singh S, Hassan D, Aldawsari HM, Molugulu N, Shukla R, Kesharwani P. Immune Checkpoint Inhibitors: A Promising Anticancer Therapy. *Drug Discov Today* (2020) 25:223–9. doi: 10.1016/j.drudis.2019.11.003
54. Jiao Y, Yi M, Xu L, Chu Q, Yan Y, Luo S, et al. CD38: Targeted Therapy in Multiple Myeloma and Therapeutic Potential for Solid Cancers. *Expert Opin Investig Drugs* (2020) 29:1295–308. doi: 10.1080/13543784.2020.1814253
55. Laudisi F, Cherubini F, Monteleone G, Stolfi C. STAT3 Interactors as Potential Therapeutic Targets for Cancer Treatment. *Int J Mol Sci* (2018) 19:1787. doi: 10.3390/ijms19061787
56. Carpenter RL, Lo HW. STAT3 Target Genes Relevant to Human Cancers. *Cancers (Basel)* (2014) 6:897–925. doi: 10.3390/cancers6020897
57. Wu WY, Li J, Wu ZS, Zhang CL, Meng XL. STAT3 Activation in Monocytes Accelerates Liver Cancer Progression. *BMC Cancer* (2011) 11:506. doi: 10.1186/1471-2407-11-506

Conflict of Interest: The authors declare that the research was conducted in the absence of any commercial or financial relationships that could be construed as a potential conflict of interest.

Publisher's Note: All claims expressed in this article are solely those of the authors and do not necessarily represent those of their affiliated organizations, or those of the publisher, the editors and the reviewers. Any product that may be evaluated in this article, or claim that may be made by its manufacturer, is not guaranteed or endorsed by the publisher.

frontiers in Immunology

CASE REPORT
published: 06 January 2022
doi: 10.3389/fimmu.2021.784861

Case Report: Addition of PD-1 Antibody Camrelizumab Overcame Resistance to Trastuzumab Plus Chemotherapy in a HER2-Positive, Metastatic Gallbladder Cancer Patient

Li Wang[1†], Xiaomo Li[2†], Yurong Cheng[1], Jing Yang[1], Si Liu[2], Tonghui Ma[2], Li Luo[3], Yanping Hu[3], Yi Cai[4] and Dong Yan[1*]*

[1] Department of Oncology, Beijing Luhe Hospital Affiliated to Capital Medical University, Beijing, China, [2] Department of Translational Medicine, Genetron Health (Beijing) Technology, Co. Ltd, Beijing, China, [3] Department of Pathology, Beijing Luhe Hospital Affiliated to Capital Medical University, Beijing, China, [4] Independent Researcher, Ellicott City, MD, United States

HER2 amplification/overexpression is a common driver in a variety of cancers including gallbladder cancer (GBC). For patients with metastatic GBC, chemotherapy remains the standard of care with limited efficacy. The combination of HER2 antibody trastuzumab plus chemotherapy is the frontline treatment option for patients with HER2-positive breast cancer and gastric cancer. Recently, this regime also showed antitumor activity in HER2-positive GBC. However, resistance to this regime represents a clinical challenge. Camrelizumab is a novel PD-1 antibody approved for Hodgkin lymphoma and hepatocellular carcinoma in China. In this study, we presented a HER2-positive metastatic GBC patient who was refractory to trastuzumab plus chemotherapy but experienced significant clinical benefit after the addition of camrelizumab. Our case highlights the potential of immunotherapy in combination with HER2-targeted therapy in HER2-positive GBC. We also demonstrated that two immune-related adverse events (irAEs) associated with camrelizumab can be managed with an anti-VEGF agent apatinib. This case not only highlights the importance of irAE management in patients treated with camrelizumab, but also demonstrates the potential of PD-1 antibody plus trastuzumab in HER2-positive GBC patients who have developed resistance to chemotherapy and trastuzumab-based targeted therapy.

Keywords: gallbladder cancer, *HER2* amplification, trastuzumab resistance, combination immunotherapy, camrelizumab, irAE, case report

OPEN ACCESS

Edited by:
Bo Qin,
Mayo Clinic, United States

Reviewed by:
Thuy Vu,
University of Texas MD Anderson Cancer Center, United States
Chongqi Tu,
Sichuan University, China
Lixuan Wei,
Mayo Clinic, United States

****Correspondence:***
Dong Yan
yd15yt88@163.com
Yi Cai
yicai108@gmail.com

[†]These authors have contributed equally to this work and share first authorship

Specialty section:
This article was submitted to Cancer Immunity and Immunotherapy, a section of the journal Frontiers in Immunology

Received: *28 September 2021*
Accepted: *15 December 2021*
Published: *06 January 2022*

Citation:
Wang L, Li X, Cheng Y, Yang J, Liu S, Ma T, Luo L, Hu Y, Cai Y and Yan D (2022) Case Report: Addition of PD-1 Antibody Camrelizumab Overcame Resistance to Trastuzumab Plus Chemotherapy in a HER2-Positive, Metastatic Gallbladder Cancer Patient. Front. Immunol. 12:784861. doi: 10.3389/fimmu.2021.784861

INTRODUCTION

Biliary tract cancers (BTCs) are low-incidence epithelial malignancies in the biliary tree, including gallbladder cancer (GBC) and cholangiocarcinoma (CCA). From 1990 to 2017, the global incidence and mortality of BTCs increased by 76% and 65%, respectively (1). Recently, FGFR inhibitors (pemigatinib and infigratinib) and IDH1 inhibitor ivosidenib have significantly improved the outcomes of CCA patients harboring *FGFR2* or *IDH1* alterations, respectively (2). The FDA approvals of these agents and the endorsement from the latest NCCN guideline demonstrated that the treatment of CCA finally enters the era of precision therapy (3). In contrast, chemotherapy is the only systemic treatment available for advanced or metastatic GBC patients, and its clinical benefit is limited, with a median overall survival (OS) of less than one year (2). Given the dismal prognosis of GBC patients, a biomarker-guided personalized treatment strategy should be explored in this BTC subtype without targeted therapy or immunotherapy options (3, 4).

Genomic profiling studies revealed that the amplification or overexpression of *ERBB2/HER2* is a major targetable mutation in GBC (5–7). HER2 is a member of the ERBB family of receptor tyrosine kinases and an established therapeutic target in breast, gastric and gastroesophageal junction (GEJ) cancers (8). A variety of HER2-directed agents including monoclonal antibodies, tyrosine kinase inhibitors, and antibody-drug conjugates (ADCs), have significantly improved the outcomes of patients with HER2-positive breast cancer and become the front-line treatment options for this disease (8).

Cancer immunotherapy agents such as immune checkpoint inhibitors have caused a paradigm shift in the landscape of cancer treatment. In addition to monotherapy, immune checkpoint inhibitors combined with HER2-directed therapies, provide a promising strategy to combat trastuzumab resistance in various HER2-positive cancers. For instance, in the phase 1b/2 PANACEA trial, the combination of PD-1 antibody pembrolizumab and trastuzumab showed activity and durable clinical benefit in patients with trastuzumab-resistant, HER2-positive breast cancer (9). Similarly, pembrolizumab plus trastuzumab and chemotherapy showed superior efficacy in HER2-positive gastric/GEJ cancers, which resulted in the accelerated approval of this triplet regime as the first-line treatment by the FDA (10). In this study, we encountered a HER2-positive, metastatic GBC patient refractory to chemotherapy and HER2-targeted therapy plus chemotherapy. Surprisingly, he responded to a series of combination therapies containing trastuzumab plus a novel PD-1 antibody camrelizumab. Our results suggest that the combination of PD-1 antibody plus trastuzumab with or without chemotherapy could be feasible treatment options for trastuzumab-resistant, HER2-positive, advanced GBC.

CASE PRESENTATION

In September 2018, a 67-year-old Chinese man was admitted to our hospital due to a gallbladder mass revealed by ultrasonography during routine physical examination. His baseline Karnofsky Performance Status (KPS) was 100. Radical resection was performed on October 9th, 2018, and postoperative pathology revealed a stage IIIA (T3N0M0) moderately-differentiated GBC. A summary of his treatment history is illustrated in **Figure 1A**. Immunohistochemical (IHC) staining was positive for HER2 (3+) and negative for PD-L1 (**Figure 1B**). The patient received five cycles of capecitabine. A follow-up chest CT scan in April 2019 revealed disease progression in the lung and his KPS score dropped to 80. Biopsy of a pulmonary lesion confirmed staged IV (T3N0M1) GBC. IHC staining was positive for HER2 (3+), CK8/18, CK19, AE1/AE3 and negative for PD-L1, TTF-1, Napsin-A, p40, and p63. Treatment was changed to S-1 monotherapy for one cycle before the addition of gemcitabine. After three cycles, a new liver lesion and increased bilirubin level were noted. Treatment was switched to oxaliplatin and paclitaxel, but left off after one cycle due to disease progression, as well as multiple adverse events including limbs numbness, grade 2 peripheral neurotoxicity, grade 3 diarrhea, increased γ-glutamyltranspeptidase level, and severe abdominal pain (numeric rating scale of 8-9).

The failure of chemotherapy led us to explore the possibility of targeted therapy. A multi-gene next-generation sequencing (NGS) testing (Onco Panscan^{TM}, Genetron Health) was performed on the primary lesion and a pulmonary nodule to identify potential therapeutic targets (**Figure 1C** and **Supplemental Table 1**). Genomic profiling of the pulmonary lesion showed the presence of *TP53* S241Y, *ARID2* R273*, *EGFR* E872K mutations, *HER2* amplification (fold change, 8.7), and a high tumor mutational burden (TMB) of 10.33 mutations per megabase (mut/Mb). The *EGFR* E872K mutation, originally found in a bile duct carcinoma patient, was associated with activation of EGFR signaling, a common mechanism for acquired trastuzumab resistance in HER2-positive esophagogastric (EG) cancer (11, 12). To target *HER2* amplification and putative activation of EGFR signaling mediated by the *EGFR* E872K mutation, this patient was treated with a triplet regime consisting of trastuzumab (6mg/kg, Q3W), HER2/EGFR inhibitor afatinib (30mg, QD), and capecitabine (2500mg/m^2 on days 1-14, Q3W) in August 2019. In the first dose of trastuzumab infusion, the patient experienced chills and fever, which were resolved by antipyretic treatment. In September 2019, this combination therapy was discontinued when new brain metastases and pulmonary progression of disease were noted (**Figure 2A**).

Because HER2-targeting antibody-drug conjugates (ADCs) such as ado-trastuzumab emtansine (T-DM1) and fam-trastuzumab deruxtecan (T-DXd) were not approved in China at that time, we set out to explore the possibility of immunotherapy given the TMB-H status of the pulmonary metastases. In the basket study of the KEYNOTE-158 trial, pembrolizumab showed durable antitumor activity in a subset of patients with advanced biliary adenocarcinoma irrespective of PD-L1 status (13). In a single-center phase 2 trial, the combination of pembrolizumab plus trastuzumab and chemotherapy achieved a disease control rate of 100% and an objective response rate (ORR) of 83% in HER2-positive metastatic esophagogastric adenocarcinoma irrespective of PD-L1 status (14). Based on these results and the affordability of a

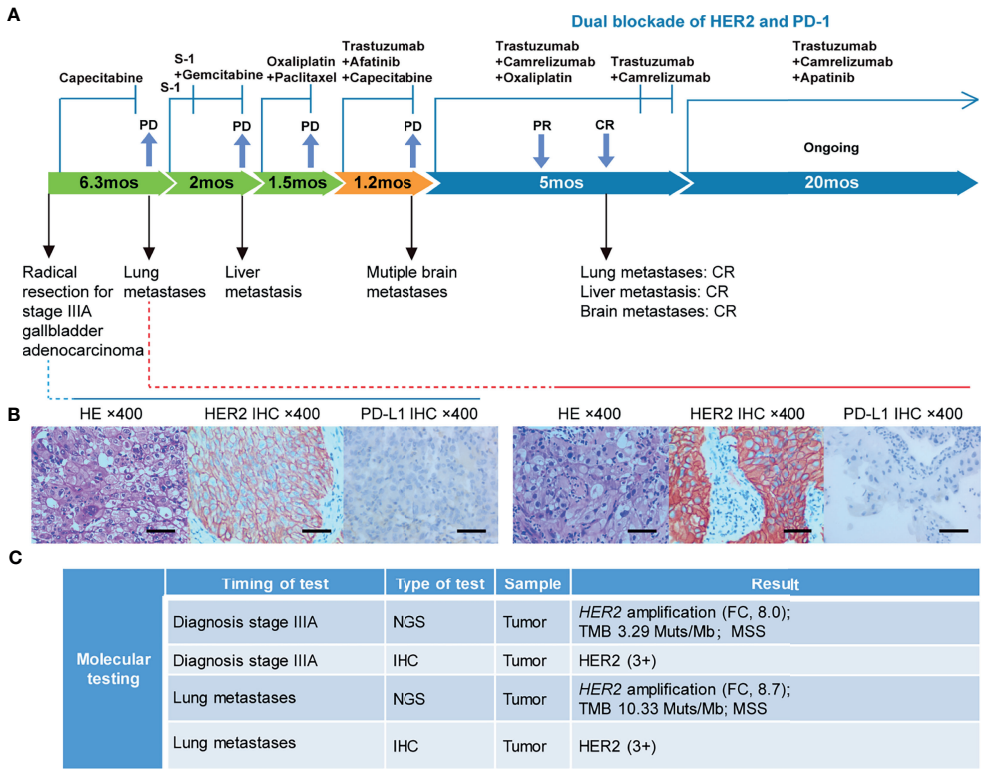

	Timing of test	Type of test	Sample	Result
Molecular testing	Diagnosis stage IIIA	NGS	Tumor	*HER2* amplification (FC, 8.0); TMB 3.29 Muts/Mb; MSS
	Diagnosis stage IIIA	IHC	Tumor	HER2 (3+)
	Lung metastases	NGS	Tumor	*HER2* amplification (FC, 8.7); TMB 10.33 Muts/Mb; MSS
	Lung metastases	IHC	Tumor	HER2 (3+)

FIGURE 1 | Case summary. **(A)** Summary of disease course, treatment procedure, and key molecular findings. PR, partial response; CR, complete response; PD, progressive disease; mo, months. **(B)** H&E, HER2, and PD-L1 staining of the primary tumor and lung metastasis. Scale bars: 25 μm. H&E: hematoxylin and eosin. **(C)** Detailed molecular alterations of the primary tumor and lung metastasis. FC, fold change; MSS, microsatellite stable; TMB, tumor mutational burden.

domestic PD-1 antibody camrelizumab, a triplet regime of camrelizumab (200mg, Q3W), trastuzumab (6mg/kg, Q3W), and oxaliplatin (130mg/m^2, Q3W) were administered for six cycles. In the first cycle, radical cryoablation was performed to treat the lung metastases. After three cycles, regression of all metastases involving multiple organs was noted. The lesions of the lung, liver, and brain completely regressed after five cycles (**Figure 2A**). The patient's CA199, which continued to increase during chemotherapy and HER2-directed therapy, quickly fell into the normal range after the addition of camrelizumab, indicative of response to the combination regime (**Figure 2B**). Oxaliplatin was discontinued after six cycles due to grade 2 thrombocytopenia, which was subsequently resolved with recombinant human interleukin-11 (rhIL-11) treatment. The patient continued on maintenance camrelizumab plus trastuzumab, with a KPS score of 90. After cycle 2 of camrelizumab, the patient developed grade 1 reactive cutaneous capillary endothelial proliferation (RCCEP), a novel immune-related adverse event (irAE) observed in the majority of patients treated with camrelizumab (15, 16). The symptoms of RCCEP reached grade 2 in cycles 3-4 when the patient developed one cutaneous nodule with a diameter larger than 10mm and bleeding. Apatinib, a small-molecule VEGFR2 inhibitor, has been approved to treat gastric cancer in China (17). The addition of low-dose apatinib to camrelizumab significantly reduced the frequency of RCCEP in clinical studies (18–20). Based on these results, apatinib (250mg, QD) was added to the treatment regime. The patient's RCCEP became grade 1 on week 3, and completely regressed on week 6 (**Figure 3A**). Interestingly, the addition of apatinib also led to the complete resolution of an endothelial neovessel-based nodule in the right buccal mucosa, a putative camrelizumab-related irAE (**Figure 3B**). Apatinib was then decreased to 250mg, twice a week with no recurrence of RCCEP. The patient remained in remission until the last follow-up in November 2021 with a KPS score of 90.

DISCUSSION

Biliary tract cancers (BTCs), including cholangiocarcinoma (CCA) and gallbladder cancer (GBC), are a group of gastrointestinal cancers with low incidence and poor prognosis (21). BTCs are generally refractory to chemotherapy and the 5-year survival rate of BTC patients ranges from 5% to 15% (22). HER2 overexpression is detected in 13%-31% of GBC cases and is a promising candidate for targeted therapy clinical trials (23–25). HER2 is an established therapeutic target in HER2-positive breast, gastric, and gastroesophageal junction (GEJ) cancers (8, 26). Multiple HER2-directed agents have been approved to treat HER2-positive breast cancer, including trastuzumab, pertuzumab, margetuximab, trastuzumab emtansine (T-DM1), trastuzumab deruxtecan (T-

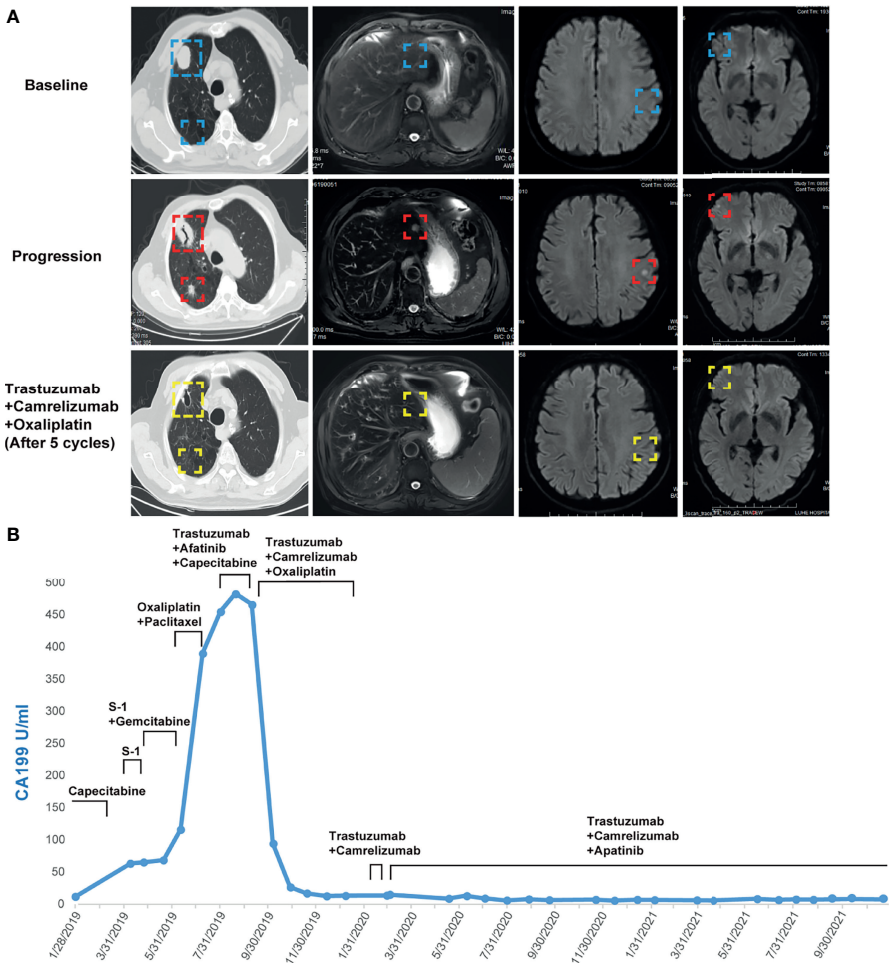

FIGURE 2 | **(A)** Computed tomography and MRI images showing the patient's baseline disease, progression on S-1 plus gemcitabine in the liver metastatic lesion, progression on trastuzumab plus afatinib and capecitabine in the brain and lung metastatic lesions, and response to camrelizumab plus trastuzumab and oxaliplatin in the liver, brain, and lung metastatic lesions. **(B)** Dynamics of cancer antigen 199 (CA199) (U/ml) levels during the entire disease course.

DXd/DS-8201), neratinib, lapatinib, and tucatinib (27). However, the options of HER2-targeted therapies for HER2-positive gastrointestinal cancers are very limited. For instance, only trastuzumab and trastuzumab deruxtecan are approved for HER2-positive gastric/GEJ cancer (28). Unlike HER2-positive breast cancer and gastric/GEJ cancer, there is no HER2-directed therapy approved for HER2-positive BTC. Multiple HER2-directed agents, including receptor tyrosine kinase inhibitors, monoclonal antibodies, and antibody-drug conjugates, have been or are currently being tested in ongoing trials for patients with BTC. Lapatinib, a HER2 receptor tyrosine kinase inhibitor (TKI), failed to show activity in two phase 2 trials for unselected patients with BTC (29, 30). In the phase 2 SUMMIT basket trial, neratinib achieved an ORR of 12% and a median PFS of 2.8 months in 25 patients with *HER2*-mutated BTC (31). The combination of trastuzumab and pertuzumab resulted in an ORR of 23% in a multicenter, open-label, phase 2a trial for HER2-positive, metastatic BTC (32). In a phase 2 basket trial (NCT02675829), trastuzumab emtansine (T-DM1) resulted in an ORR of 16.7% in 6 patients with *HER2*-amplified BTC (7). In a phase 1 trial for pretreated, HER2-expressing (IHC > 1+), non-breast/non-gastric solid tumors, trastuzumab deruxtecan achieved partial response in two BTC patients (33).

Cancer immunotherapy has led to a paradigm shift in cancer treatment. Recent clinical studies reported a synergistic effect of the combination of immune checkpoint inhibitors with HER2-directed agents in HER2-positive gastric/GEJ cancers (34, 35). Interim analysis of the ongoing KEYNOTE-811 trial showed that the triplet regime of pembrolizumab, trastuzumab, and chemotherapy resulted in a substantial, statistically significant increase in ORR versus the duplet regime of trastuzumab and chemotherapy as first-line therapy for HER2-positive metastatic gastric/GEJ cancer (10). Based on these results, FDA granted accelerated approval of pembrolizumab in combination with trastuzumab and chemotherapy as the first-line treatment for patients with locally advanced unresectable or metastatic HER2 positive gastric/GEJ cancer.

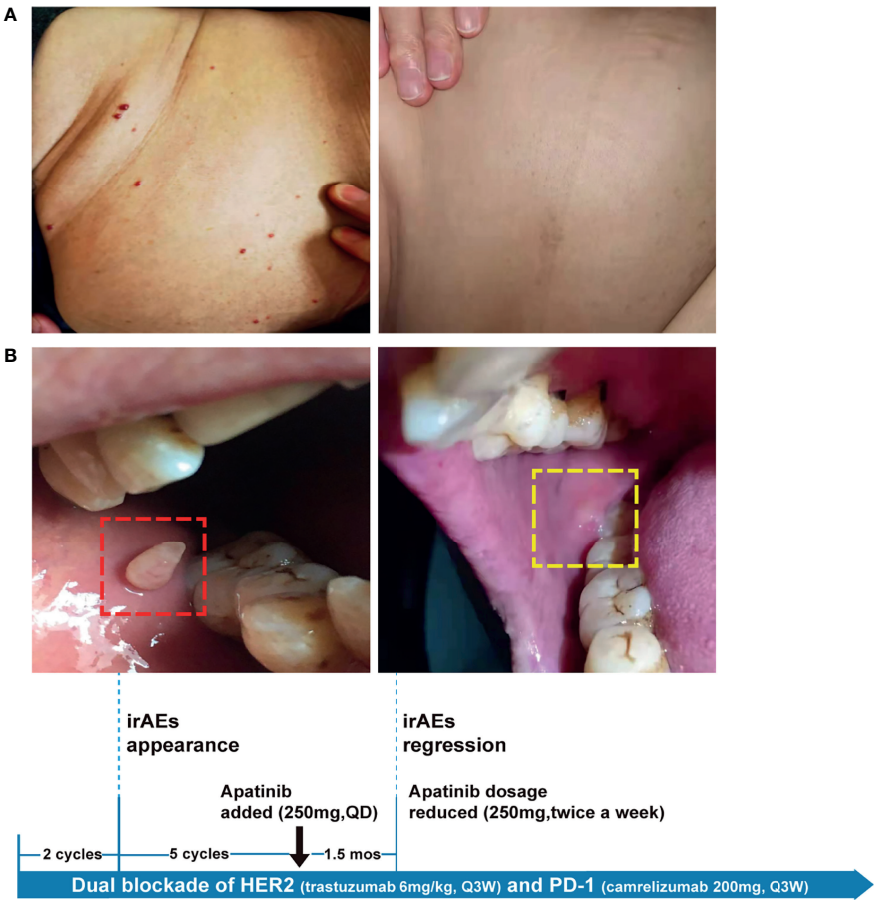

FIGURE 3 | The management of camrelizumab-related irAEs with anti-VEGF agent apatinib. Representative images showing irAEs of **(A)** RCCEP, **(B)** mucosal membrane and their resolution after apatinib treatment. irAE, immune-related adverse event; RCCEP, reactive cutaneous capillary endothelial proliferation.

Currently, PD-L1 is the most widely used biomarker to guide the selection of patients to receive PD-1/PD-L1 immune checkpoint blockade therapy (36). One intriguing observation of this case study is that the clinical response to PD-1/HER2 dual blockade did not correlate with the PD-L1-negative status of the primary tumor and lung metastases. Interestingly, in some PD-1/HER2 dual blockade trials of HER2-positive gastrointestinal cancers, the clinical benefit did not correlate with PD-L1 status either. For instance, in the CP-MGAH22–05 phase 1b/2 trial for HER2-positive gastroesophageal carcinoma patients, pembrolizumab plus HER2 antibody margetuximab resulted in disease control rate of 72% and 56% in HER2 IHC-positive/PD-L1-positive and HER2 IHC-positive/PD-L1-negative patients, respectively (34). Similarly, in the phase 2 trial testing the efficacy of pembrolizumab plus trastuzumab in patients with HER-2 positive esophagogastric cancer, the median PFS in the PD-L1-negative group was numerically longer than that of the PD-L1-positive group (14.6 versus 10.3 months, respectively; $p = 0.56$) (35). Together, these results indicated that HER2-positive GBC patients with PD-L1-negative status should be enrolled in future clinical trials of dual PD-1/HER2 blockade therapy as well.

Tumor mutational burden (TMB) is a useful but imperfect predictive biomarker for cancer immunotherapy. Based on results of the KEYNOTE-158 trial, FDA recently approved pembrolizumab for patients who have solid tumors with a TMB greater than 10 mut/Mb (37). This threshold was determined by the FoundationOne CDx (F1CDx) assay, which targets a genomic region of ~0.8 Mb covering 324 cancer-related genes (38). The gold standard to measure TMB is whole exome sequencing (WES), which is impractical to use in the clinic right now. For accurate TMB assessment, multi-gene panels covering at least 1 Mb are generally recommended (38, 39). The phase 2 KEYNOTE-158 trial covered 10 different rare cancers including biliary adenocarcinoma (37). Whether the results of these rare cancers can be extended to common cancers is a controversial issue (40, 41). It is recommended that the application of TMB as an immune biomarker should be cancer-type specific and in combination with other immune biomarkers (38–40). Further investigations are required to fully explore the potential of TMB as an immune biomarker for GBC treatment.

The timely recognition and mitigation of serious immune-related adverse events (irAEs) are essential for the optimal

management of cancer patients treated with ICIs. A novel ICI-related irAE, reactive cutaneous capillary endothelial proliferation (RCCEP), represents the most common irAE associated with camrelizumab (42–44). To address this issue, the Chinese Society of Clinical Oncology (CSCO) recently developed an RCCEP management guideline, which recommended special interventions for grade 2 RCCEP with large nodules or bleeding (45). Although the mechanism of RCCEP is still unknown, it was observed that RCCEP correlates with increased expression of VEGF-A and activation of VEGFR-2 receptor, two key players of VEGF signaling (45). Interestingly, a retrospective meta-analysis revealed that the median resolution time of RCCEP was 6.5 months in patients treated with camrelizumab alone but 2.2 months if camrelizumab was combined with anti-VEGF therapy (45). Consistently, several clinical studies showed that the addition of VEGFR-2 inhibitor apatinib significantly reduced the frequency of RCCEP or alleviated symptoms of RCCEP in patients treated with camrelizumab (46–49). Together, these results indicated that anti-VEGF therapy could be a promising strategy for the management of camrelizumab-related RCCEP.

In summary, we applied a triplet combination of camrelizumab, trastuzumab, and chemotherapy to overcome the resistance to chemotherapy and HER2-targeted therapy in a HER2-positive GBC patient. The response was maintained after the withdraw of chemotherapy. Our case demonstrated that the combination of PD-1 antibody plus trastuzumab with or without chemotherapy can produce robust and durable responses in metastatic HER2-positive GBC resistant to trastuzumab and chemotherapy. Some of the camrelizumab-related irAEs may be managed by the anti-VEGF agent apatinib. Future investigation of PD-1 antibody plus trastuzumab with or without chemotherapy as the frontline treatments for HER2-positive GBC is warranted.

DATA AVAILABILITY STATEMENT

The original contributions presented in the study are included in the article/**Supplementary Material**. Further inquiries can be directed to the corresponding authors.

ETHICS STATEMENT

Written informed consent was obtained from the individual(s) for the publication of any potentially identifiable images or data included in this article.

AUTHOR CONTRIBUTIONS

DY, conceptualization, methodology, supervision, writing-reviewing and editing. YC, conceptualization, investigation, and writing-original draft preparation. LW and XL, methodology, visualization, investigation, and writing-original draft preparation. YRC, JY, and SL, investigation, data curation, and validation. TM, validation, writing-reviewing and editing. LL and YH, methodology and validation. All authors contributed to the article and approved the submitted version.

SUPPLEMENTARY MATERIAL

The Supplementary Material for this article can be found online at: https://www.frontiersin.org/articles/10.3389/fimmu.2021.784861/full#supplementary-material

REFERENCES

1. Ouyang G, Liu Q, Wu Y, Liu Z, Lu W, Li S, et al. The Global, Regional, and National Burden of Gallbladder and Biliary Tract Cancer and Its Attributable Risk Factors in 195 Countries and Territories, 1990 to 2017: A Systematic Analysis for the Global Burden of Disease Study 2017. *Cancer* (2021) 127:2238–50. doi: 10.1002/cncr.33476
2. Valle JW, Kelley RK, Nervi B, Oh DY, Zhu AX. Biliary Tract Cancer. *Lancet (London England)* (2021) 397:428–44. doi: 10.1016/s0140-6736(21)00153-7
3. Benson AB, D'Angelica MI, Abbott DE, Anaya DA, Anders R, Are C, et al. Hepatobiliary Cancers, Version 2.2021, NCCN Clinical Practice Guidelines in Oncology. *J Natl Compr Cancer Netw JNCCN* (2021) 19:541–65. doi: 10.6004/jnccn.2021.0022
4. Zhu AX, Macarulla T, Javle MM, Kelley RK, Lubner SJ, Adeva J, et al. Final Results From ClarIDHy, a Global, Phase III, Randomized, Double-Blind Study of Ivosidenib (IVO) Versus Placebo (PBO) in Patients (Pts) With Previously Treated Cholangiocarcinoma (CCA) and an Isocitrate Dehydrogenase 1 (IDH1) Mutation. *J Clin Oncol* (2021) 39:266–6. doi: 10.1200/JCO.2021.39.3_suppl.266
5. Nepal C, Zhu B, O'Rourke CJ, Bhatt DK, Lee D, Song L, et al. Integrative Molecular Characterisation of Gallbladder Cancer Reveals Micro-Environment-Associated Subtypes. *J Hepatol* (2021) 74:1132–44. doi: 10.1016/j.jhep.2020.11.033
6. Lin J, Cao Y, Yang X, Li G, Shi Y, Wang D, et al. Mutational Spectrum and Precision Oncology for Biliary Tract Carcinoma. *Theranostics* (2021) 11:4585–98. doi: 10.7150/thno.56539
7. Mondaca S, Razavi P, Xu C, Offin M, Myers M, Scaltriti M, et al. Genomic Characterization of ERBB2-Driven Biliary Cancer and a Case of Response to Ado-Trastuzumab Emtansine. *JCO Precis Oncol* (2019) 3:1–9. doi: 10.1200/po.19.00223
8. Oh DY, Bang YJ. HER2-Targeted Therapies - a Role Beyond Breast Cancer. Nature reviews. *Clin Oncol* (2020) 17:33–48. doi: 10.1038/s41571-019-0268-3
9. Loi S, Giobbie-Hurder A, Gombos A, Bachelot T, Hui R, Curigliano G, et al. Pembrolizumab Plus Trastuzumab in Trastuzumab-Resistant, Advanced, HER2-Positive Breast Cancer (PANACEA): A Single-Arm, Multicentre, Phase 1b-2 Trial. *Lancet Oncol* (2019) 20:371–82. doi: 10.1016/s1470-2045(18)30812-x
10. Janjigian YY, Kawazoe A, Yanez PE, Luo S, Lonardi S, Kolesnik O, et al. Pembrolizumab Plus Trastuzumab and Chemotherapy for HER2+ Metastatic Gastric or Gastroesophageal Junction (G/GEJ) Cancer: Initial Findings of the Global Phase 3 KEYNOTE-811 Study. *J Clin Oncol* (2021) 39:4013–3. doi: 10.1200/JCO.2021.39.15_suppl.4013
11. Leone F, Cavalloni G, Pignochino Y, Sarotto I, Ferraris R, Piacibello W, et al. Somatic Mutations of Epidermal Growth Factor Receptor in Bile Duct and Gallbladder Carcinoma. *Clin Cancer Res Off J Am Assoc Cancer Res* (2006) 12:1680–5. doi: 10.1158/1078-0432.Ccr-05-1692
12. Sanchez-Vega F, Hechtman JF, Castel P, Ku GY, Tuvy Y, Won H, et al. EGFR and MET Amplifications Determine Response to HER2 Inhibition in ERBB2-Amplified Esophagogastric Cancer. *Cancer Discov* (2019) 9:199–209. doi: 10.1158/2159-8290.Cd-18-0598
13. Bang Y-J, Ueno M, Malka D, Chung HC, Nagrial A, Kelley RK, et al. Pembrolizumab (Pembro) for Advanced Biliary Adenocarcinoma: Results From the KEYNOTE-028 (KN028) and KEYNOTE-158 (KN158) Basket Studies. *J Clin Oncol* (2019) 37:4079–9. doi: 10.1200/JCO.2019.37.15_suppl.4079
14. Janjigian YY, Chou JF, Simmons M, Momtaz P, Sanchez-Vega F, Shcherba M, et al. First-Line Pembrolizumab (P), Trastuzumab (T), Capecitabine (C) and

Oxaliplatin (O) in HER2-Positive Metastatic Esophagogastric Adenocarcinoma (mEGA). *J Clin Oncol* (2019) 37:62–2. doi: 10.1200/JCO.2019.37.4_suppl.62
15. Chen X, Ma L, Wang X, Mo H, Wu D, Lan B, et al. Reactive Capillary Hemangiomas: A Novel Dermatologic Toxicity Following Anti-PD-1 Treatment With SHR-1210. *Cancer Biol Med* (2019) 16:173–81. doi: 10.20892/j.issn.2095-3941.2018.0172
16. Song Y, Wu J, Chen X, Lin T, Cao J, Liu Y, et al. Multicenter, Phase II Study of Camrelizumab in Relapsed or Refractory Classical Hodgkin Lymphoma. *Clin Cancer Res* (2019) 25:7363–9. doi: 10.1158/1078-0432.Ccr-19-1680
17. Li J, Qin S, Xu J, Xiong J, Wu C, Bai Y, et al. Randomized, Double-Blind, Placebo-Controlled Phase III Trial of Apatinib in Patients With Chemotherapy-Refractory Advanced or Metastatic Adenocarcinoma of the Stomach or Gastroesophageal Junction. *J Clin Oncol* (2016) 34:1448–54. doi: 10.1200/jco.2015.63.5995
18. Xu J, Zhang Y, Jia R, Yue C, Chang L, Liu R, et al. Anti-PD-1 Antibody SHR-1210 Combined With Apatinib for Advanced Hepatocellular Carcinoma, Gastric, or Esophagogastric Junction Cancer: An Open-Label, Dose Escalation and Expansion Study. *Clin Cancer Res* (2019) 25:515–23. doi: 10.1158/1078-0432.Ccr-18-2484
19. Zhao S, Ren S, Jiang T, Zhu B, Li X, Zhao C, et al. Low-Dose Apatinib Optimizes Tumor Microenvironment and Potentiates Antitumor Effect of PD-1/PD-L1 Blockade in Lung Cancer. *Cancer Immunol Res* (2019) 7:630–43. doi: 10.1158/2326-6066.Cir-17-0640
20. Zhou C, Gao G, Wang YN, Zhao J, Chen G, Liu Z, et al. Efficacy of PD-1 Monoclonal Antibody SHR-1210 Plus Apatinib in Patients With Advanced Nonsquamous NSCLC With Wild-Type EGFR and ALK. *J Clin Oncol* (2019) 37:9112–2. doi: 10.1200/JCO.2019.37.15_suppl.9112
21. Valle JW, Lamarca A, Goyal L, Barriuso J, Zhu AX. New Horizons for Precision Medicine in Biliary Tract Cancers. *Cancer Discov* (2017) 7:943–62. doi: 10.1158/2159-8290.Cd-17-0245
22. Hundal R, Shaffer EA. Gallbladder Cancer: Epidemiology and Outcome. *Clin Epidemiol* (2014) 6:99–109. doi: 10.2147/clep.S37357
23. Roa I, de Toro G, Schalper K, de Aretxabala X, Churi C, Javle M. Overexpression of the HER2/neu Gene: A New Therapeutic Possibility for Patients With Advanced Gallbladder Cancer. *Gastrointestinal Cancer Res GCR* (2014) 7:42–8.
24. Vivaldi C, Fornaro L, Ugolini C, Niccoli C, Musettini G, Pecora I, et al. HER2 Overexpression as a Poor Prognostic Determinant in Resected Biliary Tract Cancer. *Oncol* (2020) 25:886–93. doi: 10.1634/theoncologist.2019-0922
25. Hiraoka N, Nitta H, Ohba A, Yoshida H, Morizane C, Okusaka T, et al. Details of Human Epidermal Growth Factor Receptor 2 Status in 454 Cases of Biliary Tract Cancer. *Hum Pathol* (2020) 105:9–19. doi: 10.1016/j.humpath.2020.08.006
26. Denduluri N, Somerfield MR, Chavez-MacGregor M, Comander AH, Dayao Z, Eisen A, et al. Selection of Optimal Adjuvant Chemotherapy and Targeted Therapy for Early Breast Cancer: ASCO Guideline Update. *J Clin Oncol Off J Am Soc Clin Oncol* (2021) 39:685–93. doi: 10.1200/jco.20.02510
27. Gradishar WJ, Moran MS, Abraham J, Aft R, Agnese D, Allison KH, et al. NCCN Guidelines® Insights: Breast Cancer, Version 4.2021. *J Natl Compr Cancer Netw JNCCN* (2021) 19:484–93. doi: 10.6004/jnccn.2021.0023
28. Nakamura Y, Kawazoe A, Lordick F, Janjigian YY, Shitara K. Biomarker-Targeted Therapies for Advanced-Stage Gastric and Gastro-Oesophageal Junction Cancers: An Emerging Paradigm. *Nat Rev Clin Oncol* (2021) 18:473–87. doi: 10.1038/s41571-021-00492-2
29. Ramanathan RK, Belani CP, Singh DA, Tanaka M, Lenz HJ, Yen Y, et al. A Phase II Study of Lapatinib in Patients With Advanced Biliary Tree and Hepatocellular Cancer. *Cancer Chemother Pharmacol* (2009) 64:777–83. doi: 10.1007/s00280-009-0927-7
30. Peck J, Wei L, Zalupski M, O'Neil B, Villalona Calero M, Bekaii-Saab T. HER2/neu may Not be an Interesting Target in Biliary Cancers: Results of an Early Phase II Study With Lapatinib. *Oncology* (2012) 82:175–9. doi: 10.1159/000336488
31. Harding JJ, Cleary JM, Quinn DI, Braña I, Moreno V, Borad MJ, et al. Targeting HER2 (ERBB2) Mutation-Positive Advanced Biliary Tract Cancers With Neratinib: Results From the Phase II SUMMIT 'Basket' Trial. *J Clin Oncol* (2021) 39:320–0. doi: 10.1200/JCO.2021.39.3_suppl.320
32. Javle M, Borad MJ, Azad NS, Kurzrock R, Abou-Alfa GK, George B, et al. Pertuzumab and Trastuzumab for HER2-Positive, Metastatic Biliary Tract Cancer (MyPathway): A Multicentre, Open-Label, Phase 2a, Multiple Basket Study. *Lancet Oncol* (2021) 22(9):1290–300. doi: 10.1016/s1470-2045(21)00336-3
33. Tsurutani J, Iwata H, Krop I, Jänne PA, Doi T, Takahashi S, et al. Targeting HER2 With Trastuzumab Deruxtecan: A Dose-Expansion, Phase I Study in Multiple Advanced Solid Tumors. *Cancer Discov* (2020) 10:688–701. doi: 10.1158/2159-8290.Cd-19-1014
34. Catenacci DVT, Kang YK, Park H, Uronis HE, Lee KW, Ng MCH, et al. Margetuximab Plus Pembrolizumab in Patients With Previously Treated, HER2-Positive Gastro-Oesophageal Adenocarcinoma (CP-MGAH22-05): A Single-Arm, Phase 1b-2 Trial. *Lancet Oncol* (2020) 21:1066–76. doi: 10.1016/s1470-2045(20)30326-0
35. Janjigian YY, Maron SB, Chatila WK, Millang B, Chavan SS, Alterman C, et al. First-Line Pembrolizumab and Trastuzumab in HER2-Positive Oesophageal, Gastric, or Gastro-Oesophageal Junction Cancer: An Open-Label, Single-Arm, Phase 2 Trial. *Lancet Oncol* (2020) 21:821–31. doi: 10.1016/s1470-2045(20)30169-8
36. Doroshow DB, Bhalla S, Beasley MB, Sholl LM, Kerr KM, Gnjatic S, et al. PD-L1 as a Biomarker of Response to Immune-Checkpoint Inhibitors. *Nat Rev Clin Oncol* (2021) 18:345–62. doi: 10.1038/s41571-021-00473-5
37. Marabelle A, Fakih M, Lopez J, Shah M, Shapira-Frommer R, Nakagawa K, et al. Association of Tumour Mutational Burden With Outcomes in Patients With Advanced Solid Tumours Treated With Pembrolizumab: Prospective Biomarker Analysis of the Multicohort, Open-Label, Phase 2 KEYNOTE-158 Study. *Lancet Oncol* (2020) 21:1353–65. doi: 10.1016/s1470-2045(20)30445-9
38. Sha D, Jin Z, Budczies J, Kluck K, Stenzinger A, Sinicrope FA. Tumor Mutational Burden as a Predictive Biomarker in Solid Tumors. *Cancer Discov* (2020) 10:1808–25. doi: 10.1158/2159-8290.Cd-20-0522
39. Jardim DL, Goodman A, de Melo Gagliato D, Kurzrock R. The Challenges of Tumor Mutational Burden as an Immunotherapy Biomarker. *Cancer Cell* (2021) 39:154–73. doi: 10.1016/j.ccell.2020.10.001
40. McGrail DJ, Pilié PG, Rashid NU, Voorwerk L, Slagter M, Kok M, et al. High Tumor Mutation Burden Fails to Predict Immune Checkpoint Blockade Response Across All Cancer Types. *Ann Oncol Off J Eur Soc Med Oncol* (2021) 32:661–72. doi: 10.1016/j.annonc.2021.02.006
41. Rousseau B, Foote MB, Maron SB, Diplas BH, Lu S, Argilés G, et al. The Spectrum of Benefit From Checkpoint Blockade in Hypermutated Tumors. *N Engl J Med* (2021) 384:1168–70. doi: 10.1056/NEJMc2031965
42. Huang J, Xu J, Chen Y, Zhuang W, Zhang Y, Chen Z, et al. Camrelizumab Versus Investigator's Choice of Chemotherapy as Second-Line Therapy for Advanced or Metastatic Oesophageal Squamous Cell Carcinoma (ESCORT): A Multicentre, Randomised, Open-Label, Phase 3 Study. *Lancet Oncol* (2020) 21:832–42. doi: 10.1016/s1470-2045(20)30110-8
43. Zhou C, Chen G, Huang Y, Zhou J, Lin L, Feng J, et al. Camrelizumab Plus Carboplatin and Pemetrexed Versus Chemotherapy Alone in Chemotherapy-Naive Patients With Advanced Non-Squamous Non-Small-Cell Lung Cancer (CameL): A Randomised, Open-Label, Multicentre, Phase 3 Trial. *Lancet Respir Med* (2021) 9:305–14. doi: 10.1016/s2213-2600(20)30365-9
44. Yang Y, Qu S, Li J, Hu C, Xu M, Li W, et al. Camrelizumab Versus Placebo in Combination With Gemcitabine and Cisplatin as First-Line Treatment for Recurrent or Metastatic Nasopharyngeal Carcinoma (CAPTAIN-1st): A Multicentre, Randomised, Double-Blind, Phase 3 Trial. *Lancet Oncol* (2021) 22:1162–74. doi: 10.1016/s1470-2045(21)00302-8
45. Expert Committee on Safety Management of Antitumor Drugs of Chinese Society of Clinical Oncology. Expert Consensus on the Clinical Diagnosis and Treatment of Reactive Skin Capillary Hyperplasia Caused by Camrelizumab. *Chin Clin Oncol* (2020) 25:840–8. doi: 10.3969/j.issn.1009-0460.2020.09.012
46. Li W, Wei Z, Yang X, Huang G, Han X, Ni Y, et al. Salvage Therapy of Reactive Capillary Hemangiomas: Apatinib Alleviates the Unique Adverse Events Induced by Camrelizumab in non-Small Cell Lung Cancer. *J Cancer Res Ther* (2019) 15:1624–8. doi: 10.4103/jcrt.JCRT_997_19
47. Fan Y, Zhao J, Wang Q, Huang D, Li X, Chen J, et al. Camrelizumab Plus Apatinib in Extensive-Stage SCLC (PASSION): A Multicenter, Two-Stage, Phase 2 Trial. *J Thorac Oncol Off Publ Int Assoc Study Lung Cancer* (2021) 16:299–309. doi: 10.1016/j.jtho.2020.10.002
48. Xu J, Shen J, Gu S, Zhang Y, Wu L, Wu J, et al. Camrelizumab in Combination With Apatinib in Patients With Advanced Hepatocellular Carcinoma (RESCUE): A Nonrandomized, Open-Label, Phase II Trial. *Clin Cancer Res Off J Am Assoc Cancer Res* (2021) 27:1003–11. doi: 10.1158/1078-0432.Ccr-20-2571
49. Lan C, Shen J, Wang Y, Li J, Liu Z, He M, et al. Camrelizumab Plus Apatinib in Patients With Advanced Cervical Cancer (CLAP): A Multicenter, Open-Label, Single-Arm, Phase II Trial. *J Clin Oncol Off J Am Soc Clin Oncol* (2020) 38:4095–106. doi: 10.1200/jco.20.01920

Conflict of Interest: XL, SL, and TM are employees of Genetron Health (Beijing) Technology, Co. Ltd.

The remaining authors declare that the research was conducted in the absence of any commercial or financial relationships that could be construed as a potential conflict of interest.

Publisher's Note: All claims expressed in this article are solely those of the authors and do not necessarily represent those of their affiliated organizations, or those of the publisher, the editors and the reviewers. Any product that may be evaluated in this article, or claim that may be made by its manufacturer, is not guaranteed or endorsed by the publisher.

frontiers in Immunology

REVIEW
published: 07 January 2022
doi: 10.3389/fimmu.2021.807648

Potential Role of the Gut Microbiome In Colorectal Cancer Progression

Jaeho Kim and Heung Kyu Lee *

Graduate School of Medical Science and Engineering, Korea Advanced Institute of Science and Technology (KAIST), Daejeon, South Korea

An increasing number of studies have revealed that the progression of colorectal cancer (CRC) is related to gut microbiome composition. Under normal conditions, the gut microbiome acts as a barrier to other pathogens or infections in the intestine and modulates inflammation by affecting the host immune system. These gut microbiota are not only related to the intestinal inflammation associated with tumorigenesis but also modulation of the anti-cancer immune response. Thus, they are associated with tumor progression and anti-cancer treatment efficacy. Studies have shown that the gut microbiota can be used as biomarkers to predict the effect of immunotherapy and improve the efficacy of immunotherapy in treating CRC through modulation. In this review, we discuss the role of the gut microbiome as revealed by recent studies of the growth and progression of CRC along with its synergistic effect with anti-cancer treatment modalities.

Keywords: gut microbiota, colorectal cancer, immunotherapy, chemotherapy, immune checkpoint inhibitors

OPEN ACCESS

Edited by:
Ti Wen,
The First Affiliated Hospital of China Medical University, China

Reviewed by:
Philip Brandon Busbee, University of South Carolina, United States
Ana Maria Caetano Faria, Federal University of Minas Gerais, Brazil

***Correspondence:**
Heung Kyu Lee
heungkyu.lee@kaist.ac.kr

Specialty section:
This article was submitted to Cancer Immunity and Immunotherapy, a section of the journal Frontiers in Immunology

Received: *02 November 2021*
Accepted: *17 December 2021*
Published: *07 January 2022*

Citation:
Kim J and Lee HK (2022) Potential Role of the Gut Microbiome In Colorectal Cancer Progression. Front. Immunol. 12:807648. doi: 10.3389/fimmu.2021.807648

INTRODUCTION

Colorectal cancer (CRC) is one of the most common types of cancer and is the third highest leading cause of death worldwide (1). Numerous epidemiological studies have demonstrated that the prevalence of CRC is related to a western diet and intake of dietary fiber, thus highlighting the important relationship between diet and CRC (2–5). In this context, the gut environment, including the microbiome, has been in the spotlight and has emerged as an important factor related to CRC (6).

A multitude of microorganisms live in the intestines of mammals. In the human intestine, there are more than 1000 species and 10^{14} microorganisms forming a colony (7). They play an important role in maintaining a normal physiologic environment, including energy metabolism, interacting with the normal gut barrier system, promoting the survival of epithelial cells, and, importantly, protecting our body against other external or opportunistic pathogens (8). Over the past few decades, studies have shown that the gut microbiome influences the host significantly (9–11). Dysbiosis in the intestines is known to be associated with the pathogenesis of a variety of diseases, including neurological, gastrointestinal, and metabolic diseases (12). Changes in the gut microbiome can be induced by eating habits or changes in environmental factors and studies have shown that changes in the gut microbiome induce CRC through inflammatory diseases, microbial metabolites, or virulence factors (13–15). The gut microbiome has been demonstrated to affect not only the generation of CRC, but also its progression. Furthermore, the gut microbiome has been associated with controlling the efficacy of cancer treatment and the toxicities of

therapeutic agents. Thus, therapeutic agents, such as probiotics, that can control the gut microbiome are expected to among the most effective approaches for helping to fight CRC (16, 17).

Recent advances in our understanding of the role of the gut microbiome are due to the development of technologies, such as 16S rRNA sequencing, that enable the discovery of many microorganisms in the intestine that could not be identified previously (18). Many studies related to metabolomics and metagenomics describe the effects of these gut microbes on the human body, and some studies revealed their involvement in cancer prevention, tumorigenesis, and anti-cancer effects (19, 20). In particular, changes in gut microbial metabolites, such as short-chain fatty acids (SCFAs), polyphenols, vitamins, tryptophan catabolites, and polyamines produced or affected by the gut microbiota, may have a wide range of effects on the formation and progression of CRC and even metastasis (21). As our understanding of the role of the anti-cancer immune response in the tumor microenvironment during cancer progression and treatment increases, the effect of the gut microbiome on tumor immunity is also receiving greater attention (21). It is known that changes in the gut microbiota not only affect tumor immunotherapy, but also affect therapeutic toxicity (22). Thus, modulation of the gut microbiome can be used as a novel treatment modality.

The gut microbiome has emerged as an important factor in various diseases, and the relationship between the gut microbiome and CRC has become an important issue in several studies. In this review, the potential role of the gut microbiome will be reviewed with a focus on how the gut microbiome affects the tumorigenesis processes associated with CRC. Furthermore, we discuss methods of gut microbiome modulation that can be used to treat CRC.

CORRELATION BETWEEN CRC AND GUT MICROBIOME

With changes in western dietary habits worldwide, the incidence of CRC is expected to increase steadily, resulting in 2.2 million new cases by 2030 (23). Studies have shown that approximately 90% of CRC occurs sporadically and the remainder is caused by genetic factors or exposure to specific environmental factors (24–27). In particular, lifestyle factors such as physical inactivity, smoking history, western diet, low fiber intake, alcohol intake, and obesity are major influences on CRC. It is important to note that most of these environmental factors can induce changes in the gut microbiota (26, 28, 29). Many studies have confirmed that susceptibility to CRC or tumor progression is affected by changes in the gut microbiome, which has been found to induce inflammation, DNA damage, or metabolites produced from microorganisms (30).

Evidence from several studies has suggested the existence of a close link between the gut microbiome and the host during the development of CRC (31–33). Studies using high-throughput microbiome sequencing have been conducted to investigate the microbiome community in tumor-formed and normal colon tissues (27), enabling a better understanding of the differences in gut microbiome between CRC and healthy patients. Reports have shown that the diversity and richness of the gut microbiome decreases in CRC patients (33, 34). In particular, analysis of the gut microbiome of CRC patients revealed that significant changes in specific microbial groups occurs, leading researchers to hypothesize that these changes might have a greater impact on the mucosal immune response of CRC patients compared to that of healthy individuals (34). A total of 11 operational taxonomic units (OTUs) belonging to the genera *Enterococcus*, *Escherichia*/*Shigella*, *Klebsiella*, *Streptococcus*, and *Peptostreptococcus* were significantly found to be more abundant in the gut microbiota of CRC patients, while 5 OTUs belonging to *Roseburia* and other butyrate-producing bacteria from the *Lachnospiraceae* family were less abundant (35). In addition, dysbiosis was observed in the gut microbiome of CRC patients as the balance between microorganisms was disrupted (36). Dysbiosis of gut microbiota and increased intestinal permeability induce colonic inflammation and may cause the promotion or progression of CRC (37). *Fusobacterium nucleatum* (*F. nucleatum*) is significantly increased in human CRC compared to healthy patients (38). Moreover, early-stage CRC patients (advanced adenoma) have a different microbiome composition compared to advanced-stage CRC patients (definitive CRC) (35, 39). These studies indicate a very close correlation between CRC and the gut microbiome; however, further investigation is still required to fully elucidate the effect of the gut microbiome on CRC.

INFLUENCE OF THE GUT MICROBIOME ON CRC FORMATION

Although much is still unknown about the formation of CRC, chronic inflammation has been implicated in the initiation of malignancy. It is estimated that approximately 20% of malignant tumors occurring in the colon are preceded by chronic inflammation (40). During carcinogenesis, inflammatory cytokines and chemokines produced by cancerous cells attract immature myeloid cells or pro-inflammatory helper T cells. This pro-tumorigenic microenvironment is characterized by the synthesis of growth and angiogenic factors, as well as tissue remodeling enzymes, and the suppression of anti-tumor T-cell responses, favoring tumor progression (41).

Knowledge that the gut microbiome affects CRC formation was first obtained in the early 1970s. When the colon was exposed to a carcinogen called 1,2-dimethlylhydrazine in a germ-free mouse model, the degree of CRC formation was found to be significantly reduced (42). At the time, it was not possible to specify which bacteria caused this phenomenon. However, a similar experiment using various colon cancer models confirmed that the presence or absence of intestinal microbes had a significant effect on the formation of colon cancer (43, 44). Since then, many studies using high-throughput microbiome sequencing have identified the various intestinal microorganisms that affect CRC formation.

Streptococcus bovis (*S. bovis*) has been reported as one of the risk factors for CRC (45–47). *S. bovis* is normally colonized in the gastrointestinal tract. Thus, the occurrence of *S. bovis*-induced endocarditis or bacteremia was an early clue to its involvement in colon cancer (45). The association between inflammation and colon carcinogenesis was confirmed when the relationship between the pro-inflammatory potential of *S. bovis* proteins and their carcinogenic properties was observed (48, 49). *S. bovis* has been found to play an active role in CRC development, perhaps through an inflammation-based sequence of tumor development or propagation involving interleukin (IL)-1, cyclooxygenase-2 (COX-2), and IL-8 (48).

F. nucleatum is one of the most widely known strains related to CRC tumor formation (50). Metagenomic analysis showed that the commensal *Fusobacterium* spp. are associated with CRC in humans; however, it remains unclear whether this is indirect or causal (38). Castellarin and coworkers confirmed that the transcripts of the strain were increased approximately 400 times in CRC tumor tissue compared to normal tissue (50). In a study using the adenomatous polyposis coli (*APC)* $^{+/-}$ mouse CRC model, *F. nucleatum* developed a pro-inflammatory environment which induced neoplasia progression in intestinal epithelial cells and recruited tumor-infiltrating immune cells (38). In addition, studies demonstrated that IL-17a was highly expressed in CRC patients with abundant *F. nucleatum* (51). This strain induces early carcinogenesis through increased bacterial adherence in the mucosal surface (52). *F. nucleatum* produces a unique protein called Fusobacterium adhesin A (FadA), which induces activation of the β-catenin signaling pathway after binding to E-cadherin, which is a potent oncogenic stimulator.

Enterococcus faecalis (*E. faecalis*) is a gut commensal bacterium that produces a superoxide from the autoxidation of membrane-associated demethylmenaquinone (53). Infection with *E. faecalis* induces DNA damage to intestinal epithelial cells by forming the superoxide. Thus, the abundance of *E. faecalis* was shown to be significantly increased in CRC patients compared to healthy individuals (35, 54, 55). Moreover, *in vitro* and *in vivo* studies demonstrated that *E. faecalis* can produce hydroxyl radicals (56, 57), which are potent mutagens that cause DNA breaks, point mutations, and protein-DNA crosslinking, thereby contributing to chromosomal instability and CRC risk (58).

Enterotoxigenic *Bacteroides fragilis* (*ETBF*) is a bacterium that produces *B. fragilis* toxin (BFT) and causes diarrhea and inflammatory bowel disease (IBD) (59–62). This strain plays a role in promoting tumors by elevating signal transducer and activator of transcription 3 (STAT3) and the Th17 response during colon tumorigenesis (60). Although STAT3 activation is required for colon tumorigenesis, it alone is not sufficient to trigger colon tumorigenesis by *ETBF*. Notably, IL-17-dependent nuclear factor kappa B (NF-κB) activation results in the formation of a proximal to distal mucosal gradient of CXC chemokines, which mediates the recruitment of CXCR2-expressing polymorphonuclear immature myeloid cells to cause *ETBF*-mediated distal colon tumorigenesis in parallel (62).

Peptostreptococcus anaerobius (*P. anaerobius*) induces a pro-inflammatory immune microenvironment and promotes tumor formation in the intestine. This strain plays a role in tumor formation by increasing the expression of pro-inflammatory cytokines in a mouse model and recruiting tumor-infiltrating immune cells such as immunosuppressive myeloid-derived suppressor cells (63). *P. anaerobius* increases the levels of reactive oxidative species that interact with toll-like receptor (TLR) 2 and TLR4 in colon cells to promote cholesterol synthesis and cell proliferation, ultimately causing dysplasia of colon cells (64).

Salmonella infections and colonization can be chronic and increase the risk of chronic cholecystitis and other gastrointestinal diseases, including cancers (65). Salmonella promotes colon tumorigenesis by relying on AvrA protein, which can activate both the Wnt/b-catenin and STAT3 signaling pathways in colon tumor cells (66–68). Salmonella also produces a genotoxin called typhoid toxin, which damages DNA *via* the phosphoinositide 3-kinase (PI3K) pathway in colonic epithelial cells (69). The reduced DNA repair capacity and inability to activate appropriate checkpoint responses have been associated with increased genomic instability in APC-deficient cells exposed to genotoxin. *Campylobacter jejuni* produces a cytolethal distending toxin (CDT), a genetic toxin with DNAse activity that causes DNA double-strand breaks and promotes colorectal tumorigenesis (70). Rapamycin, which inhibits mammalian target of mTOR signaling in mammals, has been shown to attenuate *C. jejuni*-induced colitis and carcinogenesis (70, 71).

Sulfate-reducing bacteria (SRB) are a microbiome component that is of particular interest with respect to colitis (72). These microorganisms can produce hydrogen sulfide (H_2S) by using methionine and cysteine as substrates. Studies have shown increased amounts of SRB in the stool of CRC patients compared to healthy individuals (73). H_2S produced by SRB can stimulate CRC progression by inhibiting butyrate oxidation and destroying the gut barrier, as well as induce DNA damage through reactive oxygen species (ROS) (74, 75).

Research to understand the relationship between other intestinal microbes with CRC formation is still ongoing. Thus, the bacteria discussed above do not constitute all of the causative bacteria of CRC.

INFLUENCE OF GUT THE MICROBIOME ON CRC PROGRESSION

The gut microbiome affects not only the formation of colon malignancy, but also its progression. Published literature related to the development of CRC has demonstrated that many bacteria affect tumor development and growth. In addition, it was observed that the progression of colon adenoma was promoted in a spontaneous CRC mouse model characterized by expression of mutated *Apc*, a tumor suppressor gene (76). This section will describe research findings associated with progression-related mechanisms rather than tumor formation. **Figure 1** summarizes the bacteria and their mechanisms of involvement in CRC initiation and progression.

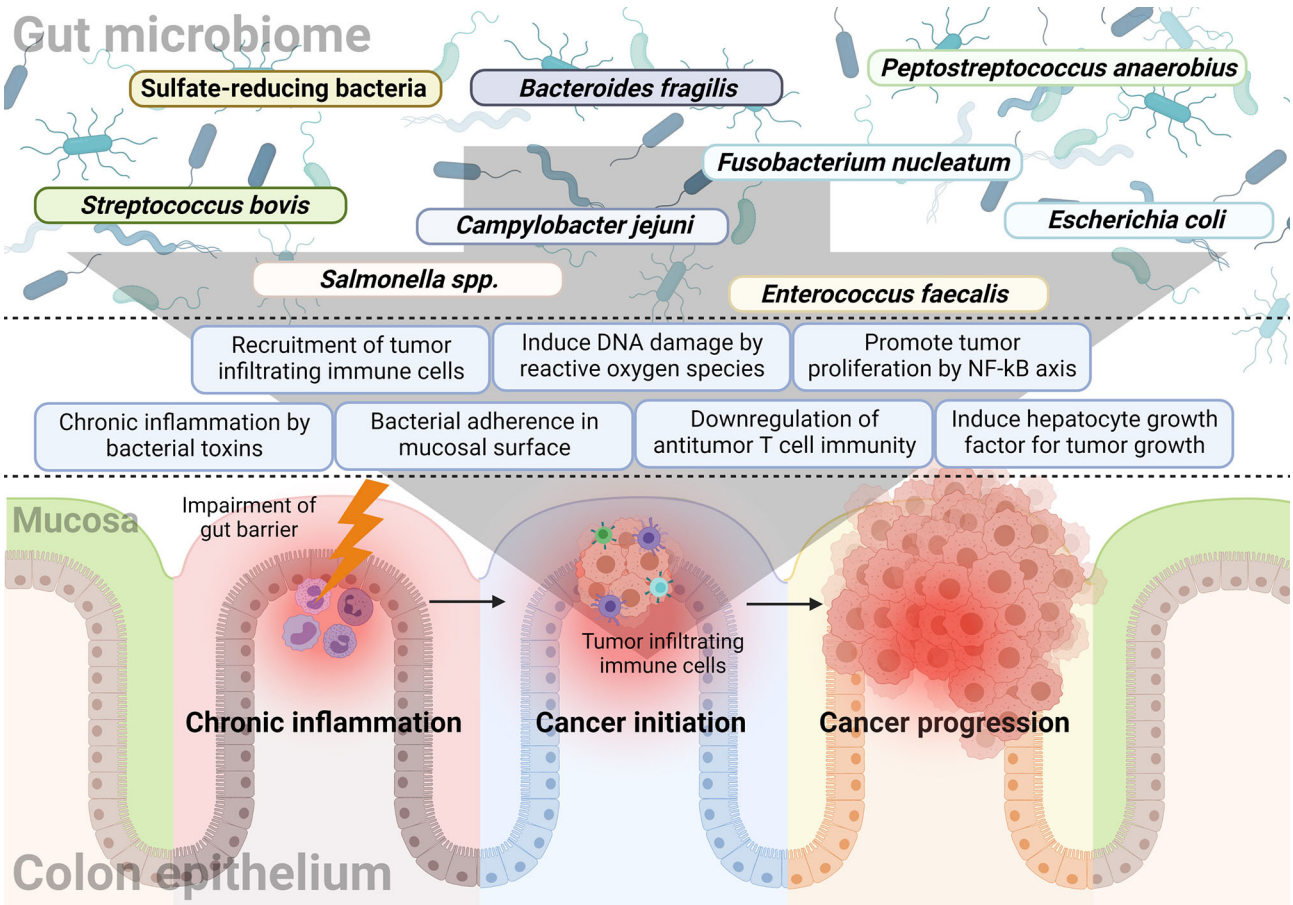

FIGURE 1 | The relationship between the gut microbiome and sequential progression of colorectal carcinoma. Specific gut microorganisms induce chronic inflammation in the colorectal epithelium. For example, typhoid toxin or colibactin secreted by *Salmonella* or *E. coli*, respectively, leads to pro-inflammatory cytokine production and bacterial adherence. Chronic inflammation is one of the major causes of CRC and increased ROS with epithelial cell DNA damage also play a major role in cancer initiation by the gut microbiome. Some microorganisms like *F. nucleatum* and *B. fragilis* induce a tumor-favorable immune microenvironment by reducing CD3+ T cell density along with the recruitment and proliferation of CD4+CCR6+IL17A+ Th17 cells. Furthermore, bacterial components such as putative cell wall binding repeat 2 surface protein in *P. anaerobius* activate the NF-κB signaling pathway in CRC tumor cells and promote tumor cell proliferation. Colibactin-producing *E. coli* encodes enzymes responsible for HGF synthesis and induces senescence and tumor growth.

The presence of *F. nucleatum* is associated with worse prognosis in CRC patients (77, 78). Expression of tumor necrosis factor alpha, β-catenin, and NF-κB was increased in the *F. nucleatum*-abundant group and COX-2, matrix metallopeptidase 9, and NF-κB were highly expressed in the *B. fragilis*-abundance group. Immunohistochemical analysis showed that Kirsten rat sarcoma virus (KRAS) and proto-oncogene B-Raf (BRAF) expression were increased in the presence of *F. nucleatum* and *B. fragilis* (78). *F. nucleatum*-high cases were inversely associated with the density of CD3+ T cells (79). Experimental evidence suggests that *F. nucleatum* can promote colonic tumor development by downregulation of anti-tumor T cell-mediated adaptive immunity. Natural killer cells (NK cells) were also found to be affected by *F. nucleatum* in various carcinomas including CRC (80). Gur and colleagues found that the Fap2 protein of *F. nucleatum* directly interacts with T cell immunoreceptor with Ig and ITIM domains (TIGIT) to inhibit the cytotoxicity of NK cells.

ETBF was also revealed to support the progression of malignancy as well as tumorigenesis (81). This strain induces the secretion of exosome-like nanoparticles in intestinal epithelial cell lines and contains chemokine CC motif ligand 20 and prostaglandin E2 in the particle. Thus, *ETBF* induces the recruitment and proliferation of CD4+CCR6+IL17A+ Th17 cells *via* the IL-17 signaling pathway, thereby participating in tumorigenesis and cancer cell growth.

Long, et al. found that the surface protein of *P. anaerobius*, putative cell wall binding repeat 2 (PCWBR2), promotes CRC development in $APC^{+/-}$ mice (63). PCWBR2 initiates the oncogenic PI3K-Akt signaling pathway that directly binds to the intestinal epithelial cell receptor integrin α2/β1 and promotes tumor cell proliferation *via* the PCWBR2-integrin α2/β1-PI3K-Akt-NF-κB signaling axis.

Escherichia coli (*E. coli*), which is the most highly abundant strain residing in the intestine, is also closely related to the growth of CRC. Studies have shown that the level of mucosal-associated *E. coli* is increased in CRC tumor tissues compared with in normal colon tissues (82). The pathogenic *E. coli* strain showed a correlation with inflammation and ROS production, which may propagate tumor infiltration (83). *E. coli* has polyketide synthase which codes for production of colibactin, the polyketide-peptide genotoxin found to play a significant impact on tumor growth (84, 85). In a xenograft model, colibactin-producing *E. coli* indirectly promotes tumor growth by inducing hepatocyte growth factor (HGF) (86). HGF is the main mechanical link between pks+ (which encodes enzymes responsible for HGF synthesis) *E. coli*-induced senescence and tumor growth. Other factors, including microRNA-20a-5p, sentrin-specific protease 1 (SENP1), and activated HGF receptors, are also affected by the presence of pks+ *E. coli* in human CRC.

In contrast, the presence or enrichment of certain intestinal strains leads to anti-cancer effects on the growth of CRC. Numerous animal studies have shown several emerging chemical candidates as key mechanisms for probiotics to induce protective effects against CRC. *Faecalibacterium prausnitzii* is a potential probiotic that can downregulate the NF-kB pathway in gut epithelial cells by producing hydrophobic microbial anti-inflammatory molecules and prevent colitis in animal models (87). *Lactobacillus rhamnosus* GG and *Bifidobacterium lactis* Bb12 help to prevent abnormal epithelial proliferation in patients with a history of polyps and improve the intestinal epithelial tight junction barrier (88). *Lactobacilli* and *Bifidobacteria* were suggested to play a role in suppressing tumor progression and volume in a CRC mouse model (89, 90). The presence of these probiotics was confirmed to induce increasing SCFA production, thus inducing apoptosis and inhibiting tumor proliferation (91). Butyrate, one of the SCFA metabolites produced by probiotics, can induce the expansion of T reg lymphocytes for regulating the immune response in colorectal tissues and suppressing carcinogenesis and tumor growth (92).

INFLUENCE OF THE GUT MICROBIOME ON CRC TREATMENT

Because the gut microbiome has been closely associated with CRC, numerous studies have been focused on investigating its effect on CRC treatment. Research related to the effect of gut microbiome on tumor treatment is the most important part of the cancer-microbiome research field and many studies are being conducted in combination with various treatment modalities to apply it to clinical cancer treatment. In addition to existing chemotherapeutic agents or radiotherapy, new discoveries are being made about the synergistic effects of the gut microbiome with immune checkpoint inhibitors (ICIs) (93). **Figure 2** summarizes the research findings discussed below.

CHEMOTHERAPY

The gut microbiota can modulate the efficacy of conventional chemotherapy. For example, it is known that certain gut microbiota may play a role in regulating cytotoxicity by participating in the metabolic process of anti-cancer drugs. The anti-cancer effect of platinum-based chemotherapeutic agents such as oxaliplatin and CpG oligodeoxynucleotides was decreased in mice treated with antibiotics (94), which exhibited lower cytokine secretion and ROS production, resulting in reduced tumor necrosis following anti-tumor therapy in the MC38 mouse colon tumor transplant model.

Gemcitabine has been shown to convert into an inactivated form with reduced anti-cancer effect when a specific gammaproteobacteria is present in the tumor (95). Gammaproteobacteria contain a long isoform of the cytidine deaminase enzyme which converts gemcitabine into an inactivated form. The anti-cancer effect was shown to be suppressed when the bacteria were eliminated by antibiotic treatment in a mouse model of CRC (95). Even in mouse tumor experiments using 5-fluorouracil (5-FU), antibiotic administration reduced the anti-cancer effect of 5-FU administration in the CRC model (96). In 16S rRNA seq analysis, pathogenic bacteria such as *Escherichia shigella* and *Enterobacter* were significantly increased when antibiotics were administered, and these changes were restored by taking probiotics.

F. nucleatum, which was previously known to greatly influence tumor initiation and progression, affects CRC treatment outcomes as well as CRC risk and dysplasia. A qPCR analysis based on colorectal tissue samples from 122 CRC patients confirmed a better prognosis occurred in patients with low *F. nucleatum* levels (77, 97). The level of *F. nucleatum* enrichment was positively correlated with poor response to 5-FU and oxalipatin in CRC patients (98). *F. nucleatum* stimulates the TLR4 and Myd88 innate immune signals and interferes with apoptosis, contributing to activation of the autophagy pathway and CRC chemoresistance (98).

RADIOTHERAPY

Dysbiosis caused by radiation therapy has the potential to adversely affect the other treatment modalities of CRC. Analysis of the gut microbiome after radiation treatment showed a decrease in commensal bacteria such as *Bifidobacterium*, *Faecalibacterium*, and *Clostridium* spp., as well as an increase in *Bacteroides* and *Enterococcus* spp (99). In addition, in the case of patients receiving radiation therapy to the pelvic region, there was a tendency for the *Fusobacteria* taxa to increase by about 3% (100). These changes show the potential for tumor-promoting capacities. These microbiota can pass through the impaired gut barrier as a result of epithelial inflammatory damage caused by radiation therapy, leading to an additional intestinal inflammatory response and tissue damage (101).

IMMUNOTHERAPY

Certain intestinal microbes are involved in tumor growth by regulating the immune response. Studies have been conducted to

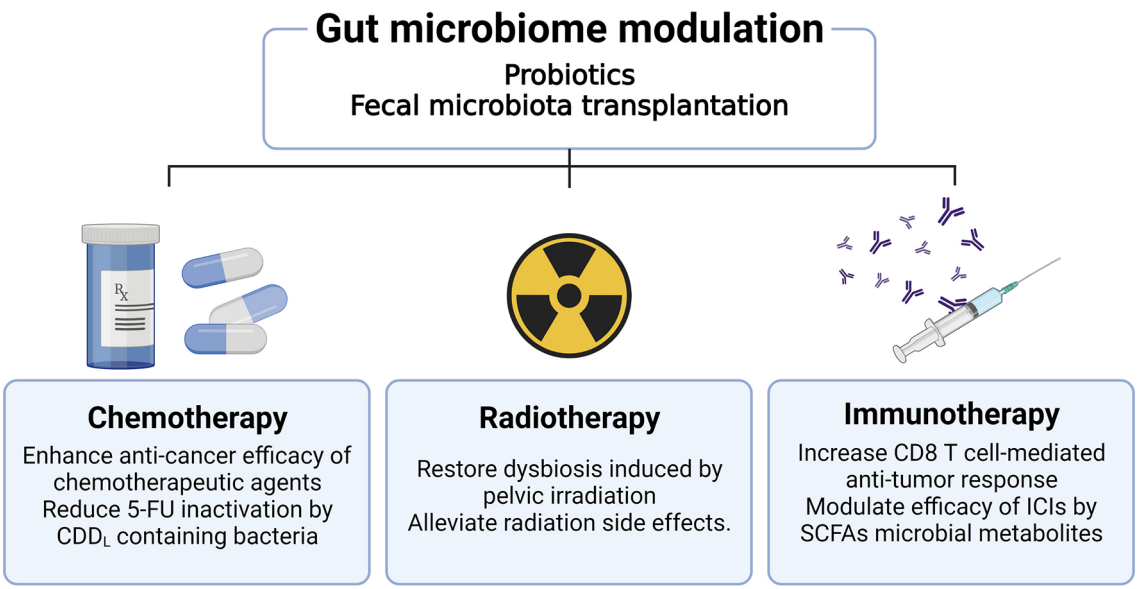

FIGURE 2 | Effects of gut microbiome modulation on cancer treatment. Therapies which modulate the gut microbiome, including administration of probiotics or fecal microbiota transplantation, improve the efficacy of cancer treatment. Administration of antibiotics can reduce the efficacy of oxaliplatin and CpG oligodeoxynucleotides chemotherapeutic agents. The use of antibiotics increases pathogenic bacteria such as *Escherichia shigella* and *Enterobacter*, as well as reduces the anti-cancer effect of 5-FU. Radiation of the pelvic area causes dysbiosis and has the potential to affect the treatment modality of CRC. Furthermore, radiation-induced gut epithelial damage worsens the prognosis of CRC patients. These radiation side effects can be ameliorated through fecal microbiome transplantation as well as probiotics administration. The gut microbiota plays a role in modulating mucosal immunity in the colorectal region, acting to improve the efficacy of immunotherapy by enhancing the CD8+ T cell immune response or SCFA metabolite production.

elucidate the mechanism of intestinal microbes and how they affect the efficacy of immunotherapeutic agents. In 2015, it was reported that the commensal gut microbiome could enhance the anti-tumor efficacy of programmed death-ligand 1 (PD-L1) ICIs through two mouse studies. Cytotoxic T-lymphocyte-associated protein 4 (CTLA-4) inhibitors are one of the most widely used ICIs in clinical practice. The efficacy of CTLA-4 inhibitors was demonstrated to be altered by the population of the gut microbiome (102). The literature has identified an important role for *Bacteroides* species in the immunostimulatory modulation of CTLA-4 blockade. The modulation of ICI efficacy mediated by bacterial species in the gut microbiome is not limited to CTLA-4 signaling. The efficacy of a PD-L1 inhibitor was also shown to be modulated by the gut microbiota composition in a mouse tumor model (103). Recent studies have indicated that the anti-tumor effect was found associated with various bacteria such as *Akkermansia*, *Faecalibacterium*, *Clostridiales*, and *Bifidobacterium* spp (104–106). Although some details remain to be understood, this anti-tumor effect has been partially attributed to SCFA microbial metabolites such as butyrate and propionate (107). Another mechanism for modulation of ICIs is that host immune cells can interact directly with specific bacteria. *Akkermansia muciniphila* improves the efficacy of immunotherapeutic agents in an IL-12-dependent manner through direct interaction with dendritic cells in the lymph node (106). *Bacteroides* spp. can also directly increase Th1 and CD8 T cell anti-tumor immune responses (102).

MICROBIOME MODULATION FOR COLON CANCER TREATMENT

Growing evidence clearly illustrates the significant influence that the gut microbiome has on tumors. Thus, it is not surprising that attempts have been made to inhibit tumor growth or modulate the efficacy of tumor therapy by regulating the gut microbiota. Efforts are ongoing to increase the effectiveness of tumor treatment and reduce side effects through fecal microbiome transplantation as well as probiotic therapy.

We discussed results from studies showing that *Lactobacilli* and *Bifidobacterium* affect the occurrence and progression of CRC in animal models (89–91). Some probiotics can help to not only enhance the effects of anti-cancer therapeutic agents but also alleviate the side effects caused by conventional cancer treatments (108). However, these probiotics also have the potential to act as opportunistic pathogens that can easily penetrate the intestinal barrier and immune environment after weakening by intestinal tumors (109). Appropriate probiotics with appropriate administration methods that can enhance anti-cancer effects and alleviate side effects are needed.

Fecal microbiota transplantation (FMT) is an emerging biotherapeutic method for altering the microbiota by transplanting stool information from healthy donors to patients (110). FMT can be applied to various gastrointestinal diseases including *C. difficile* infection, IBD, and restored eubiosis (111, 112). Many efforts are being made to apply FMT in the clinic as a tumor treatment. Reports have shown that FMT

could be used to overcome resistance to immunosuppressants in the CRC mouse model (113). In addition, FMT can be helpful in alleviating the side effects of ICIs such as immune checkpoint inhibitor-associated colitis (114). Complete resolution of colitis through FMT was sustained for 53 days after one dose and for 78 days after two doses. Although clinical application as a treatment for CRC is still unexplored, a recent FMT study of melanoma patients reported that FMT succeeded in overcoming resistance to immunotherapy in patients who did not respond to immunotherapy (115, 116). These results suggest that FMT can be effectively used in the treatment of CRC. However, since the gut microbiome environment consists of a very large network with many unknowns remaining, more research is needed before microbiome modulation can be administered as an anti-cancer treatment in CRC.

CONCLUSION

Various animal and clinical experiments have demonstrated that changes in the composition of the gut microbiota affect the initiation of precancerous cancer lesions and cancer progression. Because the colorectal region is a site where changes in the gut microbiota can influence the organs directly, CRC is considered to be affected by the gut microbiome more than other tumors. Studies of the gut microbiome revealed that dysbiosis occurred more frequently in CRC patients than in healthy people. The proportion of butyrate-producing bacteria was found to be reduced along with inflammation in the intestine while opportunistic pathogens were increased. Epidemiological studies have highlighted dietary factors such as western eating habits and reduced dietary fiber intake as risk factors for CRC, suggesting the gut microbiome as one of the mechanisms linking these factors to CRC. Dietary fiber can be fermented into SCFAs by intestinal bacteria and animal experiments demonstrated that various SCFAs such as butyrate could affect cancer initiation and progression. Finally, the use of antibiotics may also be a risk factor for CRC and studies of the gut microbiome demonstrate its involvement in this effect.

Many published results have demonstrated that the gut microbiome acts as an important key factor in the initiation and progression of carcinoma in the treatment of CRC. However, we still understand only a small part of the gut microbiome and further research is needed to elucidate the underlying mechanisms and to modulate the gut microbiome as an important strategy in the treatment and prevention of CRC. This review describes the gut microbiome strains that affect each stage of the tumorigenesis process, including the underlying mechanisms, supplying an overview of the microbiota species likely involved in future studies examining the associations between the gut microbiome and CRC.

AUTHOR CONTRIBUTIONS

JK and HL wrote the manuscript. All authors contributed to the article and approved the submitted version.

FUNDING

This study was supported by the National Research Foundation of Korea (NRF-2021M3A9D3026428 and NRF-2021M3A9H3015688) funded by the Ministry of Science and ICT of Korea.

ACKNOWLEDGMENTS

Figures were created with BioRender.com.

REFERENCES

1. Sung H, Ferlay J, Siegel RL, Laversanne M, Soerjomataram I, Jemal A, et al. Global Cancer Statistics 2020: GLOBOCAN Estimates of Incidence and Mortality Worldwide for 36 Cancers in 185 Countries. *CA A Cancer J Clin* (2021) 71:(3):209–49. doi: 10.3322/caac.21660
2. Wu GD, Chen J, Hoffmann C, Bittinger K, Chen YY, Keilbaugh SA, et al. Linking Long-Term Dietary Patterns With Gut Microbial Enterotypes. *Science* (2011) 334(6052):105–8. doi: 10.1126/science.1208344
3. De Almeida CV, de Camargo MR, Russo E, Amedei A. Role of Diet and Gut Microbiota on Colorectal Cancer Immunomodulation. *World J Gastroenterol* (2019) 25(2):151–62. doi: 10.3748/wjg.v25.i2.151
4. Murphy N, Moreno V, Hughes DJ, Vodicka L, Vodicka P, Aglago EK, et al. Lifestyle and Dietary Environmental Factors in Colorectal Cancer Susceptibility. *Mol Aspects Med* (2019) 69:2–9. doi: 10.1016/j.mam.2019.06.005
5. Zheng X, Hur J, Nguyen LH, Liu J, Song M, Wu K, et al. Comprehensive Assessment of Diet Quality and Risk of Precursors of Early-Onset Colorectal Cancer. *JNCI: J Natl Cancer Inst* (2020) 113(5):543–52. doi: 10.1093/jnci/djaa164
6. Costello EK, Lauber CL, Hamady M, Fierer N, Gordon JI, Knight R. Bacterial Community Variation in Human Body Habitats Across Space and Time. *Science* (2009) 326(5960):1694–7. doi: 10.1126/science.1177486
7. Thursby E, Juge N. Introduction to the Human Gut Microbiota. *Biochem J* (2017) 474(11):1823–36. doi: 10.1042/BCJ20160510
8. Tremaroli V, Bäckhed F. Functional Interactions Between the Gut Microbiota and Host Metabolism. *Nature* (2012) 489(7415):242–9. doi: 10.1038/nature11552
9. Shreiner AB, Kao JY, Young VB. The Gut Microbiome in Health and in Disease. *Curr Opin Gastroenterol* (2015) 31(1):69. doi: 10.1097/MOG.0000000000000139
10. Busnelli M, Manzini S, Chiesa G. The Gut Microbiota Affects Host Pathophysiology as an Endocrine Organ: A Focus on Cardiovascular Disease. *Nutrients* (2019) 12(1):79. doi: 10.3390/nu12010079
11. Fan Y, Pedersen O. Gut Microbiota in Human Metabolic Health and Disease. *Nat Rev Microbiol* (2021) 19(1):55–71. doi: 10.1038/s41579-020-0433-9
12. Helmink BA, Khan MW, Hermann A, Gopalakrishnan V, Wargo JAJNm. The Microbiome, Cancer, and Cancer Therapy. *Nat Med* (2019) 25: (3):377–88. doi: 10.1038/s41591-019-0377-7
13. Song M, Chan AT, Sun JJ. Influence of the Gut Microbiome, Diet, and Environment on Risk of Colorectal Cancer. *Gastroenterology* (2020) 158 (2):322–40. doi: 10.1053/j.gastro.2019.06.048
14. Wang J, Chen W-D, Wang Y-D. The Relationship Between Gut Microbiota and Inflammatory Diseases: The Role of Macrophages. *Front Microbiol* (2020) 11:1065. doi: 10.3389/fmicb.2020.01065
15. Lavelle A, Sokol H. Gut Microbiota-Derived Metabolites as Key Actors in Inflammatory Bowel Disease. *Nat Rev Gastroenterol Hepatol* (2020) 17 (4):223–37. doi: 10.1038/s41575-019-0258-z

16. Allen J, Sears CL. Impact of the Gut Microbiome on the Genome and Epigenome of Colon Epithelial Cells: Contributions to Colorectal Cancer Development. *Genome Med* (2019) 11(1):1–18. doi: 10.1186/s13073-019-0621-2
17. Chattopadhyay I, Dhar R, Pethusamy K, Seethy A, Srivastava T, Sah R, et al. Exploring the Role of Gut Microbiome in Colon Cancer. *Appl Biochem Biotechnol* (2021) 193:1780–99. doi: 10.1007/s12010-021-03498-9
18. Schloss PD. Identifying and Overcoming Threats to Reproducibility, Replicability, Robustness, and Generalizability in Microbiome Research. *mBio* (2018) 9(3):e00525–18. doi: 10.1128/mBio.00525-18
19. Zhang X, Li L, Butcher J, Stintzi A, Figeys D. Advancing Functional and Translational Microbiome Research Using Meta-Omics Approaches. *Microbiome* (2019) 7(1):1–12. doi: 10.1186/s40168-019-0767-6
20. Cho I, Blaser MJ. The Human Microbiome: At the Interface of Health and Disease. *Nat Rev Genet* (2012) 13(4):260–70. doi: 10.1038/nrg3182
21. Johnson CH, Spilker ME, Goetz L, Peterson SN, Siuzdak G. Metabolite and Microbiome Interplay in Cancer Immunotherapy. *Cancer Res* (2016) 76 (21):6146–52. doi: 10.1158/0008-5472.CAN-16-0309
22. Zitvogel L, Ma Y, Raoult D, Kroemer G, Gajewski TF. The Microbiome in Cancer Immunotherapy: Diagnostic Tools and Therapeutic Strategies. *Science* (2018) 359(6382):1366–70. doi: 10.1126/science.aar6918
23. Arnold M, Sierra MS, Laversanne M, Soerjomataram I, Jemal A, Bray F. Global Patterns and Trends in Colorectal Cancer Incidence and Mortality. *Gut* (2017) 66(4):683–91. doi: 10.1136/gutjnl-2015-310912
24. Sánchez-Alcoholado L, Ramos-Molina B, Otero A, Laborda-Illanes A, Ordóñez R, Medina JA, et al. The Role of the Gut Microbiome in Colorectal Cancer Development and Therapy Response. *Cancers (Basel)* (2020) 12(6):1406. doi: 10.3390/cancers12061406
25. Feng Q, Liang S, Jia H, Stadlmayr A, Tang L, Lan Z, et al. Gut Microbiome Development Along the Colorectal Adenoma-Carcinoma Sequence. *Nat Commun* (2015) 6:6528. doi: 10.1038/ncomms7528
26. Nakatsu G, Li X, Zhou H, Sheng J, Wong SH, Wu WKK, et al. Gut Mucosal Microbiome Across Stages of Colorectal Carcinogenesis. *Nat Commun* (2015) 6(1):8727. doi: 10.1038/ncomms9727
27. Yu J, Feng Q, Wong SH, Zhang D, Liang QY, Qin YW, et al. Metagenomic Analysis of Faecal Microbiome as a Tool Towards Targeted non-Invasive Biomarkers for Colorectal Cancer. *Gut* (2017) 66(1):70. doi: 10.1136/gutjnl-2015-309800
28. Feng Q, Liang S, Jia H, Stadlmayr A, Tang L, Lan Z, et al. Gut Microbiome Development Along the Colorectal Adenoma–Carcinoma Sequence. *Nat Commun* (2015) 6(1):6528. doi: 10.1038/ncomms7528
29. Garcia-Gonzalez AP, Ritter AD, Shrestha S, Andersen EC, Yilmaz LS, Walhout AJM. Bacterial Metabolism Affects the C. Elegans Response to Cancer Chemotherapeutics. *Cell* (2017) 169(3):431–41.e8. doi: 10.1016/j.cell.2017.03.046
30. Cheng Y, Ling Z, Li L. The Intestinal Microbiota and Colorectal Cancer. *Front Immunol* (2020) 11:615056. doi: 10.3389/fimmu.2020.615056
31. Cipe G, Idiz UO, Firat D, Bektasoglu H. Relationship Between Intestinal Microbiota and Colorectal Cancer. *World J Gastroint Oncol* (2015) 7 (10):233–40. doi: 10.4251/wjgo.v7.i10.233
32. Zackular JP, Baxter NT, Iverson KD, Sadler WD, Petrosino JF, Chen GY, et al. The Gut Microbiome Modulates Colon Tumorigenesis. *mBio* (2013) 4 (6):e00692–13. doi: 10.1128/mBio.00692-13
33. Chen W, Liu F, Ling Z, Tong X, Xiang C. Human Intestinal Lumen and Mucosa-Associated Microbiota in Patients With Colorectal Cancer. *PloS One* (2012) 7(6):e39743. doi: 10.1371/journal.pone.0039743
34. Saffarian A, Mulet C, Regnault B, Amiot A, Tran-Van-Nhieu J, Ravel J, et al. Crypt- and Mucosa-Associated Core Microbiotas in Humans and Their Alteration in Colon Cancer Patients. *mBio* (2019) 10(4):e01315–19. doi: 10.1128/mBio.01315-19
35. Wang T, Cai G, Qiu Y, Fei N, Zhang M, Pang X, et al. Structural Segregation of Gut Microbiota Between Colorectal Cancer Patients and Healthy Volunteers. *ISME J* (2012) 6(2):320–9. doi: 10.1038/ismej.2011.109
36. Coker OO, Nakatsu G, Dai RZ, Wu WKK, Wong SH, Ng SC, et al. Enteric Fungal Microbiota Dysbiosis and Ecological Alterations in Colorectal Cancer. *Gut* (2019) 68(4):654–62. doi: 10.1136/gutjnl-2018-317178
37. Dzutsev A, Goldszmid RS, Viaud S, Zitvogel L, Trinchieri G. The Role of the Microbiota in Inflammation, Carcinogenesis, and Cancer Therapy. *Eur J Immunol* (2015) 45(1):17–31. doi: 10.1002/eji.201444972
38. Kostic AD, Chun E, Robertson L, Glickman JN, Gallini CA, Michaud M, et al. Fusobacterium Nucleatum Potentiates Intestinal Tumorigenesis and Modulates the Tumor-Immune Microenvironment. *Cell Host Microbe* (2013) 14(2):207–15. doi: 10.1016/j.chom.2013.07.007
39. Viljoen KS, Dakshinamurthy A, Goldberg P, Blackburn JM. Quantitative Profiling of Colorectal Cancer-Associated Bacteria Reveals Associations Between Fusobacterium Spp., Enterotoxigenic Bacteroides Fragilis (ETBF) and Clinicopathological Features of Colorectal Cancer. *PloS One* (2015) 10 (3):e0119462. doi: 10.1371/journal.pone.0119462
40. Grivennikov SI. Inflammation and Colorectal Cancer: Colitis-Associated Neoplasia. *Semin Immunopathol* (2013) 35(2):229–44. doi: 10.1007/s00281-012-0352-6
41. Francescone R, Hou V, Grivennikov SI. Microbiome, Inflammation, and Cancer. *Cancer J* (2014) 20(3):181–9. doi: 10.1097/PPO.0000000000000048
42. Reddy BS, Narisawa T, Wright P, Vukusich D, Weisburger J, Wynder E. Colon Carcinogenesis With Azoxymethane and Dimethylhydrazine in Germ-Free Rats. *Cancer Res* (1975) 35(2):287–90.
43. Reddy BS, Narisawa T, Weisburger J. Colon Carcinogenesis in Germ-Free Rats With Intrarectal 1, 2-Dimethylhydrazine and Subcutaneous Azoxymethane. *Cancer Res* (1976) 36(8):2874–6.
44. Son JS, Khair S, Pettet DWIII, Ouyang N, Tian X, Zhang Y, et al. Altered Interactions Between the Gut Microbiome and Colonic Mucosa Precede Polyposis in Apcmin/+ Mice. *PloS One* (2015) 10: (6):e0127985. doi: 10.1371/journal.pone.0127985
45. Gupta A, Madani R, Mukhtar HJ. Streptococcus Bovis Endocarditis, A Silent Sign for Colonic Tumour. *Colorectal Dis* (2010) 12(3):164–71. doi: 10.1111/j.1463-1318.2009.01814.x
46. Srivastava A, Walter N, Atkinson P. Streptococcus Bovis Infection of Total Hip Arthroplasty in Association With Carcinoma of Colon. *J Surg Orthop Adv* (2010) 19(2):125–8.
47. Boleij A, van Gelder MM, Swinkels DW, Tjalsma HJ. Clinical Importance of Streptococcus Gallolyticus Infection Among Colorectal Cancer Patients: Systematic Review and Meta-Analysis. *Clin Infect Dis* (2011) 53(9):870–8. doi: 10.1093/cid/cir609
48. Biarc J, Nguyen IS, Pini A, Gosse F, Richert S, Thierse D, et al. Carcinogenic Properties of Proteins With Pro-Inflammatory Activity From Streptococcus Infantarius (Formerly s. bovis). *Carcinogenesis* (2004) 25(8):1477–84. doi: 10.1093/carcin/bgh091
49. Abdulamir AS, Hafidh RR, Bakar FA. Molecular Detection, Quantification, and Isolation of Streptococcus Gallolyticus Bacteria Colonizing Colorectal Tumors: Inflammation-Driven Potential of Carcinogenesis *via* IL-1, COX-2, and IL-8. *Mol Cancer* (2010) 9(1):249. doi: 10.1186/1476-4598-9-249
50. Castellarin M, Warren RL, Freeman JD, Dreolini L, Krzywinski M, Strauss J, et al. Fusobacterium Nucleatum Infection is Prevalent in Human Colorectal Carcinoma. *Genome Res* (2012) 22(2):299–306. doi: 10.1101/gr.126516.111
51. Ye X, Wang R, Bhattacharya R, Boulbes DR, Fan F, Xia L, et al. Fusobacterium Nucleatum Subspecies Animalis Influences Proinflammatory Cytokine Expression and Monocyte Activation in Human Colorectal Tumors. *Cancer Prev Res (Phila)* (2017) 10:(7):398–409. doi: 10.1158/1940-6207.CAPR-16-0178
52. Rubinstein MR, Wang X, Liu W, Hao Y, Cai G, YWJCh H, et al. Fusobacterium Nucleatum Promotes Colorectal Carcinogenesis by Modulating E-Cadherin/β-Catenin Signaling via its Fada Adhesin. *Cell Host Microbe* (2013) 14(2):195–206. doi: 10.1016/j.chom.2013.07.012
53. Winters MD, Schlinke TL, Joyce WA, Glore SR, Huycke MM. Prospective Case-Cohort Study of Intestinal Colonization With Enterococci That Produce Extracellular Superoxide and the Risk for Colorectal Adenomas or Cancer. *Am J Gastroenterol* (1998) 93(12):2491–500. doi: 10.1111/j.1572-0241.1998.00710.x
54. Wang X, Huycke MM. Extracellular Superoxide Production by Enterococcus Faecalis Promotes Chromosomal Instability in Mammalian Cells. *Gastroenterology* (2007) 132(2):551–61. doi: 10.1053/j.gastro.2006.11.040
55. Wang X, Allen TD, May RJ, Lightfoot S, Houchen CW, Huycke M. Enterococcus Faecalis Induces Aneuploidy and Tetraploidy in Colonic Epithelial Cells Through a Bystander Effect. *Cancer Res* (2008) 68 (23):9909–17. doi: 10.1158/0008-5472.CAN-08-1551
56. Huycke MM, Moore D, Joyce W, Wise P, Shepard L, Kotake Y, et al. Extracellular Superoxide Production by Enterococcus Faecalis Requires

Demethylmenaquinone and is Attenuated by Functional Terminal Quinol Oxidases. *Mol Microbiol* (2001) 42(3):729–40. doi: 10.1046/j.1365-2958.2001.02638.x
57. Huycke MM, Moore DR. *In Vivo* Production of Hydroxyl Radical by Enterococcus Faecalis Colonizing the Intestinal Tract Using Aromatic Hydroxylation. *Free Radical Biol Med* (2002) 33(6):818–26. doi: 10.1016/S0891-5849(02)00977-2
58. Evans MD, Dizdaroglu M, Cooke MS. Oxidative DNA Damage and Disease: Induction, Repair and Significance. *Mutat Res* (2004) 567(1):1–61. doi: 10.1016/j.mrrev.2003.11.001
59. Sears C. Enterotoxigenic Bacteroides Fragilis: A Rogue Among Symbiotes. *Clin Microbiol Rev* (2009) 22(2):349–69. doi: 10.1128/CMR.00053-08
60. Wu S, Rhee K-J, Albesiano E, Rabizadeh S, Wu X, Yen H-R, et al. A Human Colonic Commensal Promotes Colon Tumorigenesis via Activation of T Helper Type 17 T Cell Responses. *Nat Med* (2009) 15(9):1016–22. doi: 10.1038/nm.2015
61. Sears CL, Geis AL, Housseau F. Bacteroides Fragilis Subverts Mucosal Biology: From Symbiont to Colon Carcinogenesis. *J Clin Invest* (2014) 124 (10):4166–72. doi: 10.1172/JCI72334
62. Chung L, Orberg ET, Geis AL, Chan JL, Fu K, Shields CED, et al. Bacteroides Fragilis Toxin Coordinates a Pro-Carcinogenic Inflammatory Cascade via Targeting of Colonic Epithelial Cells. *Cell Host Microbe* (2018) 23(2):203–14.e5. doi: 10.1016/j.chom.2018.01.007
63. Long X, Wong CC, Tong L, Chu ES, Szeto CH, Go MY, et al. Peptostreptococcus Anaerobius Promotes Colorectal Carcinogenesis and Modulates Tumour Immunity. *Nat Microbiol* (2019) 4(12):2319–30. doi: 10.1038/s41564-019-0541-3
64. Tsoi H, Chu ESH, Zhang X, Sheng J, Nakatsu G, Ng SC, et al. Peptostreptococcus Anaerobius Induces Intracellular Cholesterol Biosynthesis in Colon Cells to Induce Proliferation and Causes Dysplasia in Mice. *Gastroenterology* (2017) 152(6):1419–33.e5. doi: 10.1053/j.gastro.2017.01.009
65. Gradel KO, Nielsen HL, Schønheyder HC, Ejlertsen T, Kristensen B, Nielsen H. Increased Short- and Long-Term Risk of Inflammatory Bowel Disease After Salmonella or Campylobacter Gastroenteritis. *Gastroenterology* (2009) 137(2):495–501. doi: 10.1053/j.gastro.2009.04.001
66. Lu R, Wu S, Zhang YG, Xia Y, Liu X, Zheng Y, et al. Enteric Bacterial Protein Avra Promotes Colonic Tumorigenesis and Activates Colonic Beta-Catenin Signaling Pathway. *Oncogenesis* (2014) 3(6):e105. doi: 10.1038/oncsis.2014.20
67. Lu R, Wu S, Y-g Z, Xia Y, Zhou Z, Kato I, et al. Salmonella Protein Avra Activates the STAT3 Signaling Pathway in Colon Cancer. *Neoplasia* (2016) 18(5):307–16. doi: 10.1016/j.neo.2016.04.001
68. Wang J, Lu R, Fu X, Dan Z, Zhang Y-G, Chang X, et al. Novel Regulatory Roles of Wnt1 in Infection-Associated Colorectal Cancer. *Neoplasia* (2018) 20(5):499–509. doi: 10.1016/j.neo.2018.03.001
69. Martin OC, Bergonzini A, d'Amico F, Chen P, Shay JW, Dupuy J, et al. Infection With Genotoxin-Producing Salmonella Enterica Synergises With Loss of the Tumour Suppressor APC in Promoting Genomic Instability *via* the PI3K Pathway in Colonic Epithelial Cells. *Cell Microbiol* (2019) 21(12): e13099. doi: 10.1111/cmi.13099
70. He Z, Gharaibeh RZ, Newsome RC, Pope JL, Dougherty MW, Tomkovich S, et al. Campylobacter Jejuni Promotes Colorectal Tumorigenesis Through the Action of Cytolethal Distending Toxin. *Gut* (2019) 68(2):289–300. doi: 10.1136/gutjnl-2018-317200
71. Sun X, Threadgill D, Jobin C. Campylobacter Jejuni Induces Colitis Through Activation of Mammalian Target of Rapamycin Signaling. *Gastroenterology* (2012) 142(1):86–95.e5. doi: 10.1053/j.gastro.2011.09.042
72. Figliuolo VR, dos Santos LM, Abalo A, Nanini H, Santos A, Brittes NM, et al. Sulfate-Reducing Bacteria Stimulate Gut Immune Responses and Contribute to Inflammation in Experimental Colitis. *Life Sci* (2017) 189:29–38. doi: 10.1016/j.lfs.2017.09.014
73. Yachida S, Mizutani S, Shiroma H, Shiba S, Nakajima T, Sakamoto T, et al. Metagenomic and Metabolomic Analyses Reveal Distinct Stage-Specific Phenotypes of the Gut Microbiota in Colorectal Cancer. *Nat Med* (2019) 25(6):968–76. doi: 10.1038/s41591-019-0458-7
74. Louis P, Hold GL, Flint HJ. The Gut Microbiota, Bacterial Metabolites and Colorectal Cancer. *Nat Rev Microbiol* (2014) 12(10):661–72. doi: 10.1038/nrmicro3344
75. Marquet P, Duncan SH, Chassard C, Bernalier-Donadille A, Flin T. Lactate Has the Potential to Promote Hydrogen Sulphide Formation in the Human Colon. *FEMS Microbiol Lett* (2009) 299(2):128–34. doi: 10.1111/j.1574-6968.2009.01750.x
76. Li L, Li X, Zhong W, Yang M, Xu M, Sun Y, et al. Gut Microbiota From Colorectal Cancer Patients Enhances the Progression of Intestinal Adenoma in Apcmin/+ Mice. *EBioMedicine* (2019) 48:301–15. doi: 10.1016/j.ebiom.2019.09.021
77. Mima K, Nishihara R, Qian ZR, Cao Y, Sukawa Y, Nowak JA, et al. Fusobacterium Nucleatum in Colorectal Carcinoma Tissue and Patient Prognosis. *Gut* (2016) 65(12):1973–80. doi: 10.1136/gutjnl-2015-310101
78. Wei Z, Cao S, Liu S, Yao Z, Sun T, Li Y, et al. Could Gut Microbiota Serve as Prognostic Biomarker Associated With Colorectal Cancer Patients' Survival? A Pilot Study on Relevant Mechanism. *Oncotarget* (2016) 7(29):46158. doi: 10.18632/oncotarget.10064
79. Mima K, Sukawa Y, Nishihara R, Qian ZR, Yamauchi M, Inamura K, et al. Fusobacterium Nucleatum and T Cells in Colorectal Carcinoma. *JAMA Oncol* (2015) 1(5):653–61. doi: 10.1001/jamaoncol.2015.1377
80. Gur C, Ibrahim Y, Isaacson B, Yamin R, Abed J, Gamliel M, et al. Binding of the Fap2 Protein of Fusobacterium Nucleatum to Human Inhibitory Receptor TIGIT Protects Tumors From Immune Cell Attack. *Immunity* (2015) 42(2):344–55. doi: 10.1016/j.immuni.2015.01.010
81. Deng Z, Mu J, Tseng M, Wattenberg B, Zhuang X, Egilmez NK, et al. Enterobacteria-Secreted Particles Induce Production of Exosome-Like S1P-Containing Particles by Intestinal Epithelium to Drive Th17-Mediated Tumorigenesis. *Nat Commun* (2015) 6(1):6956. doi: 10.1038/ncomms7956
82. Bonnet M, Buc E, Sauvanet P, Darcha C, Dubois D, Pereira B, et al. Colonization of the Human Gut by E. Coli and Colorectal Cancer Risk. *Clin Cancer Res* (2014) 20(4):859–67. doi: 10.1158/1078-0432.CCR-13-1343
83. Veziant J, Gagnière J, Jouberton E, Bonnin V, Sauvanet P, Pezet D, et al. Association of Colorectal Cancer With Pathogenic Escherichia Coli: Focus on Mechanisms Using Optical Imaging. *World J Clin Oncol* (2016) 7(3):293–301. doi: 10.5306/wjco.v7.i3.293
84. Cuevas-Ramos G, Petit CR, Marcq I, Boury M, Oswald E, Nougayrède J-P. Escherichia Coli Induces DNA Damage *In Vivo* and Triggers Genomic Instability in Mammalian Cells. *Proc Natl Acad Sci USA* (2010) 107 (25):11537–42. doi: 10.1073/pnas.1001261107
85. Arthur JC, Gharaibeh RZ, Mühlbauer M, Perez-Chanona E, Uronis JM, McCafferty J, et al. Microbial Genomic Analysis Reveals the Essential Role of Inflammation in Bacteria-Induced Colorectal Cancer. *Nat Commun* (2014) 5:4724. doi: 10.1038/ncomms5724
86. Cougnoux A, Dalmasso G, Martinez R, Buc E, Delmas J, Gibold L, et al. Bacterial Genotoxin Colibactin Promotes Colon Tumour Growth by Inducing a Senescence-Associated Secretory Phenotype. *Gut* (2014) 63 (12):1932–42. doi: 10.1136/gutjnl-2013-305257
87. Quévrain E, Maubert MA, Michon C, Chain F, Marquant R, Tailhades J, et al. Identification of an Anti-Inflammatory Protein From Faecalibacterium Prausnitzii, a Commensal Bacterium Deficient in Crohn's Disease. *Gut* (2016) 65(3):415–25. doi: 10.1136/gutjnl-2014-307649
88. Rafter J, Bennett M, Caderni G, Clune Y, Hughes R, Karlsson PC, et al. Dietary Synbiotics Reduce Cancer Risk Factors in Polypectomized and Colon Cancer Patients. *Am J Clin Nutr* (2007) 85(2):488–96. doi: 10.1093/ajcn/85.2.488
89. Lee HA, Kim H, Lee K-W, Park K-Y. Dead Nano-Sized Lactobacillus Plantarum Inhibits Azoxymethane/Dextran Sulfate Sodium-Induced Colon Cancer in Balb/C Mice. *J Med Food* (2015) 18(12):1400–5. doi: 10.1089/jmf.2015.3577
90. Talero E, Bolivar S, Ávila-Román J, Alcaide A, Fiorucci S, Motilva V. Inhibition of Chronic Ulcerative Colitis-Associated Adenocarcinoma Development in Mice by VSL3. *Inflamm Bowel Dis* (2015) 21(5):1027–37. doi: 10.1097/MIB.0000000000000346
91. Gamallat Y, Meyiah A, Kuugbee ED, Hago AM, Chiwala G, Awadasseid A, et al. Lactobacillus Rhamnosus Induced Epithelial Cell Apoptosis, Ameliorates Inflammation and Prevents Colon Cancer Development in an

Animal Model. *Biomed Pharmacother* (2016) 83:536–41. doi: 10.1016/j.biopha.2016.07.001
92. Singh N, Gurav A, Sivaprakasam S, Brady E, Padia R, Shi H, et al. Activation of Gpr109a, Receptor for Niacin and the Commensal Metabolite Butyrate, Suppresses Colonic Inflammation and Carcinogenesis. *Immunity* (2014) 40 (1):128–39. doi: 10.1016/j.immuni.2013.12.007
93. Roy S, Trinchieri G. Microbiota: A Key Orchestrator of Cancer Therapy. *Nat Rev Cancer* (2017) 17(5):271–85. doi: 10.1038/nrc.2017.13
94. Iida N, Dzutsev A, Stewart CA, Smith L, Bouladoux N, Weingarten RA, et al. Commensal Bacteria Control Cancer Response to Therapy by Modulating the Tumor Microenvironment. *Science* (2013) 342(6161):967–70. doi: 10.1126/science.1240527
95. Geller LT, Barzily-Rokni M, Danino T, Jonas OH, Shental N, Nejman D, et al. Potential Role of Intratumor Bacteria in Mediating Tumor Resistance to the Chemotherapeutic Drug Gemcitabine. *Science* (2017) 357 (6356):1156–60. doi: 10.1126/science.aah5043
96. Yuan L, Zhang S, Li H, Yang F, Mushtaq N, Ullah S, et al. The Influence of Gut Microbiota Dysbiosis to the Efficacy of 5-Fluorouracil Treatment on Colorectal Cancer. *Biomed Pharmacother = Biomed Pharmacother* (2018) 108:184–93. doi: 10.1016/j.biopha.2018.08.165
97. Flanagan L, Schmid J, Ebert M, Soucek P, Kunicka T, Liska V, et al. Fusobacterium Nucleatum Associates With Stages of Colorectal Neoplasia Development, Colorectal Cancer and Disease Outcome. *Eur J Clin Microbiol Infect Dis* (2014) 33(8):1381–90. doi: 10.1007/s10096-014-2081-3
98. Yu T, Guo F, Yu Y, Sun T, Ma D, Han J, et al. Fusobacterium Nucleatum Promotes Chemoresistance to Colorectal Cancer by Modulating Autophagy. *Cell* (2017) 170(3):548–63.e16. doi: 10.1016/j.cell.2017.07.008
99. Touchefeu Y, Montassier E, Nieman K, Gastinne T, Potel G, Bruley Des Varannes S, et al. Systematic Review: The Role of the Gut Microbiota in Chemotherapy- or Radiation-Induced Gastrointestinal Mucositis - Current Evidence and Potential Clinical Applications. *Alimentary Pharmacol Ther* (2014) 40(5):409–21. doi: 10.1111/apt.12878
100. Nam YD, Kim HJ, Seo JG, Kang SW, Bae JW. Impact of Pelvic Radiotherapy on Gut Microbiota of Gynecological Cancer Patients Revealed by Massive Pyrosequencing. *PloS One* (2013) 8(12):e82659. doi: 10.1371/journal.pone.0082659
101. Al-Qadami G, Van Sebille Y, Le H, Bowen J. Gut Microbiota: Implications for Radiotherapy Response and Radiotherapy-Induced Mucositis. *Expert Rev Gastroenterol Hepatol* (2019) 13(5):485–96. doi: 10.1080/17474124.2019.1595586
102. Vetizou M, Pitt JM, Daillere R, Lepage P, Waldschmitt N, Flament C, et al. Anticancer Immunotherapy by CTLA-4 Blockade Relies on the Gut Microbiota. *Science* (2015) 350(6264):1079. doi: 10.1126/science.aad1329
103. Sivan A, Corrales L, Hubert N, Williams JB, Aquino-Michaels K, Earley ZM, et al. Commensal Bifidobacterium Promotes Antitumor Immunity and Facilitates Anti-PD-L1 Efficacy. *Science* (2015) 350(6264):1084–9. doi: 10.1126/science.aac4255
104. Gopalakrishnan V, Spencer CN, Nezi L, Reuben A, Andrews MC, Karpinets TV, et al. Gut Microbiome Modulates Response to Anti-PD-1 Immunotherapy in Melanoma Patients. *Science* (2018) 359(6371):97–103. doi: 10.1126/science.aan4236
105. Matson V, Fessler J, Bao R, Chongsuwat T, Zha Y, Alegre M-L, et al. The Commensal Microbiome is Associated With Anti–PD-1 Efficacy in Metastatic Melanoma Patients. *Science* (2018) 359(6371):104–8. doi: 10.1126/science.aao3290
106. Routy B, Le Chatelier E, Derosa L, Duong CPM, Alou MT, Daillere R, et al. Gut Microbiome Influences Efficacy of PD-1-Based Immunotherapy Against Epithelial Tumors. *Science* (2018) 359(6371):91–7. doi: 10.1126/science.aan3706
107. Hayase E, Jenq RR. Role of the Intestinal Microbiome and Microbial-Derived Metabolites in Immune Checkpoint Blockade Immunotherapy of Cancer. *Genome Med* (2021) 13(1), 107. doi: 10.1186/s13073-021-00923-w
108. Rodriguez-Arrastia M, Martinez-Ortigosa A, Rueda-Ruzafa L, Folch Ayora A, Ropero-Padilla C. Probiotic Supplements on Oncology Patients' Treatment-Related Side Effects: A Systematic Review of Randomized Controlled Trials. *Int J Environ Res Public Health* (2021) 18(8):4265. doi: 10.3390/ijerph18084265
109. Veiga P, Suez J, Derrien M, Elinav E. Moving From Probiotics to Precision Probiotics. *Nat Microbiol* (2020) 5(7):878–80. doi: 10.1038/s41564-020-0721-1
110. Aroniadis OC, Brandt L. Fecal Microbiota Transplantation: Past, Present and Future. *Curr Opin Gastroenterol* (2013) 29(1):79–84. doi: 10.1097/MOG.0b013e32835a4b3e
111. Van Nood E, Vrieze A, Nieuwdorp M, Fuentes S, Zoetendal EG, De Vos WM, et al. Duodenal Infusion of Donor Feces for Recurrent Clostridium Difficile. *N Engl J Med* (2013) 368(5):407–15. doi: 10.1056/NEJMoa1205037
112. Paramsothy S, Kamm MA, Kaakoush NO, Walsh AJ, van den Bogaerde J, Samuel D, et al. Multidonor Intensive Faecal Microbiota Transplantation for Active Ulcerative Colitis: A Randomised Placebo-Controlled Trial. *Lancet* (2017) 389(10075):1218–28. doi: 10.1016/S0140-6736(17)30182-4
113. Rosshart SP, Vassallo BG, Angeletti D, Hutchinson DS, Morgan AP, Takeda K, et al. Wild Mouse Gut Microbiota Promotes Host Fitness and Improves Disease Resistance. *Cell* (2017) 171(5):1015–28.e13. doi: 10.1016/j.cell.2017.09.016
114. Wang Y, Wiesnoski DH, Helmink BA, Gopalakrishnan V, Choi K, DuPont HL, et al. Fecal Microbiota Transplantation for Refractory Immune Checkpoint Inhibitor-Associated Colitis. *Nat Med* (2018) 24(12):1804–8. doi: 10.1038/s41591-018-0238-9
115. Davar D, Dzutsev AK, McCulloch JA, Rodrigues RR, Chauvin J-M, Morrison RM, et al. Fecal Microbiota Transplant Overcomes Resistance to Anti–PD-1 Therapy in Melanoma Patients. *Science* (2021) 371(6529):595–602. doi: 10.1126/science.abf3363
116. Baruch EN, Youngster I, Ben-Betzalel G, Ortenberg R, Lahat A, Katz L, et al. Fecal Microbiota Transplant Promotes Response in Immunotherapy-Refractory Melanoma Patients. *Science* (2021) 371(6529):602–9. doi: 10.1126/science.abb5920

Conflict of Interest: The authors declare that the research was conducted in the absence of any commercial or financial relationships that could be construed as a potential conflict of interest.

frontiers in Oncology

CASE REPORT
published: 13 January 2022
doi: 10.3389/fonc.2021.759652

Case Report: Favorable Response and Manageable Toxicity to the Combination of Camrelizumab, Oxaliplatin, and Oral S-1 in a Patient With Advanced Epstein–Barr Virus-Associated Gastric Cancer

Wanrui Lv[†], *Ke Cheng*[†], *Xiaofen Li*, *Lusi Feng*, *Hancong Li*, *Jia Li*, *Chen Chang and Dan Cao*[*]

Department of Medical Oncology, Cancer Center, West China Hospital, Sichuan University, Chengdu, China

OPEN ACCESS

Edited by:
Yanhong Deng,
The Sixth Affiliated Hospital of Sun Yat-sen University, China

Reviewed by:
Jun Nishikawa,
Yamaguchi University, Japan
Bing Luo,
Qingdao University, China

***Correspondence:**
Dan Cao
caodan316@163.com

[†]*These authors have contributed equally to this work*

Specialty section:
This article was submitted to Cancer Immunity and Immunotherapy, a section of the journal Frontiers in Oncology

Received: *16 August 2021*
Accepted: *20 December 2021*
Published: *13 January 2022*

Citation:
Lv W, Cheng K, Li X, Feng L, Li H, Li J, Chang C and Cao D (2022) Case Report: Favorable Response and Manageable Toxicity to the Combination of Camrelizumab, Oxaliplatin, and Oral S-1 in a Patient With Advanced Epstein–Barr Virus-Associated Gastric Cancer. Front. Oncol. 11:759652. doi: 10.3389/fonc.2021.759652

Some pertinent studies have demonstrated that Epstein–Barr virus-associated gastric cancer (EBVaGC) patients showed a favorable clinical outcome to immunotherapy and Epstein–Barr virus (EBV)-positive status might be a potential biomarker for immunotherapy in gastric cancer (GC). However, knowledge of given exposure to EBVaGC to the first-line immunotherapy is largely inadequate. Moreover, whether camrelizumab can be as effective as other PD-1 inhibitors in the treatment of advanced EBVaGC has not been reported. We report a case of advanced EBVaGC patient with a positive expression of PD-L1, enriched PD-L1+CD68+macrophages, and high TMB who had a long-term partial response and manageable toxicity to the combined approach of camrelizumab (a novel PD-1 inhibitor) and oxaliplatin plus oral S-1 (SOX). As the first-line treatment of advanced EBVaGC patients, camrelizumab combined with SOX regimen may provide a novel combined approach with favorable response and manageable safety. Combination of multiple biomarkers could have a higher effective predictive capacity to immunotherapy. Integrated treatment (chemo-immunotherapy and radiotherapy) might be the optimal strategy for patients with oligometastasis. It deserves prospective research to further validate the efficacy.

Keywords: EBV-associated gastric cancer, camrelizumab, immunotherapy, programmed cell death ligand-1 (PD-L1) positive, favorable response, manageable toxicity

INTRODUCTION

Gastric cancer (GC) remains a significant burden worldwide with an estimated 1,089,103 new cases and 768,793 deaths in 2020 (1). The prognosis and survival are much worse for advanced GC. Based on the CheckMate 649 trial (2), nivolumab combined with fluoropyrimidine and oxaliplatin has been adopted as the first-line treatment for advanced GC patients with HER2 overexpression negative and PD-L1 CPS ≥5 in the NCCN guideline (3). Epstein–Barr virus-associated gastric

cancer (EBVaGC), as one of four subtypes of gastric carcinoma, accounts for ~9% of GC (4, 5). Although very limited data in EBVaGCs are known, some pertinent studies have demonstrated that EBVaGC patients showed a favorable clinical outcome to immunotherapy and EBV-positive status might be a potential biomarker for immunotherapy in GC. Kim et al. showed a striking result that compared with the overall response rate (ORR) of 85.7% in microsatellite instability-high metastatic gastric cancer (mGC), ORR in EBV-positive mGC is 100% (6). In a prospective observational study, 66.7% of EBVaGC patients showed a partial response (PR) after combined immunotherapy (7). Plausible explanations contributing to favorable efficacy of the anti-PD-1 antibody in EBVaGC mainly involve the EBV-related cancer-intrinsic characteristics, including the tumor-associated immune cell-rich phenotype as well as the overexpression of PD-L1. Since late-stage EBVaGC patients receiving treatments only comprise ~3% of GC cases, knowledge of given exposure to EBVaGC to the first-line immunotherapy is largely inadequate. Trials of applying nivolumab and pembrolizumab to the first-line treatment of advanced GC have been carried out one after another and achieved corresponding success (2, 8). Whether the aforementioned observations in these anti-PD-1 antibodies may analogously be extended to advanced GC treated with camrelizumab, especially EBVaGC, has not been reported. We herein report a case of a metastatic EBVaGC patient with an overexpression of PD-L1, enriched PD-L1+CD68+macrophages, and high TMB who had early tumor shrinkage, deep response, long-term duration of response, and manageable toxicity to camrelizumab, a novel PD-1 blockade, in combination with standard chemotherapy as a first-line setting.

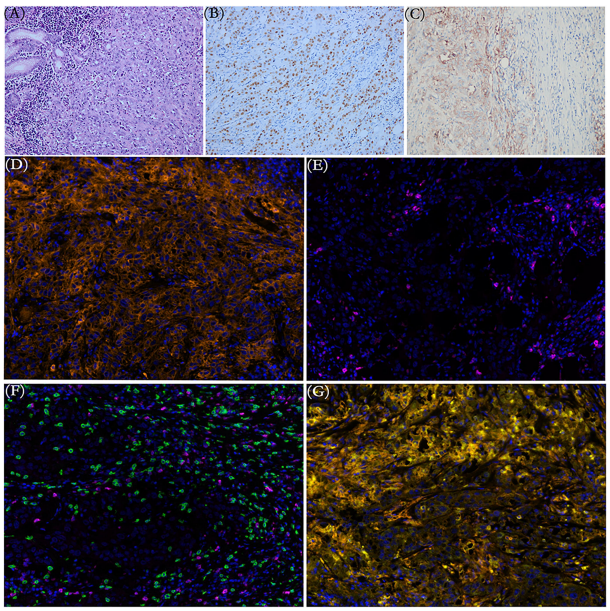

FIGURE 1 | **(A)** Representative pathological image of gastric mass magnifications shows intense infiltrate of lymphocytes within the primary tumor (hematoxylin and eosin). **(B)** The brown cells in EBER-ISH ×200 magnification images are the cells harboring EBV infection (EBV-encoded small RNA *in situ* hybridization, EBER-ISH). **(C)** Immunohistochemical staining indicated broadly positive programmed death-ligand 1 (PD-L1) expression in the primary tumor. **(D–G)** Multiplex immunohistochemical analysis from a variety of cells in the tumor microenvironment. **(D)** PD-L1+ cells (orange). **(E)** PD-1+ cells (purple). **(F)** CD8+T cells (green). **(G)** PD-L1+ CD68+ macrophages (yellow). Original magnification ×200.

CASE PRESENTATION

A 56-year-old Chinese woman was admitted to our hospital emergency room in September 2020 with repeat fatigue, abdominal distension, and melena for 1 month. Abdominal computerized tomography (CT) suggested obviously uneven thickening and strengthening of the gastric body and gastric antrum wall, possibly accompanied by ulcers and multiple lymph nodes adjacent to the stomach enlarged. Gastroscopic examination revealed a giant ulcerative lesion located in the posterior wall of the gastric antrum, with the invasion of stomach angle and pylorus. Subsequent pathological examination of the biopsy showed poorly differentiated adenocarcinoma. On September 19, 2020, she underwent radical gastrectomy for distal gastric cancer and D2 lymphadenectomy. Pathohistological results of distal gastric cancer resection showed that the tumor was poorly differentiated adenocarcinoma with lymphoid stroma component (**Figure 1**), without any cancer in the surgical margin and metastasis to regional lymph nodes. An EBV-encoded RNA (EBER) assay demonstrated strong positive staining parallel to the tumor harboring EBV infection (**Figure 1**). Meanwhile, the immunohistochemistry indicated that MLH1, MSH2, MSH6, and PMS2 were overexpressed (pMMR) and human epidermal growth factor receptor 2 (HER2) was not amplified. The tumor was confirmed as pT4bN0M0 poorly gastric antrum differentiated adenocarcinoma with lymphoid stroma component (EBER-ISH+ and HER2-). The outcomes of next-generation sequencing (NGS) verified fifteen gene mutations (**Table 1**), a high tumor mutation burden (TMB) with 10.8 Muts/Mb, and microsatellite stable (MSS)

TABLE 1 | The fifteen gene mutations of the patient.

Gene	Mutations	Mutation abundance (%)
PIK3CA	c.1634A>C p.E545A	10.93%
ABL1	c.3010C>T p.P1004S	8.51%
ARID1B	c.4296G>A p.M1432I	10.41%
CASP8	c.1414C>T p.R472*	10.86%
EPHA5	c.414C>A p.N138K	8.84%
FBXW7	c.1258C>T p.H420Y	8.79%
JAK2	c.1258C>T p.H420Y	8.79%
MLH3	c.1258C>T p.H420Y	11.7%
MYCL	c.1034C>T p.S345F	9.8%
NF2	c.1034C>T p.S345F	19.7%
PTPN11	c.1508G>T p.G503V	19.7%
RAD21	c.335A>C p.E112A	10.27%
RICTOR	c.872C>T p.T291I	2.16%
SOX9	c.872C>T p.T291I	0.46%
TET2	c.5059C>T p.Q1687*	0.69%

**means the termination codons. c.5059C>T p.Q1687* :aminoacids changes from Glutarnine(Q) to termination codons (*).*

status. Immunohistochemical (IHC) data of the tumor tissue suggested that the positive expression of PD-L1 protein and the tumor proportion score (TPS) was 70% and the combined positive score (CPS) was 75 (**Figure 1**). The immune microenvironment was examined by multiplex immunohistochemical staining and quantitative analysis (**Figure 1** and **Table 2**). Two months after the operation, abdominal CT showed enlargement of mass located in the gastrocolic ligament (**Figure 2**), which indicated metastatic lymph node (LN). Oxaliplatin 200 mg on day 1 plus oral S-1 60 mg twice a day, from days 1 to 14, along with camrelizumab 200 mg on day 1, repeated every 3 weeks, was administered as first-line treatment. Then, radiographic evaluation was performed every 8 weeks by enhanced CT. The significant resolution of the lymph node was observed after two cycles' exposure of regimen SOX combined with camrelizumab, and the best efficacy evaluation was PR based on RECIST 1.1. Early tumor shrinkage was observed after 8 weeks, and persistent shrinkage of LN was achieved after 4 cycles (**Figure 2**). From then on, she had been exposed to SOX combined with camrelizumab up to 8 months and still achieved continuous PR. Moreover, the quality of life of the patient was good. Chemotherapy-associated AEs (grade 1 nausea, vomit and grade 2 anemia, grade 2 decreased neutrophil count, and decreased white blood cell count) were observed, and grade 1 reactive cutaneous capillary endothelial proliferation (RCCEP) was presented without any other immune-related adverse event. After 7 cycles' SOX plus camrelizumab, the lesion was still unresectable due to whole abdominal adhesions. After multidisciplinary team (MDT) consultation, the patient underwent external-beam radiotherapy (EBRT) and received 50 Gy/25 fractions. She received S-1 and camrelizumab as the maintenance therapy up to 10 cycles followed by EBRT. Tumor is gradually and continuously shrinking in the latest visit and in deep response with a >80% decrease in size (**Figure 2**). Until now, PFS reached at least 12 months and the duration of response was beyond 10 months with manageable toxicity.

TABLE 2 | Tumor-infiltrating immune cell test results.

Test indicators (multiplex IHC)	Test result
CD8+ T cells	+(10.59%)
PD-1+ cells	+(1.07%)
CD8+PD-1+ T cells	+(0.33%)
CD68+ macrophage cells	+(38.71%)
CD68+PD-L1+ macrophage	+(28.83%)

DISCUSSION

Searching for electrical databases, few clinical studies have focused on camrelizumab combined with chemotherapy as a first-line setting for gastric cancer, let alone for EBVaGC. As far as we know, this is the first report to show long-term response and safety of camrelizumab combined with chemotherapy in the first-line treatment of advanced EBVaGC. The cancer of the patient shown in this case quickly metastasized in a short period of time after the operation, which reflected the high degree of malignancy and poor biological behavior of the tumor. Then, early tumor shrinkage to PR was observed after two cycles' exposure of camrelizumab combined with SOX regimen and persistency of response was observed. Notably, the median OS was 13.1 months in the nivolumab-plus-chemotherapy arm (patients with PD-L1 CPS ≥5) and the median PFS was 7.7 months (95% CI 7.0–9.2) with nivolumab plus chemotherapy in the CheckMate 649 study (2), in contrast, the PFS benefit (beyond 12 months) was more prominent in our case, which could be translated into a long-term survival benefit for this patient. The favorable responses of this patient may attribute to the unique characteristics of EBV-related cancers. Enriched tumor-infiltrating immune cells (lymphocyte and tumor-associated macrophages) exist in the EBVaGC microenvironment (9, 10). The density of CD68+macrophages was significantly higher in EBVaGC patients compared to Epstein–Barr virus-negative gastric cancer (EBVnGC), which was positively correlated with the expression rate of PD-L1 (11, 12). Compared with EBVnGC, the density of

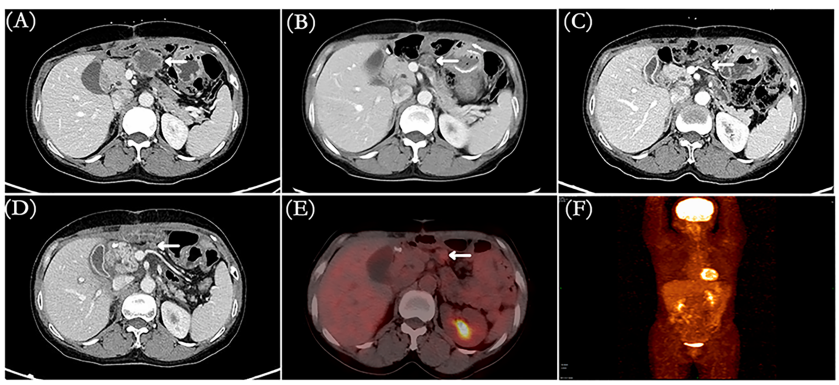

FIGURE 2 | **(A)** CT image presented lymph node metastasis before treatment. **(B)** CT image showed early tumor shrinkage to PR after two cycles' treatment. **(C)** CT image showed that lymph node metastasis was smaller (sustained PR) after four cycles. **(D–F)** CT and PET/CT images indicated lymph node metastasis with decrease >80% in size and mild uptake on 18F-FDG-PET/CT after seven cycles' SOX + camrelizumab and three cycles' S-1 + camrelizumab (total ten cycles). White arrows: lymph node metastasis.

PD-L1+ tumor infiltrating immune cells was significantly greater in EBVaGC (10). Interestingly, several studies have shown that the quantity of PD-L1+CD68+macrophage may serve as an independent prognostic factor for survival or be significantly associated with favorable outcome to immunotherapy-based treatment in other malignancies, such as non-small-cell lung cancer, testicular lymphoma, and breast cancer (13–15). Hence, the quantity of PD-L1+CD68+macrophage may also serve as both an independent prognostic factor of EBVaGC and an effective predictor of EBVaGC in immunotherapy. Concordantly, through multiplex immunohistochemistry (mIHC), numerous infiltrated CD8+T lymphocytes and CD68+PD-L1+macrophages were observed in our case (**Figure 1** and **Table 2**), which provides a good antitumor environment. Next, the high levels of PD-L1 in cancer cells and inflammatory cells may be another interpretation for favorable outcomes (10). As the interaction of PD-L1 in cancer cells and programmed cell death protein 1 (PD-1) on the surface of T-cells enables tumor cells to escape from antitumor immunity, the high expression of PD-L1 in EBVaGC can be considered to be related to tumor progression (16). Accordingly, treatment with anti-PD-1/PD-L1 may prevent this interaction, thereby restoring the immune response against cancer cells. Thirdly, the high TMB in this patient may also play an important role in favorable outcomes. Although the predictive role of TMB in immunotherapy is still controversial, many immune-based studies indicated that due to its influence to invigoration of immune cells, patients with high TMB showed better curative effect to immune checkpoint inhibitors (ICIs) than those with non-high-TMB (6, 17).

Camrelizumab, a novel PD-1 inhibitor, possesses the characteristics of lower IC50 and EC50 values, increased affinity, and higher PD-1 receptor occupancy rate (>85%), which results in enhanced antitumor activity, compared to other PD-1 inhibitors (18, 19). Furthermore, camrelizumab showed impressive efficacy and manageable toxicity in a wide spectrum of solid tumors, including Hodgkin lymphoma (20), B-cell lymphoma (21), esophageal squamous cell carcinoma (22), gastric and gastroesophageal junction cancer (23), hepatocellular carcinoma (23), nasopharyngeal cancer, and non-squamous, non-small cell lung cancer (24). Hence, the possibility of long-term tolerance coming from low toxicity should be taken into account. No serious adverse events have been shown during the treatment outside of grade 1 nausea and vomit, grade 2 anemia, decreased neutrophil count, and decreased white blood cell count, which were more prone to chemotherapy-related toxicities. Under prolonged exposure to camrelizumab, mild RCCEPs were observed without any other immune-related adverse event. Further follow-up is needed.

The complexity of the relationship between cancer and the immune system renders it difficult to identify a single predictive biomarker. Although favorable clinical outcomes were observed in patients with EBV-negative PD-L1 positive treated with chemotherapy plus PD-L1 antibody in a published study (25), PD-L1 expression levels might not be a robust predictor for anti-PD-1/PD-L1 therapies in GC (25–27). Commonly, EBVaGC patients showed a favorable clinical outcome to immunotherapy, and almost EBV+GC cases presented high PD-L1 CPS (28, 29), just as this patient with CPS = 75, and this phenomenon was seldom seen in EBVnGC. Hence, we believed that the EBV-positive status might be a superior predictor than PD-L1 for immunotherapy in GC (7, 30). Could the combination of different factors become a more accurate biomarker? High PD-L1, enriched PD-L1+CD68 +macrophages, and high TMB were presented in this patient with EBVaGC. Combination of multiple biomarkers could have a higher efficacy predictive capacity to immunotherapy. This speculation was consistent with a previous study in which 3 patients with EBVaGC showing PR were PD-L1 positive and at the last follow-up, their durations of the response were 13.8, 18, and 10 months, respectively (7), whose finding highlighted the long-lasting nature of immunotherapy. This assumption requires further large-scale clinical trials for verification.

To our knowledge, this is the first case with high PD-L1 (TPS = 70%, CPS = 75), enriched PD-L1+CD68+macrophages (28.83%), and high TMB (10.8 Muts/Mb). EBVaGC was treated with camrelizumab combined with oxaliplatin and S-1 as the first-line therapy. Early tumor shrinkage, deep response, durable PFS, and manageable toxicities were exhibited. Moreover, multidisciplinary approaches—camrelizumab plus SOX (induction therapy), radiotherapy (local therapy), and camrelizumab plus S-1 (maintenance therapy)—might be the more suitable integrated treatment for this patient with oligometastatic lesion. It remained unclear, however, whether prominent PD-L1+CD68+macrophages were a common finding in EBVaGC or just for our patient. Next, cross talk among PD-L1+CD68+macrophages, T cells, and cancer cells was unknown. Additionally, repeated mIHC examinations, although better, were difficult to apply in real-world clinical practice.

In conclusion, the present study suggests that camrelizumab combined with SOX might be a promising and well-tolerated regimen as the first-line treatment in metastatic EBVaGC with high PD-L1 CPS and enriched PD-L1+CD68+macrophages in the tumor microenvironment. For a highly heterogeneous malignancy, we recommend gene sequencing and multiplex immunohistochemical to find a new strategy. It deserves prospective research to further validate the efficacy.

DATA AVAILABILITY STATEMENT

The original contributions presented in the study are included in the article/supplementary material. Further inquiries can be directed to the corresponding author.

ETHICS STATEMENT

The studies involving human participants were reviewed and approved by West China Hospital of Sichuan University Biomedical Research Ethics Committee. The patients/participants provided their written informed consent to

participate in this study. Written informed consent was obtained from the individual(s) for the publication of any potentially identifiable images or data included in this article.

AUTHOR CONTRIBUTIONS

XL and HL performed the radiological analysis of CT images. LF, CC, and JL collected the clinical data. WL and KC wrote the first draft of the manuscript. DC wrote the sections of the manuscript. All authors contributed to the article and approved the submitted version.

FUNDING

This research was partly supported by Sichuan Province Health Planning Committee Research Project (No. 19PJ083).

REFERENCES

1. Sung H, Ferlay J, Siegel RL, Laversanne M, Soerjomataram I, Jemal A, et al. Global Cancer Statistics 2020: GLOBOCAN Estimates of Incidence and Mortality Worldwide for 36 Cancers in 185 Countries. *CA: Cancer J Clin* (2021) 71(3):209–49. doi: 10.3322/caac.21660
2. Janjigian YY, Shitara K, Moehler M, Garrido M, Salman P, Shen L, et al. First-Line Nivolumab Plus Chemotherapy Versus Chemotherapy Alone for Advanced Gastric, Gastro-Oesophageal Junction, and Oesophageal Adenocarcinoma (CheckMate 649): A Randomised, Open-Label, Phase 3 Trial. *Lancet (London England)* (2021) 398(10294):27–40. doi: 10.1016/s0140-6736(21)00797-2
3. *Gastric Cancer, Version 5.2021, NCCN Clinical Practice Guidelines in Oncology* (2021). Available at: https://www.nccn.org/professionals/physician_gls/pdf/gastric.pdf.
4. Murphy G, Pfeiffer R, Camargo MC, Rabkin CS. Meta-Analysis Shows That Prevalence of Epstein-Barr Virus-Positive Gastric Cancer Differs Based on Sex and Anatomic Location. *Gastroenterology* (2009) 137(3):824–33. doi: 10.1053/j.gastro.2009.05.001
5. Zhang W. TCGA Divides Gastric Cancer Into Four Molecular Subtypes: Implications for Individualized Therapeutics. *Chin J Cancer* (2014) 33 (10):469–70. doi: 10.5732/cjc.014.10117
6. Kim H, Hong JY, Lee J, Park SH, Park JO, Park YS, et al. Clinical Sequencing to Assess Tumor Mutational Burden as a Useful Biomarker to Immunotherapy in Various Solid Tumors. *Ther Adv Med Oncol* (2021) 13:1758835921992992. doi: 10.1177/1758835921992992
7. Xie T, Liu Y, Zhang Z, Zhang X, Gong J, Qi C, et al. Positive Status of Epstein-Barr Virus as a Biomarker for Gastric Cancer Immunotherapy: A Prospective Observational Study. *J Immunother (Hagerstown Md: 1997)* (2020) 43 (4):139–44. doi: 10.1097/cji.0000000000000316
8. Shitara K, Van Cutsem E, Bang YJ, Fuchs C, Wyrwicz L, Lee KW, et al. Efficacy and Safety of Pembrolizumab or Pembrolizumab Plus Chemotherapy vs Chemotherapy Alone for Patients With First-Line, Advanced Gastric Cancer: The KEYNOTE-062 Phase 3 Randomized Clinical Trial. *JAMA Oncol* (2020) 6(10):1571–80. doi: 10.1001/jamaoncol.2020.3370
9. Grogg KL, Lohse CM, Pankratz VS, Halling KC, Smyrk TC. Lymphocyte-Rich Gastric Cancer: Associations With Epstein-Barr Virus, Microsatellite Instability, Histology, and Survival. *Modern Pathol: An Off J United States Can Acad Pathol Inc* (2003) 16(7):641–51. doi: 10.1097/01.Mp.0000076980.73826.C0
10. Derks S, Liao X, Chiaravalli AM, Xu X, Camargo MC, Solcia E, et al. Abundant PD-L1 Expression in Epstein-Barr Virus-Infected Gastric Cancers. *Oncotarget* (2016) 7(22):32925–32. doi: 10.18632/oncotarget.9076
11. Jia X, Guo T, Li Z, Zhang M, Feng Y, Dong B, et al. Clinicopathological and Immunomicroenvironment Characteristics of Epstein-Barr Virus-Associated Gastric Cancer in a Chinese Population. *Front Oncol* (2020) 10:586752. doi: 10.3389/fonc.2020.586752
12. Wang YL, Gong Y, Lv Z, Li L, Yuan Y. Expression of PD1/PDL1 in Gastric Cancer at Different Microsatellite Status and its Correlation With Infiltrating Immune Cells in the Tumor Microenvironment. *J Cancer* (2021) 12(6):1698–707. doi: 10.7150/jca.40500
13. Liu Y, Zugazagoitia J, Ahmed FS, Henick BS, Gettinger SN, Herbst RS, et al. Immune Cell PD-L1 Colocalizes With Macrophages and Is Associated With Outcome in PD-1 Pathway Blockade Therapy. *Clin Cancer Res: An Off J Am Assoc Cancer Res* (2020) 26(4):970–7. doi: 10.1158/1078-0432.Ccr-19-1040
14. Pollari M, Brück O, Pellinen T, Vähämurto P, Karjalainen-Lindsberg ML, Mannisto S, et al. PD-L1(+) Tumor-Associated Macrophages and PD-1(+) Tumor-Infiltrating Lymphocytes Predict Survival in Primary Testicular Lymphoma. *Haematologica* (2018) 103(11):1908–14. doi: 10.3324/haematol.2018.197194
15. Wang J, Browne L, Slapetova I, Shang F, Lee K, Lynch J, et al. Multiplexed Immunofluorescence Identifies High Stromal CD68(+)PD-L1(+) Macrophages as a Predictor of Improved Survival in Triple Negative Breast Cancer. *Sci Rep* (2021) 11(1):21608. doi: 10.1038/s41598-021-01116-6
16. Cho J, Kang MS, Kim KM. Epstein-Barr Virus-Associated Gastric Carcinoma and Specific Features of the Accompanying Immune Response. *J Gastric Cancer* (2016) 16(1):1–7. doi: 10.5230/jgc.2016.16.1.1
17. Wei XL, Xu JY, Wang DS, Chen DL, Ren C, Li JN, et al. Baseline Lesion Number as an Efficacy Predictive and Independent Prognostic Factor and its Joint Utility With TMB for PD-1 Inhibitor Treatment in Advanced Gastric Cancer. *Ther Adv Med Oncol* (2021) 13:1758835921988996. doi: 10.1177/1758835921988996
18. Lickliter JD, Gan HK, Voskoboynik M, Arulananda S, Gao B, Nagrial A, et al. A First-In-Human Dose Finding Study of Camrelizumab in Patients With Advanced or Metastatic Cancer in Australia. *Drug Design Dev Ther* (2020) 14:1177–89. doi: 10.2147/dddt.S243787
19. Mo H, Huang J, Xu J, Chen X, Wu D, Qu D, et al. Safety, Anti-Tumour Activity, and Pharmacokinetics of Fixed-Dose SHR-1210, an Anti-PD-1 Antibody in Advanced Solid Tumours: A Dose-Escalation, Phase 1 Study. *Br J Cancer* (2018) 119(5):538–45. doi: 10.1038/s41416-018-0100-3
20. Nie J, Wang C, Liu Y, Yang Q, Mei Q, Dong L, et al. Addition of Low-Dose Decitabine to Anti-PD-1 Antibody Camrelizumab in Relapsed/Refractory Classical Hodgkin Lymphoma. *J Clin Oncol: Off J Am Soc Clin Oncol* (2019) 37 (17):1479–89. doi: 10.1200/jco.18.02151
21. Mei Q, Zhang W, Liu Y, Yang Q, Rasko JEJ, Nie J, et al. Camrelizumab Plus Gemcitabine, Vinorelbine, and Pegylated Liposomal Doxorubicin in Relapsed/Refractory Primary Mediastinal B-Cell Lymphoma: A Single-Arm, Open-Label, Phase II Trial. *Clin Cancer Res: An Off J Am Assoc Cancer Res* (2020) 26(17):4521–30. doi: 10.1158/1078-0432.Ccr-20-0514
22. Huang J, Xu J, Chen Y, Zhuang W, Zhang Y, Chen Z, et al. Camrelizumab Versus Investigator's Choice of Chemotherapy as Second-Line Therapy for Advanced or Metastatic Oesophageal Squamous Cell Carcinoma (ESCORT): A Multicentre, Randomised, Open-Label, Phase 3 Study. *Lancet Oncol* (2020) 21(6):832–42. doi: 10.1016/s1470-2045(20)30110-8
23. Xu J, Zhang Y, Jia R, Yue C, Chang L, Liu R, et al. Anti-PD-1 Antibody SHR-1210 Combined With Apatinib for Advanced Hepatocellular Carcinoma, Gastric, or Esophagogastric Junction Cancer: An Open-Label, Dose Escalation and Expansion Study. *Clin Cancer Res: An Off J Am Assoc Cancer Res* (2019) 25(2):515–23. doi: 10.1158/1078-0432.Ccr-18-2484
24. Fang W, Yang Y, Ma Y, Hong S, Lin L, He X, et al. Camrelizumab (SHR-1210) Alone or in Combination With Gemcitabine Plus Cisplatin for Nasopharyngeal Carcinoma: Results From Two Single-Arm, Phase 1 Trials. *Lancet Oncol* (2018) 19(10):1338–50. doi: 10.1016/s1470-2045(18)30495-9
25. Kawazoe A, Yamaguchi K, Yasui H, Negoro Y, Azuma M, Amagai K, et al. Safety and Efficacy of Pembrolizumab in Combination With S-1 Plus Oxaliplatin as a First-Line Treatment in Patients With Advanced Gastric/Gastroesophageal Junction Cancer: Cohort 1 Data From the KEYNOTE-659 Phase IIb Study. *Eur J Cancer (Oxford England: 1990)* (2020) 129:97–106. doi: 10.1016/j.ejca.2020.02.002

26. Kang YK, Boku N, Satoh T, Ryu MH, Chao Y, Kato K, et al. Nivolumab in Patients With Advanced Gastric or Gastro-Oesophageal Junction Cancer Refractory to, or Intolerant of, at Least Two Previous Chemotherapy Regimens (ONO-4538-12, ATTRACTION-2): A Randomised, Double-Blind, Placebo-Controlled, Phase 3 Trial. *Lancet (Lond Engl)* (2017) 390 (10111):2461–71. doi: 10.1016/s0140-6736(17)31827-5
27. Bang YJ, Ruiz EY, Van Cutsem E, Lee KW, Wyrwicz L, Schenker M, et al. Randomised Trial of Avelumab Versus Physician's Choice of Chemotherapy as Third-Line Treatment of Patients With Advanced Gastric or Gastro-Oesophageal Junction Cancer: Primary Analysis of JAVELIN Gastric 300. *Ann Oncol: Off J Eur Soc Med Oncol* (2018) 29(10):2052–60. doi: 10.1093/annonc/mdy264
28. Yang J, Liu Z, Zeng B, Hu G, Gan R. Epstein-Barr Virus-Associated Gastric Cancer: A Distinct Subtype. *Cancer Lett* (2020) 495:191–9. doi: 10.1016/j.canlet.2020.09.019
29. Naseem M, Barzi A, Brezden-Masley C, Puccini A, Berger MD, Tokunaga R, et al. Outlooks on Epstein-Barr Virus Associated Gastric Cancer. *Cancer Treat Rev* (2018) 66:15–22. doi: 10.1016/j.ctrv.2018.03.006
30. Kim ST, Cristescu R, Bass AJ, Kim KM, Odegaard JI, Kim K, et al. Comprehensive Molecular Characterization of Clinical Responses to PD-1 Inhibition in Metastatic Gastric Cancer. *Nat Med* (2018) 24(9):1449–58. doi: 10.1038/s41591-018-0101-z

Conflict of Interest: The authors declare that the research was conducted in the absence of any commercial or financial relationships that could be construed as a potential conflict of interest.

Publisher's Note: All claims expressed in this article are solely those of the authors and do not necessarily represent those of their affiliated organizations, or those of the publisher, the editors and the reviewers. Any product that may be evaluated in this article, or claim that may be made by its manufacturer, is not guaranteed or endorsed by the publisher.

frontiers in Immunology

ORIGINAL RESEARCH
published: 18 January 2022
doi: 10.3389/fimmu.2021.783243

Safety and Efficacy of Camrelizumab in Combination With Nab-Paclitaxel Plus S-1 for the Treatment of Gastric Cancer With Serosal Invasion

*Ju-Li Lin[1,2], Jian-Xian Lin[1,2,3], Jun Peng Lin[1,2], Chao-Hui Zheng[1,2], Ping Li[1,2,3], Jian-Wei Xie[1,2], Jia-bin Wang[1,2,3], Jun Lu[1,2], Qi-Yue Chen[1,2] and Chang-Ming Huang[1,2,3]**

[1] Department of Gastric Surgery, Fujian Medical University Union Hospital, Fuzhou, China, [2] Department of General Surgery, Fujian Medical University Union Hospital, Fuzhou, China, [3] Key Laboratory of Ministry of Education of Gastrointestinal Cancer, Fujian Medical University, Fuzhou, China

Objective: To investigate the safety and efficacy of camrelizumab in combination with nab-paclitaxel plus S-1 for the treatment of gastric cancer with serosal invasion.

Method: Two hundred patients with gastric cancer with serosal invasion who received neoadjuvant therapy from January 2012 to December 2020 were retrospectively analyzed. According to the different neoadjuvant therapy regimens, the patients were divided into the following three groups: the SOX group (S-1 + oxaliplatin) (72 patients), SAP group (S-1 + nab-paclitaxel) (95 patients) and C-SAP group (camrelizumab + S-1 + nab-paclitaxel) (33 patients).

Result: The pathological response (TRG 1a/1b) in the C-SAP group (39.4%) was not significantly different from that in the SAP group (26.3%) and was significantly higher than that in the SOX group (18.1%). The rate of ypT0 in the C-SAP group (24.2%) was higher than that in the SAP group (6.3%) and the SOX group (5.6%). The rate of ypN0 in the C-SAP group (66.7%) was also higher than that in the SAP group (38.9%) and the SOX group (36.1%). The rate of pCR in the C-SAP group (21.2%) was higher than that in the SAP group (5.3%) and the SOX group (2.8%). The use of an anti-PD-1 monoclonal antibody was an independent protective factor for TRG grade (1a/1b). The use of camrelizumab did not increase postoperative complications or the adverse effects of neoadjuvant therapy.

Conclusion: Camrelizumab combined with nab-paclitaxel plus S-1 could significantly improve the rate of tumor regression grade (TRG 1a/1b) and the rate of pCR in gastric cancer with serosal invasion.

Keywords: gastric cancer, camrelizumab (SHR-1210), neoadjuvant chemotherapy, tumor regression rate, pCR

OPEN ACCESS

Edited by:
Ti Wen,
The First Affiliated Hospital of China Medical University, China

Reviewed by:
Juli Bai,
The University of Texas Health Science Center at San Antonio, United States
Changhua Zhang,
Sun Yat-sen University, China

***Correspondence:**
Chang-Ming Huang
hcmlr2002@163.com
orcid.org/0000-0002-0019-885X

Specialty section:
This article was submitted to Cancer Immunity and Immunotherapy, a section of the journal Frontiers in Immunology

Received: *25 September 2021*
Accepted: *27 December 2021*
Published: *18 January 2022*

Citation:
Lin J-L, Lin J-X, Lin JP, Zheng C-H, Li P, Xie J-W, Wang J-b, Lu J, Chen Q-Y and Huang C-M (2022) Safety and Efficacy of Camrelizumab in Combination With Nab-Paclitaxel Plus S-1 for the Treatment of Gastric Cancer With Serosal Invasion. Front. Immunol. 12:783243. doi: 10.3389/fimmu.2021.783243

INTRODUCTION

Gastric cancer is the fifth most common malignant tumor worldwide and the third leading cause of cancer-related death (1, 2). Surgical resection remains the only radical treatment available for patients with nonmetastatic gastric cancer. Because the recurrence rate remains high, multidisciplinary therapy, including neoadjuvant chemotherapy, has gradually become important for the treatment of advanced gastric cancer. In Europe and the Americas, docetaxel, oxaliplatin, fluorouracil, and leucovorin (the FLOT regimen) have become the standard neoadjuvant chemotherapy for advanced gastric cancer (CT2/N+M0) (3, 4). Compared with epirubicin, cisplatin, and fluorouracil or capecitabine (ECF/ECX regimen), the FLOT regimen has shown superiority in terms of pathological responses and overall survival outcomes. In China, the results of the RESOLVE trial (5) showed that the SOX regimen increased the overall survival rate of advanced gastric cancer (cT4aN+M0/cT4bN×M0) patients and the 3-year disease-free survival rate.

The KEYNOTE-059 (6) and ATTRACTION-2 (7) trials confirmed that PD-1 monoclonal antibody treatment provides significant survival benefit and good safety for advanced, recurrent or metastatic gastric/GEJ adenocarcinoma. Currently, the benefit of immunotherapy combined with neoadjuvant chemotherapy for locally advanced gastric cancer remains unclear. The safety and efficacy of immunotherapy in combination with neoadjuvant chemotherapy have not been reported in gastric cancer with serosal invasion. Therefore, the objective of this study was to investigate the safety and efficacy of camrelizumab in combination with nab-paclitaxel plus S-1 for the treatment of gastric cancer with serosal invasion.

METHODS

Patient Selection

This study retrospectively analyzed the clinicopathological data of 200 patients who received SOX, nab-paclitaxel + S-1 or camrelizumab + nab-paclitaxel + S-1 neoadjuvant therapy and radical gastrectomy at the Fujian Union Hospital from January 2012 to December 2020. The inclusion criteria were as follows: gastric adenocarcinoma confirmed by gastroscopy and pathology before surgery; clinical stage: cT4, lymph node N1 to N3, nondistant metastasis (M0); ECOG score 0-2; and blood index, liver and kidney function, and cardiopulmonary function indicating that patients could tolerate chemotherapy or surgery. The exclusion criteria were as follows: distant metastasis or highly suspected metastasis; incomplete pathological diagnosis; gastric stump cancer; gastric cancer; emergency surgery; and combination with other malignant tumors.

Abbreviations: S-1, tegafur gimeracil oteracil potassium capsule; TRG, tumor regression grade; pCR, pathological complete response; the FLOT regimen, docetaxel, oxaliplatin, fluorouracil, and leucovorin; ECF/ECX regimen, epirubicin, cisplatin, and fluorouracil or capecitabine.

Neoadjuvant Therapy

We divided the patients into three groups according to the different neoadjuvant drug treatments: the SOX group (oxaliplatin + S-1), SAP group (nab-paclitaxel + S-1), and C-SAP group (camrelizumab + nab-paclitaxel + S-1). The specific scheme was as follows.

The cycle of SOX chemotherapy consisted of the following:

Day 1: Intravenous oxaliplatin 130 mg/m^2

Days 1–14: S-1 at 120 mg/day for surface area ≥ 1.5 m^2, 100 mg/day for surface area between 1.25 and 1.5 m^2, and 80 mg/day for surface area < 1.25 m^2 were administered 2 times daily.

The next chemotherapy was repeated on the 22nd day.

The cycle of nab-paclitaxel + S-1 chemotherapy consisted of the following.

Day 1: Intravenous nab-paclitaxel 260 mg/m^2 over 30 min. Dose reductions (220 mg/m^2, 180 mg/m^2, or 150 mg/m^2) were permitted in patients with severe hematological or nonhematological toxicity.

Days 1–14: S-1 at 120 mg/day for surface area ≥ 1.5 m^2, 100 mg/day for surface area between 1.25 and 1.5 m^2, and 80 mg/day for surface area < 1.25 m^2 were administered 2 times daily.

The next chemotherapy was repeated on the 22nd day.

The cycle of camrelizumab + nab-paclitaxel+S-1 chemotherapy consisted of the following.

Day 1: Intravenous camrelizumab 200 mg

Day 1: Intravenous nab-paclitaxel 260 mg/m^2 over 30 min. Dose reductions (220 mg/m^2, 180 mg/m^2, or 150 mg/m^2) were permitted in patients with severe hematological or nonhematological toxicity.

Days 1–14: S-1 at 120 mg/day for surface area ≥ 1.5 m^2, 100 mg/day for surface area between 1.25 and 1.5 m^2, and 80 mg/day for surface area < 1.25 m^2 were administered 2 times daily.

The next chemotherapy was repeated on the 22nd day.

Surgery

Patients underwent surgical resection between 2 and 4 weeks after the completion of neoadjuvant chemotherapy. Exploratory laparoscopy was routinely performed to exclude peritoneal or distant metastases. The scope of lymph node dissection was updated according to Japanese gastric cancer treatment guidelines (4th English edition) (8). TNM staging was performed according to the 8th edition of the AJCC/TNM staging system for gastric cancer (9).

Study Endpoints

The primary endpoint of this study was the rate of tumor regression grade (TRG 1a/1b). The secondary end points included pCR, TNM stage, total number of lymph nodes, positive lymph nodes, complete (R0) resection rate, surgical complications, and neoadjuvant treatment-related adverse effects.

Pathological Response

Tumor regression grade (TRG) was determined according to the Becker criteria (10, 11) and included "Grade 1a" (complete tumor regression, i.e., 0% residual tumor per tumor bed),

"Grade 1b" (subtotal tumor regression, i.e., <10% residual tumor per tumor bed) "Grade 2" (partial tumor regression, i.e., 10–50% residual tumor per tumor bed), and "Grade 3" (minimal or no tumor regression, i.e., > 50% residual tumor per tumor bed).

Pathologic complete response (pCR) was defined as no invasive disease within submitted and evaluated gross lesions and histologically negative nodes based on central review.

Tumor Staging

Radiologists followed the guidelines of the Response Evaluation Criteria in Solid Tumors (RECIST version 1.1) for the determination of radiological response to neoadjuvant chemotherapy (12). Two specialized radiologists independently evaluated the response rate, and the final result was determined after reviewing both sets of results.

Neoadjuvant Therapy Cycles

CT evaluation was performed after 2 and 4 cycles of neoadjuvant therapy. Some patients could not tolerate the side effects of neoadjuvant therapy, so the neoadjuvant therapy cycle was less than 4 cycles. Some patients completed 4 cycles of neoadjuvant therapy. Because R0 resection could not be performed after CT evaluation, more cycles were added before surgery.

Postoperative Complications

Postoperative complications were defined as events occurring within 30 days after the procedure, the severity of which was assessed by the Clavien-Dindo classification system (13, 14).

Evaluation of Adverse Effects

Adverse effects were recorded according to the National Cancer Institute Common Terminology Criteria for Adverse Events (CTCAE 4.0). Drug dose or timing was adjusted for patients with grade three or worse adverse effects.

Ethics

The study was approved by the ethics committee of Fujian Union Hospital. All of the patients signed informed consent documents.

Statistical Methods

All of the data were analyzed by SPSS software (SPSS, Chicago, IL, USA), version 22.0. The chi-square test or Fisher's exact test was used for comparisons of categorical variables. The independent sample t test or the Mann-Whitney U test was used for comparisons of continuous variables. Univariate logistic regression analysis was used to analyze the clinicopathological data of TRG (1a/1b). $P < 0.05$ was considered statistically significant.

RESULTS

Clinical Characteristics

A total of 200 patients were included in this study, including the SOX group (72 patients), SAP group (95 patients) and C-SAP group (33 patients) (**Supplemental Figure 1**). There were no significant differences in age, sex, ECOG score, Baumann classification or tumor location among the three groups (all $P > 0.05$). The number of patients with tumor size > 5 cm was greater in the C-SAP group (51.5%) and the SAP group (48.4%) than in the SOX group (36.1%) (all $P < 0.05$). The proportion of poorly differentiated/undifferentiated tumors in the C-SAP group (69.7%) and the SAP group (63.2%) was higher than that in the SOX group (all $P < 0.05$). The proportion of patients with ≥ 4 cycles of preoperative neoadjuvant treatment in the SAP group (81.1%) was higher than that in the C-SAP group (66.7%) and the SOX group (36.1%) (all $P < 0.05$) (**Table 1**).

Pathological Response

There was no significant difference in the rate of TRG grade (1a + 1b) between the C-SAP group (39.4%) and the SAP group (26.3%) ($P > 0.05$), but the rate in these two groups was higher than that in the SOX group (18.1%) ($P < 0.05$). The proportion of ypT0 in the C-SAP group (24.2%) was higher than that in the SAP group (6.3%) and the SOX group (5.6%). The proportion of ypN0 in the C-SAP group (66.7%) was higher than that in the SAP group (38.9%) and the SOX group (36.1%). The proportion of pCR in the C-SAP group (21.2%) was higher than that in the SAP group (5.3%) and the SOX group (2.8%) (both $P < 0.05$). There was no significant difference in the proportion of TRG grade (1a + 1b), the proportion of ypT0, the proportion of ypN0 or the proportion of pCR between the SAP group and the SOX group ($P > 0.05$) (**Table 2**). **Supplemental Figure 3** shows the effects of different neoadjuvant chemotherapy regimens and cycles on TRG in detail. The rate of TRG (1a + 1b) of patients receiving ≥ 4 cycles of neoadjuvant therapy group was higher than that of patients receiving ≤ 3 cycles of neoadjuvant therapy in C-SAP; The rate of TRG (1a + 1b) of patients receiving ≥ 4 cycles of neoadjuvant therapy was lower than that of patients receiving ≤ 3 cycles of neoadjuvant therapy in the SAP and SOX groups.

Risk Factors for Pathological Response

By univariate analysis, we found that the influencing factors of TRG (1a + 1b) included tumor size, Baumann classification, the use of PD-1, tumor location and pathological differentiation type. The multivariate analysis showed that tumor size > 5 cm was an independent risk factor (OR = 3.791, 95% CI = 1.513-9.501, P = 0.004), while the use of PD-1 was an independent protective factor (OR = 0.36, 95% CI = 0.152-0.852, P = 0.02) (**Supplemental Table 1**). By univariate analysis, we found that the factors influencing lymph node staging (ypN0) included tumor size, Baumann classification, tumor location and the use of PD-1. The multivariate analysis showed that middle gastric cancer was an independent risk factor (OR = 3.653, 95% CI = 1.163-8.275, P = 0.002), while the use of PD-1 was an independent protective factor (OR = 0.215, 95% CI = 0.88-0.525, P = 0.001) (**Supplemental Table 2**).

Comparison of Postoperative Conditions

There were no significant differences in the type of gastrectomy, surgical approach, R0 resection, nerve invasion or vascular

TABLE 1 | Demographic data before surgery.

Baseline variable	C-SAP group (n = 33)	SAP group (n = 95)	*P** value	SOX group (n = 72)	*P*$^{\#}$ value	*P*$^{\&}$ value
Gender			0.486		0.908	0.448
Male	26 (78.8)	69 (72.6)		56 (77.8)		
Female	7 (21.2)	26 (27.4)		16 (22.2)		
Age			0.988		0.962	0.969
< 60	13 (39.4)	31 (32.6)		27 (37.5)		
>= 60	20 (60.6)	64 (67.4)		45 (62.5)		
median	61.9 + 10.6	61.9 +12.3		62 + 10.8		
ECOG			0.530		0.379	0.724
0	29 (87.9)	87 (91.6)		67 (93.1)		
1	4 (12.1)	8 (8.4)		5 (6.9)		
Tumor size						
<= 5 cm	16 (48.5)	49 (51.6)	0.550	46 (63.9)	0.01	0.03
> 5 cm	17 (51.5)	46 (48.4)		26 (36.1)		
median (cm)	5.5	5.1		4.8		
Baumann type			0.786		0.214	0.354
2-3	26 (78.8)	73 (76.8)		59 (81.9)		
4	7 (21.2)	22 (23.2)		13 (18.1)		
Neoadjuvant cycle			0.010		0.001	0.001
<= 3	11 (33.3)	18 (18.9)		46 (63.9)		
>= 4	22 (66.7)	77 (81.1)		26 (36.1)		
Tumor location			0.530		0.379	0.724
Upper	18 (54.5)	46 (48.4)		37 (51.4)		
Middle	10 (30.3)	22 (23.2)		19 (26.4)		
Lower	5 (15.2)	27 (28.4)		16 (22.2)		
Differentiation			0.235		0.001	0.001
Well and middle	10 (30.3)	35 (36.8)		37 (51.4)		
Poor and underdifferentiated	23 (69.7)	60 (63.2)		35 (48.6)		

*P**: C-SAP vs. SAP *P*$^{\#}$: C-SAP vs. SOX *P*$^{\&}$: SAP vs. SOX.

invasion among the three groups (all P > 0.05). There were no significant differences in the number of harvested lymph nodes and positive lymph nodes between the C-SAP and SAP groups (all P > 0.05). The number of harvested lymph nodes in the C-SAP group was greater than that in the SOX group, and the number of positive lymph nodes in the C-SAP group was lower than that in the SOX group (all P < 0.05) (**Supplemental Figure 2**). In the SAP group, the treatment of 1 patient (1.1%) was combined with partial hepatectomy. In the SOX group, the treatment of 1 patient (1.4%) was combined with transverse colectomy, and 1 patient (1.4%) received body and tail pancreatectomy (**Table 3**).

Postoperative Complications

The overall complication rate was 25.5%, the Grade II complication rate was 22.5%, the Grade III complication rate was 3.5%, and there were no Grade IV or V complications.

There were no significant differences in the proportions of postoperative complications among the three groups (C-SAP (24.2%), SAP (22.1%) and SOX (31.9%)) (P > 0.05). The proportion of Grade II complications was 18.2% in the C-SAP group, 18.9% in the SAP group and 29.2% in the SOX group, with no significant differences (P > 0.05). The proportion of Grade III complications was 6.1% in the C-SAP group, 3.2% in the SAP group and 2.8% in the SOX group, with no significant differences (P > 0.05). There were no significant differences in the rates of pneumonia, abdominal infection, postoperative bleeding or anastomotic leakage among the three groups (P > 0.05) (**Table 4**).

Adverse Effects Associated With Neoadjuvant Therapy

We analyzed the adverse effects associated with neoadjuvant therapy. The most common adverse effects (Grades 3 and 4) were decreased WBC count, decreased neutrophil count and increased serum AST/ALT ratio. Neutrophil count decreased (Grades 3, 4) in the C-SAP group (24.8%) and the SAP group (23.2%) and were significantly higher than in the SOX group (9.7%) (P < 0.05), but there was no significant difference between the C-SAP group and the SAP group (P>0.05). WBC decreased (Grade s3 and4) in the C-SAP group (15.2%) and the SAP group (21.1%) and was higher than in the SOX group (5.6%), but there was no significant difference between the C-SAP group and the SAP group (P > 0.05). Serum AST/ALT increased in the C-SAP group (24.2%), SAP group (12.6%) and SOX group (20.8%), and there were no significant differences among the three groups (P > 0.05). The levels of anemia (Grades 3 and 4) in the C-SAP group (3.0%), SAP group (2.1%) and SOX group (6.9%) (P>0.05) were not significantly different. The platelet count was decreased (Grades 3 and 4) in the C-SAP group (6.1%), SAP group (3.2%) and SOX group (5.6%), and there was no significant difference among the three groups (P > 0.05). There was no significant difference in the rate of febrile neutropenia among the C-SAP (3.0%), SAP (5.3%) and SOX (2.8%) groups (P > 0.05) (**Table 5**).

TABLE 2 | Differences in response among the three groups.

Baseline variable	C-SAP group (n = 33)	SAP group (n = 95)	P^* value	SOX group (n = 72)	$P^{\#}$ value	$P^{\&}$ value
TRG			0.034		0.029	0.543
TRG1a	8 (24.2)	6 (6.3)		4 (5.6)		
TRG1b	5 (15.2)	19 (20.0)		9 (12.5)		
TRG2	6 (18.2)	32 (33.7)		24 (33.3)		
TRG3	14 (42.4)	38 (40.0)		35 (48.6)		
subgroup analysis			0.157		0.019	0.207
TRG1a-1b	13 (39.4)	25 (26.3)		13 (18.1)		
TRG2-3	20 (60.6)	70 (73.7)		59 (81.9)		
ypTstage			0.027		0.078	0.039
T0	8 (24.2)	6 (6.3)		4 (5.6)		
T1	2 (6.1)	11 (11.6)		4 (5.6)		
T2	4 (12.1)	12 (12.6)		5 (6.9)		
T3	13 (39.4)	55 (57.9)		37 (51.4)		
T4a	5 (15.2)	11 (11.6)		21 (29.2)		
T4b	1 (3.0)	0		1 (1.4)		
ypNstage			0.055		0.056	0.563
N0	22 (66.7)	37 (38.9)		26 (36.1)		
N1	5 (15.2)	21 (22.1)		14 (19.4)		
N2	2 (6.1)	15 (15.8)		12 (16.7)		
N3a	2 (6.1)	17 (17.9)		11 (15.3)		
N3b	2 (6.1)	5 (5.3)		9 (12.5)		
ypTNMstage			0.015		0.003	0.504
pCR	7 (21.2)	5 (5.3)		2 (2.8)		
I	6 (18.2)	17 (17.9)		9 (12.5)		
II	12 (36.4)	35 (36.8)		25 (34.7)		
III	8 (24.2)	38 (40.0)		36 (50.0)		
ypTstage			0.004		0.014	1
T0	8 (24.22)	6 (6.3)		4 (5.6)		
T1-T4b	25 (75.8)	89 (93.7)		68 (94.4)		
ypNstage			0.006		0.004	0.708
N0	22 (66.7)	37 (38.9)		26 (36.1)		
N1-N3b	11 (33.3)	58 (61.1)		46 (63.9)		
ypTstage			0.006		0.002	0.686
pCR	7 (21.2)	5 (5.3)		2 (2.8)		
I-III	26 (78.8)	90 (94.7)		70 (97.2)		
Radiological response			0.754		0.918	0.587
PR	30 (90.9)	88 (92.6)		65 (90.3)		
SD	3 (9.1)	7 (7.4)		7 (9.7)		

P^*: C-SAP vs. SAP $P^{\#}$: C-SAP vs. SOX $P^{\&}$: SAP vs. SOX.

DISCUSSION

The safety and efficacy of immunotherapy in combination with neoadjuvant chemotherapy have not been reported in gastric cancer with serosal invasion. This study is the first to investigate the safety and efficacy of camrelizumab in combination with nab-paclitaxel plus S-1 for the treatment of gastric cancer with serosal invasion. The results showed that camrelizumab in combination with neoadjuvant chemotherapy significantly increased the rate of tumor regression grade (TRG grade 1a/1b) and the rate of pCR in gastric cancer with serosal invasion and did not increase postoperative complications or neoadjuvant treatment-related adverse effects.

For patients receiving neoadjuvant chemotherapy, tumor regression grade is an important factor affecting the overall survival rate (11). The SOX regimen is a commonly used neoadjuvant chemotherapy regimen in the Asian population. A large-scale, randomized, controlled trial (RESOLVE) (5) from China showed that the SOX regimen has good application prospects as a neoadjuvant chemotherapy for advanced gastric cancer. The results of a phase II clinical trial (Dragon III) (15) revealed that the rate of tumor regression grade (TRG grade 1a/1b) in locally advanced gastric cancer (cT4/NxM0) treated with the SOX regimen was 32.4%. A nab-paclitaxel regimen and camrelizumab combined with a nab-paclitaxel regimen in the treatment of locally advanced gastric cancer have not been reported. In this study, the rate of tumor regression grade (TRG grade 1a/1b) in the C-SAP group (39.4%) was not significantly different from that in the SAP group (26.3%) but was significantly higher than that in the SOX group (18.1%). Therefore, camrelizumab combined with neoadjuvant chemotherapy could increase the tumor regression grade (TRG grade 1a/1b).

Pathological complete response (pCR) has been shown to correlate with overall survival (OS) outcomes (16). More than ten studies focusing on immunotherapy combined with

TABLE 3 | Clinicopathological results after surgery.

Baseline variable	C-SAP group (n = 33)	SAP group (n = 95)	P* value	SOX group (n = 72)	P# value	P& value
Type of gastrectomy			0.44		0.503	0.493
Partial	4 (12.4)	17 (17.9)		14 (19.4)		
Total	29 (87.9)	78 (82.1)		58 (80.6)		
Surgical approach			0.109		1.000	0.156
Laparoscopy	31 (93.9)	95 (100)		69 (95.8)		
Open	2 (6.1)	0		3 (4.2)		
Combination organ dissection						
Transverse colon				1 (1.4)		
Body and tail of pancreas				1 (1.4)		
Partial left liver		1 (1.1)				
Extent of resection			0.578		0.568	0.889
R0	32 (97.0)	94 (98.9)		68 (94.4)		
R1	1 (3.0)	1 (1.1)		4 (5.6)		
Nerve invasion			0.144		0.924	0.048
No	25 (75.8)	58 (61.7)		51 (71.8)		
Yes	8 (24.2)	36 (38.3)		20 (28.2)		
Vessel invasion			0.107		0.506	0.3
No	24 (72.7)	54 (56.8)		50 (69.4)		
Yes	9 (27.3)	41 (432.2)		22 (30.6)		
Harvested lymph nodes			0.569		0.039	< 0.001
Median	41.3 ± 19.3	43.1 ± 14.0		34.8 ± 10.5		
Positive lymph nodes			0.124		0.033	0.517
Median	2.2 ± 5.2	4.3 ± 6.9		4.9 ± 6.6		

P, C-SAP vs. SAP; P#, C-SAP vs. SOX; P&, SAP vs. SOX.*

neoadjuvant chemotherapy for the treatment of gastric cancer have been conducted, most of which evaluated pCR as the primary endpoint. The rate of pCR was 22.2% (2/9) when sintilimab was combined with the FLOT regimen for the neoadjuvant treatment of gastric or gastroesophageal junction (GEJ) adenocarcinoma (17). The rate of pCR was 23.1 (6/26) when sintilimab plus oxaliplatin/capecitabine (CapeOx) was used as a neoadjuvant therapy for patients with locally advanced, resectable gastric (G)/esophagogastric junction (GEJ) adenocarcinoma (18). The rate of pCR was 8% (2/26) when camrelizumab was combined with FOLFOX as a neoadjuvant therapy for resectable locally advanced gastric and gastroesophageal junction adenocarcinoma (19). In this study, the rate of pCR in the C-SAP group was 21.2% (7/33), similar to that observed in previous studies, and it was significantly higher than that in the SAP group (5.3%, 5/95) and the SOX group (2.8%, 2/72). Therefore, the results of this study showed that camrelizumab combined with neoadjuvant chemotherapy could improve the rate of pCR.

In the Dragon III study (15), univariate analyses showed that TRG was correlated with sex, nerve invasion, vascular invasion and postoperative pathological stage. However, the general clinical data of the three groups of patients in this study were not balanced. The number of patients with tumor size > 5 cm in the C-SAP group (51.5%) and the SAP group (48.4%) was higher than that in the SOX group (36.1%). The number of patients with poorly differentiated/undifferentiated tumors in the C-SAP group (69.7%) and the SAP group (63.2%) was higher than that in the SOX group (all P < 0.05). However, the multivariate analysis showed that tumor size > 5 cm was an independent risk factor, while the use of camrelizumab was an independent protective factor.

TABLE 4 | Postoperative complications.

Baseline variable	C-SAP group (n = 33)	SAP group (n = 95)	P* value	SOX group (n = 72)	P# value	P& value
Postoperative complications (yes)	8 (24.2)	21 (22.1)	0.801	23 (31.9)	0.422	0.153
Clavien Dindo grading						
Grade I-II	6 (18.2)	18 (18.9)	0.923	21 (29.2)	0.232	0.122
Pulmonary infection	5 (15.2)	14 (14.7)	0.954	16 (21.3)	0.455	0.263
Abdominal infection	1 (3.0)	4 (4.2)	1.000	5 (11.3)	0.761	0.715
Grade III	2 (6.1)	3 (3.2)	0.826	2 (2.8)	0.790	1.000
Bleeding	1 (3.0)	1 (1.1)	1.000	1 (1.3)	1.000	1.000
Obstruction	0	0	NA	1 (1.3)	> 0.99	> 0.99
Anastomotic leakage	1 (3.0)	2 (2.1)	1	0	> 0.99	> 0.99
Grade IV	0	0	NA	0	NA	NA
Grade V	0	0	NA	0	NA	NA

P, C-SAP vs. SAP; P#, C-SAP vs. SOX; P&, SAP vs. SOX.*
NA, Not applicable.

TABLE 5 | Neoadjuvant treatment adverse effects.

Baseline Variable	C-SAP group (n=33)	SAP group (n=95)	P* value	SOX group (n=72)	P# value	P& value
WBC decreased			0.461		0.103	0.005
Grade 0, 1, 2	28 (84.8)	75 (78.9)		68 (94.4)		
Grade 3, 4	5 (15.2)	20 (21.1)		4 (5.6)		
Neutrophil count decreased			0.899		0.048	0.023
Grade 0, 1, 2	25 (75.8)	73 (76.8)		65 (90.3)		
Grade 3, 4	8 (24.8)	22 (23.2)		7 (9.7)		
Anemia			1.000		0.422	0.122
Grade 0, 1, 2	32 (97.0)	93 (97.9)		67 (93.1)		
Grade 3, 4	1 (3.0)	2 (2.1)		5 (6.9)		
Platelet count decreased			0.458		0.918	0.444
Grade 0, 1, 2	31 (93.9)	92 (96.8)		68 (94.4)		
Grade 3, 4	2 (6.1)	3 (3.2)		4 (5.6)		
Serum AST/ALT increase			0.114		0.695	0.154
Normal	25 (75.8)	83 (87.4)		57 (79.2)		
Increase	8 (24.2)	12 (12.6)		15 (20.8)		
Febrile neutropenia			0.601		1.000	0.427
No	32 (97.0)	90 (94.7)		70 (97.2)		
Yes	1 (3.0)	5 (5.3)		2 (2.8)		

P, C-SAP vs SAP; P#, C-SAP vs SOX; P&, SAP vs SOX.*

The postoperative safety of patients after neoadjuvant therapy remains unclear. Li et al (20) reported that laparoscopic distal gastrectomy appeared to offer better postoperative safety than open distal gastrectomy for patients with locally advanced gastric cancer who received neoadjuvant chemotherapy. Li et al. reported that the LADG group was less likely to have Clavien-Dindo Grade II complications than the ODG group (6 [13%] vs. 20 [40%]; P = 0.004). Six patients (13%) in the LADG group and 2 patients (4%) in the ODG group had Grade III or higher complications (P = 0.25). Only 1 patient (2%) in the laparoscopic group had Grade IV complications, and no Grade V complications were reported. In our study, the overall complication rate of the whole group was 25.5%, the complication rate of Grade II events was 22.5%, and the complication rate of Grade III events was 3.5%. There were no Grade IV or V events reported, similar to the findings reported by Li et al. Additionally, the rate of Grade II complications was 18.2% in the C-SAP group, 18.9% in the SAP group and 29.2% in the SOX group. The rate of Grade III complications was 6.1% in the C-SAP group, 3.2% in the SAP group and 2.8% in the SOX group. Therefore, camrelizumab combined with neoadjuvant chemotherapy did not increase postoperative complications.

The WBC decreased (Grades 3, 4) by 41% in patients treated weekly with SAP in the ABSOLUTE trial (21). There was no significant difference in terms of WBC decreases (Grades 3 and 4) among the three groups in our study. There was no significant difference in terms of neutrophil count decreases (Grades 3 and 4) between the C-SAP and SAP groups. In this study, only one patient suffered febrile neutropenia (3%) in the C-SAP group, similar to that observed in the weekly SAP group (3%) in the ABSOLUTE trial, while there was no significant difference in terms of febrile neutropenia among the three groups. Therefore, camrelizumab combined with neoadjuvant chemotherapy is safe.

Although there was no significant difference in TRG between the C-SAP and SAP groups, we found that the rate of TRG (1a + 1b) in the C-SAP group was higher than that in the SAP group. Camrelizumab might be the reason for the difference between the two groups. Therefore, for gastric cancer patients with cT4a/T4b, the use of camrelizumab might predict a higher rate of TRG (1a + 1b). In addition, the rates of yPCR, yT0 and yN0 in the C-SAP group were significantly higher than those in the SAP group. The reason for the difference was the use of camrelizumab.

The optimal cycles of neoadjuvant therapy are controversial. A possible reason is that patients with obvious tumor regression receive 3-4 cycles of neoadjuvant therapy before surgery. Patients with no obvious tumor regression were asked to receive more cycles on the basis of 3-4 cycles. For patients in the SAP and SOX groups, the rate of TRG (1a + 1b) of patients receiving ≥ 4 cycles of neoadjuvant therapy was lower than that receiving ≤ 3 cycles of neoadjuvant therapy in the SAP and SOX groups. Therefore, the optimal neoadjuvant therapy cycle for these patients is 3 cycles. For patients in the C-SAP group, the rate of TRG (1a + 1b) of patients receiving ≥ 4 cycles of neoadjuvant therapy was higher than that of patients receiving ≤ 3 cycles of neoadjuvant therapy. Therefore, the optimal neoadjuvant therapy cycle for these patients is 4 cycles.

There are several limitations of this study. First, this study was a real-world, retrospective study with selection bias. Our center did not use the chemotherapy regimen of camrelizumab + SOX. Second, the number of patients in the C-SAP group was relatively small. PD-L1 expression was not measured, and differences in CPS could have affected the results of this study. Most of the patients in this study were followed up for less than 3 years.

In conclusion, camrelizumab in combination with nab-paclitaxel plus S-1 could significantly improve the rate of tumor regression grade (TRG 1a/1b) and the rate of pCR in gastric cancer with serosal invasion and did not increase postoperative complications or neoadjuvant treatment-related adverse effects. The results of this study must be further confirmed by prospective, randomized, controlled trials.

DATA AVAILABILITY STATEMENT

The raw data supporting the conclusions of this article will be made available by the authors, without undue reservation.

ETHICS STATEMENT

The studies involving human participants were reviewed and approved by the ethics committee of Fujian Union Hospital. The patients/participants provided their written informed consent to participate in this study.

AUTHOR CONTRIBUTIONS

Study concepts, statistical analysis, data analysis, and interpretation, manuscript preparation, and manuscript editing: J-LL, J-XL, JPL, C-MH. Study design, data acquisition, quality control of data, and algorithms: J-LL, J-XL, JPL, C-HZ, PL, J-WX, J-BW, JL, Q-YC, C-MH. All authors contributed to the article and approved the submitted version.

FUNDING

The second batch of special support funds for Fujian Province innovation and entrepreneurship talents (2016B013).

SUPPLEMENTARY MATERIAL

The Supplementary Material for this article can be found online at: https://www.frontiersin.org/articles/10.3389/fimmu.2021.783243/full#supplementary-material

Supplementary Figure 1 | Diagram.

Supplementary Figure 2 | There was no significant difference in terms of the total number of lymph nodes and positive lymph nodes between the C-SAP and SAP groups (all $P > 0.05$). However, the total number of lymph nodes in the C-SAP group was greater than that in the SOX group, and the number of positive lymph nodes in the C-SAP group was less than that in the SOX group (all $P < 0.05$).

Supplementary Figure 3 | Different neoadjuvant chemotherapy regimens and cycles on TRG.

REFERENCES

1. Siegel RL, Miller KD, Jemal A. Cancer Statistics, 2018. *CA Cancer J Clin* (2018) 68(1):7–30. doi: 10.3322/caac.21442
2. Ferlay J, Soerjomataram I, Dikshit R, Eser S, Mathers C, Rebelo M, et al. Cancer Incidence and Mortality Worldwide: Sources, Methods and Major Patterns in GLOBOCAN 2012. *Int J Cancer* (2015) 136(5):E359–86. doi: 10.1002/ijc.29210
3. Al-Batran SE, Hofheinz RD, Pauligk C, Kopp HG, Haag GM, Luley KB, et al. Histopathological Regression After Neoadjuvant Docetaxel, Oxaliplatin, Fluorouracil, and Leucovorin Versus Epirubicin, Cisplatin, and Fluorouracil or Capecitabine in Patients With Resectable Gastric or Gastro-Oesophageal Junction Adenocarcinoma (FLOT4-AIO): Results From the Phase 2 Part of a Multicentre, Open-Label, Randomised Phase 2/3 Trial. *Lancet Oncol* (2016) 17(12):1697–708. doi: 10.1016/S1470-2045(16)30531-9
4. Al-Batran SE, Homann N, Pauligk C, Goetze TO, Meiler J, Kasper S, et al. Perioperative Chemotherapy With Fluorouracil Plus Leucovorin, Oxaliplatin, and Docetaxel Versus Fluorouracil or Capecitabine Plus Cisplatin and Epirubicin for Locally Advanced, Resectable Gastric or Gastro-Oesophageal Junction Adenocarcinoma (FLOT4): A Randomised, Phase 2/3 Trial. *Lancet* (2019) 393(10184):1948–57. doi: 10.1016/S0140-6736(18)32557-1
5. Ji J, Shen L, Li Z, Zhang X, Liang H, Xue Y, et al. Perioperative Chemotherapy of Oxaliplatin Combined With S-1 (SOX) Versus Postoperative Chemotherapy of SOX or Oxaliplatin With Capecitabine (XELOX) in Locally Advanced Gastric Adenocarcinoma With D2 Gastrectomy: A Randomized Phase III Trial (RESOLVE Trial). *Ann Oncol* (2019) 30(v877). doi: 10.1093/annonc/mdz394.033
6. Fuchs CS, Doi T, Jang RW, Muro K, Satoh T, Machado M, et al. Safety and Efficacy of Pembrolizumab Monotherapy in Patients With Previously Treated Advanced Gastric and Gastroesophageal Junction Cancer: Phase 2 Clinical KEYNOTE-059 Trial. *JAMA Oncol* (2018) 4(5):e180013. doi: 10.1001/jamaoncol.2018.0013
7. Kang YK, Boku N, Satoh T, Ryu MH, Chao Y, Kato K, et al. Nivolumab in Patients With Advanced Gastric or Gastro-Oesophageal Junction Cancer Refractory to, or Intolerant of, at Least Two Previous Chemotherapy Regimens (ONO-4538-12, ATTRACTION-2): A Randomised, Double-Blind, Placebo-Controlled, Phase 3 Trial. *Lancet* (2017) 390(10111):2461–71. doi: 10.1016/S0140-6736(17)31827-5
8. Japanese Gastric Cancer A. Japanese Gastric Cancer Treatment Guidelines 2014 (Ver. 4). *Gastric Cancer* (2017) 20(1):1–19. doi: 10.1007/s10120-016-0622-4
9. Doescher J, Veit JA, Hoffmann TK. The 8th Edition of the AJCC Cancer Staging Manual. *HNO* (2017) 65(12):956–61. doi: 10.1007/s00106-017-0391-3
10. Becker K, Mueller JD, Schulmacher C, Ott K, Fink U, Busch R, et al. Histomorphology and Grading of Regression in Gastric Carcinoma Treated With Neoadjuvant Chemotherapy. *Cancer* (2003) 98(7):1521–30. doi: 10.1002/cncr.11660
11. Becker K, Langer R, Reim D, Novotny A, Meyer zum Buschenfelde C, Engel J, et al. Significance of Histopathological Tumor Regression After Neoadjuvant Chemotherapy in Gastric Adenocarcinomas: A Summary of 480 Cases. *Ann Surg* (2011) 253(5):934–9. doi: 10.1097/SLA.0b013e318216f449
12. Eisenhauer EA, Therasse P, Bogaerts J, Schwartz LH, Sargent D, Ford R, et al. New Response Evaluation Criteria in Solid Tumours: Revised RECIST Guideline (Version 1.1). *Eur J Cancer* (2009) 45(2):228–47. doi: 10.1016/j.ejca.2008.10.026
13. Dindo D, Demartines N, Clavien PA. Classification of Surgical Complications: A New Proposal With Evaluation in a Cohort of 6336 Patients and Results of a Survey. *Ann Surg* (2004) 240(2):205–13. doi: 10.1097/01.sla.0000133083.54934.ae
14. Clavien PA, Sanabria JR, Strasberg SM. Proposed Classification of Complications of Surgery With Examples of Utility in Cholecystectomy. *Surgery* (1992) 111(5):518–26.
15. Sah BK, Zhang B, Zhang H, Li J, Yuan F, Ma T, et al. Neoadjuvant FLOT Versus SOX Phase II Randomized Clinical Trial for Patients With Locally Advanced Gastric Cancer. *Nat Commun* (2020) 11(1):6093. doi: 10.1038/s41467-020-19965-6
16. Li Z, Shan F, Wang Y, Zhang Y, Zhang L, Li S, et al. Correlation of Pathological Complete Response With Survival After Neoadjuvant Chemotherapy in Gastric or Gastroesophageal Junction Cancer Treated With Radical Surgery: A Meta-Analysis. *PloS One* (2018) 13(1):e0189294. doi: 10.1371/journal.pone.0189294
17. Li N, Li Z, Fu Q, Zhang B, Luo S. 160p Phase II Study of Sintilimab Combined With FLOT Regimen for Neoadjuvant Treatment of Gastric or Gastroesophageal Junction (GEJ) Adenocarcinoma. *Ann Oncol* (2020) 31:S1302. doi: 10.1016/j.annonc.2020.10.181
18. Jiang H, Yu X, Kong M, Ma Z, Teng L. Sintilimab Plus Oxaliplatin/Capecitabine (CapeOx) as Neoadjuvant Therapy in Patients With Locally Advanced, Resectable Gastric (G)/esophagogastric Junction (GEJ) Adenocarcinoma. *J Clin Oncol* (2021) 39(3_suppl):211–1. doi: 10.1200/JCO.2021.39.3_suppl.211
19. Liu Y, Han G, Li H, Zhao y, Zhuang J, Li D, et al. Camrelizumab Combined With FOLFOX as Neoadjuvant Therapy for Resectable Locally Advanced Gastric and Gastroesophageal Junction Adenocarcinoma. *J Clin Oncol* (2020) 38(15_suppl):4536–6. doi: 10.1200/JCO.2020.38.15_suppl.4536

20. Li Z, Shan F, Ying X, Zhang Y, E JY, Wang Y, et al. Assessment of Laparoscopic Distal Gastrectomy After Neoadjuvant Chemotherapy for Locally Advanced Gastric Cancer: A Randomized Clinical Trial. *JAMA Surg* (2019) 154(12):1093–101. doi: 10.1001/jamasurg.2019.3473
21. Shitara K, Takashima A, Fujitani K, Koeda K, Hara H, Nakayama N, et al. Nab-Paclitaxel Versus Solvent-Based Paclitaxel in Patients With Previously Treated Advanced Gastric Cancer (ABSOLUTE): An Open-Label, Randomised, Non-Inferiority, Phase 3 Trial. *Lancet Gastroenterol Hepatol* (2017) 2(4):277–87. doi: 10.1016/S2468-1253(16)30219-9

Conflict of Interest: The authors declare that the research was conducted in the absence of any commercial or financial relationships that could be construed as a potential conflict of interest.

frontiers in Immunology

ORIGINAL RESEARCH
published: 24 January 2022
doi: 10.3389/fimmu.2021.758040

CX3CR1 Acts as a Protective Biomarker in the Tumor Microenvironment of Colorectal Cancer

Yuanyi Yue[1], *Qiang Zhang*[2] *and Zhengrong Sun*[3*]

[1] Department of Gastroenterology Medicine, Shengjing Hospital of China Medical University, Shenyang, China, [2] Department of Pulmonary and Critical Care Medicine, Shengjing Hospital of China Medical University, Shenyang, China, [3] BioBank, Shengjing Hospital of China Medical University, Shenyang, China

OPEN ACCESS

Edited by:
Bo Qin,
Mayo Clinic, United States

Reviewed by:
Jinhui Liu,
Nanjing Medical University, China
Lixuan Wei,
Mayo Clinic, United States

***Correspondence:**
Zhengrong Sun
sunzr@sj-hospital.org

Specialty section:
This article was submitted to Cancer Immunity and Immunotherapy, a section of the journal Frontiers in Immunology

Received: *13 August 2021*
Accepted: *28 December 2021*
Published: *24 January 2022*

Citation:
Yue Y, Zhang Q and Sun Z (2022) CX3CR1 Acts as a Protective Biomarker in the Tumor Microenvironment of Colorectal Cancer. Front. Immunol. 12:758040. doi: 10.3389/fimmu.2021.758040

The tumor microenvironment (TME) plays an important role in the pathogenesis of many cancers. We aimed to screen the TME-related hub genes of colorectal adenoma (CRAD) and identify possible prognostic biomarkers. The gene expression profiles and clinical data of 464 CRAD patients in The Cancer Genome Atlas (TCGA) database were downloaded. The Estimation of STromal and Immune cells in MAlignant Tumours using Expression data (ESTIMATE) algorithm was performed to calculate the ImmuneScore, StromalScore, and EstimateScore. Thereafter, differentially expressed genes (DEGs) were screened. Gene Ontology (GO), Kyoto Encyclopedia of Genes and Genomes (KEGG) pathway, and protein–protein interaction (PPI) analysis were performed to explore the roles of DEGs. Furthermore, univariate and multivariate Cox analyses were accomplished to identify independent prognostic factors of CRAD. CX3CR1 was selected as a hub gene, and the expression was confirmed in colorectal cancer (CRC) patients and cell lines. The correlations between CX3CR1 and tumor-infiltrating immune cells were estimated by Tumor IMmune Estimation Resource database (TIMER) and CIBERSORT analysis. Besides, we investigated the effects of coculture with THP-1-derived macrophages with HCT8 cells with low CX3CR1 expression on immune marker expression, cell viability, and migration. There were significant differences in the ImmuneScore and EstimateScore among different stages. Patients with low scores presented significantly lower lifetimes than those in the high-score group. Moreover, we recognized 1,578 intersection genes in ImmuneScore and StromalScore, and these genes were mainly enriched in numerous immune-related biological processes. CX3CR1 was found to be associated with immune cell infiltration levels, immune marker expression, and macrophage polarization. Simultaneous silencing of CX3CR1 and coculture with THP-1 cells further regulated macrophage polarization and promoted the cell proliferation and migration of CRC cells. CX3CR1 was decreased in CRAD tissues and cell lines and was related to T and N stages,

tumor differentiation, and prognosis. Our results suggest that CX3CR1 contributes to the recruitment and regulation of immune-infiltrating cells and macrophage polarization in CRC and TAM-induced CRC progression. CX3CR1 may act as a prognostic biomarker in CRC.

Keywords: colorectal cancer, tumor microenvironment, ESTIMATE algorithm, stromal, immune, prognosis, CX3CR1

INTRODUCTION

Colorectal cancer (CRC) is one of the most common malignant gastrointestinal cancers (1) and ranks the fifth leading cause of cancer-related death in China (2). CRC has been well-acknowledged as a heterogeneous disease, which presents various differences in clinical features, molecular genetic alterations, and prognosis (3). Some factors, such as age, diet, environment, unhealthy lifestyle, obesity, inflammatory bowel disease (IBD), gene mutation, gut microbiota, and family history of colon cancers, have been reported to be at high risk of developing the tumor (4–7). Among the influencing factors, molecular genetic changes have been considered as one of the important key characteristics contributing to the progression of cancers (8, 9).

Growing evidence suggests that the tumor microenvironment (TME) plays a critical role in the progression and prognosis of malignant tumors (10, 11), including CRC (12, 13). The TME is the location of tumor appearance, comprising many cells, mediators, and molecules (14, 15). Among the cells, infiltrating stromal and immune cells are the two foremost members of the TME, which significantly contributes to cancer biology (16, 17). It has been demonstrated that the early stage of CRC is characterized by a high content of stromal cells and the infiltration of immune cells, with unfavorable and favorable prognosis of refeeding syndrome (RFS), respectively (18). In addition, the immune and stromal stratification of CRC is responsible for molecular subtypes and tailored immunotherapy (19). However, little information is available regarding the TME-related genes that could identify potential prognostic biomarkers for CRC. The Estimation of STromal and Immune cells in MAlignant Tumours using Expression data (ESTIMATE) algorithm is an accurate method to calculate the specific gene data expression signature to evaluate the infiltration of stromal and immune cells and tumor purity. It is a broad, novel, and reliable algorithm that has been administered in data mining of several cancers, and this method has been proven effective in several large independent databases (20–24). ESTIMATE algorithm includes Immunescore, StromalScore, and ESTIMATEScore. Immunescore is the percentage of Immune cells, which is a scoring system based on the quantitative analysis of cytotoxic T cells and memory T cells in the core of the tumor (CT) and the invasive margin (IM) of the tumor (25). StromalScore is the percentage of stromal cells, and EstimateScore is the sum of the ImmuneScore and StromalScore (26). A higher ImmuneScore or StromalScore is indicative of the presence of a significant immune or stromal component in the TME, and ESTIMATEScore is the sum of immune and stromal score. In other words, high tumor purity is related to the unfavorable prognosis of patients. Although the ESTIMATE algorithm is based on cancer tissue data, it is effective in evaluating cellular data as well (27). Several studies have confirmed that the scores are associated with the clinicopathological characteristics and chemotherapeutic drug resistance in various types of tumors, and that ESTIMATE could be used as an indicator for patient prognosis assessment (27–29).

Therefore, in the current study, we aimed to evaluate the ImmuneScore and StromalScore in the TME based on CRC data acquired from The Cancer Genome Atlas (TCGA) database by single-sample gene set enrichment analysis (ssGSEA). Moreover, we further explored the stromal-immune score-based gene signature related to the prognosis of CRC. Our results might shed insight into the improvement of novel prognostic biomarkers and treatments, specifically immunotherapies, for patients with CRC.

MATERIALS AND METHODS

The Cancer Genome Atlas Data Download and Processing

In this analysis, we downloaded the expression datasets of fragments per kilobase of exon per million mapped fragments (FPKM) from TCGA website (https://portal.gdc.cancer.gov/). The samples were screened according to the clinical information. The principles of sample selection were listed as follows: 1) Primary tumor tissues were selected; 2) Complete information for tumor-node-metastasis (TNM) staging and stage were selected, and the samples without relevant follow-up data and incomplete information were removed; 3) The samples without clinical survival information were removed; 4) Five-year survival data could be obtained from the patients whose survival time is more than 1 month and less than 5 years. According to the above inclusion and exclusion criteria, a total of 464 colorectal adenoma (CRAD) samples were included for subsequent analysis.

Calculation of ImmuneScore, StromalScore, and EstimateScore

After selecting the samples, we extracted the expression matrix from the samples and then calculated the immune purity of the expression matrix using the "estimate" R package. We performed ssGSEA method for each sample, and the immune infiltration (ImmuneScore), overall stromal content (StromalScore), and the combined (EstimateScore) were calculated by ESTIMATE algorithms (21).

Overall Survival Analysis

Kaplan–Meier plots were performed to investigate the prognosis of patients with CRAD. The individuals were assigned to the high-score group (the values of >optimal cutoff) and low-score group (the values of <optimal cutoff) based on the optimal cutoff values of the ImmuneScore and StromalScore. Maximally selected rank statistics (30) were performed to ascertain the optimal cutoff. The "survminer" in R package was performed to detect the survival analyses.

Selection of Differentially Expressed Genes

The patients were divided into high-score and low-score groups based on the optimal cutoff mentioned above. The selection of DEGs was performed according to the published method (31) by using "edgeR" R package with *P*-value <0.01 and |logFC| >1. Volcano plot was further used to visualize the DEGs. Moreover, Venn diagrams were performed to detect the upregulated or downregulated intersection genes of DEGs in the immune and stromal groups using a website tool (http://bioinformatics.psb.ugent.be/webtools/Venn/).

Enrichment Analysis of Intersection Genes

Gene Ontology (GO) and Kyoto Encyclopedia of Genes and Genomes (KEGG) enrichment analyses were performed by "ClusterProfiler" R package and ClueGO plug-in in Cytoscape software (3.6.1 version) (32).

Construction of Protein–Protein Interaction Network

The PPI network was constructed by STRING (http://string-db.org) (33) with an interaction combined score >0.7. The interaction nodes of the protein were visualized by using Cytoscape (34), and enrichment analysis of each cluster was analyzed with ClueGo software (35). In addition, Molecular Complex Detection (MCODE) was used to investigate the key subnetworks in PPI networks. The parameters of clustering and scoring were selected as follows: MCODE score ≥5, degree cutoff = 2, node score cutoff = 0.2, max depth = 100, and k-score = 2. Genes with the highest MCODE score in the PPI network were selected as the hub genes.

Univariate and Multivariate Cox Analyses

Univariate and multivariate Cox analyses were performed to assess the independent prognostic factors associated with patients' survival. Hub gene expression, T stage, N stage, M stage, and Stage were selected as covariates. Hazard ratios (HRs) were used to recognize protective (HR <1) or risky genes (HR >1), and the most relevant gene for the prognosis of CRAD was obtained by regression analysis.

Tumor Microenvironment Analysis

The abundance of immune infiltrates was estimated by Tumor IMmune Estimation Resource database (TIMER; cistrome.shinyapps.io/timer) (36) and CIBERSORT analysis. The correlation between CX3CR1 expression and the abundance of infiltrating immune cells, including tumor purity, B cells, $CD8^+$ T cells, $CD4^+$ T cells, macrophages, neutrophils, and dendritic cells (DCs), was analyzed. Furthermore, the interconnections between CX3CR1 expression and molecular biomarkers of tumor-infiltrating immune cells were investigated by correlation modules. For further investigation, CIBERSORT was used to estimate the abundance of different immune cell types in the TME. It is a deconvolution algorithm for calculating the abundance of immune cell infiltration for each sample, which is based on a gene set of 22 sets of immune cell-associated genes (37) (https://cibersort.stanford.edu/). RNA sequencing (RNA-seq) data of CRC samples were divided into low CX3CR1 expression group and high CX3CR1 expression group according to the median level of CX3CR1. Data were imported into CIBERSORT and LM22 signature matrix.

Subjects

A total of 60 (38 males and 22 females, mean age: 58 years old) CRC tumors and matched adjacent non-tumor tissues were acquired from subjects at Shengjing Hospital of China Medical University between 2014 and 2015. The collected samples were immediately frozen after the operation and stored at -80°C until use. Patients' information, including gender, ages, tumor location, size, TNM classification, and differentiation, was collected. All individuals did not receive any preoperative treatments. Our study was permitted by the Medical Ethics Committee of Shengjing Hospital of China Medical University (No. 2014PS13), and informed consent was acquired from each individual.

Cell Lines

Human normal intestinal mucous cell line CCC-HIE-2, human CRC cell lines (CaCO-2, HCT8, HCT-116, and LoVo), and human THP-1 monocytes were acquired from the American Type Culture Collection (ATCC, Manassas, VA, USA). These cell lines were routinely cultured in Dulbecco's modified Eagle's medium (DMEM; Gibco, Grand Island, NY) supplemented with 10% fetal bovine serum (FBS; Gibco) and 2 mM L-glutamine (Gibco), 100 U/ml penicillin (Invitrogen, Carlsbad, CA, USA), and 100 μg/ml streptomycin (Invitrogen). They were maintained at 37°C in a 5% CO_2 atmosphere.

Coculture of THP-1 With HCT8

The CRC cells HCT8 and THP-1-derived macrophages were cocultured with a non-contact cell culture insert (0.4 μM; Corning, NY, USA). The THP-1 cells were seeded into the upper chamber at a density of 5×10^5 cells/ml, and they were induced to differentiate into M2 macrophages by administration of 350 nm phorbol-12-myristate-13-acetate (PMA; Sigma-Aldrich, St. Louis, MO, USA) for 6 h and interleukin (IL)-4 for 18 h. The ratio of M2 cells to HCT8 cells was 1:4. After washing with phosphate-buffered saline (PBS), the cells were incubated for another 24 h to remove the effect of PMA. The HCT8 cells (2.5×10^5 cells/ml) were placed in the lower chamber for 24 h to allow adherence. Thereafter, the THP-1-derived macrophages

were directly put on the top of plates containing the HCT8 cells and were then incubated for 24 h in serum-free RPMI 1640.

Transient Transfection

Small interfering RNA for CX3CR1 (si-CX3CR1, 150 nM) was transfected into HCT8 to knockdown CX3CR1. si-CX3CR1 was designed and produced by Genechem (Shanghai, China). The sequence of si-CX3CR1 was as follows: 5′-CTTGTCTGATCTGC TGTTT-3′. Cell transfection was performed by using Lipofectamine® 2000 (Invitrogen) at indicated times.

Cell Counting Kit-8

After transfection with si-NC or si-CX3XR1 in the absence or presence of coculture, the HCT8 cells were seeded into 96-well plates (5×10^3 cells/well). Thereafter, the cell viability was assessed using Cell Counting Kit-8 (CCK-8; Japan Dojindo Molecular Technologies) at 24, 48, 72, and 96 h according to the manufacturer's instructions.

Migration Assay

After transfection with si-NC or si-CX3XR1 in the absence or presence of coculture, cell migration assay was conducted using 24-well Transwell plates (8.0 μm; Corning, NY, USA). The macrophages or cancer cells (5×10^4, HCT8-si-NC, HCT-8-si-CX3CR1) were planted into the upper chambers, and 600 μl RPMI 1640 containing 10% FBS were placed into the lower chambers. Thereafter, the Transwell plates were incubated in a 37°C, 5% CO_2 incubator for 48 h and then fixed in 4% formaldehyde for half an hour and stained with 0.01% crystal violet. Non-migrating cells were carefully removed with a cotton swab, and the cells that had migrated to the lower chambers were counted under the microscope.

Quantitative Real-Time Reverse Transcription PCR

Total RNA was extracted from the samples, and cells using TRIzol reagent (Invitrogen). Reverse-transcription reactions were performed using an M-MLV Reverse Transcriptase kit (Roche Molecular Biochemicals) according to the manufacturer's protocol. Real-time PCR was carried out using a standard SYBR Green PCR kit (Qiagen, Hilden, Germany). Glyceraldehyde-3-phosphate dehydrogenase (GAPDH) was used as an internal reference. The sequences of different primers were summarized in **Table 1**. Each sample was analyzed in triplicate, and relative quantitation of gene expression levels was determined using $2^{-\triangle\triangle CT}$ method.

Western Blot

Proteins were extracted from the samples and cells using radioimmunoprecipitation assay (RIPA) lysis buffer (Beyotime, Shanghai, China). Thereafter, the acquired proteins were separated using sodium dodecyl sulfate (SDS)-polyacrylamide gel electrophoresis (PAGE) and transferred onto polyvinylidene fluoride (PVDF) membranes (Beyotime). The membranes were then incubated with anti-CX3CR1 primary antibody (SAB2900202; Sigma-Aldrich, St. Louis, MO, USA) at 4°C overnight and with horseradish peroxidase-conjugated secondary antibody (A2691, Sigma-Aldrich) for 1 h at room temperature. Enhanced chemiluminescence (ECL) plus Kit (GE Healthcare, Little Chalfont, Buckinghamshire, UK) was used to analyze the chemiluminescence intensity of each membrane and then quantitated by ImageJ software (NIH, Bethesda, MD, USA). GAPDH was used as a housekeeping gene.

Statistical Analyses

All analyses were conducted with R version 3.5.3 (http://www.R-project.org), along with its appropriate packages. Survival analysis was performed using Kaplan–Meier method with the log-rank test. Univariate and multivariate analysis Cox proportional hazards model was used to assess the potential independent factors with the prognosis. For the *in vitro* experiments, the acquired data are presented as the mean ± standard deviation (SD). The differences were evaluated with Student's *t*-tests (for 2 groups) or one-way analysis of variance (ANOVA) for 3 and/or more than 3 groups

TABLE 1 | The sequences of different primers.

Gene		Sequence (5′ -> 3′)
CX3CR1	Forward	ACTTTGAGTACGATGATTTGGCT
	Reverse	GGTAAATGTCGGTGACACTCTT
NOS2	Forward	TTCAGTATCACAACCTCAGCAAG
	Reverse	TGGACCTGCAAGTTAAAATCCC
IRF5	Forward	GGGCTTCAATGGGTCAACG
	Reverse	GCCTTCGGTGTATTTCCCTG
PTGS2	Forward	CTGGCGCTCAGCCATACAG
	Reverse	CGCACTTATACTGGTCAAATCCC
CD163	Forward	TTTGTCAACTTGAGTCCCTTCAC
	Reverse	TCCCGCTACACTTGTTTTCAC
VSIG4	Forward	GGGGCACCTAACAGTGGAC
	Reverse	GTCTGAGCCACGTTGTACCAG
MS4A4A	Forward	ACCATGCAAGGAATGGAACAG
	Reverse	TTCCCATGCTAAGGCTCATCA
GAPDH	Forward	ACACCCACTCCTCCACCTTT
	Reverse	TTACTCCTTGGAGGCCATGT

CX3CR1, C-X3-C motif chemokine receptor 1; NOS2, nitric oxide synthase 2; IRF5, interferon regulatory factor 5; PTGS2, prostaglandin-endoperoxide synthase 2; VSIG4, V-set and immunoglobulin domain containing 4; membrane-spanning 4-domains, subfamily A, member 4A; GAPDH, glyceraldehyde-3-phosphate dehydrogenase.

using SPSS Statistics 19.0 software (IBM, Armonk, NY, USA). For the CIBERSORT algorithm, it was performed with 1,000 simulations, and the results were filtered according to $P < 0.05$. After obtaining the abundance of immune cell infiltration in each sample, correlations between these immune cells and CX3CR1 expression levels were calculated based on the Spearman coefficient, and differences in immune cell infiltration between high and low CX3CR1 expression groups were calculated using the Wilcoxon log-rank test. $P < 0.05$ was regarded as statistically significant.

RESULTS

ImmuneScore and ESTIMATEScore Correlate With Clinical Data and Prognosis in Patients with Colorectal Adenoma

A total of 464 samples were used to analyze in the current study according to TCGA data. ESTIMATE algorithm was used to calculate the StromalScore, ImmuneScore, and ESTIMATEScore. According to the clinical data extracted from TCGA (**Supplementary Table S1**), we observed that there was no significant difference among different stages in the StromalScore ($P = 0.053$; **Figure 1A**). However, there were statistical differences among different stages in the ImmuneScore ($P = 0.00066$; **Figure 1B**) and ESTIMATEScore ($P = 0.023$; **Figure 1C**). The StromalScore ranged from -2,286.02 to 1,695.44, ImmuneScore ranged from -741.19 to 2,489.81, and ESTIMATEScore ranged from -3,027.21 to 4,185.25. The scores were summarized in **Supplementary Table S2**. The distribution of StromalScore, ImmuneScore, and ESTIMATEScore was shown in **Figures 1D–F**, and the cut points respectively were -1,431.83, -305.47, and -1,013.54. To further explore the potential correlation between clinical overall survival (OS) of patients with CRAD and their three scores, we assigned the 464 patients into the high-score group (the values >optimal cutoff) and the low-score group (the values <optimal cutoff). Thereafter, we assessed the potential correlation with Kaplan–Meier survival analysis. The results showed that patients with high scores presented significantly longer lifetimes than those in the low-score group for StromalScore ($P = 0.032$; **Figure 1G**), ImmuneScore ($P = 0.00055$; **Figure 1H**), and ESTIMATEScore ($P = 0.0025$; **Figure 1I**). These results implied that both ImmuneScore and ESTIMATEScore correlated with clinical data and prognosis in patients with CRAD, while StromalScore only correlated with the prognosis but not the clinical data.

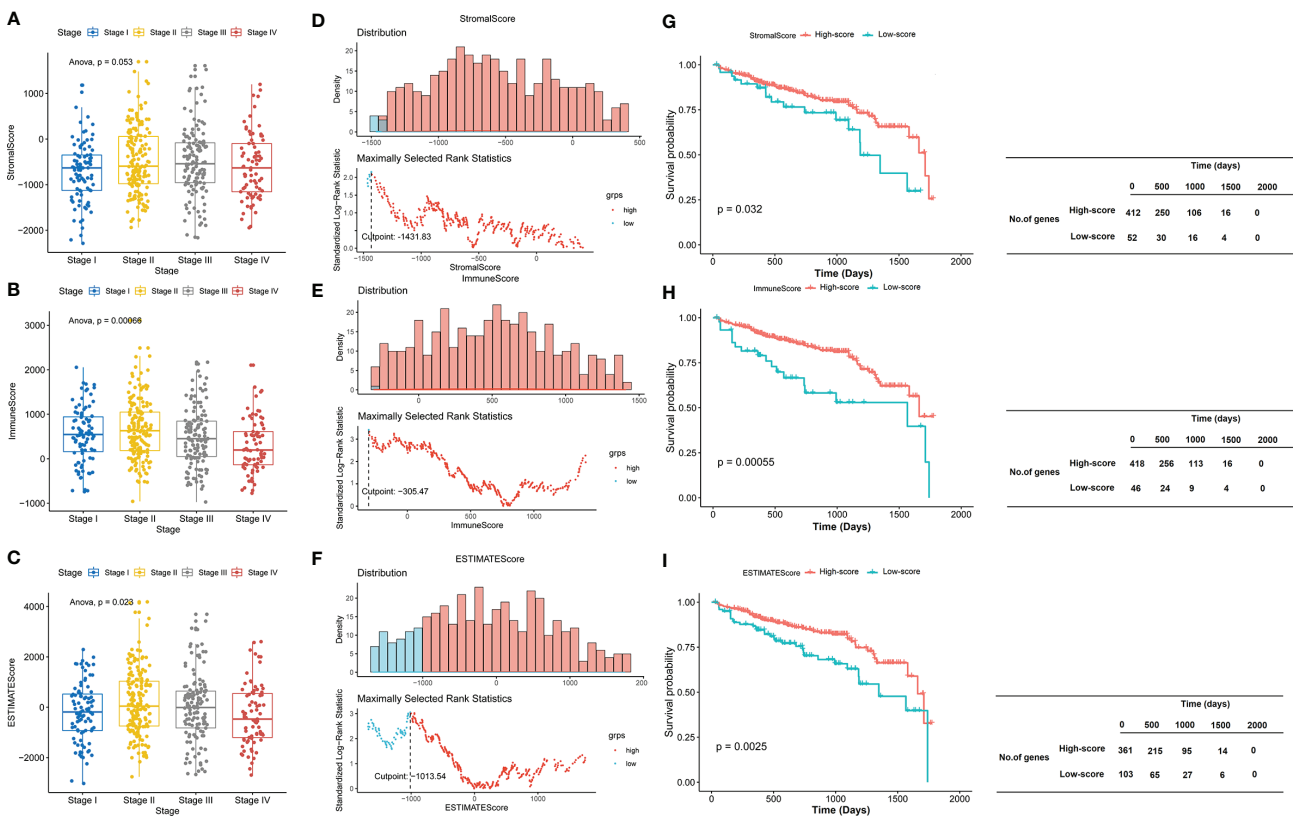

FIGURE 1 | ImmuneScore and ESTIMATEScore correlate with clinical data and prognosis in patients with CRAD. **(A–C)** The boxplot of StromalScore, ImmuneScore, and ESTIMATEScore of CRAD patients in different stages. **(D–F)** The distribution of StromalScore, ImmuneScore, and ESTIMATEScore. **(G–I)** Kaplan–Meier survival analysis of StromalScore, ImmuneScore, and ESTIMATEScore. CRAD, colorectal adenoma.

Identification of Differentially Expressed Genes Based on ImmuneScore and StromalScore

The expression profile data of 464 patients with CRAD were further examined to detect DEGs by using "edgeR" R package. A total of 2,773 and 2,705 DEGs were respectively screened in CRAD sample cells based on ImmuneScore and StromalScore. Volcano plots were performed to visualize the distribution of DEGs of ImmuneScore and StromalScore. Upregulated or downregulated genes were characterized respectively with red or green dots (**Figures 2A, B**). Venn diagrams were accomplished to detect the upregulated or downregulated intersection genes of DEGs. Among them, we recognized 2,426 upregulated genes and 347 downregulated genes in StromalScore and 1,838 upregulated genes and 867 downregulated genes in ImmuneScore. A total of 1,353 upregulated intersection genes and 225 downregulated intersection genes were selected for further analysis (**Figures 2C, D**). Upregulated and downregulated DEGs were respectively listed in **Supplementary Tables S3**, **S4**.

Gene Ontology and Kyoto Encyclopedia of Genes and Genomes Pathway Enrichment Analyses

We further explored the GO and KEGG pathway enrichment analysis of 1,578 intersection genes by two different methods: the "ClusterProfiler" R package and the ClueGO plug-in in Cytoscape software. All the GO terms and KEGG pathways were recorded in **Supplementary Tables S5**, **S6**, respectively. Top 20 GO terms and Top 10 KEGG pathways were presented in the current study using the "ClusterProfiler" R package. As shown in **Figure 3A**, we found that the DEGs were mainly enriched in the regulation of lymphocyte activation, T-cell activation, leukocyte migration, positive regulation of cell activation and leukocyte cell–cell adhesion, and so on. Moreover, the KEGG enrichment analysis of DEGs was primarily enriched in cytokine–cytokine receptor interaction, viral protein interaction with cytokine and cytokine receptor, *Staphylococcus aureus* infection, hematopoietic cell lineage, rheumatoid arthritis, and chemokine signaling pathway, etc.

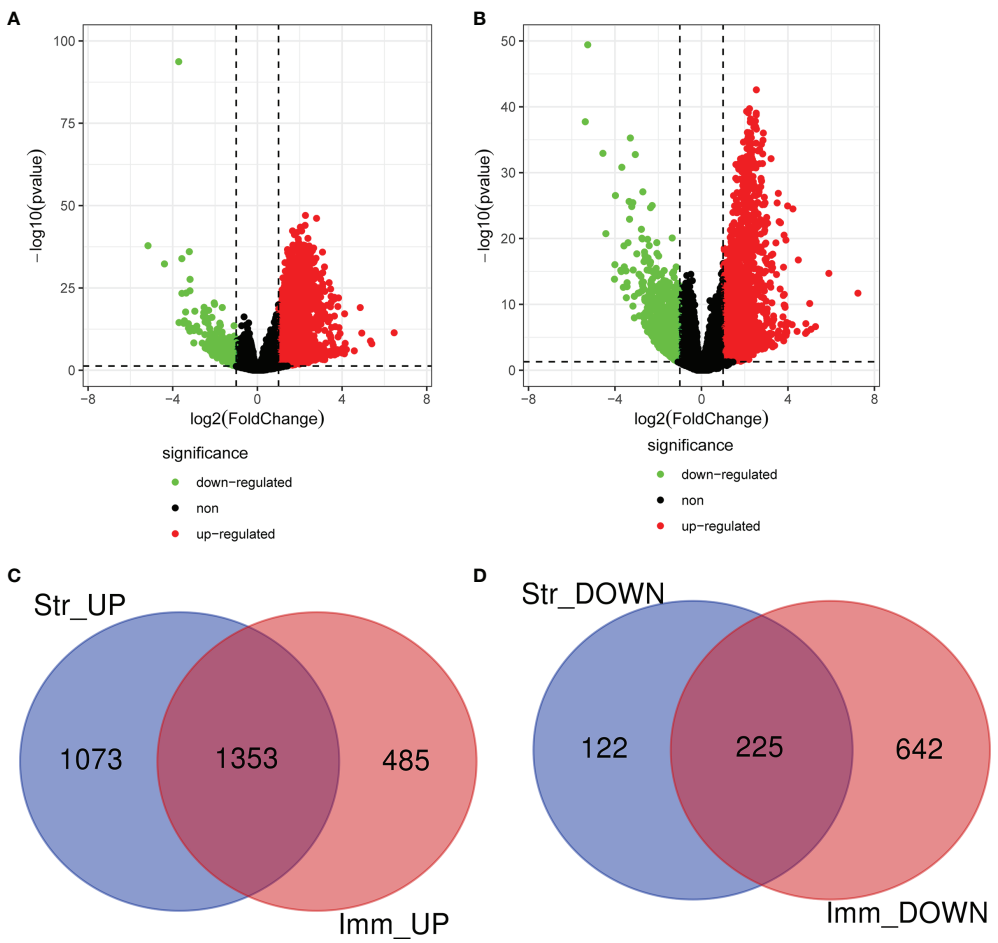

FIGURE 2 | Identification of DEGs based on ImmuneScore and StromalScore. **(A)** The distribution of DEGs of ImmuneScore using volcano plots. **(B)** The distribution of DEGs of StromalScore using volcano plots. **(C)** Upregulated intersection genes of DEGs detected by Venn diagrams. **(D)** Downregulated intersection genes of DEGs detected by Venn diagrams. DEGs, differentially expressed genes.

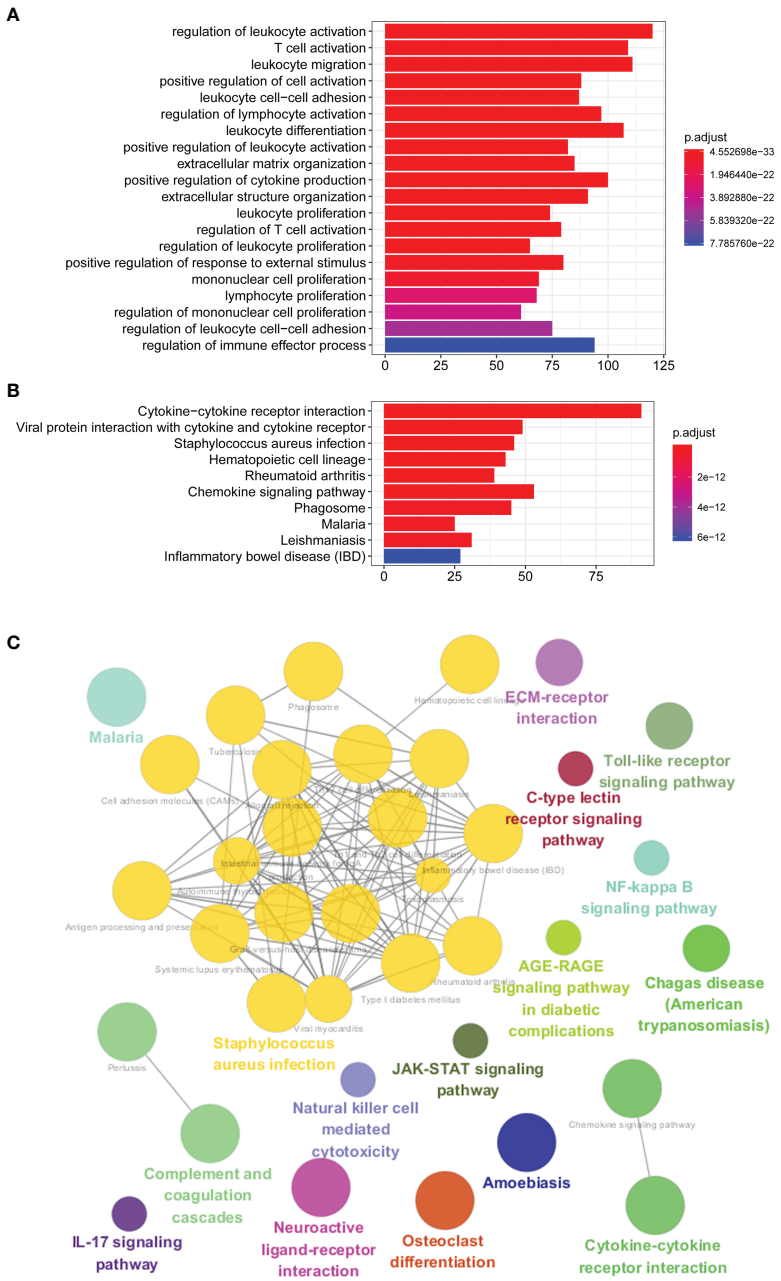

FIGURE 3 | GO and KEGG pathway enrichment analyses. **(A)** Top 20 GO terms of the intersection DEGs using "ClusterProfiler" R package. **(B)** Top 10 KEGG pathways of the intersection DEGs using "ClusterProfiler" R package. **(C)** GO terms and KEGG pathway using ClueGO method. GO, Gene Ontology; KEGG, Kyoto Encyclopedia of Genes and Genomes; DEGs, differentially expressed genes.

(**Figure 3B**). The results of GO terms and KEGG pathway using ClueGO method were shown in **Figure 3C**. Interestingly, we found that the results of immune-related genes in GO term biological process (BP) and KEGG pathways were achieved only from the upregulated DEGs. The dotplot for the enriched GO and KEGG analysis of upregulated and downregulated DEGs was demonstrated in **Figure 4**. Therefore, we performed further analyses on upregulated DEGs only.

Protein–Protein Interaction Construction and Module Analysis of Upregulated Differentially Expressed Genes

PPI network of upregulated 1,353 DEGs for CRAD was constructed with STRING tool and Cytoscape software (**Figure 5A**). There were 836 nodes in the network with the interaction combined score >0.7 and 6,662 pairs of interaction relationships (**Supplementary Table S7**). The circle size in the

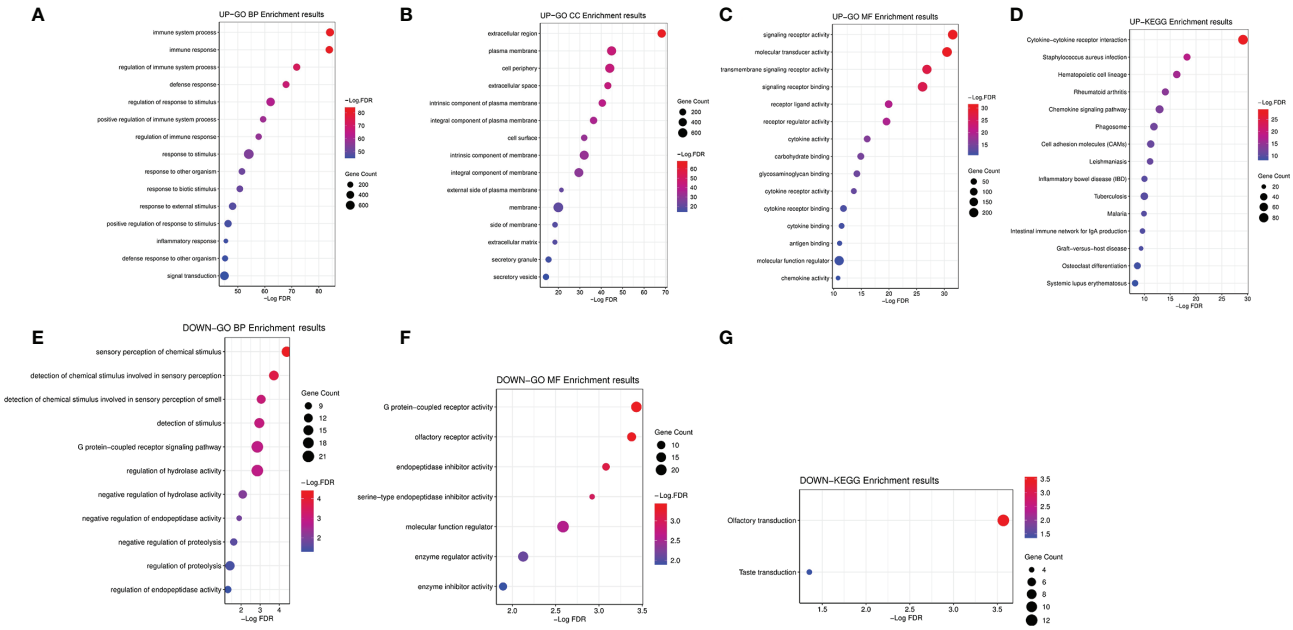

FIGURE 4 | The dotplot for the enriched GO and KEGG analysis of upregulated and downregulated DEGs. **(A)** The dotplot for the enriched GO BP of upregulated DEGs. **(B)** The dotplot for the enriched GO CC of upregulated DEGs. **(C)** The dotplot for the enriched GO MF of upregulated DEGs. **(D)** The dotplot for the enriched KEGG analysis of upregulated DEGs. **(E)** The dotplot for the enriched GO BP of downregulated DEGs. **(F)** The dotplot for the enriched GO MF of downregulated DEGs. **(G)** The dotplot for the enriched KEGG analysis of downregulated DEGs. GO, Gene Ontology; KEGG, Kyoto Encyclopedia of Genes and Genomes; DEGs, differentially expressed genes; BP, biological process; MF, molecular function; CC, cellular component.

figure indicated the degree of the corresponding node. The larger the circle, the greater importance of the corresponding node in the network found. Furthermore, we used Cytotype MCODE software to investigate Clustering analysis of the above PPI network. According to the threshold value, we selected the first significant module with 62 hub genes (**Figure 5B** and **Supplementary Table S8**). The functional analysis of 62 hub genes was preliminarily screened by the Cytoscape software with ClueGO plug-in. The results were shown in **Figure 5C**, which was consistent with the above KEGG results. Therefore, we confirmed that the analysis results were reliable.

CX3CR1 Acts as a Biomarker of Progression and Prognosis in Colorectal Adenoma

To further confirm the independent prognosis factors of patients with CRAD, we used iterative univariable Cox regression to judge the prognostic value of each gene included in the study. Then, we included all genes to conduct multivariable Cox regression, which employed Akaike information criterion (AIC)-based stepwise methods to train a model and is totally different from step 1. And genes that meet $P < 0.05$ of both univariable and multivariable Cox regression were deeded the prognostic genes. Finally, the number of these prognostic genes was eight. The univariate Cox analysis results were shown in **Table 2**, and we observed that there were significant differences in G protein subunit gamma 8 (GNG8), histamine receptor H3 (HRH3), C-C motif chemokine ligand 19 (CRCL19), C-X-C motif chemokine receptor 5 (CXCR5), somatostatin receptor 3 (SSTR3), opioid-related nociceptin receptor 1 (OPRL1), C-X3-C motif chemokine receptor 1 (CX3CR1), and purinergic receptor P2Y13 (P2RY13). The multivariate Cox analysis data showed that there was statistical significance in CX3CR1 (**Figure 6A**). All univariate and multivariate results were shown in **Supplementary Tables S9**, **S10**, respectively. We verified this result by analyzing the relationship between the expression of CX3CR1 and the prognosis of patients with CRAD. As indicated in **Figure 6B**, patients in the low-score group presented poorer 5-year survival consequences than those in the high-score group ($P = 0.01$). These data implied that CX3CR1 might act as a biomarker of progression and prognosis in patients with CRAD.

CX3CR1 Is Associated With Immune Cell Infiltration Levels

The differential expression of CX3CR1 between tumor and adjacent normal tissues was analyzed using the DiffExp module of the TIMER database. As demonstrated in **Figure 7A**, the results revealed that the levels of CX3CR1 were differentially expressed in various cancer types, including colon adenocarcinoma (COAD) ($P < 0.001$). It has been reported that tumor–infiltrating lymphocytes (TILs) are critical survival predictors in cancer patients, and tumor purity plays a significant role in determining CRC prognosis (38). Thus, we used the gene module of the TIMER database to explore whether CX3CR1

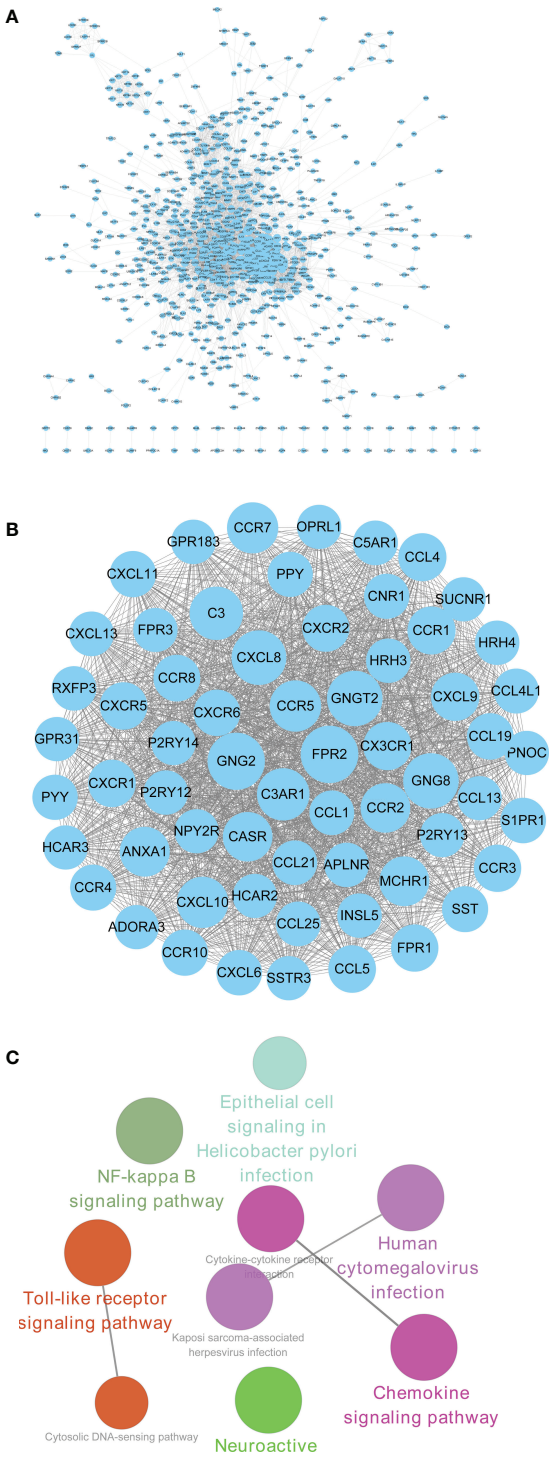

FIGURE 5 | PPI construction and module analysis of upregulated DEGs. **(A)** PPI network of upregulated intersection DEGs using STRING tool and Cytoscape software. **(B)** The first significant module with 62 hub genes. **(C)** The functional analysis of 62 hub genes screened by the Cytoscape software with ClueGO plug-in. PPI, protein–protein interaction; DEGs, differentially expressed genes.

expression was related to infiltration levels in CRC. As shown in **Figure 7B**, CX3CR1 was negatively correlated with purity (cor = -0.161, P = 1.15e-03) and positively correlated with B cells (cor = 0.257, P = 1.61e-07), $CD8^+$ T cells (cor = 0.194, P = 8.01e-07), $CD4^+$ T cells (cor = 0.456, P = 4.97e-22), macrophages (cor = 0.534, P = 3.39e-31), neutrophils (cor = 0.331, P = 1.04e-11), and

TABLE 2 | Univariate Cox proportional hazards regression analyses of clinical parameters and hub genes in patients with CRAD.

Cells	coef	HR (95% CI for HR)	*P* value
GNG8	0.194	1.21 (1.11–1.32)	0.0000117
HRH3	0.433	1.54 (1.26–1.88)	0.0000183
CCL19	0.0167	1.02 (1.01–1.03)	0.000826
CXCR5	3.58	36 (3.6–359)	0.00228
SSTR3	1.61	5.01 (1.54–16.3)	0.00733
OPRL1	0.518	1.68 (1.08–2.6)	0.0202
CX3CR1	-1	0.367 (0.144–0.938)	0.0363
P2RY13	-0.259	0.772 (0.596–0.998)	0.0486

CI, confidence interval; HR, hazard ratio; GNG8, G protein subunit gamma 8; HRH3, histamine receptor H3; CRCL19, C-C motif chemokine ligand 19; CXCR5, C-X-C motif chemokine receptor 5; SSTR3, somatostatin receptor 3; OPRL1, opioid-related nociceptin receptor 1; CX3CR1, C-X3-C motif chemokine receptor 1; P2RY13, purinergic receptor P2Y13; CRAD, colorectal adenoma.

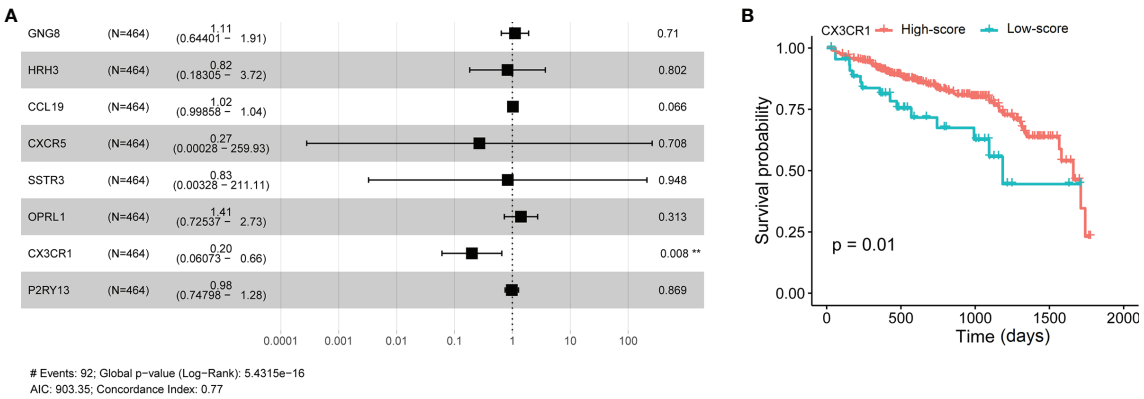

FIGURE 6 | Multivariate Cox analyses of hub genes and survival analysis of CX3CR1 in patients with CRAD. **(A)** Multivariate Cox analyses of hub genes in patients with CRAD. **(B)** Survival analysis of CX3CR1 in patients with CRAD. GNG8, G protein subunit gamma 8; HRH3, histamine receptor H3; CRCL19, C-C motif chemokine ligand 19; CXCR5, C-X-C motif chemokine receptor 5; SSTR3, somatostatin receptor 3; OPRL1, opioid-related nociceptin receptor 1; CX3CR1, C-X3-C motif chemokine receptor 1; P2RY13, purinergic receptor P2Y13; CRAD, colorectal adenoma.

dendritic cells (DCs) (cor = 0.464, P = 8.17e-23). Furthermore, we examined the correlation between CX3CR1 expression and immune markers of different immune cells using the correlation module of the TIMER database in COAD, including monocyte markers (CD86 and CSF1R), tumor-associated macrophage (TAM) markers (CCL2, CD68, and IL10), M1 macrophage markers (NOS2, IRF5, and PTGS2), and M2 macrophage markers (VSIG4, MS4A4A, and CD163). The results showed that CX3CR1 expression was correlated with that of most monocytes, TAM, and M1 and M2 macrophage markers in COAD (**Figure 7C**). For further exploration, CIBERSORT analysis indicated that the high expression of CX3CR1 was positively correlated with resting DCs (cor = 0.25, P = 1.75e-06), resting mast cells (cor = 0.21, P = 2.62e-05), M2 macrophages (cor = 0.33, P = 6.74e-10), and plasma cells (cor = 0.17, P = 0.002) and negatively correlated with activated DCs (cor = -0.11, P = 0.008), activated natural killer (NK) cells (cor = -0.20, P = 8.73e-05), and activated mast cells (cor = -0.14, P = 0.006). No significant difference was observed in resting NK cells (cor = -0.08, P = 0.123) (**Figure 7D**). These data suggested that CX3CR1 was associated with immune cell infiltration levels in CRC pathology.

Coculture of THP-1 and HCT8 Cells With Low CX3CR1 Expression Regulates Macrophage Polarization and Promotes Proliferation and Migration

To further confirm the above results, we subsequently assessed the effects of coculture of THP-1 and CRC cells with low CX3CR1 expression on CRC cell functions. Firstly, we analyzed the protein expression of CX3CR1 in different CRC cell lines. The data revealed that the protein expression of CX3CR1 was significantly diminished in different CRC cell lines compared to the human normal intestinal mucous cell line CCC-HIE-2 (P < 0.05 or P < 0.01; **Figure 7E**), with the highest level in HCT8 cells. Then, the effects of coculture on the mRNA expression of M1 and M2 macrophage markers were explored. The findings revealed that, compared to the control group, silencing of CX3CR1 or coculture with THP-1 cells could significantly increase the mRNA levels of M1 macrophage markers (NOS2, IRF5, and PTGS2) (P < 0.001) but decrease the mRNA levels of M2 macrophage markers (VSIG4, MS4A4A, and CD163) (P < 0.01 or P < 0.001), while simultaneous silencing of CX3CR1 and coculture with THP-1 cells further enhanced the above functions (P < 0.05, P < 0.01, or P < 0.001; **Figure 7F**).

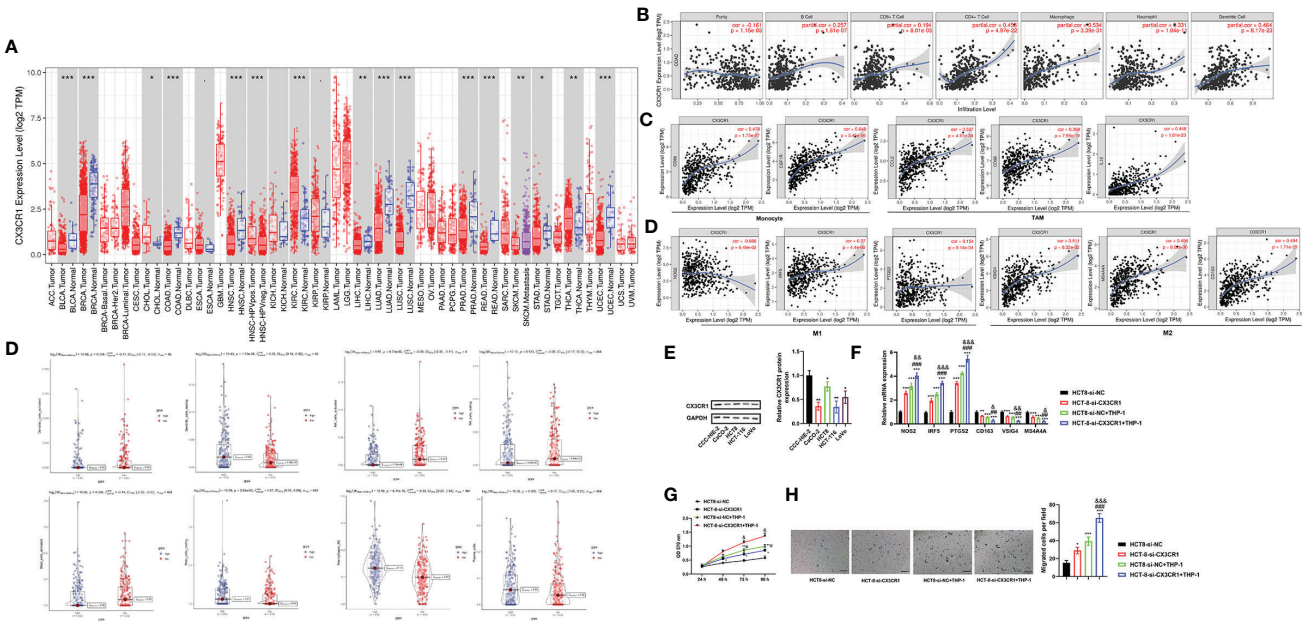

FIGURE 7 | CX3CR1 is associated with immune cell infiltration levels and contributes to TAM-induced CRC progression. **(A)** The differential expression of CX3CR1 between tumor and adjacent normal tissues in COAD analyzed by the DiffExp module of the TIMER database. **(B)** The association between CX3CR1 expression and infiltration levels in COAD analyzed by the gene module of the TIMER database. **(C)** The correlation between CX3CR1 expression and immunological markers in COAD analyzed by the correlation module of the TIMER database. **(D)** The correlation between CX3CR1 expression and immune cell infiltration levels analyzed by CIBERSORT analysis. **(E)** The protein expression of CX3CR1 in different CRC cell lines. **(F–H)** The effects of coculture of THP-1 and HCT8 cells with low CX3CR1 expression on the mRNA expression of monocyte, TAM, M1 and M2 macrophage markers, proliferation and migration. $^{*}P < 0.05$, $^{***}P < 0.01$, $^{***}P < 0.001$ compared to the HCT-8-si-NC group; $^{\#}P < 0.05$, $^{\#\#}P < 0.01$, $^{\#\#\#}P < 0.001$ compared to the HCT-8-si-CX3CR1 group; $^{\&}P < 0.05$, $^{\&\&}P < 0.01$, $^{\&\&\&}P < 0.001$ compared to the HCT-8-si-NC+THP-1 group. CX3CR1, C-X3-C motif chemokine receptor 1; CRC, colorectal cancer; TAM, tumor-associated macrophage; COAD, colon adenocarcinoma; NOS2, nitric oxide synthase 2; IRF5, interferon regulatory factor 5; PTGS2, prostaglandin-endoperoxide synthase 2; VSIG4, V-set and immunoglobulin domain containing 4; membrane-spanning 4-domains, subfamily A, member 4A; TIMER, Tumor IMmune Estimation Resource database.

Next, the effects of coculture on the proliferation and migration of cancer cells were investigated. As demonstrated in **Figures 7G, H**, the data revealed that, compared to the control group, the cell viability and number of migrated cells were significantly promoted by silencing of CX3CR1 or coculture with THP-1 cells and were further elevated by simultaneous silencing of CX3CR1 and coculture with THP-1 cells ($P < 0.05$, $P < 0.01$, or $P < 0.001$). These data implied that CX3CR1 contributed to the recruitment and regulation of immune infiltrating cells and macrophage polarization in CRC, as well as TAM-induced CRC progression.

Verification of CX3CR1 Expression in Human Colorectal Cancer Tissues

To further verify the expression of CX3CR1 and the potential functional role of CX3CR1 in CRC, we enrolled a total of 60 patients with CRC and analyzed the mRNA and protein expressions of CX3CR1 in the tumor tissues. As revealed in **Figure 8A**, the data showed that, compared to the non-tumor tissues, the mRNA expression of CX3CR1 was significantly downregulated in the tumor tissues ($P < 0.01$). In addition, 12 pairs of tissues were randomly chosen to assess the protein expression of CX3CR1. In line with the mRNA results, the protein expression of CX3CR1 was also statistically reduced in the tumor tissues compared with the non-tumor tissues ($P < 0.01$ or $P < 0.001$; **Figure 8B**). In addition, we investigated the relationship between CX3CR1 expression and CRC clinicopathological parameters, including gender, age, tumor location, TNM stage, and tumor size and differentiation. Among these 60 patients, 28 patients were categorized as high expression group and the remaining 32 patients were categorized as low expression group. As indicated in **Table 3**, CX3CR1 was not significantly related to age, gender, tumor location, size, and M stage but was associated with T and N stages, tumor differentiation, and prognosis of the tumor. These findings suggested that CX3CR1 may function as a potential prognostic biomarker in CRC.

DISCUSSION

CRC is a highly heterogeneous disease with increasing incidence and mortality. Immunotherapy has emerged as a novel approach for the management of CRC (19, 39, 40). Although many patients with CRC are immunoresponsive, some adverse effects, such as toxicity, have been reported recently (40). Therefore, there is an unmet need for exploring the targeting immunotherapy to the TME, since the TME plays an important role in the progression and development of cancers, as well as in responses to therapies, particularly immunotherapies (41). Moreover, the TME-related genes could be used as favorable predictors to evaluate patients'

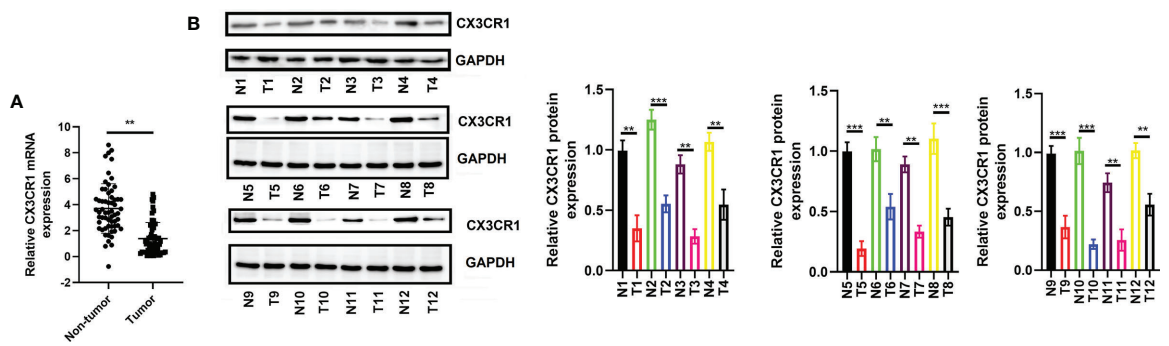

FIGURE 8 | Expression of CX3CR1 in patients with CRC. **(A)** The mRNA expression of CX3CR1 in the enrolled 60 patients. **(B)** The protein expression of CX3CR1 in the 12 pairs of tissues. CX3CR1, C-X3-C motif chemokine receptor 1; CRC, colorectal cancer. $^{**}P < 0.01$, $^{***}P < 0.001$ compared to the corresponding groups.

TABLE 3 | Correlation between CX3CR1 expression and clinicopathological characteristics of CRC.

Characteristics		Cases	CX3CR1 expression		*P* value
			Low	High	
Gender	Male	38	20	18	0.886
	Female	22	12	10	
Age	<60	26	14	12	0.944
	≥60	34	18	16	
Tumor location					
	Colon	40	21	19	0.582
	Rectum	20	12	8	
T stage					
	T1–2	36	12	24	0.000
	T3–4	24	18	4	
N stage					
	N0	32	12	20	0.009
	N1–2	28	20	8	
M stage					
	M0	34	16	18	0.265
	M1	22	16	10	
Differentiation					
	Low	12	5	7	0.003
	Medium	36	22	14	
	High	12	5	7	
Size					
	<4.5 cm	31	16	15	0.782
	≥4.5 cm	29	16	13	

CX3CR1, C-X3-C motif chemokine receptor 1; CRC, colorectal cancer.

survival, thereby improving the clinical consequence. In the current study, we performed a comprehensive analysis of the stromal and immune cells, the TME-associated genes, and the clinical prognosis of CRAD patients.

Firstly, we used the ESTIMATE algorithm to analyze the associations between the ImmuneScore, StromalScore, and EstimateScore and the stages and survival rates in CRAD patients acquired from TCGA database. ESTIMATE algorithm is a broad, novel, and reliable algorithm that has been administered in the data mining of many cancers (21). Our data showed that the StromalScore, ImmuneScore, and EstimateScore were generally decreased with the stage of disease malignancy. There were statistical differences in the latter two, which indicated that immune infiltration and tumor purity might significantly contribute to the development of CRAD. Moreover, the survival analysis revealed that the high three scores presented a longer lifetime than those with low scores. Combining these results, we demonstrated that the clinical consequences of CRAD patients were markedly affected by the TME, which were in line with previous studies (16, 42, 43).

Subsequently, we identified a total of 1,578 intersection genes. GO and KEGG pathway analyses established that the intersection genes were mainly enriched in the tumor immune response and the maintenance of TNM. For instance, the GO results indicated that the interaction genes were principally enriched in the regulation of leukocyte activation, T-cell activation, leukocyte

migration/cell–cell adhesion/differentiation, and extracellular matrix (ECM)/structure organization, and the KEGG pathway demonstrated that they were specifically enriched in cytokine–cytokine receptor interaction and chemokine signaling pathway. Furthermore, according to the DEGs of the PPI network analysis, we identified and selected 62 hub genes as the first important module, and the KEGG pathway analyzed by ClueGO showed that these hub genes were also enriched in cytokine–cytokine receptor interaction and chemokine signaling pathway, etc. Our data supported previous investigations on the essential role of immune cells and ECM molecular components in the establishment of the TME, as well as the relationship between the progression and development of CRC and the TME (44–47).

To reveal the potential independent prognostic biomarkers for CRC, we performed univariate and multivariate Cox analysis by evaluating 62 hub genes and pathologic stages. After removal of insignificant variables, we found that pathologic stages (TNM) and several genes including GNG8, HRH3, CCL19, CXCR5, SSTR3, OPRL1, CX3CR1, and P2RY13 were significantly correlated with the prognosis of CRC in the univariate Cox analysis. At present, the TNM staging system has been well considered as the most frequently used predictor of OS and recurrence in CRC (48). Our results also confirmed that all stages were significantly correlated with the prognosis of CRC. GNG8 is a protein-coding gene, which is involved in GTPase activity and obsolete signal transducer activity. A previous bioinformatics analysis suggested that GNG8 was downregulated in CRC (49). However, the biological function of GNG8 in CRC remains uncertain to date. HRH3 is a presynaptic receptor, which mediates the discharge of histamine from histaminergic neurons and other neurotransmitters from different types of neurons (50). Recent research confirmed that HRH3 was involved in tumor growth and metastasis (51, 52). CCL19 belongs to the chemokine family, while CXCR5 and CX3CR1 are both chemokine receptors. These three factors play significant roles in many cancers, including CRC (53, 54). Interestingly, a previous study observed that CX3CR1 ectopic expression improved the recruitment of adoptively transferred T cells toward CX3CL1-generated cancers, leading to the augmentation of T-cell infiltration and reduction of tumor growth (55). SSTR3 is a well-known G-protein-coupled plasma membrane receptor and is activated by neuropeptides. It has been reported that SSTR3 was decreased with the Dukes' stages in CRC (56). P2RY13 is a G-protein-coupled receptor, and it was reported to be decreased upon epidermal growth factor (EGF)- and hypoxia-induced epithelial–mesenchymal transition (EMT) in breast cancer cells (57, 58). Additionally, P2RY13 was also involved in the identification of M1 macrophages in CRC (59). However, multivariate Cox analysis showed that only T stage, N stage, and CX3CR1 were independent risk factors that could affect the prognosis of CRC. In addition, the survival of CX3CR1 also confirmed that the low score of CX3CR1 indicated a lower lifetime.

CX3CR1, located on chromosome 3p22.2, is a key chemokine receptor with a single ligand, which belongs to the G-protein-coupled receptor (GPCR) superfamily (60). It is a proinflammatory leukocyte receptor specific for the chemokine CX3CL1 [fractalkine (FKN)] (61). CX3CR1 includes four exons and three introns and is expressed by infiltrating immune cells (e.g., monocytes, $CD8^+$ T cells, and NK cells) (62) and tissue-resident cells (e.g., macrophages and DCs) (63). Previous studies have revealed that the CX3CL1/CX3CR1 axis is responsible for numerous pathological processes, such as atherosclerosis (60), atherogenesis (64), nervous system diseases (65), vasculitis (66), abnormal heart function (67), and cancer development (68, 69). In addition, CX3CL1:CX3CR1 axis has been confirmed to play critical roles in the TME (70) and mediates several cellular functions, including cell proliferation, apoptosis, migration, and invasion by activation of phosphatidylinositol-3-kinases/protein-serine-threonine kinase (PI3K/AKT) and MAPK kinases, Src, and/or eNOS signaling pathways (71). However, the CX3CL1:CX3CR1 axis presents either pro- or antitumor effects in different cancers (72). For example, patients with a high expression of CX3CR1 were reported to be an independent negative prognosis factor in pancreatic ductal adenocarcinoma (73). Compared to the normal tissues, reduced expression of CX3CR1 was found in macrophages infiltrating CRC tissues (74). In contrast, a high expression of CX3CL1 was observed to have a positively strong association with a high number of stromal $CD8^+$ T cells, NK cells, and intratumoral DCs in breast cancer (75). CX3CL1 was related to the density of TILs and was found to be one of the biomarkers for identifying CRC patients (76). Contrary to our results, a previous study suggested that CX3CR1 (lack of the allele I249) might play a limited or insignificant role in CRC, and plasma FKN/CX3CL1 does not appear to be a valuable tumor marker in CRC (77). These results implied that the effects of CX3CR1 might be heterogeneous even in the same cancers. To further confirm our bioinformatics results, we analyzed the expression of CX3CR1 in CRC tissues and cell lines, as well as the relationship between CX3CR1 and clinical parameters. As demonstrated in our *in vitro* experiments, we confirmed the lower expression of CX3CR1 in CRC tissues and cell lines. In addition, we observed that lower expression of CX3CR1 was correlated with tumor T and N stages, differentiation, and poorer prognosis.

Recently, the immune function of CX3CL1:CX3CR1 axis has been explored. For example, the expression of CX3CL1 has been confirmed to result in the infiltration of NK cells, DCs, $CD4^+$, and $CD8^+$ T cells into the tumor, which leads to an increase in the antitumor immune response (75). A previous research suggested that transduction with CX3CR1 increases T-cell recruitment into the TME in an animal model of CRC (55). On another front, $CX3CR1^-CD8^+$ T cells were reported to be functionally suppressed in the TME (78). To further explore the immune functions of CX3CR1, we investigated the associations between CX3CR1 expression and TILs and immune marker expression using TIMER database and CIBERSORT analysis. Interestingly, we observed that CX3CR1 expression was negatively related to purity but positively correlated with B cells, $CD8^+$ T cells, $CD4^+$ T cells, macrophages, neutrophils, and DCs. In addition, we observed that the high expression of CX3CR1 was positively correlated with resting DCs, resting mast

cells, M2 macrophages, and plasma cells and negatively correlated with activated DCs, activated NK cells, and activated mast cells. These results indicated that CX3CR1 was associated with immune cell infiltration levels. The correlation between CX3CR1 and the expression of immune marker gene expression strongly suggested that CX3CR1 can regulate immune cell infiltration and interact within the TME. We detected a correlation between CX3CR1 and M1/M2 macrophage markers, which suggests that CX3CR1 might contribute to CRC by regulation of macrophage polarization. Macrophages are important innate immune cells that serve as a first line of defense against pathogenic insults to tissues. Nevertheless, TAM induces the expression of cytokines and chemokines that can inhibit antitumor immunity and promote cancer progression in different cancer types (79). Therefore, the protective effects of CX3CR1 on CRC might be by suppression of TAM-induced CRC progression. To confirm this, we used a coculture system to analyze the effects of coculture of THP-1 and CRC cells with low CX3CR1 expression on M1/M2 macrophage marker gene expression and cell proliferation and migration in CRC. As expected, coculture with THP-1-derived macrophages significantly promoted CRC cell proliferation and migration, which were in line with previous studies (80–82). Interestingly, our study found that simultaneous silencing of CX3CR1 and coculture with THP-1 cells further regulated macrophage polarization and promoted cell proliferation and migration of CRC cells. To our knowledge, this is the first report on the immune function of CX3CR1 with macrophages in cancer development.

Though our research achieved highly valued data, some limitations should be unneglectable. This study was performed only based on TCGA database; hence, a more comprehensive analysis should be implemented to illuminate the complicated relationship between the TME and CRC. Moreover, more immune-related experiments, such as the changes of CX3CR1 on the proportion changes of immune cells, should be performed to confirm the roles of CX3CR1 in the TME of CRC.

In conclusion, we comprehensively investigated the correlation between the TME-related genes and CRC by using the ESTIMATE algorithm based on TCGA database. Our data suggested that CX3CR1 might be a potential prognostic biomarker in the TME of CRC.

DATA AVAILABILITY STATEMENT

The original contributions presented in the study are included in the article/**Supplementary Material**. Further inquiries can be directed to the corresponding author.

ETHICS STATEMENT

The studies involving human participants were reviewed and approved by The Medical Ethics Committee of Shengjing Hospital of China Medical University. The patients/participants provided their written informed consent to participate in this study.

AUTHOR CONTRIBUTIONS

Conception and design: ZS. Administrative support: QZ. Provision of study materials or patients: YY. Collection and assembly of data: YY and QZ. Data analysis and interpretation: YY and QZ. Article writing: All authors. Final approval of article: All authors. All authors contributed to the article and approved the submitted version.

FUNDING

This research did not receive any specific grant from funding agencies in the public, commercial, or not-for-profit sectors.

SUPPLEMENTARY MATERIAL

The Supplementary Material for this article can be found online at: https://www.frontiersin.org/articles/10.3389/fimmu.2021.758040/full#supplementary-material

REFERENCES

1. Bahrami A, Hassanian SM. Targeting RAS Signaling Pathway as a Potential Therapeutic Target in the Treatment of Colorectal Cancer. *J Cell Physiol* (2018) 2333:2058–66. doi: 10.1002/jcp.25890
2. Chen W, Zheng R, Baade PD, Zhang S, Zeng H, Bray F, et al. Cancer Statistics in China 2015. *CA Cancer J Clin* (2016) 66(2):115–32. doi: 10.3322/caac.21338
3. Bahrami A, Shahidsales S, Khazaei M, Ghayour-Mobarhan M, Maftouh M, Hassanian SM. C-Met as a Potential Target for the Treatment of Gastrointestinal Cancer: Current Status and Future Perspectives. *J Cell Physiol* (2017) 232(10):2657–73. doi: 10.1002/jcp.25794
4. Simon K. Colorectal Cancer Development and Advances in Screening. *Clin Interv Aging* (2016) 11:967–76. doi: 10.2147/cia.s109285
5. Maida M, Macaluso FS, Ianiro G, Mangiola F, Sinagra E, Hold G, et al. Screening of Colorectal Cancer: Present and Future. *Expert Rev Anticancer Ther* (2017) 17(12):1131–46. doi: 10.1080/14737140.2017.1392243
6. Bresalier RS. Early Detection of and Screening for Colorectal Neoplasia. *Gut Liver* (2009) 3(2):69–80. doi: 10.5009/gnl.2009.3.2.69
7. Yue YY, Fan XY, Zhang Q, Lu YP, Wu S, Wang S, et al. Bibliometric Analysis of Subject Trends and Knowledge Structures of Gut Microbiota. *World J Clin cases* (2020) 8(13):2817–32. doi: 10.12998/wjcc.v8.i13.2817
8. Kinzler KW, Vogelstein B. Lessons From Hereditary Colorectal Cancer. *Cell* (1996) 87(2):159–70. doi: 10.1016/s0092-8674(00)81333-1
9. Yue Y, Zhang Q, Wu S, Wang S, Cui C, Yu M, et al. Identification of Key Genes Involved in JAK/STAT Pathway in Colorectal Cancer. *Mol Immunol* (2020) 128:287–97. doi: 10.1016/j.molimm.2020.10.007
10. Witz IP. Tumor-Microenvironment Interactions: Dangerous Liaisons. *Adv Cancer Res* (2008) 100:203–29. doi: 10.1016/S0065-230X(08)00007-9
11. Swartz MA, Iida N, Roberts EW, Sangaletti S, Wong MH, Yull FE, et al. Tumor Microenvironment Complexity: Emerging Roles in Cancer Therapy. *Cancer Res* (2012) 72(10):2473–80. doi: 10.1158/0008-5472.CAN-12-0122
12. Pedrosa L, Esposito F, Thomson TM, Maurel J. The Tumor Microenvironment in Colorectal Cancer Therapy. *Cancers (Basel)* (2019) 11(8). doi: 10.3390/cancers11081172
13. Peddareddigari VG, Wang D, Dubois RN. The Tumor Microenvironment in Colorectal Carcinogenesis. *Cancer Microenviron* (2010) 3(1):149–66. doi: 10.1007/s12307-010-0038-3

14. Hanahan D, Coussens LM. Accessories to the Crime: Functions of Cells Recruited to the Tumor Microenvironment. *Cancer Cell* (2012) 21(3):309–22. doi: 10.1016/j.ccr.2012.02.022
15. Hanahan D, Weinberg RA. The Hallmarks of Cancer. *Cell* (2000) 100(1):57–70. doi: 10.1016/s0092-8674(00)81683-9
16. Chen P, Yang Y, Zhang Y, Jiang S, Li X, Wan J. Identification of Prognostic Immune-Related Genes in the Tumor Microenvironment of Endometrial Cancer. *Aging (Albany NY)* (2020) 12(4):3371–87. doi: 10.18632/aging.102817
17. Bussard KM, Mutkus L, Stumpf K, Gomez-Manzano C, Marini FC. Tumor-Associated Stromal Cells as Key Contributors to the Tumor Microenvironment. *Breast Cancer Res* (2016) 18(1):84. doi: 10.1186/s13058-016-0740-2
18. Wirapati P, Qu X, Ling H, Emre E, Sabine T, Omar K. Prognostic Stromal and Immune Response Expression Patterns in Early-Stage Colorectal Cancer Predicted by Genes Intrinsically Expressed by Tumor Epithelial Cells. *J Clin Oncol* (2019) 37(15_suppl):3601–1. doi: 10.1200/JCO.2019.37.15_suppl.3601
19. Becht E, de Reyniès A, Giraldo NA, Pilati C, Buttard B, Lacroix L, et al. Immune and Stromal Classification of Colorectal Cancer Is Associated With Molecular Subtypes and Relevant for Precision Immunotherapy. *Clin Cancer Res* (2016) 22(16):4057–66. doi: 10.1158/1078-0432.ccr-15-2879
20. Chen CH, Lu YS, Cheng AL, Huang CS, Kuo WH, Wang MY, et al. Disparity in Tumor Immune Microenvironment of Breast Cancer and Prognostic Impact: Asian Versus Western Populations. *Oncologist* (2020) 25(1):e16–23. doi: 10.1634/theoncologist.2019-0123
21. Yoshihara K, Shahmoradgoli M, Martínez E, Vegesna R, Kim H, Torres-Garcia W, et al. Inferring Tumour Purity and Stromal and Immune Cell Admixture From Expression Data. *Nat Commun* (2013) 4:2612. doi: 10.1038/ncomms3612
22. Vincent KM, Findlay SD, Postovit LM. Assessing Breast Cancer Cell Lines as Tumour Models by Comparison of mRNA Expression Profiles. *Breast Cancer Res* (2015) 17:114. doi: 10.1186/s13058-015-0613-0
23. Yan H, Qu J, Cao W, Liu Y, Zheng G, Zhang E, et al. Identification of Prognostic Genes in the Acute Myeloid Leukemia Immune Microenvironment Based on TCGA Data Analysis. *Cancer. Immunol Immunother* (2019) 68(12):1971–8. doi: 10.1007/s00262-019-02408-7
24. Ren H, Hu D, Mao Y, Su X. Identification of Genes With Prognostic Value in the Breast Cancer Microenvironment Using Bioinformatics Analysis. *Med Sci Monit* (2020) 26:e920212. doi: 10.12659/msm.920212
25. Galon J, Pagès F, Marincola FM, Angell HK, Thurin M, Lugli A, et al. Cancer Classification Using the Immunoscore: A Worldwide Task Force. *J Transl Med* (2012) 10:205. doi: 10.1186/1479-5876-10-205
26. Xue YN, Xue YN, Wang ZC, Mo YZ, Wang PY, Tan WQ. A Novel Signature of 23 Immunity-Related Gene Pairs Is Prognostic of Cutaneous Melanoma. *Front Immunol* (2020) 11:576914. doi: 10.3389/fimmu.2020.576914
27. Liu W, Ye H, Liu YF, Xu CQ, Zhong YX, Tian T, et al. Transcriptome-Derived Stromal and Immune Scores Infer Clinical Outcomes of Patients With Cancer. *Oncol Lett* (2018) 15(4):4351–7. doi: 10.3892/ol.2018.7855
28. Ke ZB, Wu YP, Huang P, Hou J, Chen YH, Dong RN, et al. Identification of Novel Genes in Testicular Cancer Microenvironment Based on ESTIMATE Algorithm-Derived Immune Scores. *J Cell Physiol* (2021) 236(1):706–13. doi: 10.1002/jcp.29898
29. Yang L, Yang Y, Meng M, Wang W, He S, Zhao Y, et al. Identification of Prognosis-Related Genes in the Cervical Cancer Immune Microenvironment. *Gene* (2021) 766:145119. doi: 10.1016/j.gene.2020.145119
30. Hothorn T, Zeileis A. Generalized Maximally Selected Statistics. *Biometrics* (2008) 64(4):1263–9. doi: 10.1111/j.1541-0420.2008.00995.x
31. Jin W, Zhang Y. Exploration of the Molecular Characteristics of the Tumor-Immune Interaction and the Development of an Individualized Immune Prognostic Signature for Neuroblastoma. *J Cell Physiol* (2021) 236(1):294–308. doi: 10.1002/jcp.29842
32. Yu G, Wang LG, Han Y, He QY. Clusterprofiler: An R Package for Comparing Biological Themes Among Gene Clusters. *Omics* (2012) 16(5):284–7. doi: 10.1089/omi.2011.0118
33. Szklarczyk D, Gable AL, Lyon D, Junge A, Wyder S, Huerta-Cepas J, et al. STRING V11: Protein-Protein Association Networks With Increased Coverage, Supporting Functional Discovery in Genome-Wide Experimental Datasets. *Nucleic Acids Res* (2019) 47(D1):D607–13. doi: 10.1093/nar/gky1131
34. Shannon P, Markiel A, Ozier O, Baliga NS, Wang JT, Ramage D, et al. Cytoscape: A Software Environment for Integrated Models of Biomolecular Interaction Networks. *Genome Res* (2003) 13(11):2498–504. doi: 10.1101/gr.1239303
35. Bindea G, Mlecnik B, Hackl H, Charoentong P, Tosolini M, Kirilovsky A, et al. ClueGO: A Cytoscape Plug-in to Decipher Functionally Grouped Gene Ontology and Pathway Annotation Networks. *Bioinformatics* (2009) 25(8):1091–3. doi: 10.1093/bioinformatics/btp101
36. Li T, Fan J, Wang B, Traugh N, Chen Q, Liu JS, et al. TIMER: A Web Server for Comprehensive Analysis of Tumor-Infiltrating Immune Cells. *Cancer Res* (2017) 77(21):e108–10. doi: 10.1158/0008-5472.can-17-0307
37. Newman AM, Liu CL, Green MR. Robust Enumeration of Cell Subsets From Tissue Expression Profiles. *Nat Methods* (2015) 12(5):453–7. doi: 10.1038/nmeth.3337
38. Mao Y, Feng Q, Zheng P, Yang L, Liu T, Xu Y, et al. Low Tumor Purity is Associated With Poor Prognosis, Heavy Mutation Burden, and Intense Immune Phenotype in Colon Cancer. *Cancer Manag Res* (2018) 10:3569–77. doi: 10.2147/cmar.s171855
39. Basile D, Garattini SK, Bonotto M, Ongaro E, Casagrande M, Cattaneo M, et al. Immunotherapy for Colorectal Cancer: Where Are We Heading? *Expert Opin Biol Ther* (2017) 17(6):709–21. doi: 10.1080/14712598.2017.1315405
40. Wrobel P, Ahmed S. Current Status of Immunotherapy in Metastatic Colorectal Cancer. *Int J Colorectal Dis* (2019) 34(1):13–25. doi: 10.1007/s00384-018-3202-8
41. Fridman WH, Pagès F, Sautès-Fridman C, Galon J. The Immune Contexture in Human Tumours: Impact on Clinical Outcome. *Nat Rev Cancer* (2012) 12(4):298– 306. doi: 10.1038/nrc3245
42. Li J, Li X, Zhang C, Zhang C, Wang H. A Signature of Tumor Immune Microenvironment Genes Associated With the Prognosis of Non–Small Cell Lung Cancer. *Oncol Rep* (2020) 43(3):795–806. doi: 10.3892/or.2020.7464
43. Zeng Q, Zhang W, Li X, Lai J, Li Z. Bioinformatic Identification of Renal Cell Carcinoma Microenvironment-Associated Biomarkers With Therapeutic and Prognostic Value. *Life Sci* (2020) 243:117273. doi: 10.1016/j.lfs.2020.117273
44. Schneider K, Marbaix E, Bouzin C, Hamoir M, Mahy P, Bol V, et al. Immune Cell Infiltration in Head and Neck Squamous Cell Carcinoma and Patient Outcome: A Retrospective Study. *Acta Oncol* (2018) 57(9):1165–72. doi: 10.1080/0284186X.2018.1445287
45. Cammarota R, Bertolini V, Pennesi G, Bucci EO, Gottardi O, Garlanda C, et al. The Tumor Microenvironment of Colorectal Cancer: Stromal TLR-4 Expression as a Potential Prognostic Marker. *J Transl Med* (2010) 8:112. doi: 10.1186/1479-5876-8-112
46. Lin YC, Mahalingam J, Chiang JM, Su PJ, Chu YY, Lai HY, et al. Activated But Not Resting Regulatory T Cells Accumulated in Tumor Microenvironment and Correlated With Tumor Progression in Patients With Colorectal Cancer. *Int J Cancer* (2013) 132(6):1341–50. doi: 10.1002/ijc.27784
47. Sakai N, Yoshidome H, Shida T, Kimura F, Shimizu H, Ohtsuka M, et al. CXCR4/CXCL12 Expression Profile is Associated With Tumor Microenvironment and Clinical Outcome of Liver Metastases of Colorectal Cancer. *Clin Exp Metastasis* (2012) 29(2):101–10. doi: 10.1007/s10585-011-9433-5
48. Chen JH, Zhai ET, Yuan YJ, Wu KM, Xu JB, Peng JJ, et al. Systemic Immune-Inflammation Index for Predicting Prognosis of Colorectal Cancer. *World J Gastroenterol* (2017) 23(34):6261–72. doi: 10.3748/wjg.v23.i34.6261
49. Qi Y, Qi H, Liu Z, He P, Li B. Bioinformatics Analysis of Key Genes and Pathways in Colorectal Cancer. *J Comput Biol* (2019) 26(4):364–75. doi: 10.1089/cmb.2018.0237
50. Sundvik M, Panula P. Interactions of the Orexin/Hypocretin Neurones and the Histaminergic System. *Acta Physiol (Oxf)* (2015) 213(2):321–33. doi: 10.1111/apha.12432
51. Yu D, Zhao J, Wang Y, Hu J, Zhao Q, Li J, et al. Upregulated Histamine Receptor H3 Promotes Tumor Growth and Metastasis in Hepatocellular Carcinoma. *Oncol Rep* (2019) 41(6):3347–54. doi: 10.3892/or.2019.7119
52. Francis H, DeMorrow S, Venter J, Kopriva S, Vaculin B, Savage J, et al. The Activation of H3/H4 Histamine Receptors Induces a Decrease in Cholangiocarcinoma Growth. *Cancer Res* (2008) 68(9 Supplement):3602–2.
53. Lu J, Zhao J, Feng H, Wang P, Zhang Z, Zong Y, et al. Antitumor Efficacy of CC Motif Chemokine Ligand 19 in Colorectal Cancer. *Dig Dis Sci* (2014) 59(9):2153–62. doi: 10.1007/s10620-014-3138-y
54. Qi XW, Xia SH, Yin Y, Jin LF, Pu Y, Hua D, et al. Expression Features of CXCR5 and its Ligand, CXCL13 Associated With Poor Prognosis of

Advanced Colorectal Cancer. *Eur Rev Med Pharmacol Sci* (2014) 18 (13):1916–24.
55. Siddiqui I, Erreni M, van Brakel M, Debets R, Allavena P. Enhanced Recruitment of Genetically Modified CX3CR1-Positive Human T Cells Into Fractalkine/CX3CL1 Expressing Tumors: Importance of the Chemokine Gradient. *J Immunother Cancer* (2016) 4:21. doi: 10.1186/s40425-016-0125-1
56. Qiu CZ, Wang C, Huang ZX, Zhu SZ, Wu YY, Qiu JL. Relationship Between Somatostatin Receptor Subtype Expression and Clinicopathology, Ki-67, Bcl-2 and P53 in Colorectal Cancer. *World J Gastroenterol* (2006) 12(13):2011–5. doi: 10.3748/wjg.v12.i13.2011
57. Davis FM, Kenny PA, Soo ET, van Denderen BJ, Thompson EW, Cabot PJ, et al. Remodeling of Purinergic Receptor-Mediated Ca2+ Signaling as a Consequence of EGF-Induced Epithelial-Mesenchymal Transition in Breast Cancer Cells. *PloS One* (2011) 6(8):e23464. doi: 10.1371/journal.pone.0023464
58. Azimi I, Beilby H, Davis FM, Marcial DL, Kenny PA, Thompson EW, et al. Altered Purinergic Receptor-Ca^{2+} Signaling Associated With Hypoxia-Induced Epithelial-Mesenchymal Transition in Breast Cancer Cells. *Mol Oncol* (2016) 10(1):166–78. doi: 10.1016/j.molonc.2015.09.006
59. Wu Y, Zhang S, Yan J. IRF1 Association With Tumor Immune Microenvironment and Use as a Diagnostic Biomarker for Colorectal Cancer Recurrence. *Oncol Lett* (2020) 19(3):1759–70. doi: 10.3892/ol.2020.11289
60. Liu H, Jiang D. Fractalkine/CX3CR1 and Atherosclerosis. *Clin Chim Acta* (2011) 412(13-14):1180–6. doi: 10.1016/j.cca.2011.03.036
61. Clark AK, Staniland AA, Malcangio M. Fractalkine/CX3CR1 Signalling in Chronic Pain and Inflammation. *Curr Pharm Biotechnol* (2011) 12(10):1707–14. doi: 10.2174/138920111798357465
62. Bazan JF, Bacon KB, Hardiman G, Wang W, Soo K, Rossi D, et al. A New Class of Membrane-Bound Chemokine With a CX3C Motif. *Nature* (1997) 385(6617):640–4. doi: 10.1038/385640a0
63. Lee M, Lee Y, Song J, Lee J, Chang SY. Tissue-Specific Role of CX(3)CR1 Expressing Immune Cells and Their Relationships With Human Disease. *Immune Netw* (2018) 18(1):e5. doi: 10.4110/in.2018.18.e5
64. Landsman L, Bar-On L, Zernecke A, Kim KW, Krauthgamer R, Shagdarsuren E, et al. CX3CR1 is Required for Monocyte Homeostasis and Atherogenesis by Promoting Cell Survival. *Blood* (2009) 113(4):963–72. doi: 10.1182/blood-2008-07-170787
65. Fuhrmann M, Bittner T, Jung CK, Burgold S, Page RM, Mitteregger G, et al. Microglial Cx3cr1 Knockout Prevents Neuron Loss in a Mouse Model of Alzheimer's Disease. *Nat Neurosci* (2010) 13(4):411–3. doi: 10.1038/nn.2511
66. Li C, He J, Zhong X, Gan H, Xia Y. CX3CL1/CX3CR1 Axis Contributes to Angiotensin II-Induced Vascular Smooth Muscle Cell Proliferation and Inflammatory Cytokine Production. *Inflammation* (2018) 41(3):824–34. doi: 10.1007/s10753-018-0736-4
67. Weisheit CK, Kleiner JL, Rodrigo MB, Niepmann ST, Zimmer S, Duerr GD, et al. CX3CR1 is a Prerequisite for the Development of Cardiac Hypertrophy and Left Ventricular Dysfunction in Mice Upon Transverse Aortic Constriction. *PloS One* (2021) 16(1):e0243788. doi: 10.1371/journal.pone.0243788
68. Schmall A, Al-Tamari HM, Herold S, Kampschulte M, Weigert A, Wietelmann A, et al. Macrophage and Cancer Cell Cross-Talk *via* CCR2 and CX3CR1 is a Fundamental Mechanism Driving Lung Cancer. *Am J Respir Crit Care Med* (2015) 191(4):437–47. doi: 10.1164/rccm.201406-1137OC
69. Wei LM, Cao S, Yu WD, Liu YL, Wang JT. Overexpression of CX3CR1 is Associated With Cellular Metastasis, Proliferation and Survival in Gastric Cancer. *Oncol Rep* (2015) 33(2):615–24. doi: 10.3892/or.2014.3645
70. Conroy MJ, Lysaght J. CX3CL1 Signaling in the Tumor Microenvironment. *Adv Exp Med Biol* (2020) 1231:1–12. doi: 10.1007/978-3-030-36667-4_1
71. Rivas-Fuentes S, Salgado-Aguayo A, Arratia-Quijada J, Gorocica-Rosete P. Regulation and Biological Functions of the CX3CL1-CX3CR1 Axis and Its Relevance in Solid Cancer: A Mini-Review. *J Cancer* (2021) 12(2):571–83. doi: 10.7150/jca.47022
72. D'Haese JG, Demir IE, Friess H, Ceyhan GO. Fractalkine/CX3CR1: Why a Single Chemokine-Receptor Duo Bears a Major and Unique Therapeutic Potential. *Expert Opin Ther Targets* (2010) 14(2):207–19. doi: 10.1517/14728220903540265
73. Xu X, Wang Y, Chen J, Ma H, Shao Z, Chen H, et al. High Expression of CX3CL1/CX3CR1 Axis Predicts a Poor Prognosis of Pancreatic Ductal Adenocarcinoma. *J Gastrointest Surg* (2012) 16(8):1493–8. doi: 10.1007/s11605-012-1921-7
74. Strasser K, Birnleitner H. Immunological Differences Between Colorectal Cancer and Normal Mucosa Uncover a Prognostically Relevant Immune Cell Profile. *Oncoimmunology* (2019) 8(2):e1537693. doi: 10.1080/2162402x.2018.1537693
75. Park MH, Lee JS, Yoon JH. High Expression of CX3CL1 by Tumor Cells Correlates With a Good Prognosis and Increased Tumor-Infiltrating CD8+ T Cells, Natural Killer Cells, and Dendritic Cells in Breast Carcinoma. *J Surg Oncol* (2012) 106(4):386–92. doi: 10.1002/jso.23095
76. Ohta M, Tanaka F, Yamaguchi H, Sadanaga N, Inoue H, Mori M. The High Expression of Fractalkine Results in a Better Prognosis for Colorectal Cancer Patients. *Int J Oncol* (2005) 26(1):41–7. doi: 10.3892/ijo.26.1.41
77. Dimberg J, Dienus O, Löfgren S, Hugander A, Wågsäter D. Polymorphisms of Fractalkine Receptor CX3CR1 and Plasma Levels of its Ligand CX3CL1 in Colorectal Cancer Patients. *Int J Colorectal Dis* (2007) 22(10):1195–200. doi: 10.1007/s00384-007-0343-6
78. Yamauchi T, Hoki T, Oba T, Saito H, Attwood K, Sabel MS, et al. CX3CR1-CD8+ T Cells are Critical in Antitumor Efficacy But Functionally Suppressed in the Tumor Microenvironment. *JCI Insight* (2020) 5(8). doi: 10.1172/jci.insight.133920
79. Pathria P, Louis TL, Varner JA. Targeting Tumor-Associated Macrophages in Cancer. *Trends Immunol* (2019) 40(4):310–27. doi: 10.1016/j.it.2019.02.003
80. Dehai C, Bo P, Qiang T, Lihua S, Fang L, Shi J, et al. Enhanced Invasion of Lung Adenocarcinoma Cells After Co-Culture With THP-1-Derived Macrophages *via* the Induction of EMT by IL-6. *Immunol Lett* (2014) 160 (1):1–10. doi: 10.1016/j.imlet.2014.03.004
81. Zhang X, Zhu M, Hong Z, Chen C. Co-Culturing Polarized M2 Thp-1-Derived Macrophages Enhance Stemness of Lung Adenocarcinoma A549 Cells. *Ann Transl Med* (2021) 9(8):709. doi: 10.21037/atm-21-1256
82. Wang X, Zhao X, Wang K, Wu L, Duan T. Interaction of Monocytes/Macrophages With Ovarian Cancer Cells Promotes Angiogenesis *In Vitro*. *Cancer Sci* (2013) 104(4):516–23. doi: 10.1111/cas.12110

Conflict of Interest: The authors declare that the research was conducted in the absence of any commercial or financial relationships that could be construed as a potential conflict of interest.

Publisher's Note: All claims expressed in this article are solely those of the authors and do not necessarily represent those of their affiliated organizations, or those of the publisher, the editors and the reviewers. Any product that may be evaluated in this article, or claim that may be made by its manufacturer, is not guaranteed or endorsed by the publisher.

frontiers | Frontiers in Immunology

ORIGINAL RESEARCH
published: 02 June 2022
doi: 10.3389/fimmu.2022.849984

Neoadjuvant Pembrolizumab and Chemotherapy in Resectable Esophageal Cancer: An Open-Label, Single-Arm Study (PEN-ICE)

Hongtao Duan[1†], Changjian Shao[1†], Minghong Pan[1†], Honggang Liu[1†], Xiaoping Dong[1], Yong Zhang[1], Liping Tong[1], Yingtong Feng[1], Yuanyuan Wang[2], Lu Wang[3], Neil B. Newman[4], Inderpal S. Sarkaria[5], John V. Reynolds[6], Francesco De Cobelli[7], Zhiqiang Ma[8], Tao Jiang[1*] and Xiaolong Yan[1*]*

[1] Department of Thoracic Surgery, Tangdu Hospital, Air Force Medical University, Xi'an, China, [2] Department of Pathology, Tangdu Hospital, Air Force Medical University, Xi'an, China, [3] Department of Pathology, Xijing Hospital, Air Force Medical University, Xi'an, China, [4] Department of Radiation Oncology, Vanderbilt-Ingram Cancer Center, Vanderbilt University Medical Center, Nashville, TN, United States, [5] Department of Cardiothoracic Surgery, The University of Pittsburgh School of Medicine and the University of Pittsburgh Medical Center, Pittsburgh, PA, United States, [6] Department of Surgery, Trinity Centre, St. James's Hospital, Dublin, Ireland, [7] Department of Radiology, IRCCS San Raffaele Scientific Institute, Milan, Italy, [8] Department of Medical Oncology, Senior Department of Oncology, The Fifth Medical Center of PLA General Hospital, Beijing, China

Background: In this single-arm study, the efficacy and safety of neoadjuvant pembrolizumab plus chemotherapy were evaluated in patients with resectable esophageal squamous cell carcinoma (ESCC).

Methods: This study included patients with ESCC of clinical stages II–IVA who underwent surgery within 4 to 6 weeks after completing treatment with pembrolizumab (200 mg) combined with a conventional chemotherapy regimen (3 cycles). The safety and efficacy of this combination treatment were evaluated as primary endpoints of the study.

Results: From April 2019 to August 2020, a total of 18 patients (including 14 men) were enrolled, of whom 13 patients progressed to surgery. Postoperative pathology revealed a major pathological response (MPR) in 9 cases (9/13, 69.2%) and a pathological complete response (pCR) in 6 cases (6/13, 46.2%). Five patients (5/18, 27.8%) experienced serious treatment-related adverse events (AEs) of grades 3–4. At the time of data cutoff (Mar 25, 2022), the shortest duration of follow-up was 17.8 months. Programmed death-ligand 1 (PD-L1) expression in pretreatment specimens was not significantly associated with the percentage of residual viable tumor (RVT) (r=–0.55, P=0.08). Changes in counts of $CD68^+$ macrophage between pre- and post-treatment specimens were weakly correlated with RVT (r=0.71; P=0.07), while a positive correlation was observed between postoperative forkhead box P3-positive $(Foxp3)^+$T cells/$CD4^+$Tcells ratios and RVT (r=0.84, P=0.03).

OPEN ACCESS

Edited by:
Yanhong Deng,
The Sixth Affiliated Hospital of Sun Yat-sen University, China

Reviewed by:
Chunxia Su,
Shanghai Pulmonary Hospital, China
Xiaorong Dong,
Huazhong University of Science and Technology, China

***Correspondence:**
Xiaolong Yan
yanxiaolong@fmmu.edu.cn
Tao Jiang
jiangtaochest@163.com
Zhiqiang Ma
mzqfmmu@163.com

†These authors have contributed equally to this work

Specialty section:
This article was submitted to Cancer Immunity and Immunotherapy, a section of the journal Frontiers in Immunology

Received: *06 January 2022*
Accepted: *28 April 2022*
Published: *02 June 2022*

Citation:
Duan H, Shao C, Pan M, Liu H, Dong X, Zhang Y, Tong L, Feng Y, Wang Y, Wang L, Newman NB, Sarkaria IS, Reynolds JV, De Cobelli F, Ma Z, Jiang T and Yan X (2022) Neoadjuvant Pembrolizumab and Chemotherapy in Resectable Esophageal Cancer: An Open-Label, Single-Arm Study (PEN-ICE). Front. Immunol. 13:849984. doi: 10.3389/fimmu.2022.849984

Conclusions: The combination of neoadjuvant immunotherapy and chemotherapy for ESCC is associated with a high pathological response and immunologic effects in the tumor microenvironment (TME). It has acceptable toxicity and great efficacy, suggesting a strong rationale for its further evaluation in randomized clinical trials (RCTs).

Trial Registration: ChiCTR2100048917.

Keywords: Pembrolizumab, chemotherapy, resectable esophageal cancer, efficacy, safety, pathological complete response (pCR), major pathological response (MPR)

1 INTRODUCTION

Esophageal cancer (EC) is the 7th most common cancer-related death globally. In China, it is the 6_{th}most common malignancy, with esophageal squamous cell carcinoma (ESCC) being the dominant subtype (1). The median overall survival (OS) of patients with advanced or metastatic EC is extremely poor. For patients who have undergone surgeries alone, OS rates are improving; nonetheless, the five-year survival rate does not exceed 50% (2).

According to the current National Comprehensive Cancer Network (NCCN) guidelines, multimodal therapy with neoadjuvant chemoradiotherapy is the recommended standard therapy for patients with T2-4aNxM0 resectable ESCC. The CROSS Study is the definitive modern randomized clinical trial (RCT), with an OS of 48.6 versus 24.0 months in the multimodal and surgery-only cohorts, respectively (3). However, a major limitation for this treatment may be a heightened risk of major respiratory complications (including pneumonia, acute respiratory distress syndrome, respiratory failure, and pulmonary embolism) and mortality postoperatively (4). Consequently, with the advent of a greater understanding of EC tumor biology and genomics, novel approaches that combine efficacy and safety are being explored.

In this regard, there is currently enormous interest in therapies that target the immune cells within the tumor microenvironment (TME). Programmed cell death protein-1 (PD-1) inhibitors have been evaluated in multiple clinical trials. In the KEYNOTE-181 study, pembrolizumab vs. chemotherapy was evaluated as a second-line treatment for advanced (unresectable or metastatic) EC. For patients with PD-L1 combined positive score (CPS) ≥10, the 12-month OS rate was 43% in the pembrolizumab group and 20% in the chemotherapy group (5). And in the KEYNOTE-590 trial, the combination of pembrolizumab and chemotherapy vs. chemotherapy was evaluated as a first-line treatment for the unresectable or metastatic EC. The survival rate at 12 months of ESCC was higher with chemoimmunotherapy versus chemotherapy (51% vs. 38%) (6). In the neoadjuvant treatment of non-small cell lung cancer (NSCLC), PD-1 inhibitors have produced excellent results. In the NCT02716038 study, NADIM study, and our recent trial, neoadjuvant chemoimmunotherapy in resectable NSCLC reported encouraging data of pathological response, with MPR (57%, 83%, 50% respectively) and pCR (33%, 63%, 30% respectively) (7–9).

Given these encouraging trends for neoadjuvant regimens including anti-PD-1 therapy, the present study aimed to explore the safety and efficacy of anti-PD-1 therapy combined with chemotherapy for resectable ESCC in neoadjuvant settings. We also preliminarily explore the correlations between pathological response and immunological parameters of the TME.

2 METHODS

2.1 Patients

Patients gave their informed consent to participate in the study, and the study was approved by the Ethics Committee of Tangdu Hospital of the Fourth Military Medical University (approval No. 202005-12-KY-07-XW-01).

In this single-arm study, 18 patients were enrolled. The eligibility criteria were: (I) aged 18 years or older; (II) Eastern Cooperative Oncology Group (ECOG) score 0-1; (III) histologically confirmed ESCC of clinical stages II–IVA (T2-4aNxM0; for theT2N0M0, the tumor length should be ≥2 cm under endoscopy; When the tumor is located in the cervical segment, the tumor boundary should be more than 5 cm away from the annular pharyngeal muscle. Lymph node with a short diameter ≥10 mm is considered as metastatic lymph node) [according to the American Joint Committee on Cancer (AJCC 8th edition)]; (IV) surgically resectable ESCC evaluated by a multidisciplinary clinical team; (V) normal hematologic, renal, and hepatic function; (VI) receiving guidance on contraception if necessary; (VII) obtained written consent inform. The exclusion criteria were: (I) patients with active autoimmune disease; (II) patients with active concurrent malignancy; (III) patients receiving ongoing systemic steroids (>10 mg daily prednisone equivalents); (IV) patients having received radiotherapy, target therapy, chemotherapy, or other immunosuppressive therapy; (V) patients severe allergic to pembrolizumab, its active substance and/or any excipients (grade ≥3); (VI) patients severely allergic to the investigational chemotherapeutic drug and/or any of its excipients (grade ≥3); (VII) history of HIV positive testing or known acquired immune deficiency syndrome; (VIII) history of hepatitis B or active hepatitis C virus infection; (IX) history of active tuberculosis; (X) pregnant women; (XI) women in the lactation state.

2.2 Procedures

All patients were arranged with pretreatment staging. It consists of upper gastrointestinal endoscopy with histological biopsy, computed tomography (CT) scan of the chest, ultrasonography of liver, pancreas, spleen, kidney and cervical lymph nodes,

pulmonary function test, echocardiography and radionuclide bone scintigraphy. For patients with suspected cervical lymph node involved, external ultrasonography of the neck with fine-needle aspiration or positron emission tomography-CT (PET-CT) was required.

All of the included patients were scheduled to receive the following drugs intravenously: pembrolizumab (200 mg) combined with conventional chemotherapy for three 21-day cycles prior to surgical resection. Chemotherapy regimens were referred to platinum-based two-drug combination chemotherapy. And the specific chemotherapeutic regimen of each patient was performed under investigators' choices. The detailed regimens were shown in **Table 1**.

After the neoadjuvant therapy was completed, reevaluation was performed to exclude patients with contraindication to surgery. The reevaluation included tests the same as pretreatment staging. Surgery was planned within 4–6 weeks after the completion of the induction regimen. McKeown or IvorLewis esophagectomy, including two-field lymphadenectomy with total mediastinal lymph node dissection, was performed according to standard institutional procedures. For patients with cervical lymph nodes involved, three-field lymph node dissection was required.

2.3 Experimental Design

The primary endpoints were safety and efficacy.

2.3.1 Safety

Adverse events (AEs) were assessed according to the Common Terminology Criteria for Adverse Events (CTCAE) V.4.0.

2.3.2 Efficacy

Efficacy was measured according to the following criteria: (I) pathological complete response (pCR), defined as the complete absence of tumor cells (corresponds with MANDARD TRG 1 and Becker grade 1a), or major pathological response (MPR), defined as <10% residual viable tumor (RVT) (it is generally corresponds with MANDARD treatment response grade(TRG) 1 and 2, or Becker pathologic response grade 1a + 1b), or incomplete pathological response, defined as ≥10% RVT (non-MPR/non-pCR) (10); (II) symptom remission, according to the Stooler classification (11); (III) treatment radiographic response, as determined using the Response Evaluation Criteria in Solid Tumors (RECIST version1.1). According to RECIST version1.1, target lesions of EC were defined as lymph nodes with a short diameter ≥15 mm, and primary esophageal lesions were not considered as target lesions. When lesions were consistent with the standards stated above, the definitions of complete response (CR), partial response (PR), stable disease (SD) and progressive disease (PD)were consistent with the standards stated in RECIST 1.1; (IV)R0 resection was defined as circumferential resection margin (CRM) greater than 1 mm and proximal - distal resection margins are free.

2.4 Evaluation of Immunologic Parameters

2.4.1 Clinical Samples

Upper gastrointestinal endoscopy with histological biopsy was carried out to obtain the pre-treatment specimens, and post-operative specimens were collected from surgical excisions. All samples were prepared for follow-up testing.

2.4.2 Immunohistochemistry

PD-L1 expression was detected in pre-treatment formalin-fixed, paraffin-embedded tumor samples using IHC. Batch assays were performed on all samples using the PD-L1 IHC SP263 pharmDx assay according to the manufacturer's instructions. The combined positive score (CPS) were evaluated by two pathologists as described previously.

2.4.3 Immune Signature of Clinical Samples

Forkhead box P3-positive (Foxp3), CD4-positive and CD8-positive tumor-infiltrating lymphocytes were compared between pre-treatment biopsy specimens and surgical specimens using multiplex immunofluorescence (mIF) (Shanghai Baili Biotechnology Co. Ltd., Shanghai, China). CD68-positive macrophages and the expression of programmed death-ligand 1 (PD-L1), tumor necrosis factor-alpha (TNF)-α, and transforming growth factor-beta 1 (TGF)-β1 were also analyzed by immunohistochemistry (online **Supplementary Methods**). The $Foxp3^+$T cells/(CD4+T cells) ratios and $Foxp3^+$T cells/(CD8+T cells) ratios were calculated.

2.5 Statistical Analysis

Demographic and safety data, as well as clinical, pathologic, radiographic, and molecular response data, were recorded using descriptive statistics. The associations between RVT and pretreatment PD-L1 expression were analyzed using Spearman's correlation analysis. Furthermore, the associations of RVT and other pretreatment and posttreatment immune parameters combined with their changes were analyzed using Spearman's correlation analysis, including the expression of TNF-α, TGF-β1, and the counts of $Foxp3^+$ $CD4^+$, $CD8^+$ T cells and $CD68^+$ macrophages. Similarly, the associations of RVT and pretreatment and posttreatment $Foxp3^+$T cells/($CD4^+$T cells) ratios and $Foxp3^+$T cells/($CD8^+$T cells) ratios combined with their changes were analyzed using Spearman's correlation analysis. Additionally, the differences in pCR between patients whose PD-L1 CPS (≥10) and CPS <10 were analyzed with χ^2 test. All P values reported are 2-sided, with the significance level set at 0.05. Statistical analyses were performed using SPSS 19.0.

3 RESULTS

3.1 Baseline Demographic and Clinical Characteristics

From April 2019 to August 2020, 18 patients were enrolled in this study (**Figure 1**), of which the median age was 64 years old and the average age was 60.9 years (ranged from 35 to 78 years). Males accounted for 77.8% (14 patients) of the patients while females accounted for 22.2% (4 patients). The locations of tumors were the middle third of esophagus (15/18, 83.3%) and the distal third of esophagus (3/18, 16.7%). Before the scheduled therapy, 7 patients (38.9%) were classified into clinical tumor stage II, 10 patients (55.6%) into stage III, and 1 patients (5.6%)

TABLE 1 | All detailed data about patients.

Patient No.	Sex	Age (years)	Location of tumor	Clinical TNM (cTNM)	Chemotherapy	RECIST 1.1	Post-Neoadjuvant therapy TNM (ypTNM)	pCR/ MPR	RVT %	PD-L1 CPS	Number of lymph nodes resected
P1	F	59	Middle	cT3N1M0 Stage III	Docetaxel (75m/m^2, D1) +Nedaplatin (80m/m^2, D1)	Non-CR/ non-PD	ypT0N0M0 Stage I	pCR	0		22
P2	M	66	Middle	cT3N1M0 Stage III	Nab-paclitaxel (260 mg/m^2,D1) +Nedaplatin (80m/m^2, D1)	Non-CR/ non-PD	ypT3N1M0 Stage IIIB		20	30	48
P3	M	54	Middle	cT4N1M0 Stage IVA	Docetaxel (75m/m^2, D1) +Nedaplatin (80m/m^2, D1)	SD	ypT4N0M0 Stage IIIB		70	<1	25
P4	M	56	Middle	cT3N2M0 Stage III	Docetaxel (75m/m^2, D1) +Nedaplatin (80m/m^2, D1)	PR	ypT3N2M0 Stage IIIB		60	15	17
P5	M	35	Distal	cT3N1M0 Stage III	Nab-paclitaxel (260 mg/m^2,D1) +Nedaplatin (80m/m^2, D1)	PR	ypT0N0M0 Stage I	pCR	0	45	16
P6	F	51	Middle	cT3N1M0 Stage III	Docetaxel (75m/m^2, D1) +Nedaplatin (80m/m^2, D1)	Non-CR/ non-PD	ypT4N0M0 Stage IIIB		65	<1	48
P7	M	66	Middle	cT3N2M0 Stage III	Nab-paclitaxel (260 mg/m^2,D1) +Nedaplatin (80m/m^2, D1)	PR	YpT1bN0M0 Stage I	MPR	9	10	25
P8	M	59	Middle	cT3N0M0 Stage II	Nab-paclitaxel (260 mg/m^2,D1) +Nedaplatin (80m/m^2, D1)	CR	ypT0N0M0 Stage I	pCR	0		15
P9	M	59	Middle	cT3N0M0 Stage II	Nab-paclitaxel (260 mg/m^2,D1) +Nedaplatin (80m/m^2, D1)	Non-CR/ non-PD	ypT2N0M0 Stage I	MPR	≤10		33
P10	M	66	Middle	cT3N1M0 Stage III	Nab-paclitaxel (260 mg/m^2,D1) +Nedaplatin (80m/m^2, D1)	PR	ypT0N0M0 Stage I	pCR	0	20	26
P11	M	64	Middle	cT3N1M0 Stage III	Nab-paclitaxel (130 mg/m^2, D1,8) +Nedaplatin (80m/m^2, D1)	Non-CR/ non-PD	ypT0N1M0 Stage IIIA	MPR	≤10		26
P12	F	65	Middle	cT3N0M0 Stage II	Nab-paclitaxel (130 mg/m^2, D1,8) +Nedaplatin (80m/m^2, D1)	CR	ypT0N0M0 Stage I	pCR	0	16	29
P13	F	57	Middle	cT3N0M0 Stage II	Nab-paclitaxel (130 mg/m^2, D1,8) +Nedaplatin (80m/m^2, D1)	CR	ypT0N0M0 Stage I	pCR	0	6	27
P14	M	78	Middle	cT3N1M0 Stage III	Nab-paclitaxel (130 mg/m^2, D1,8) +Nedaplatin (80m/m^2, D1)	Non-CR/ non-PD					
P15	M	67	Middle	cT3N0M0 Stage II	Docetaxel (75m/m^2, D1) +Nedaplatin (80m/m^2, D1)	CR					
P16	M	71	Distal	cT3N1M0 Stage III	Nab-paclitaxel (130 mg/m^2, D1,8) +Nedaplatin (80m/m^2, D1)	PR				<1	
P17	M	67	Distal	cT3N0M0 Stage II	Nab-paclitaxel (130 mg/m^2, D1,8) +Nedaplatin (80m/m^2, D1)	Non-CR/ non-PD					
P18	M	67	Middle	cT3N0M0 Stage II	Nab-paclitaxel (260 mg/m^2,D1) +Nedaplatin (80m/m^2, D1)	PD				<1	

pCR, pathological complete response; MPR, major pathological response; RVT, residual viable tumor; PD-L1, programmed death-ligand 1; CPS, combined positive score; CR, complete response; PD, progressive disease; SD, stable disease; PR, partial response.

into stage IV. The detailed data of patients were summarized in **Table 1**.

3.2 Efficacy

This study enrolled 18 patients, of whom 13 patients progressed to surgery, 4 patients refused surgery due to significant tumor regression and symptomatic relief, and 1 patient experienced disease progression (patient 18) and was given definitive chemoradiotherapy (**Figure 1**). The pathological stages of the patients who underwent surgery after treatment were as follows: stage I (8 patients), stage IIIA (1 patients), and stage IIIB (4 patients). Tumor downstaging occurred in 69.2% (9/13) of patients. In this study, R0 resection was defined as circumferential resection margin (CRM) greater than 1 mm. Therefore, R0 resection rate was 84.6% (11/13), R1 resection rate 7.7% (1/13) and R2 resection rate 7.7% (1/13). The mean number of lymph nodes resected during operation was 27.5 (range, 15–48). Postoperative pathological response revealed a pCR in 6 cases (46.2%), and an MPR in 9 cases (69.2%). **Figure 1** shows representative imaging and pathology of a patient with pCR. According to the Stooler classification, before neoadjuvant treatment, 2 patients (22.7%) had stenosis of grade 3 and 16 patients (77.3%) had stenosis of grade 2. While after therapy, 16 patients (88.9%) had grade 0 symptoms, and 2 patients (11.1%) had grade 2 symptoms, with a symptom remission rate of 94.4%. According to RECIST 1.1, 5 patients (27.8%) had a PR, and 4 patients (22.2%) attained a CR, which translated to an objective response rate (ORR) of 50% (**Figure 2**). Intriguingly, in patients achieving MPR, the size of primary lesions was all decreased and the rate of symptom remission was 100%. All detailed data were shown in **Table 1**. Representative imaging and pathology for a patient with PCR was shown in **Figure 3**.

3.3 Survival

Except for loss of follow-up of one patient, all patients had a good follow-up record. At the time of data cutoff (Mar 25, 2022), the shortest duration of follow-up was 17.8 months. and the median follow-up time of the survivors is 23.0 (17.8–29.9) months.

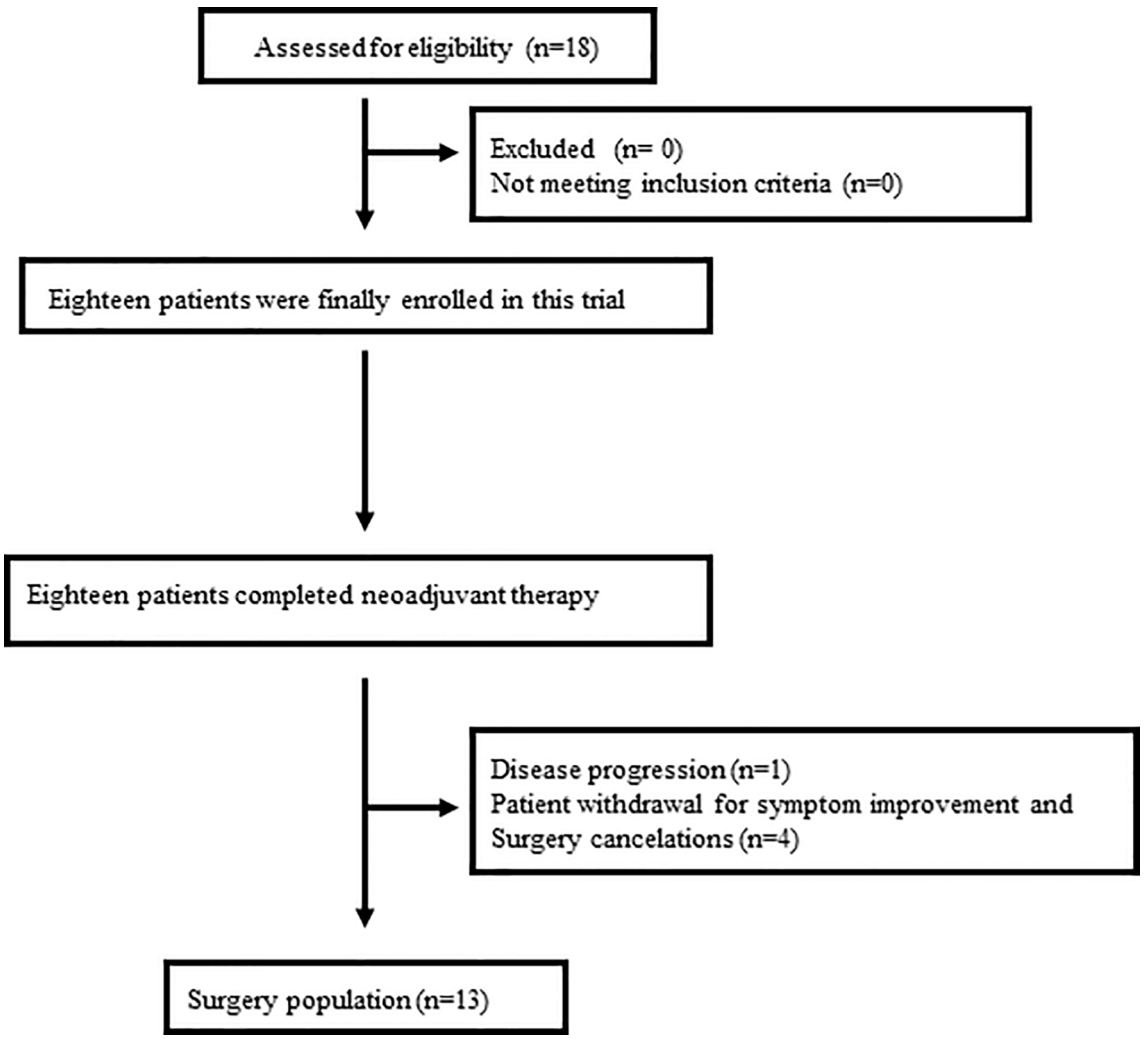

FIGURE 1 | Patients enrolled.

Kaplan-Meier analysis for OS was shown in **Figure 4A**. The median OS was 16.0 months at the non-surgery group while the surgical group has not yet reached the median OS (**Figure 4B**).

In addition, the OS rates in MPR and pCR group were slightly higher than that in non-MPR [hazard ratio (HR) =0.49; 95% confidence interval (CI): 0.06–3.96; P=0.40] and non-pCR group (HR =0.43; 95% CI: 0.06–3.14; P=0.62), respectively (**Figures 4C, D**).

3.4 Safety and Surgical Complications

AEs are shown in **Table 2**. None of the patients in the study discontinued treatment due to an AE. The most common treatment-related AEs of grade 1 or 2 were leukopenia, neutropenia, anorexia, vomiting, fatigue, and alopecia. Five patients (5/18, 27.8%) experienced serious treatment-related AEs of grade 3–4 (including anemia, neutropenia, anorexia, vomiting, fatigue, and alopecia). Hypothyroidism, skin rashes and pneumonitis were attributed as possibly being related to the immunotherapy.

Thirteen patients received surgery. Postoperative complications included hoarseness (5 cases, 38.%), pneumonia (4 cases, 30.8%), empyema (3 cases, 23.1%), atelectasis (2 cases, 15.4%), heart failure (2 cases, 15.4%), respiratory failure (1 case, 7.7%), and anastomotic leak (1 case, 7.7%). Patient 11 developed pneumonitis and pneumonia on postoperative day 1, after treatment with antimicrobial drugs and steroids (2 mg/kg), and his conditions gradually worsened until his death on postoperative day 22.

3.5 Pathologic Assessment and Genomic Analyses

Samples from 11 patients before treatment (pre-treatment) and 7 patients after three cycles of neoadjuvant immunochemotherapy (post-treatment) were obtained. Samples at both time points were available for 7 patients (patients 2, 3, 4, 5, 6, 7, 10).

The data suggested that RVT was not significantly associated with pre-treatment PD-L1 expression (r=−0.55; P=0.08)

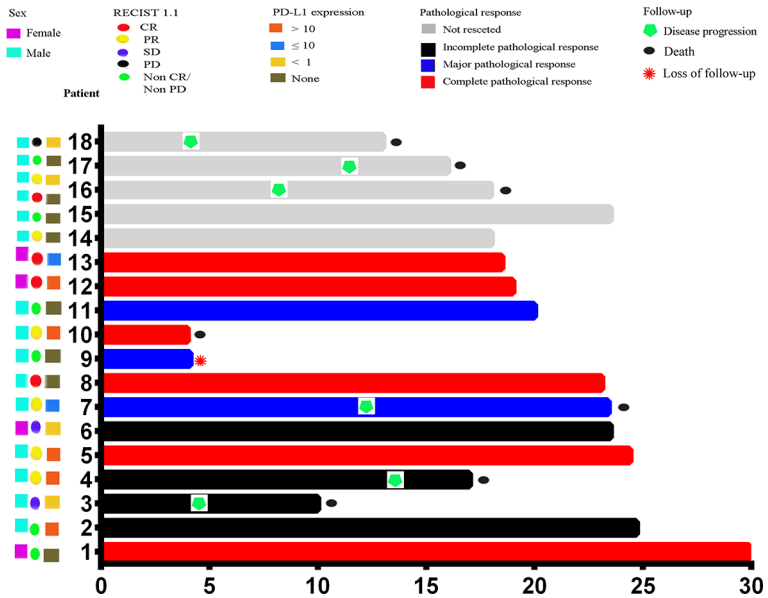

FIGURE 2 | Swimmer plot of PFS in the modified intention-to-treat population (n = 18). Each bar represents one patient. The left column shows clinical characteristics. PFS, progression-free survival.

(**Figure 5**). Additionally, between patients whose PD-L1 CPS (≥10) and CPS <10, no significant differences in pCR were identified.

Further analysis showed that the changes in counts of $CD68^+$ macrophage were found to be positively correlated with RVT (r = 0.71; P = 0.07) (**Figures 6A, B**). To explore the relationship between inflammatory cytokines and RVT, immunohistochemical methods were adopted to examine pre- and post-treatment expression of TNF-α and TGF-β1 in the pathologic specimens (**Figures 6C–F**). In this study, the post-treatment expression of TGF-β1 was increased compared to the preoperative expression, and the changes in TGF-β1 expression were positively correlated with RVT (r=0.65, P=0.11) and possibly indicated a poor prognosis (**Figures 6C, D**). However, the available data showed no significant correlation between the changes in TNF-α expression and RVT (**Figures 6E, F**). The correlations of RVT and the parameters of lymphocyte populations stated above were further explored (**Figures 7A, B**), with a positive correlation observed between postoperative $Foxp3^+$ T cells/($CD4^+$ T cells) ratios and RVT (r=0.84, P=0.03) (**Figure 7C**), positive correlation observed between changes in $Foxp3^+$ T cells/($CD4^+$ T cells) ratios and RVT (r=0.59, P=0.21) (**Figure 7D**) and negative correlation observed between the counts of postoperative $CD8^+$ T cells and RVT (r = −0.61, P=0.14) (**Figure 6E**). However, no direct correlation was found between other immune cells and RVT.

4 DISCUSSION

Different from PALACE-1, which combines immunotherapy and chemoradiotherapy for resectable EC in neoadjuvant settings, our study is the first to report on pembrolizumab combined with chemotherapy alone in the neoadjuvant treatment of EC (12). Our study was done in our hospital involving 18 patients, small sample size though, important observations were made. At the same time, our trail is the first to report neoadjuvant chemoimmunotherapy for ESCC about OS, except for loss of follow-up of one patient (4 months) and the death of patient (4.1 months), and the longest or shortest follow-up time was 29.9 or 17.8 months. The OS rates of 1-year is similar to previous studies (3, 13).

Firstly, the pCR of 46.2% was high, not dissimilar to the rates observed with chemoradiation in the CROSS trial (in ESCC, 49%) and the NEOCRTEC 5010 RCT (43.2%) (3, 13). We want to show that two patients who had moderate-severe atypical hyperplasis after surgery were identified as having pCR. This level of pathological response has not been observed in previous studies with chemotherapy alone in neoadjuvant settings, of which the pCR was typically less than 20% (12.8%) (14). Furthermore, in a recent retrospective study that performed two cycles of combination of chemotherapy and immunotherapy in neoadjuvant settings of ESCC, their results revealed a pCR of 22.2% to 35.3%, lower than the pCR in our study. It's supposed that the cycles of neoadjuvant treatment may affect the efficacy, which deserves further studies to be confirmed (15, 16). Moreover, pCR and MPR are verified to confer a survival advantage and to prolong median disease-free survival (DFS) in EC and many other cancers (10). To validate the DFS and OS benefits of neoadjuvant chemoimmunotherapy for ESCC, further exploration of this regimen could be done in this patient population. Additionally, in this study, for patients with no target-lesions, the standards of RICIST1.1 system merely consist of CR, PD, non-CR/non-PD, which makes it difficult

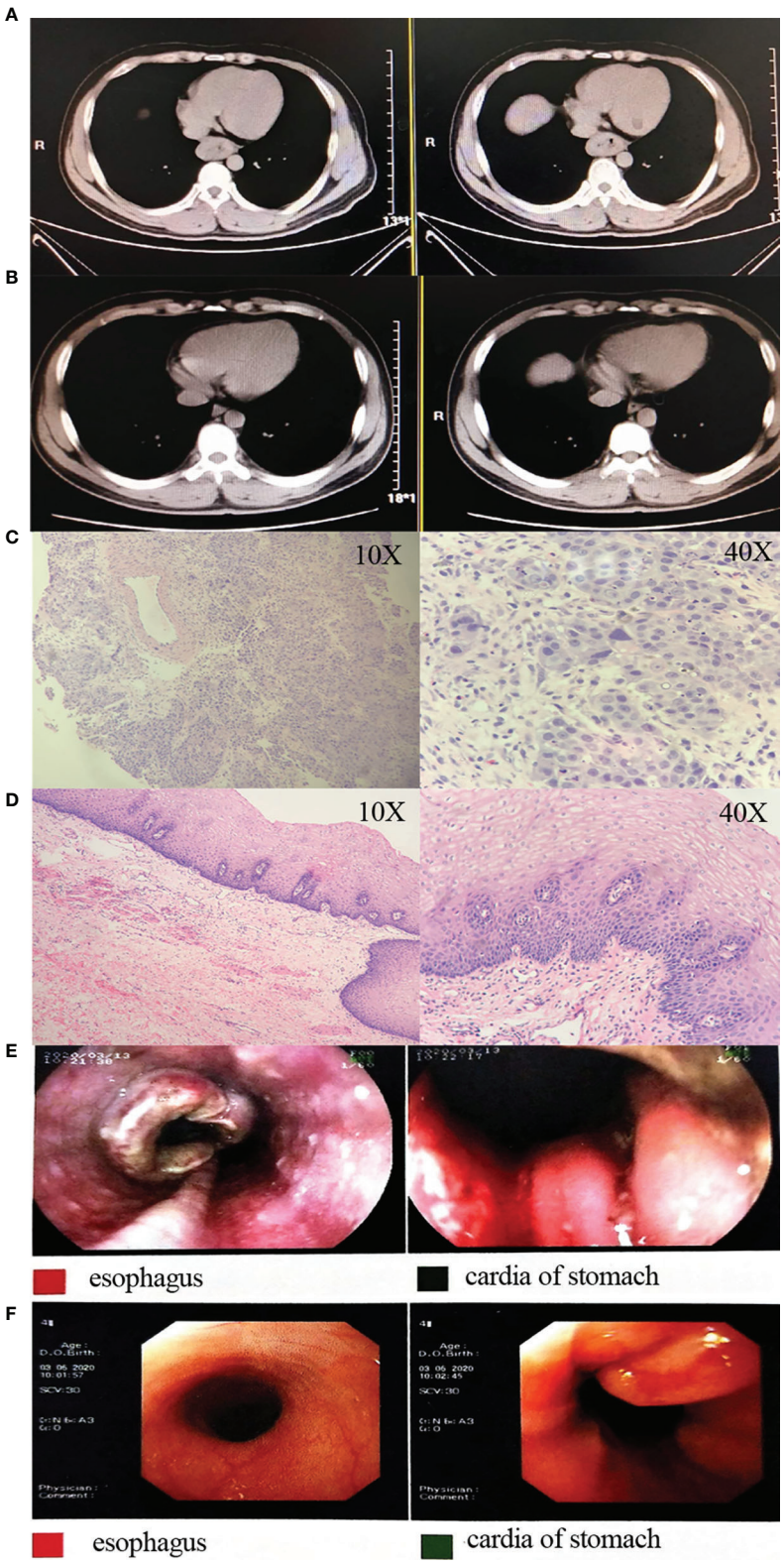

FIGURE 3 | Representative images and pathology for a patient. **(A)** Pre-treatment CT images; **(B)** post-treatment CT images; **(C)** pre-treatment HE staining images; **(D)** post operative HE staining images; **(E)** pre-treatment gastroscopy images; **(F)** post-treatment gastroscopy images. CT, computed tomography; HE, hematoxylin and eosin.

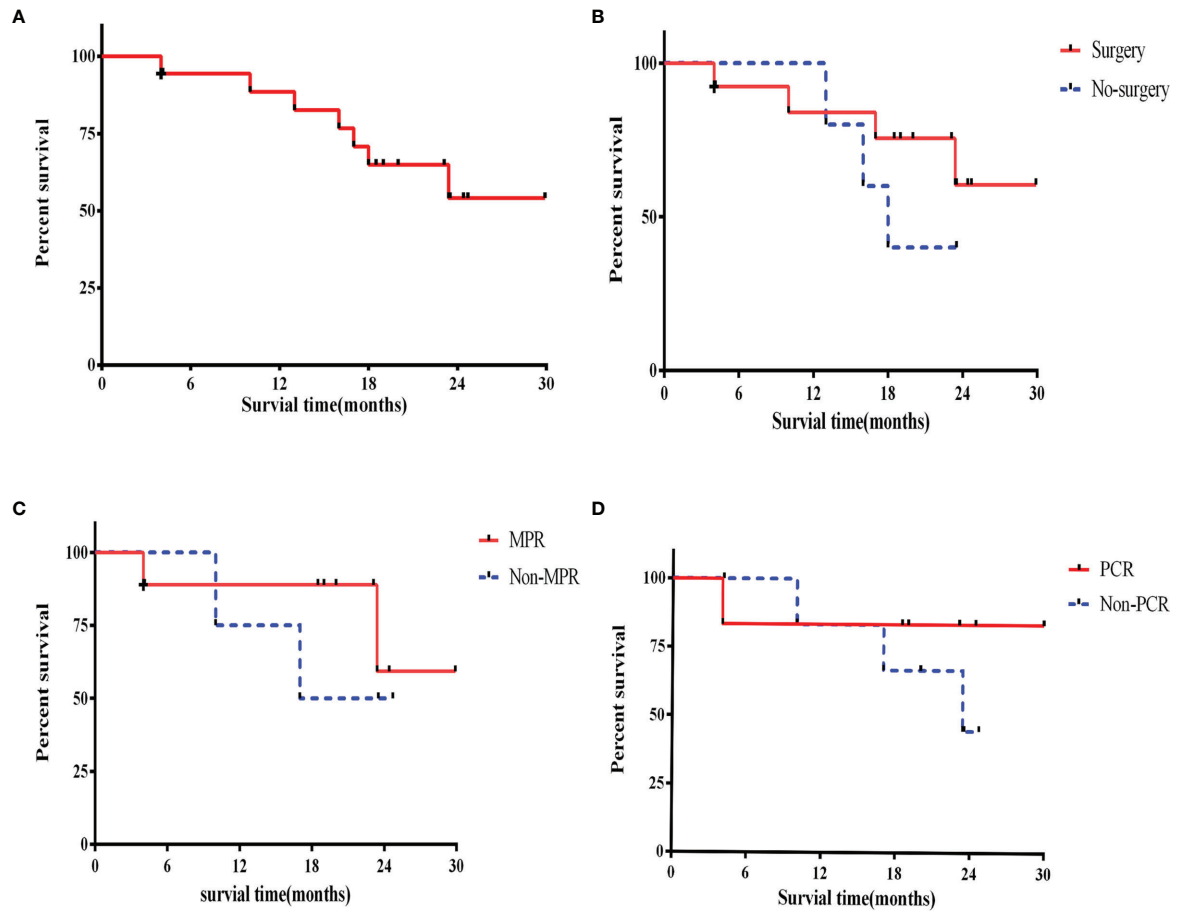

FIGURE 4 | Overall survival. **(A)** Overall survival in the intention-to-treat population; **(B)** overall survival for surgery patients and no surgery; **(C)** overall survival for MPR and non-MPR patients; **(D)** overall survival for pCR and non-pCR patients. +, censoring. MPR, major pathological response; pCR, pathological complete response.

to obtain the values of ORR. Therefore, the accuracy of RICIST1.1 system in evaluating the efficacy of neoadjuvant immunochemotherapy in ESCC needs further exploration.

We also evaluated the safety of the regimen. In our study, only 5 of 18 patients (27.8%) experienced treatment-related AEs of grade 3 or 4. The incidence of serious AEs appears to be acceptable, compared to the PALACE-1 study (65%) and NADIM study (30%) (8, 12). Furthermore, treatment with neoadjuvant pembrolizumab did not delay planned surgery. Immune-related AEs, both hypothyroidism and hypoadrenalism, were identified and relieved with supplementary treatment, with no delay to surgery. The single postoperative death (1/13; 7.7%) which had been

TABLE 2 | Treatment-related adverse events.

Variables	Any grade	Grade 1–2	Grade 3	Grade 4
Anemia	2	2	1	
Leukopenia	7	7		
Neutropenia	7	7	1	
Immune thrombocytopenic purpura	1	1		
Anorexia	8	7	1	
Vomiting	9	8	1	
Diarrhea	2	2		
Fatigue	10	9	1	
Alopecia	6	4	2	
Hypothyroidism	1	1		
Skin rashes	2	2		
Pneumonitis	1	1		

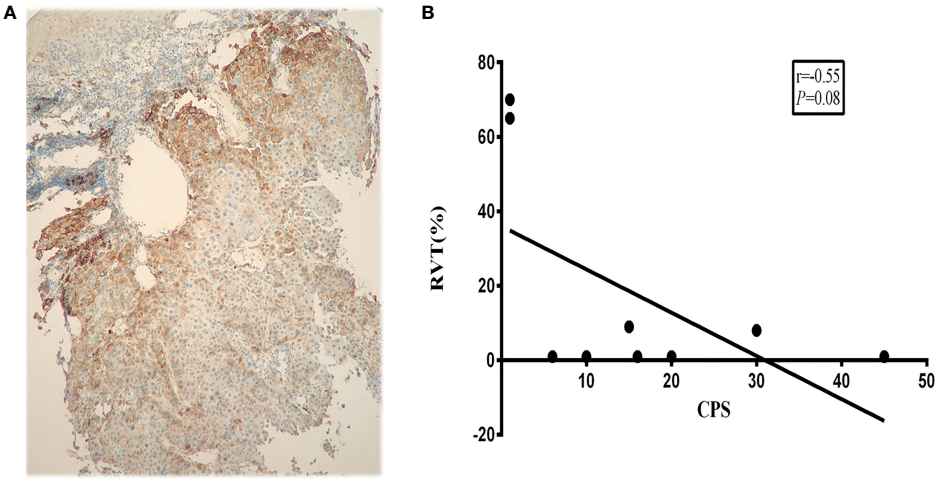

FIGURE 5 | Correlation between PD-L1 expression and RVT. **(A)** Representative PD-L1 IHC image of pre-treatment specimens; **(B)** correlation analysis of PD-L1 expression and RVT. PD-L1, programmed death-ligand 1; RVT, residual viable tumor; IHC, immunohistochemistry.

diagnosed pulmonary fibrosis (Grade 1) at a high risk of pneumonitis was diagosed to pneumonitis and pneumonia, suggesting that we need additional attention to the treatment of complications in such patients (17).

The associations between RVT and the immunologic parameters are intriguing. In the TME, tumor cells, blood vessels, immune cells, lymphocytes, cancer stem cells, and cancer-associated fibroblasts mix, and considerable immune cell activity may be stage- and context-dependent (18). Macrophages are a key component of the TME. As the principal cells of antigen recognition and presentation, they secrete TNF-α, interleukin-1β, and other cytokines, and impact the magnitude and type of T-cell response. Studies report that a high macrophage count was associated with poor OS (19), and this conclusion may also account for the positive correlation between

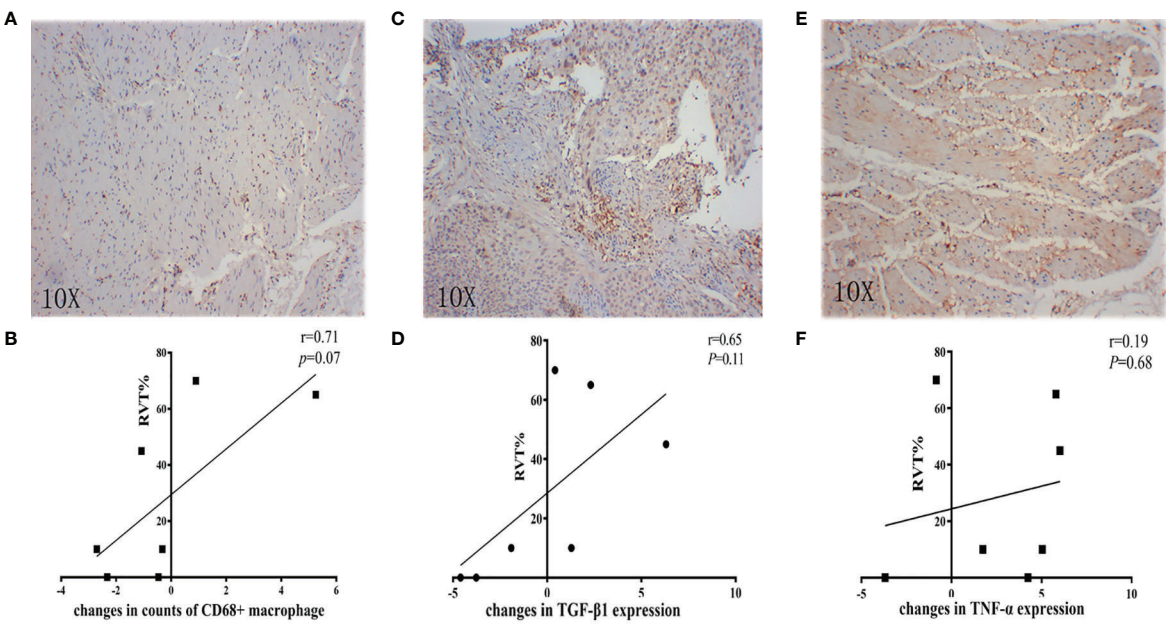

FIGURE 6 | Correlation between inflammatory parameters and RVT. **(A, C, E)** Representative IHC image of CD68, TGF-β1, and TNF-α; **(B)** correlation analysis between changes in counts of $CD68^+$ macrophage and RVT; **(D)** correlation analysis between changes in TGF-β1 expression and RVT; **(F)** correlation analysis between changes in TNF-α expression and RVT. RVT, residual viable tumor; IHC, immunohistochemistry; TGF-β1, transforming growth factor-beta 1; TNF-α, tumor necrosis factor-alpha.

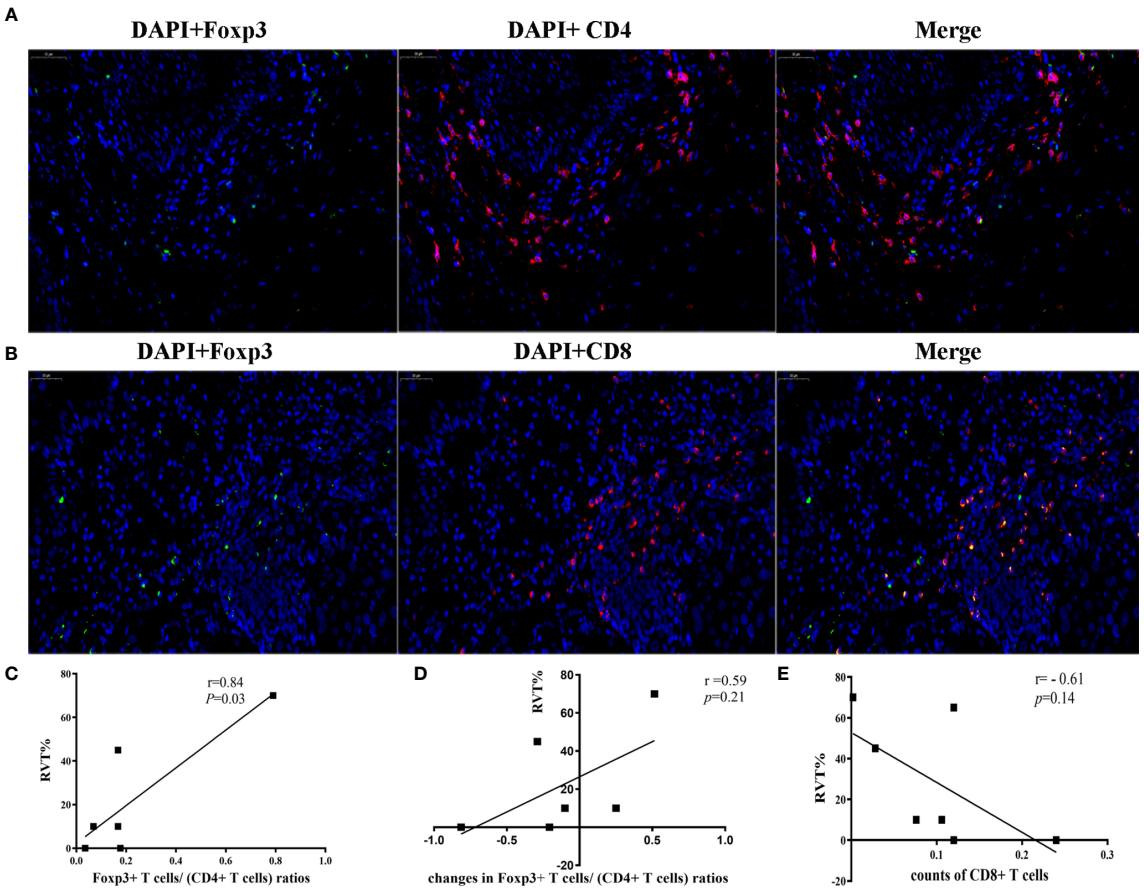

FIGURE 7 | Correlation between immune cells and RVT. **(A)** Two-color immunofluorescence analysis showing the expression of CD4, Foxp3. DAPI (blue), CD4 (red) and Foxp3 (green); **(B)** Two-color Immunofluorescence analysis showing the expression of CD8, Foxp3. DAPI (blue), CD8 (red) and Foxp3 (green); **(C)** correlation analysis between postoperative Foxp3$^+$ T cells/(CD4$^+$ T cells) ratios and RVT; **(D)** correlation analysis between changes in Foxp3$^+$ T cells/(CD4$^+$ T cells) ratios and RVT; **(E)** correlation analysis between the counts of postoperative CD8$^+$ T cells and RVT. RVT, residual viable tumor; DAPI, DAPI (4',6-diamidino-2-phenylindole) fluorescence marking the cell nucleus.

RVT and changed CD68 expression in the post-treatment pathologic tissues compared with the pre-treatment samples. Accordingly, CD68 expression may be predictive of a poor response to immunotherapy, and this requires further study. Immunosuppressive cells [i.e., regulatory T cells (Tregs, Foxp3$^+$ T)] are a part of infiltrating CD4$^+$T-cell in the TME, which significantly inhibit the T-cell-mediated anti-tumor effect and may be associated with T-cell dysfunction (20, 21). In other translational studies, Foxp3$^+$ T cells in the TME of NSCLC were associated with poor OS (22), and in our study, a positive correlation between post-treatment Foxp3$^+$ T cells/(CD4$^+$ T cells) ratios and RVT was confirmed in the context of ESCC, suggesting a prognostic role of post-treatment Foxp3$^+$ T cells/(CD4$^+$ T cells) ratios. No direct correlation was found between the counts of other T cells and RVT. These results may be attributable to the time and space heterogeneity of immunotherapy, although the specific mechanism requires further study. TGF-β1, TNF-α and other cytokines in the TME also play key roles in regulating the response to immunotherapy (23). Among these cytokines, immunoregulatory TGF-β1 suppresses the proliferation of B-cell, cytotoxic T-cell, and natural killer cell and antagonizes the biological effects of TNF-α (24). In other studies, it was reported that TGF-β signaling may counteract anti-tumor immunity by restricting the movement of T-cells in the TME (25). We hypothesized that the increases in TGF-β may predict poor pathological response. This hypothesis was supported by our findings that changes in TGF-β1 expression were positively correlated with RVT. It may be difficult that the small sample size in this study precluded a full analysis of the relationship between TNF-α, TGF-β1, and RVT, and further study is required.

There are some limitations to this study that should be noted. Firstly, other markers of relevance including the genomic profile, tumor mutational burden, and the inflammatory factor interferon-gamma were not evaluated. A further limitation is the study's small sample size; however, since it is the first clinical trial of its kind, it still has important clinical observational significance to serve as the backbone for larger analyses. Another important aspect is that the OS of patients was not

extensively explored, longer follow-up time would be used. Mostly, this is an open-label, single-arm study, so there are bias in enrollment.

5 CONCLUSIONS

In conclusion, neoadjuvant chemoimmunotherapy is safe and feasible for patients with ESCC, with an extremely high pCR and MPR and a clear impact on the TME. With adjuvant studies (such as Checkmate 577 trial) of anti-PD-1 therapy in EC having reported promising results, further RCTs and translational studies should be performed with this treatment paradigm, which appears to hold considerable potential.

DATA AVAILABILITY STATEMENT

The original contributions presented in the study are included in the article/supplementary material. Further inquiries can be directed to the corresponding authors.

ETHICS STATEMENT

The studies involving human participants were reviewed and approved by the Ethics Committee of Tangdu Hospital of the Fourth Military Medical University. The patients/participants provided their written informed consent to participate in this study. Written informed consent was obtained from the individual(s) for the publication of any potentially identifiable images or data included in this article.

AUTHOR CONTRIBUTIONS

Conception and design: XY, TJ and ZM. Administrative support: XY and TJ. Provision of study materials or patients: HD, HL, XD, YZ and LT. Collection and assembly of data: HD, CS, MP, HL, XD, YZ, LT and YF. Data analysis and interpretation: LT, YW, LW, NN, IS, JR and FDC. Manuscript writing: All authors. Final approval of manuscript: All authors. All authors contributed to the article and approved the submitted version.

FUNDING

The present study was supported by grants from the National Natural Science Foundation of China (No. 81871866) and AIRC Investigator Grant 2019 (No.23015).

ACKNOWLEDGMENTS

The authors appreciate the academic support from AME Esophageal Cancer Collaborative Group.

REFERENCES

1. Mao YS, Gao SG, Wang Q, Shi XT, Li Y, Gao WJ, et al. Analysis of a Registry Database for Esophageal Cancer From High-Volume Centers in China. *Dis Esophagus* (2020) 33(8). doi: 10.1093/dote/doz091
2. Yang H, Liu H, Chen Y, Zhu C, Fang W, Yu Z, et al. Long-Term Efficacy of Neoadjuvant Chemoradiotherapy Plus Surgery for the Treatment of Locally Advanced Esophageal Squamous Cell Carcinoma: The NEOCRTEC5010 Randomized Clinical Trial. *JAMA Surg* (2021) 156:721–9. doi: 10.1001/jamasurg.2021.2373
3. Shapiro J, van Lanschot JJB, Hulshof MCCM, van Hagen P, van Berge Henegouwen MI, Wijnhoven BPL, et al. Neoadjuvant Chemoradiotherapy Plus Surgery Versus Surgery Alone for Oesophageal or Junctional Cancer (CROSS): Long-Term Results of a Randomised Controlled Trial. *Lancet Oncol* (2015) 16:1090–8. doi: 10.1016/S1470-2045(15)00040-6
4. Kumagai K, Rouvelas I, Tsai JA, Mariosa D, Klevebro F, Lindblad M, et al. Meta-Analysis of Postoperative Morbidity and Perioperative Mortality in Patients Receiving Neoadjuvant Chemotherapy or Chemoradiotherapy for Resectable Oesophageal and Gastro-Oesophageal Junctional Cancers. *Br J Surg* (2014) 101:321–38. doi: 10.1002/bjs.9418
5. Kojima T, Shah MA, Muro K, Francois E, Adenis A, Hsu CH, et al. Randomized Phase III KEYNOTE-181 Study of Pembrolizumab Versus Chemotherapy in Advanced Esophageal Cancer. *J Clin Oncol* (2020) 38:4138–48. doi: 10.1200/JCO.20.01888
6. Sun JM, Shen L, Shah MA, Enzinger P, Adenis A, Doi T, et al. Pembrolizumab Plus Chemotherapy Versus Chemotherapy Alone for First-Line Treatment of Advanced Oesophageal Cancer (KEYNOTE-590): A Randomised, Placebo-Controlled, Phase 3 Study. *Lancet* (2021) 398:759–71. doi: 10.1016/S0140-6736(21)01234-4
7. Shu CA, Gainor JF, Awad MM, Chiuzan C, Grigg CM, Pabani A, et al. Neoadjuvant Atezolizumab and Chemotherapy in Patients With Resectable Non-Small-Cell Lung Cancer: An Open-Label, Multicentre, Single-Arm, Phase 2 Trial. *Lancet Oncol* (2020) 21:786–95. doi: 10.1016/S1470-2045(20)30140-6
8. Provencio M, Nadal E, Insa A, García-Campelo MR, Casal-Rubio J, Dómine M, et al. Neoadjuvant Chemotherapy and Nivolumab in Resectable Non-Small-Cell Lung Cancer (NADIM): An Open-Label, Multicentre, Single-Arm, Phase 2 Trial. *Lancet Oncol* (2020) 21:1413–22. doi: 10.1016/S1470-2045(20)30453-8
9. Duan H, Wang T, Luo Z, Tong L, Dong X, Zhang Y, et al. Neoadjuvant Programmed Cell Death Protein 1 Inhibitors Combined With Chemotherapy in Resectable Non-Small Cell Lung Cancer: An Open-Label, Multicenter, Single-Arm Study. *Transl Lung Cancer Res* (2021) 10:1020–8. doi: 10.21037/tlcr-21-130
10. Topalian SL, Taube JM, Pardoll DM. Neoadjuvant Checkpoint Blockade for Cancer Immunotherapy. *Science* (2020) 367(6477). doi: 10.1126/science.aax0182
11. Hong-Ke LI, Chen GF, Jian-Jie LI, Han YD, Yong-Juan SUJ. Clinical Effect of Removable Esophageal Stent Implantation and Endoscopic Probe Dilatation in the Treatment of Refractory Esophageal Stricture. *Clinical Res Prac* (2019).
12. Li C, Zhao S, Zheng Y, Han Y, Li HJE. Preoperative Pembrolizumab Combined With Chemoradiotherapy for Oesophageal Squamous Cell Carcinoma (PALACE-1). *Eur J Cancer*, (2021) 144(6):232–41. doi: 10.1016/j.ejca.2020.11.039
13. Yang H, Liu H, Chen Y, Zhu C, Fang W, Yu Z, et al. Neoadjuvant Chemoradiotherapy Followed by Surgery Versus Surgery Alone for Locally Advanced Squamous Cell Carcinoma of the Esophagus (NEOCRTEC5010): A Phase III Multicenter, Randomized, Open-Label Clinical Trial. *J Clin Oncol* (2018) 36:2796–803. doi: 10.1200/JCO.2018.79.1483
14. Peracchia A. Only Pathologic Complete Response to Neoadjuvant Chemotherapy Improves Significantly the Long Term Survival of Patients With Resectable Esophageal Squamous Cell Carcinoma: Final Report of a Randomized, Controlled Trial of Preoperative Chemotherapy Versus Surgery

Alone. *J Cancer* (2015) 91:2165–74. doi: 10.1002/1097-0142(20010601)91:11<2165::AID-CNCR1245>3.0.CO;2-H
15. Fan M, Dai L, Yan W, Yang Y, Lin Y, Chen K. Efficacy of Programmed Cell Death Protein 1 Inhibitor in Resection Transformation Treatment of Esophageal Cancer. *Thorac Cancer* (2021) 12:2182–8. doi: 10.1111/1759-7714.14054
16. Duan H, Wang T, Luo Z, Wang X, Liu H, Tong L, et al. A Multicenter Single-Arm Trial of Sintilimab in Combination With Chemotherapy for Neoadjuvant Treatment of Resectable Esophageal Cancer (SIN-ICE Study). *Ann Transl Med* (2021) 9:1700. doi: 10.21037/atm-21-6102
17. Naidoo J, Wang X, Woo KM, Iyriboz T, Halpenny D, Cunningham J, et al. Pneumonitis in Patients Treated With Anti-Programmed Death-1/Programmed Death Ligand 1 Therapy. *J Clin Oncol* (2017) 35(7):709–17. doi: 10.1200/JCO.2016.68.2005
18. Fridman WH, Pages F, Sautes-Fridman C, Galon J. The Immune Contexture in Human Tumours: Impact on Clinical Outcome. *Nat Rev Cancer* (2012) 12:298–306. doi: 10.1038/nrc3245
19. Galluzzi L, Buque A, Kepp O, Zitvogel L, Kroemer G. Immunological Effects of Conventional Chemotherapy and Targeted Anticancer Agents. *Cancer Cell* (2015) 28:690–714. doi: 10.1016/j.ccell.2015.10.012
20. Huang AC, Postow MA, Orlowski RJ, Mick R, Bengsch B, Manne S, et al. T-Cell Invigoration to Tumour Burden Ratio Associated With Anti-PD-1 Response. *Nature* (2017) 545:60–5. doi: 10.1038/nature22079
21. Galon J. Type, Density, and Location of Immune Cells Within Human Colorectal Tumors Predict Clinical Outcome. *Science* 313(5795):1960–4. doi: 10.1126/science.1129139
22. Liu J, O'Donnell J, Yan J, Madore J, Allen S, Smyth M, et al. Timing of Neoadjuvant Immunotherapy in Relation to Surgery is Crucial for Outcome. *OncoImmunology* (2019) 8:1–12. doi: 10.1080/2162402X.2019.1581530
23. Pardoll DM. The Blockade of Immune Checkpoints in Cancer Immunotherapy. *Nat Rev Cancer* (2012) 12.4(2012):252–64. doi: 10.1038/nrc3239
24. Mariathasan S, Turley SJ, Nickles D, Castiglioni A, Yuen K, Wang Y, et al. Tgfβ Attenuates Tumour Response to PD-L1 Blockade by Contributing to Exclusion of T Cells. *Nature* (2018) 554(7693):544–8. doi: 10.1038/nature25501
25. Batlle E, Massagué J. Transforming Growth Factor-β Signaling in Immunity and Cancer. *Immunity* (2019) 50.4(2019):924–40. doi: 10.1016/j.immuni.2019.03.024

Conflict of Interest: The authors declare that the research was conducted in the absence of any commercial or financial relationships that could be construed as a potential conflict of interest.

Publisher's Note: All claims expressed in this article are solely those of the authors and do not necessarily represent those of their affiliated organizations, or those of the publisher, the editors and the reviewers. Any product that may be evaluated in this article, or claim that may be made by its manufacturer, is not guaranteed or endorsed by the publisher.

frontiers | Frontiers in Immunology

TYPE Systematic Review
PUBLISHED 08 August 2022
DOI 10.3389/fimmu.2022.905651

OPEN ACCESS

EDITED BY
Yanhong Deng,
The Sixth Affiliated Hospital of Sun Yat-sen University, China

REVIEWED BY
Juan Manuel OConnor,
Alexander Fleming Specialized Medical Institute, Argentina
Zengqing Guo,
Fujian Provincial Cancer Hospital, China

*CORRESPONDENCE
Xiujuan Qu
xjqu@cmu.edu.cn

SPECIALTY SECTION
This article was submitted to Cancer Immunity and Immunotherapy, a section of the journal Frontiers in Immunology

RECEIVED 27 March 2022
ACCEPTED 18 July 2022
PUBLISHED 08 August 2022

CITATION
Guo X, Yang B, He L, Sun Y, Song Y and Qu X (2022) PD-1 inhibitors plus oxaliplatin or cisplatin-based chemotherapy in first-line treatments for advanced gastric cancer: A network meta-analysis.
Front. Immunol. 13:905651.
doi: 10.3389/fimmu.2022.905651

PD-1 inhibitors plus oxaliplatin or cisplatin-based chemotherapy in first-line treatments for advanced gastric cancer: A network meta-analysis

Xiaoyu Guo[1,2,3,4,5], Bowen Yang[1,2,3,4,5], Lingzi He[1,2,3,4,5], Yiting Sun[1,2,3,4,5], Yujia Song[1,2,3,4,5] and Xiujuan Qu[1,2,3,4,5]*

[1]Department of Medical Oncology, the First Hospital of China Medical University, Shenyang, China, [2]Key Laboratory of Anticancer Drugs and Biotherapy of Liaoning Province, the First Hospital of China Medical University, Shenyang, China, [3]Liaoning Province Clinical Research Center for Cancer, the First Hospital of China Medical University, Shenyang, China, [4]Key Laboratory of Precision Diagnosis and Treatment of Gastrointestinal Tumors, Ministry of Education, the First Hospital of China Medical University, Shenyang, China, [5]Clinical Cancer Research Center of Shenyang, the First Hospital of China Medical University, Shenyang, China

Background: Currently, there has been no direct comparison between programmed cell death protein 1 (PD-1) inhibitors plus different chemotherapy regimens in first-line treatments for advanced gastric cancer (AGC). This study performed a network meta-analysis (NMA) to evaluate the efficacy and safety of PD-1 inhibitors plus oxaliplatin- or cisplatin-based chemotherapy.

Methods: PubMed, Embase, and the Cochrane Central Register were used to seek a series of phase III randomized controlled trials (RCTs) studying on first-line PD-1 inhibitors plus chemotherapy and phase III RCTs comparing first-line oxaliplatin and cisplatin-based chemotherapy for AGC to perform NMA. The main outcome was overall survival (OS) and other outcomes included progression-free survival (PFS), objective response rate (ORR), and treatment-related adverse events (TRAEs).

Results: Eight eligible RCTs involving 5723 patients were included. Compared with PD-1 inhibitors plus cisplatin-based chemotherapy, PD-1 inhibitors plus oxaliplatin-based chemotherapy could prolong the OS without statistical significance (hazard ratio [HR]: 0.82, 95% credible interval [CI]: 0.63-1.06). However, for patients with combined positive score (CPS) ≥ 1, PD-1 inhibitors plus oxaliplatin-based chemotherapy significantly prolonged the OS (HR: 0.75, 95% CI: 0.57-0.99). PFS in PD-1 inhibitors plus oxaliplatin-based chemotherapy was significantly longer than that in PD-1 inhibitors plus cisplatin-based chemotherapy (HR: 0.72, 95% CI: 0.53-0.99). Regarding safety, the incidence of ≥ 3 TRAEs was similar between PD-1 inhibitors plus oxaliplatin-based

chemotherapy and PD-1 inhibitors plus cisplatin-based chemotherapy (RR: 0.86, 95% CI: 0.66-1.12). The surface under the cumulative ranking area curve (SUCRA) indicated that PD-1 inhibitors plus oxaliplatin-based chemotherapy ranked first for OS (97.7%), PFS (99.3%), and ORR (89.0%). For oxaliplatin-based regimens, there was no significant difference between nivolumab plus oxaliplatin-based chemotherapy and sintilimab plus oxaliplatin-based chemotherapy in terms of OS, PFS, ORR, and ≥3 TRAEs.

Conclusion: Compared with PD-1 inhibitors plus cisplatin-based chemotherapy, PD-1 inhibitors plus oxaliplatin-based chemotherapy significantly prolonged PFS. Considering both efficacy and safety, PD-1 inhibitors plus oxaliplatin-based chemotherapy might be a better option in the first-line treatment for AGC.

KEYWORDS

gastric cancer, first-line, PD-1 inhibitor, oxaliplatin, cisplatin, network meta-analysis

Introduction

Patients with advanced gastric cancer (AGC) have limited treatment options and poor prognosis (1). Chemotherapy is the standard first-line treatment for AGC, with a median overall survival (OS) of less than 1 year (2). The success in application of immune checkpoint inhibitors (ICIs) in many cancer types has prompted us to explore the utility of ICIs in AGC (3, 4). The CheckMate 649 study firstly showed that programmed cell death protein 1 (PD-1) inhibitors plus chemotherapy significantly prolonged OS compared with chemotherapy alone in the first-line treatment for AGC (5). In the recent, the data of ORIENT-16 study also support the advantage of PD-1 inhibitors plus chemotherapy in the first-line treatment for AGC (6). Based on these studies, PD-1 inhibitors in combination with chemotherapy has been recommended as the first-line treatment for AGC (7).

However, not all studies of PD-1 inhibitors based first-line treatment of AGC met their primary endpoints. In the KEYNOTE-062 study, the addition of PD-1 inhibitors to chemotherapy did not significantly prolong OS (8). One of the major differences between the KEYNOTE-062 study and the CheckMate 649 or ORIENT-16 study is the platinum used in chemotherapy. Oxaliplatin-based chemotherapy was used in the CheckMate 649 and ORIENT-16 studies, whereas cisplatin-based chemotherapy was used in the KEYNOTE-062 study. Previous studies of chemotherapy alone in the first-line treatment for AGC have shown that, compared with cisplatin, oxaliplatin has more clinical benefits and considerable advantages in safety (9–11). However, it remains unknown whether oxaliplatin also has advantage when used in combination with PD-1 inhibitors.

Although PD-1 inhibitors plus chemotherapy has been recommended as the first-line treatment for AGC, the therapeutic effect still has potential for improvement by optimizing combination regimens. Prospective clinical studies should be designed to explore combined options, but such studies require a long time to obtain results. Network meta-analysis (NMA) using data analysis from published studies can quickly answer this question and provide clinical reference. Therefore, we conducted the NMA to compare the efficacy and safety of PD-1 inhibitors combined with oxaliplatin or cisplatin-based chemotherapy in the first-line immunotherapy for AGC, hoping to provide some insights for clinical treatment decisions.

Methods

Search strategy

This NMA was conducted following the Preferred Reporting Items for Systematic Review and Meta-Analysis (PRISMA) (12) and the PRISMA extension statement for network meta-analysis (Supplementary Table 1) (13). From the PubMed, Embase, and Cochrane Central Register of randomized controlled trials, we identified qualified phase III randomized controlled trials (RCTs) containing first-line PD-1 inhibitors plus chemotherapy and phase III RCTs comparing first-line oxaliplatin and cisplatin-based chemotherapy for AGC. We searched for studies using keywords including PD-1 inhibitors, oxaliplatin, cisplatin, gastric cancer, first-line and randomized controlled trial (Supplementary Table 2). We also searched

abstracts from major conferences of the American Society of Clinical Oncology (ASCO), the European Society of Medical Oncology (ESMO), the American Association for Cancer Research (AACR), and the World Congress on Gastrointestinal Cancer (WCGC). These clinical studies were limited to those published in English before February 28, 2022.

Inclusion and exclusion criteria

We included phase III RCTs containing first-line PD-1 inhibitors plus chemotherapy and phase III RCTs comparing first-line oxaliplatin- and cisplatin-based chemotherapy for AGC to perform NMA. These trials met the following inclusion criteria: 1) Histologically confirmed AGC. 2) Two or more different-arm studies that included PD-1inhibitors plus chemotherapy and studies comparing oxaliplatin- and cisplatin-based chemotherapy in first-line treatments. 3) The hazard ratio (HR) or relative risk (RR) and its 95% credible interval (CI) of OS, progression-free survival (PFS), objective response rate (ORR) and adverse events (AEs) were available. 4) Published articles were reported in English. Exclusion criteria: 1) Trials involving the results of radiotherapy. 2) Trials only include results from special patient populations, such as elderly patients. 3) HER2 positive AGC/GEJ cancer. 4) Research for which the published data was insufficient for analysis.

Data extraction and quality evaluation

We extracted the design of the trial, sample size, median age, combined positive score (CPS) and primary endpoints of each treatment into a spreadsheet for further analysis. For AEs, we tended to use treatment-related adverse events (TRAEs) for analysis. When TRAEs were not reported, we used common AEs instead. We evaluated the qualities of RCTs included in the present NMA using ROB2 recommended by the Cochrane Collaboration (14). We assessed the following parameters as having a low risk, some concerns, or a high risk: 1) Bias arising from the randomization process. 2) Bias due to deviations from intended interventions. 3) Bias due to missing outcome data. 4) Bias in measuring the outcome. 5) Bias in selection of the reported result. Quality evaluation was performed independently by two investigators (XYG and BWY), where in cases of conflict, a third investigator (XJQ) was consulted for the purpose of conflict resolution.

Statistical analysis

The primary outcome of this study was OS. Secondary outcomes were PFS, ORR and TRAEs of grade 3 and higher (≥ 3 TRAEs). NMA was performed in a Bayesian framework using a Markov Chain Monte Carlo simulation technique within the GEMTC package in the R-Statistics and the J.A.G.S. program (15). Stata 14.0 was used to graphically display the results. For each outcome, 150,000 sample iterations were generated with 100,000 burn-ins and a thinning interval of 10 (16). Fixed and random effect models were considered and compared using deviance information criteria (DIC). If the DIC difference between the random model and the fixed model was less than 5, the fixed model should be selected (17). Model convergence was assessed using a Brooks-Gelman-Rubin diagnostic plot and trace plot (18). Heterogeneity was assessed between studies using the I^2 statistic. The estimated I^2 values under 25%, between 25% and 50%, or over 50% indicated low, moderate, or high heterogeneity respectively (19). All treatments were ranked according to the surface under the cumulative ranking area curve (SUCRA). The higher SUCRA value meant that treatment was more likely to be ranked on the top (20).

Results

Literature search and study characteristics

Literature screening was conducted according to the PRISMA procedure (Figure 1). In total, eight trials involving 5723 patients met predefined inclusion criteria. Key characteristics and specific treatments for the included trials were summarized (Table 1). Three studies compared PD-1 inhibitors plus oxaliplatin-based chemotherapy (PD-1+L-OHP) with oxaliplatin-based chemotherapy (L-OHP), and one study compared PD-1 inhibitors plus cisplatin-based chemotherapy (PD-1+DDP) with cisplatin-based chemotherapy (DDP), four studies compared L-OHP with DDP. The four treatment regimens, including PD-1+L-OHP, PD-1+DDP, L-OHP, and DDP, formed a network map of NMA (Figure 2).

Comparison between PD-1+L-OHP and PD-1+DDP

The NMA implied that compared with PD-1+DDP, PD-1+L-OHP prolonged the OS, but with no statistical significance (HR: 0.82, 95% CI: 0.63-1.06) (Figures 3A, B). As shown in Figure 3C, for patients with CPS ≥ 1, PD-1+L-OHP significantly improved the OS compared with PD-1+DDP in the first-line treatments (HR: 0.75, 95% CI: 0.57-0.99). PFS of PD-1+L-OHP was significantly longer (HR: 0.72, 95% CI: 0.53-0.99). There was no significant difference in terms of ORR between PD-1+L-OHP and PD-1+DDP (RR: 1.09, 95% CI: 0.74-1.61). As for toxicity, the incidence of ≥ 3 TRAEs was similar between PD-1+L-OHP and PD-1+DDP (RR: 1.17, 95% CI: 0.9-1.52) (Figure 4).

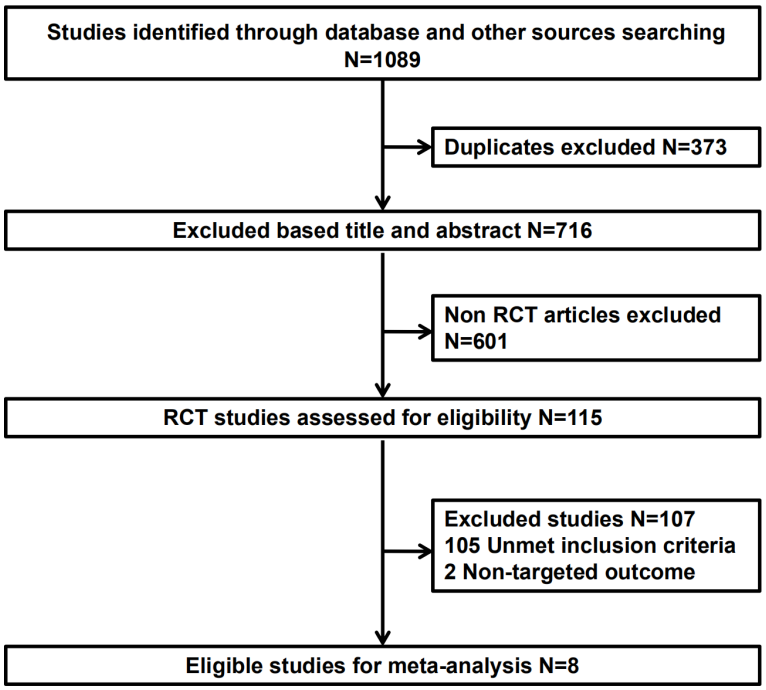

FIGURE 1
Study selection process. RCT, randomized clinical trial.

TABLE 1 Baseline characteristics of studies included in the systematic review.

Study	Treatment Arms	Sample size	Median age	Males No. (%)	CPS subgroup	Primary endpoints
KEYNOTE-062 (8)	Pem+PF[a]	257	62	195 (75.9)	≥1, ≥10	OS, PFS
	PF	250	62.5	179 (71.6)		
CheckMate 649 (5)	Niv+XELOX/FOLFOX[b]	789	62	540 (68)	≥1, ≥5	OS, PFS
	XELOX/FOLFOX	792	61	560 (71)		
ATTRACTION-4 (21)	Niv+CAPOX/SOX[c]	362	63.5	253 (69.9)	NA	OS, PFS
	CAPOX/SOX	362	65	270 (74.6)		
ORIENT-16 (6)	Sin+XELOX[d]	327	62	253 (77.4)	≥1, ≥5, ≥10	OS
	XELOX	323	60	230 (71.2)		
SOLAR (10)	TAS-118+oxaliplatin[e]	347	NA	251 (72)	NA	OS
	CS[f]	334	NA	218 (65)		
JapicCTI-101021 (9)	SOX[g]	343	65	240 (75.5)	NA	OS, PFS
	CS	342	65	237 (73.1)		
SOPP (22)	SOX	173	58	123 (71)	NA	PFS
	SP[h]	164	55	106 (65)		
SOX-GC (11)	SOX	279	NA	NA	NA	OS
	SP	279	NA	NA		

[a]Pem+PF: pembrolizumab 200 mg d1/3w+cisplatin 80 mg/m^2 d1, fluorouracil 800 mg/m^2/d1-5 or capecitabine 1000 mg/m^2 d1-14/3w.
[b]Niv+XELOX/FOLFOX: nivolumab 360 mg/3w d1 or nivolumab 240 mg/2w d1+oxaliplatin 130 mg/m^2 d1, capecitabine 1000 mg/m^2 d1-14/3w or oxaliplatin 85 mg/m^2 d1, tetrahydrofolate 400 mg/m^2 d1, fluorouracil 1200 mg/m^2 d1-2/2w.
[c]Niv+CAPOX/SOX: nivolumab 360 mg/3w d1+oxaliplatin 130 mg/m^2 d1, capecitabine 1000 mg/m^2 d1-14/3w or oxaliplatin 130 mg/m^2 d1+ S-1 40 mg/m^2 d1-14/3w.
[d]Sin+XELOX: sintilimab 3 mg/kg for body weight <60 kg, 200 mg for ≥60 kg d1/3w+oxaliplatin 130 mg/m^2 d1, capecitabine 1000 mg/m^2 d1-14/3w*6 cycles, then capecitabine 1000 mg/m^2.
[e]TAS-118+oxaliplatin: TAS-118 (S-1 40–60 mg and leucovorin 25 mg) bid d1-7 + oxaliplatin 85 mg/m^2 d1/2 w.
[f]CS: S-1 40–60 mg bid d1-21+cisplatin 60 mg/m^2 d1 or d8/5 w.
[g]SOX: S-1 80–120 mg/day d1-14+oxaliplatin 130 mg/m^2 d1/3w.
[h]SP: S-1 80 mg/m^2/day d1-14+cisplatin 60 mg/m^2 d1/3w. PFS, Progression Free Survival; OS, Overall Survival; NA, Not Available; No., number; CPS, combined positive score.

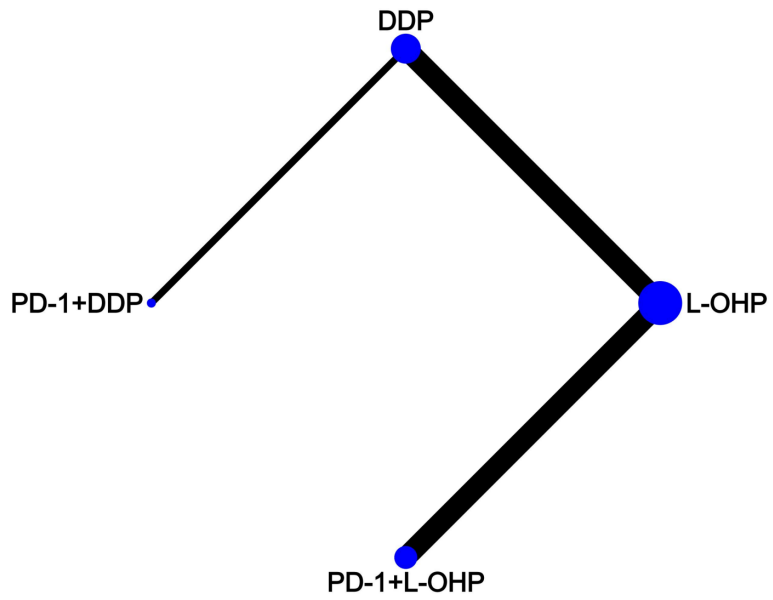

FIGURE 2
Network map. Each circular node represented a type of treatment. Circle size reflects the proportion of patients included in each treatment group. Solid lines represent randomized controlled trials (RCTs) while relative thickness represents the number of included studies. PD-1+L-OHP, PD-1 inhibitors plus oxaliplatin-based chemotherapy; PD-1+DDP, PD-1 inhibitors plus cisplatin-based chemotherapy; L-OHP, oxaliplatin-based chemotherapy; DDP, cisplatin-based chemotherapy.

Comparison between PD-1+L-OHP or PD-1+DDP and L-OHP/DDP

The OS of PD-1+L-OHP was significantly longer compared with L-OHP (HR: 0.82, 95% CI: 0.73-0.92) or DDP (HR: 0.70, 95% CI: 0.60-0.81). PD-1+L-OHP significantly reduced the risk of disease progression or death compared with patients treated with L-OHP (HR: 0.72, 95% CI: 0.62-0.83) or DDP (HR: 0.61, 95% CI: 0.5-0.73). The ORR of PD-1+L-OHP was significantly higher than L-OHP (RR: 1.23, 95% CI: 1.10-1.37) or DDP (RR: 1.23, 95% CI: 1.01-1.50). Compared with L-OHP (RR: 1.22, 95% CI: 1.05-1.43) or DDP (RR: 1.43, 95% CI: 1.13-1.80), PD-1+L-OHP exhibited a significantly higher incidence of ≥ 3 TRAEs (Figures 3A, B). However, there were no significant difference as for OS, PFS, ORR and ≥ 3 TRAEs between PD-1+DDP and L-OHP or DDP (Figures 3A, B, 4A–D).

Ranking probabilities

PD-1+L-OHP ranked first for OS (97.7%), PFS (99.3%), and ORR (89.0%). For safety, PD-1+L-OHP ranked last (4.7%) with the most incidence of ≥ 3 TRAEs (Figure 5).

Comparison of different PD-1 inhibitors in combination treatments

In the current clinical studies, PD-1 inhibitors used in immune therapy plus chemotherapy regimens were also not identical, including nivolumab (Niv) in CheckMate 649 and ATTRACTION-4, pembrolizumab (Pem) in KEYNOTE-062 and sintilimab (Sin) in ORIENT-16. To ascertain whether there was a difference among combination regimens with different PD-1 inhibitors, analysis was performed for different PD-1 inhibitor combination treatments in first-line treatments for AGC (Supplementary Figure 1).

The NMA indicated that patients treated with Sin+L-OHP (HR: 0.64, 95% CI: 0.45-0.92) significantly reduced the risk of disease progression or death compared with patients treated with Pem+DDP; there was no significant difference among Niv +L-OHP, Sin+L-OHP, and Pem+DDP in terms of OS, ORR, and ≥ 3 TRAEs (Figures 6A, B, 7A–D).

Patients with CPS ≥ 5 may benefit more from PD-1 inhibitors plus chemotherapy. In our analysis of patients with CPS ≥ 5, no significant difference was found between Niv+L-OHP and Sin+L-OHP in terms of OS (HR: 0.91, 95% CI: 0.67-1.24) and PFS (HR: 0.90, 95% CI: 0.67-1.20) (Figures 6C, 7E, F).

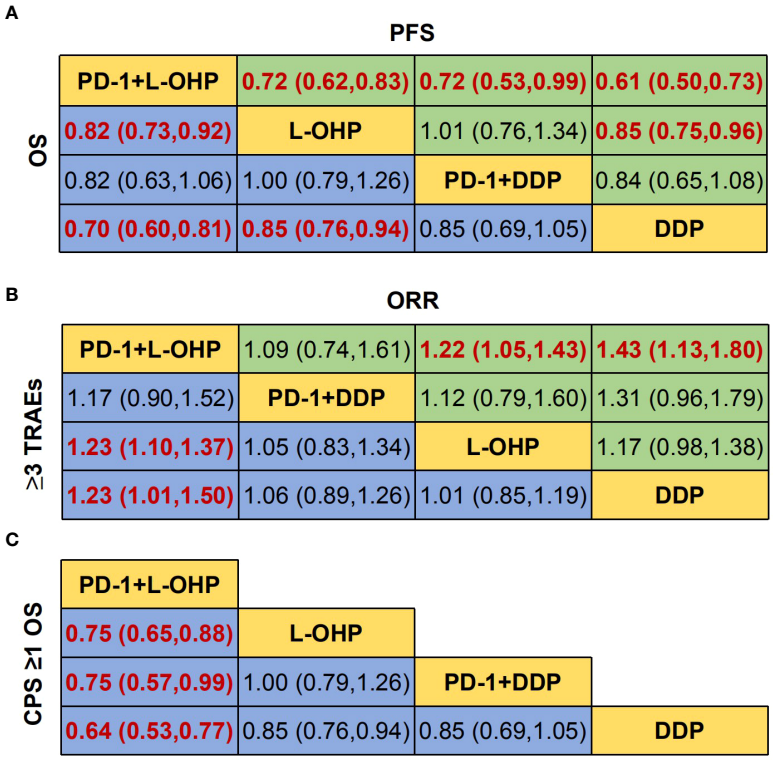

FIGURE 3
Network meta-analysis of the oxaliplatin or cisplatin-based treatments. **(A)** Hazard ratio (HR) [95% credible intervals (CI)] for overall survival (OS) and progression-free survival (PFS). **(B)** Relative risk (RR) (95% CI) for ORR and ≥3 TRAEs. **(C)** Hazard ratio (HR) [95% credible intervals (CI)] for overall survival (OS) of CPS ≥1. Data in each cell are HR or RR (95% CI) for the comparison of row-defining treatment versus column-defining treatment. HR less than 1 and RR for ORR more than 1 favored upper-row treatment. RR for ≥3 TRAEs more than 1 favored downer-row treatment. Significant results were highlighted in red and bold. PD-1+L-OHP, PD-1 inhibitors plus oxaliplatin-based chemotherapy; PD-1+DDP, PD-1 inhibitors plus cisplatin-based chemotherapy; L-OHP, oxaliplatin-based chemotherapy; DDP, cisplatin-based chemotherapy.

For different PD-1 inhibitors-based treatments, Sin+L-OHP ranked first for OS (92.5%), followed by Niv+L-OHP (77.6%), and Pem+DDP (39.8%). The SUCRAs for PFS indicated that Sin+L-OHP (97.1%) was the best, followed by Niv+L-OHP (76.7%), and Pem+DDP (37.4%). The SUCRAs for ORR showed that Niv+L-OHP (78.7%) was the best, followed by Sin+L-OHP (71.1%), and Pem+DDP (60.5%). For safety, Niv+L-OHP ranked the last (5.4%) with the most incidence of ≥ 3 TRAEs (Figure 8).

Risk of bias assessment and sensitivity analyses

The studies included in the analysis were generally at low risk of bias (Supplementary Figure 2). Trace plots and Brooks-Gelman-Rubin analysis implied that the convergence of the chosen model was acceptable (Supplementary Figure 3). The heterogeneity of outcomes in each study was low and moderate (I^2 < 50%).

Discussion

PD-1 inhibitors in combination with chemotherapy has been recommended as the first-line treatment for AGC (7). However, there has been no direct comparison between PD-1 inhibitors plus different chemotherapy regimens. Therefore, we conducted the NMA to compare the efficacy and safety of PD-1 inhibitors combined with oxaliplatin or cisplatin-based chemotherapy in the first-line immunotherapy of AGC, hoping to provide some insights for clinical treatment decisions. At present, only KEYNOTE 811 has published results for first-line treatment of HER2-positive AGC, so this study did not include HER2-positive AGC for analysis (23).

The NMA suggested that compared with PD-1+DDP, PD-1+L-OHP prolonged the OS, but the result did not achieve statistical significance (HR: 0.82, 95% CI: 0.63-1.06). However, for patients with CPS ≥ 1, PD-1+L-OHP significantly prolonged the OS (HR: 0.75, 95% CI: 0.57-0.99). PFS in PD-1+L-OHP was longer than that in PD-1+L-OHP (HR: 0.72, 95% CI: 0.53-0.99). SUCRA showed

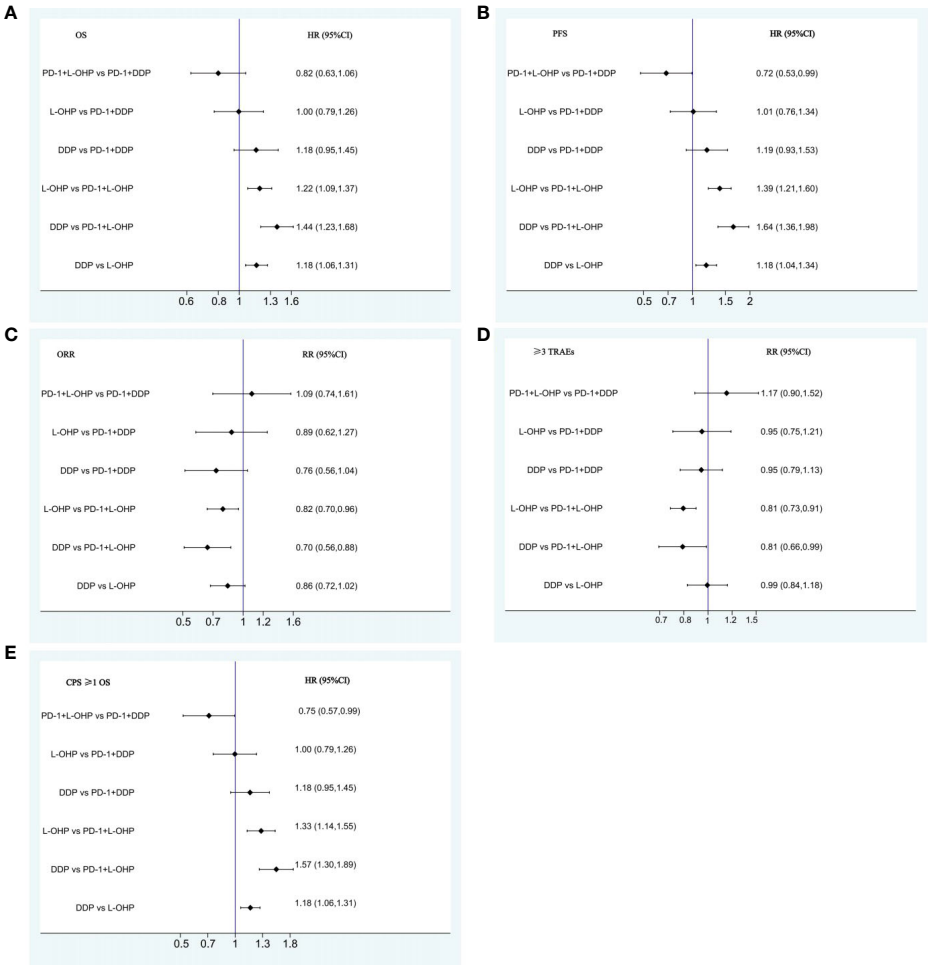

FIGURE 4
Forest plots for comparison among PD-1+L-OHP, PD-1+DDP, L-OHP, and DDP. **(A)** Forest plot for OS; **(B)** Forest plot for PFS; **(C)** Forest plot for ORR; **(D)** Forest plot for ≥3 TRAEs; **(E)** Forest plot for OS of patients with CPS ≥1. PD-1+L-OHP, PD-1 inhibitors plus oxaliplatin-based chemotherapy; L-OHP, oxaliplatin-based chemotherapy; DDP, cisplatin-based chemotherapy.

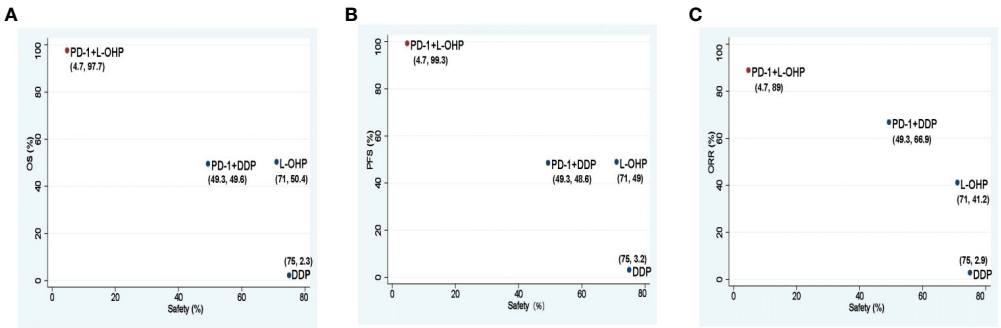

FIGURE 5
Scatter diagrams of SUCRAs among PD-1+L-OHP, PD-1+DDP, L-OHP, and DDP. **(A)** SUCRAs for safety in terms of ≥3 TRAEs and OS; **(B)** SUCRAs for safety in terms of ≥3 TRAEs and PFS; **(C)** SUCRAs for safety in terms of ≥3 TRAEs and ORR. The higher SUCRA value meant that treatment was more likely to be ranked on the top. PD-1+L-OHP, PD-1 inhibitors plus oxaliplatin-based chemotherapy; L-OHP, oxaliplatin-based chemotherapy; DDP, cisplatin-based chemotherapy; SUCRA, surface under the cumulative ranking area curve.

10.3389/fimmu.2022.905651

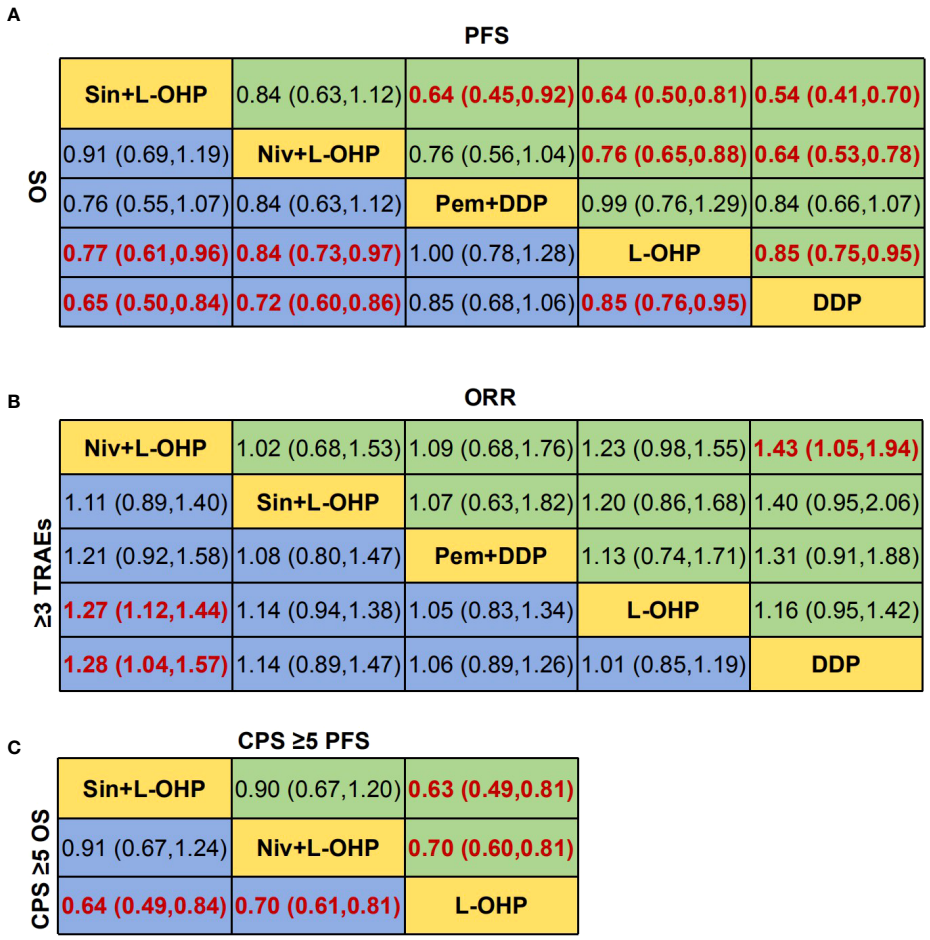

FIGURE 6
Network meta-analysis for different PD-1 inhibitor combination treatments. **(A)** Hazard ratio (HR) [95% credible intervals (CI)] for overall survival (OS) and progression-free survival (PFS). **(B)** Relative risk (RR) (95% CI) for ORR and ≥3 TRAEs. **(C)** Hazard ratio (HR) [95% credible intervals (CI)] for overall survival (OS) of CPS ≥1. Data in each cell are HR or RR (95% CI) for the comparison of row-defining treatment versus column-defining treatment. HR less than 1 and RR for ORR more than 1 favored upper-row treatment. RR for ≥3 TRAEs more than 1 favored downer-row treatment. Significant results were highlighted in red and bold. Niv+L-OHP, nivolumab plus oxaliplatin-based chemotherapy; Sin+L-OHP, sintilimab plus oxaliplatin-based chemotherapy; Pem+DDP, pembrolizumab plus cisplatin-based chemotherapy; L-OHP, oxaliplatin-based chemotherapy; DDP, cisplatin-based chemotherapy.

that PD-1+L-OHP achieved the best OS (97.7%), PFS (99.3%) and ORR (89.0%). Regarding safety, the incidence of ≥ 3 TRAEs was similar between PD-1+L-OHP and PD-1+DDP (RR: 1.17, 95% CI: 0.9-1.52). Meanwhile, compared with L-OHP/DDP, PD-1+L-OHP achieved significant improvement in OS, PFS, and ORR, while PD-1+DDP did not significantly increase clinical benefit.

As far as we know, this is the first study comparing the efficacy and safety of PD-1+L-OHP and PD-1+DDP in first-line treatments for AGC. Our NMA showed that, compared with PD-1 inhibitors plus cisplatin-based chemotherapy, PD-1 inhibitors plus oxaliplatin-based chemotherapy has potentially higher clinical benefit. In addition, in terms of safety, the incidence of ≥ 3 TRAEs was similar between PD-1+L-OHP and PD-1+DDP, but oxaliplatin-based regimens were found to have less myelosuppression and gastrointestinal toxicity, leading to better tolerance of treatment and improved quality of life than that under cisplatin-based regimens. Considering both efficacy and safety, PD-1 inhibitors plus oxaliplatin-based chemotherapy might be a better option in the first-line treatment of AGC. This result provides a basis for clinical decision-making in the first-line treatment for AGC. However, more randomized controlled trials are needed to validate the conclusions.

Basic research has proven that oxaliplatin has a stronger ICD effect than cisplatin. Oxaliplatin can regulate the three key links of ICD through interacting with various proteins in the ICD pathway. First, after oxaliplatin enters tumor cells, it causes endoplasmic reticulum stress, and calreticulin (CRT) in the endoplasmic reticulum lumen is translocated to the cell

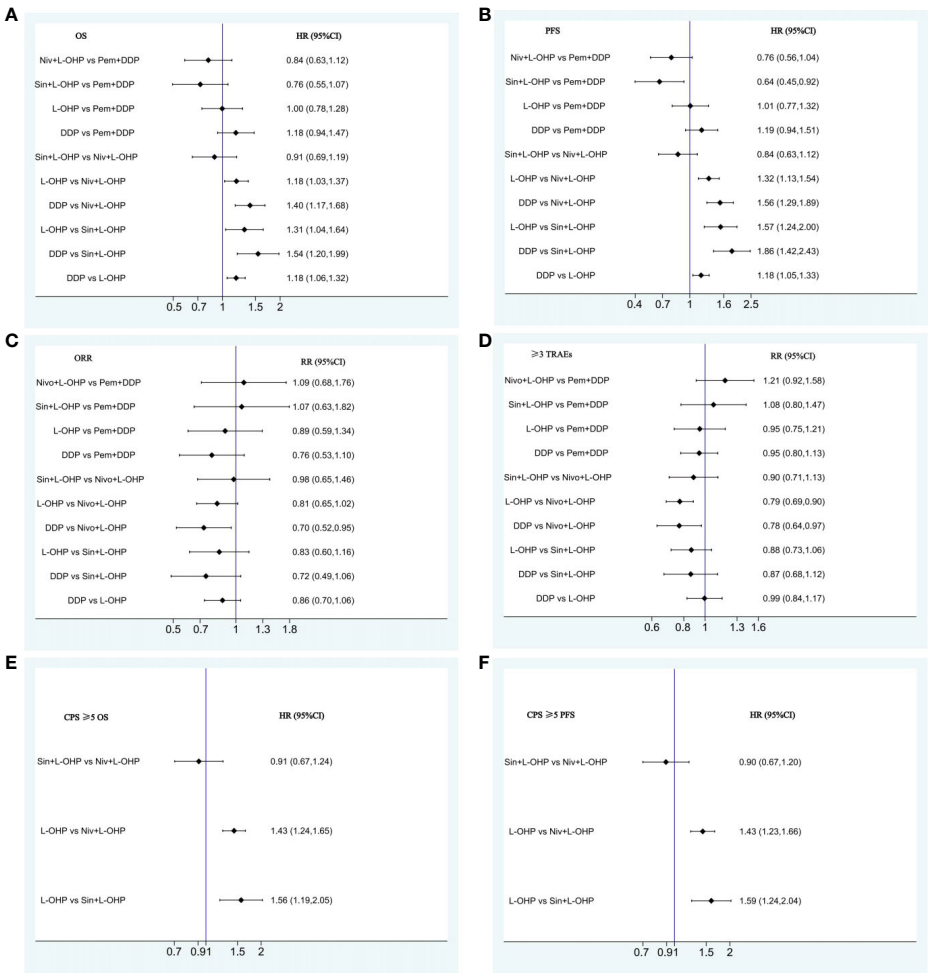

FIGURE 7
Forest plots for comparison among Niv+L-OHP, Sin+L-OHP, Pem+DDP, L-OHP, and DDP. **(A)** Forest plot for OS; **(B)** Forest plot for PFS; **(C)** Forest plot for ORR; **(D)** Forest plot for ≥3 TRAEs; **(E)** Forest plot for OS of patients with CPS ≥5; **(F)** Forest plot for PFS of patients with CPS ≥5. Niv+L-OHP, nivolumab plus oxaliplatin-based chemotherapy; Sin+L-OHP, sintilimab plus oxaliplatin-based chemotherapy; Pem+DDP, pembrolizumab plus cisplatin-based chemotherapy; L-OHP,oxaliplatin-based chemotherapy; DDP, cisplatin-based chemotherapy.

membrane and exposed on the surface of tumor cells, triggering dendritic cells (DCs) and macrophages to engulf tumor cells. Second, oxaliplatin can induce apoptotic cells to release ATP outside the cell, the excreted ATP can recruit DCs and macrophages to the tumor site and can activate DCs. Third, in the late stage of ICD, the permeability of the cell membrane changes, and the cell nuclear high mobility group box 1 (HMGB-1) is released to the outside of the cell and is associated with DCs binding to the surface receptor TLR4, activated DCs, and significantly enhanced the proliferation of DCs. Cisplatin cannot induce CRT exposure on the cell surface, while oxaliplatin induces all three key links of ICD with a stronger ICD effect (24–26). ICD can lead to an enhanced presentation of neoantigens and activation of T cells in the tumor microenvironment (27), thereby enhancing the efficacy of ICIs. Therefore, PD-1+L-OHP may be more effective than PD-1+DDP.

Although PD-1+DDP did not provide obvious benefit in AGC, a significant OS benefit in esophageal cancer was found compared with chemotherapy alone (28). A sub-group analysis of the KEYNOTE 590 study implied that the OS of PD-1+DDP was prolonged in the esophageal adenocarcinoma sub-group, but this did not reach statistical significance, while in the esophageal squamous cell carcinoma sub-group, the OS of PD-1+DDP was

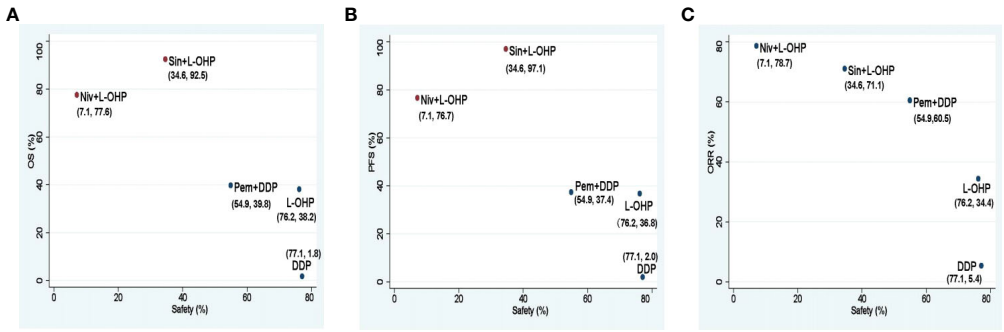

FIGURE 8
Scatter diagrams of SUCRAs among Niv+L-OHP, Sin+L-OHP, Pem+DDP, L-OHP, and DDP. **(A)** SUCRAs for safety in terms of ≥3 TRAEs and OS; **(B)** SUCRAs for safety in terms of ≥3 TRAEs and PFS; **(C)** SUCRAs for safety in terms of ≥3 TRAEs and ORR. The higher SUCRA value meant that treatment was more likely to be ranked on the top. Niv+L-OHP, nivolumab plus oxaliplatin-based chemotherapy; Sin+L-OHP, sintilimab plus oxaliplatin-based chemotherapy; Pem+DDP, pembrolizumab plus cisplatin-based chemotherapy; L-OHP,oxaliplatin-based chemotherapy; DDP, cisplatin-based chemotherapy; SUCRA, surface under the cumulative ranking area curve.

significantly better than that of chemotherapy alone. Therefore, different pathological types may have different responses to the same regimen of PD-1 inhibitors plus chemotherapy. However, there is no relevant comparison of PD-1 inhibitors plus different platinum-based chemotherapy in the treatment of esophageal cancer, which warrants further exploration. In the study of esophageal cancer, the platinum-based chemotherapy regimens contained platinum plus paclitaxel and platinum plus fluorouracil. Whether platinum plus different chemotherapy drugs affected the efficiency of PD-1 inhibitor combination therapy is also worthy of exploration.

In the current clinical studies, PD-1 inhibitors used in immune therapy plus chemotherapy regimens were also not identical, including nivolumab in CheckMate 649 and ATTRACTION-4, pembrolizumab in KEYNOTE-062 and sintilimab in ORIENT-16. To improve the affinity of the antibody, the structures of different PD-1 antibodies have been modified and optimized differently. Therefore, the efficacy and safety of different PD-1 inhibitors may not be exactly the same (29). Whether there are differences among different PD-1 inhibitor combination treatments in AGC was unknown. Our analysis suggested that patients treated with Sin +L-OHP (HR: 0.64, 95% CI: 0.45-0.92) significantly reduced the risk of disease progression or death compared with patients treated with Pem+DDP; and when combined with oxaliplatin-based chemotherapy, OS, PFS, ORR and ≥ 3 TRAEs showed no significant difference between Niv+L-OHP and Sin+L-OHP within the whole population and that population with CPS ≥ 5.

Our analysis showed that Sin+L-OHP ranked first in OS and PFS, and ranked ahead of Nivo+L-OHP in safety. Both sintilimab in ORIENT-16 and nivolumab in CheckMate 649 were combined with oxaliplatin-based chemotherapy, but except for the difference of PD-1 inhibitors, the chemotherapy regimens were not identical. The chemotherapy regimen in the CheckMate 649 study was continuous double-drug chemotherapy with oxaliplatin and fluorouracil, and in the PD-1 inhibitor plus chemotherapy group, 37% of patients discontinued treatment because of AEs (5). While the chemotherapy regimen in ORIENT-16 was oxaliplatin and fluorouracil double-drug chemotherapy for six cycles, followed by fluorouracil maintenance, and only 11.6% of patients in the PD-1 inhibitor plus chemotherapy group discontinued treatment due to AEs (6). This maintenance treatment mode in ORIENT-16 had a higher treatment completion rate. Study has shown that for patients with long-term stable disease control after chemotherapy, chemotherapy can be suspended or maintenance therapy can be performed (30). And the recent ORIENT-16 study has also demonstrated the clinical benefits and feasibility of single-agent maintenance chemotherapy after double-drug chemotherapy in the first-line treatment of PD-1 inhibitors plus chemotherapy for AGC. Therefore, considering the efficacy and safety, the single-agent maintenance treatment after double-drug chemotherapy may be a more appropriate combination chemotherapy mode of first-line PD-1 inhibitors for AGC. Regarding the duration required for double-drug chemotherapy, double-drug chemotherapy was six cycles in the ORIENT-16 study. While in the CheckMate649 study, the median duration of double-drug chemotherapy in the PD-1 inhibitor plus chemotherapy group was 4-4.6 months, which was similar to the duration of double-drug chemotherapy in ORIENT-16. For elderly and frail patients, studies have shown that reducing the dose of chemotherapy drugs to 60% of the original dose did not affect the OS (31), and the reduced dose of two-drug chemotherapy is better than single-agent chemotherapy (32, 33). However, the treatment mode and dose of PD-1 inhibitors combined with chemotherapy in elderly and frail patients need to be explored in the real world,

and the appropriate regimen and dose of PD-1 inhibitors combined with chemotherapy for the general population also need to be verified in future studies.

As so far, PD-1 inhibitors plus chemotherapy has not been proven to be a viable first-line treatment strategy for AGC in the general population. Thus, specific biomarkers are warranted to screen patients who will most benefit from PD-1 inhibitor combination therapy. In our analysis, PD-1+L-OHP was more beneficial for OS in the population with CPS ≥ 1. The expression levels of programmed cell death-ligand 1 (PD-L1) are the most commonly used efficacy predictive biomarkers in AGC clinical trials (34), and CPS proved to be a more useful assessment method than tumor proportion score (TPS) in determining PD-L1 expression (35). Based on sub-group analysis of the CheckMate 649 study, there was no significant benefit in the population with CPS < 5. In the JCO study of the CPS sub-group analysis of the randomized phase III trial, the benefit of the whole population was found to be mainly derived from the population with CPS ≥ 5, and the population with CPS < 5 had no significant benefit (36). Therefore, we are more inclined to recommend that patients with CPS ≥ 5 receive chemotherapy combined with PD-1 inhibitors as first-line treatment. However, the relationship between the expression of PD-L1 and the efficacy of PD-1 inhibitors in AGC is inconsistent, and the role of other predictive biomarkers warrants further evaluation (37). The values of microsatellite instability, tumor mutational burden, and mismatch repair deficiency (dMMR) as biomarkers for predicting response to PD-1 inhibitors have been confirmed by multiple studies (38, 39). The number of immune cells and the expression of T cell-related markers have been shown to be closely related to the response of immunotherapy (40–44). While the gut and tumor microbiota have also been found to be associated with immune checkpoint blockade responses (45). Therefore, the combination of multiple biomarkers may help to screen the immunotherapy advantaged population more accurately in the future.

Recent real-world studies have found that first-line PD-1 inhibitor-containing therapy may increase tumor response to the therapy of taxane plus ramucirumab, thereby improving second-line efficacy of AGC (46, 47). The use of PD-(L)1 inhibitors in front-line therapy can also improve the efficacy of subsequent chemotherapy (48), therefore, from the perspective of the overall treatment of AGC, the application of PD-1 inhibitors in first-line treatment is meaningful. Moreover, the combination of PD-1 inhibitors and chemotherapy also brings new hope to the transformation therapy of AGC. The transformation therapy of AGC refers to the transformation of unresectable gastric cancer into R0 resection by means of chemotherapy, radiotherapy, and targeted or immunotherapy, which can prolong the PFS and OS, and improve the quality of life. In pursuit of transformation, a regimen that achieves a higher ORR should be chosen. However, based on the current phase III study data, the ORR of first-line chemotherapy for AGC seems to have reached a bottleneck, and its ORR is unlikely to exceed 40%-50%. The ORR of PD-1 inhibitors combined with chemotherapy can reach 47.1%-85%, suggesting that it may become an effective transformation therapy regimen. In addition to immunotherapy combined with chemotherapy, phase II clinical studies of immunotherapy combined with different anti-angiogenic drugs have also achieved promising initial results, which deserve to be evaluated in further research (49, 50). And with the application of immunotherapy in first-line treatment for AGC, whether the continued application of ICIs can continue to benefit patients who have progressed on first-line immunotherapy also warrants further exploration. The treatment of AGC has entered a new era of immunotherapy, and we hope that personalized precision immunotherapy based on population screening and treatment optimization will bring more benefits to patients in the future.

Our study has some limitations. First, there are differences in ethnicity in the included studies, and Asians account for more in the assessed population. There are certain differences in the pathological characteristics and treatment response of gastric cancer between Eastern and Western populations, therefore our results may be more instructive for Asian populations. Second, some included studies comparing oxaliplatin and cisplatin-based chemotherapy did not provide PD-L1 expression data, so the sub-group analyses based on PD-L1 expression may be biased. The expression of PD-L1 mainly affects the efficacy of immunotherapy, and the efficacy of chemotherapy alone has not been reported to be related to PD-L1 expression. Therefore, the results based on PD-L1 expression in our analysis have certain reference significance, but further clinical studies are needed to verify this. Finally, the complete data of ORIENT-16 have not yet been published in the form of peer-reviewed articles. Thus, some of the data from this trial were extracted from the poster presentations released at the 2021 ESMO conference, and there might be some potential deviations as a result. Given these limitations, randomized controlled trials are needed to validate our results.

Conclusions

In the first-line treatment for AGC, compared with PD-1 inhibitors plus cisplatin-based chemotherapy, PD-1 inhibitors plus oxaliplatin-based chemotherapy had no statistically significant prolongation for OS, but significantly prolonged PFS. The incidence of ≥ 3 TRAEs was similar between PD-1 inhibitors plus oxaliplatin-based chemotherapy and PD-1 inhibitors plus cisplatin-based chemotherapy. SUCRA showed that PD-1 inhibitors plus oxaliplatin-based chemotherapy achieved the best OS, PFS, and ORR. Considering both efficacy and safety, PD-1 inhibitors plus oxaliplatin-based chemotherapy might be a better option in the first-line treatment for AGC, especially for patients with CPS ≥ 1.

Data availability statement

The original contributions presented in the study are included in the article/Supplementary Material. Further inquiries can be directed to the corresponding author.

Author contributions

XQ conceived and designed the study. XG, BY, LH, YTS and YJS contributed to data acquisition, data interpretation, statistical analysis, and drafting of the manuscript. XQ contributed to data acquisition, data interpretation, statistical analysis and reviewed the manuscript. All authors contributed to the article and approved the submitted version.

Funding

This work was supported by National Natural Science Foundation of China (81972331), "Scientist partner between China Medical University and Shenyang Branch of Chinese Academy of Sciences" Project (HZHB2022002), and Xingliao Talents Program of Liaoning Province (XLYC2008006).

Conflict of interest

The authors declare that the research was conducted in the absence of any commercial or financial relationships that could be construed as a potential conflict of interest.

Publisher's Note

Supplementary Material

The Supplementary Material for this article can be found online at: https://www.frontiersin.org/articles/10.3389/fimmu.2022.905651/full#supplementary-material

References

1. Venerito M, Link A, Rokkas T, Malfertheiner P. Review: Gastric cancer-clinical aspects. *Helicobacter* (2019) 24 Suppl 1:e12643. doi: 10.1111/hel.12643

2. Smyth EC, Nilsson M, Grabsch HI, van Grieken NC, Lordick F. Gastric cancer. *Lancet* (2020) 396(10251):635–48. doi: 10.1016/S0140-6736(20)31288-5

3. Ascierto PA, Del Vecchio M, Mandalá M, Gogas H, Arance AM, Dalle S, et al. Adjuvant nivolumab versus ipilimumab in resected stage IIIB-c and stage IV melanoma (CheckMate 238): 4-year results from a multicentre, double-blind, randomised, controlled, phase 3 trial. *Lancet Oncol* (2020) 21(11):1465–77. doi: 10.1016/S1470-2045(20)30494-0

4. Gandhi L, Rodríguez-Abreu D, Gadgeel S, Esteban E, Felip E, De Angelis F, et al. Pembrolizumab plus chemotherapy in metastatic non-small-cell lung cancer. *N Engl J Med* (2018) 378(22):2078–92. doi: 10.1056/NEJMoa1801005

5. Janjigian YY, Shitara K, Moehler M, Garrido M, Salman P, Shen L, et al. First-line nivolumab plus chemotherapy versus chemotherapy alone for advanced gastric, gastro-oesophageal unction, and oesophageal adenocarcinoma (CheckMate 649): A randomised, open-label, phase 3 trial. *Lancet* (2021) 398 (10294):27–40. doi: 10.1016/S0140-6736(21)00797-2

6. Xu JM, Jiang HP, Pan YY, Gu KS, Cang SD, Han L, et al. Sintilimab plus chemotherapy (chemo) versus chemo as the first-line treatment for advanced gastric or gastroesophageal junction (G/GEJ) adenocarcinoma (ORIENT-16). *ESMO* (2021) LBA53.

7. *NCCN clinical practice guidelines in gastric cancer (Version 2.2022)*. Available at: http://www.nccn.org.

8. Shitara K, Van Cutsem E, Bang YJ, Fuchs C, Wyrwicz L, Lee KW, et al. Efficacy and safety of pembrolizumab or pembrolizumab plus chemotherapy vs chemotherapy alone for patients with first-line, advanced gastric cancer: The KEYNOTE-062 phase 3 randomized clinical trial. *JAMA Oncol* (2020) 6 (10):1571–80. doi: 10.1001/jamaoncol.2020.3370

9. Yamada Y, Higuchi K, Nishikawa K, Gotoh M, Fuse N, Sugimoto N, et al. Phase III study comparing oxaliplatin plus s-1 with cisplatin plus s-1 in chemotherapy-naïve patients with advanced gastric cancer. *Ann Oncol* (2015) 26 (1):141–8. doi: 10.1093/annonc/mdu472

10. Kang YK, Chin K, Chung HC, Kadowaki S, Oh SC, Nakayama N, et al. S-1 plus leucovorin and oxaliplatin versus s-1 plus cisplatin as first-line therapy in patients with advanced gastric cancer (SOLAR): A randomised, open-label, phase 3 trial. *Lancet Oncol* (2020) 21(7):1045–56. doi: 10.1016/S1470-2045(20)30315-6

11. Xu RH, Wang ZQ, Shen L, Wang W, Lu JW, Dai GH, et al. S-1 plus oxaliplatin versus s-1 plus cisplatin as first-line treatment for advanced diffuse-type or mixed-type gastric/gastroesophageal junction adenocarcinoma:A randomized, phase 3 trial. *J Clin Oncol* (2019) 37(Suppl 15):4017. doi: 10.1200/JCO.2019.37.15_suppl.4017

12. Moher D, Liberati A, Tetzlaff J, Altman DGPRISMA Group. Preferred reporting items for systematic reviews and meta-analyses: The PRISMA statement. *PloS Med* (2009) 6(7):e1000097. doi: 10.1371/journal.pmed.1000097

13. Hutton B, Salanti G, Caldwell DM, Chaimani A, Schmid CH, Cameron C, et al. The PRISMA extension statement for reporting of systematic reviews incorporating network meta-analyses of health care interventions: Checklist and explanations. *Ann Intern Med* (2015) 162(11):777–84. doi: 10.7326/M14-2385

14. Higgins JP, Thomas J, Chandler J, Cumpston M, Li T, Page MJ, et al. *Cochrane handbook for systematic reviews of interventions*. Hoboken, NJ, USA: John Wiley & Sons, Inc (2019).

15. Neupane B, Richer D, Bonner AJ, Kibret T, Beyene J. Network meta-analysis using r: A review of currently available automated packages. *PloS One* (2014) 9(12): e115065. doi: 10.1371/journal.pone.0115065

16. Gelman A, Rubin DB. Inference from iterative simulation using multiple sequences. *Stat Sci* (1992) 7:457–72. doi: 10.1214/ss/1177011136

17. Dias S, Welton NJ, Caldwell DM, Ades AE. Checking consistency in mixed treatment comparison meta-analysis. *Stat Med* (2010) 29(7-8):932–44. doi: 10.1002/sim.3767

18. Brooks S, Gelman A. General methods for monitoring convergence of iterative simulations. *J Comput Graphi. Stat* (1998) 7:434–55. doi: 10.1080/10618600.1998.10474787

19. Higgins JP, Thompson SG, Deeks JJ, Altman DG. Measuring inconsistency in meta-analyses. *BMJ* (2003) 327(7414):557–60. doi: 10.1136/bmj.327.7414.557

20. Salanti G, Ades AE, Ioannidis JP. Graphical methods and numerical summaries for presenting results from multiple-treatment meta-analysis: An overview and tutorial. *J Clin Epidemiol* (2011) 64(2):163–71. doi: 10.1016/j.jclinepi.2010.03.016

21. Kang YK, Chen LT, Ryu MH, Oh DY, Oh SC, Chung HC, et al. Nivolumab plus chemotherapy versus placebo plus chemotherapy in patients with HER2-negative, untreated, unresectable advanced or recurrent gastric or gastro-oesophageal junction cancer (ATTRACTION-4): A randomised, multicentre, double-blind, placebo-controlled, phase 3 trial. *Lancet Oncol* (2022) 23(2):234–47. doi: 10.1016/S1470-2045(21)00692-6

22. Lee KW, Chung IJ, Ryu MH, Park YI, Nam BH, Oh HS, et al. Multicenter phase III trial of s-1 and cisplatin versus s-1 and oxaliplatin combination chemotherapy for first-line treatment of advanced gastric cancer (SOPP trial). *Gastric Cancer* (2021) 24(1):156–67. doi: 10.1007/s10120-020-01101-4

23. Janjigian YY, Kawazoe A, Yañez P, Li N, Lonardi S, Kolesnik O, et al. The KEYNOTE-811 trial of dual PD-1 and HER2 blockade in HER2-positive gastric cancer. *Nature* (2021) 600(7890):727–30. doi: 10.1038/s41586-021-04161-3

24. Tesniere A, Schlemmer F, Boige V, Kepp O, Martins I, Ghiringhelli F, et al. Immunogenic death of colon cancer cells treated with oxaliplatin. *Oncogene* (2010) 29(4):482–91. doi: 10.1038/onc.2009.356

25. Gatti L, Cassinelli G, Zaffaroni N, Lanzi C, Perego P. New mechanisms for old drugs: Insights into DNA-unrelated effects of platinum compounds and drug resistance determinants. *Drug Resist Update* (2015) 20:1–11. doi: 10.1016/j.drup.2015.04.001

26. Bezu L, Gomes-de-Silva LC, Dewitte H, Breckpot K, Fucikova J, Spisek R, et al. Combinatorial strategies for the induction of immunogenic cell death. *Front Immunol* (2015) 6:187. doi: 10.3389/fimmu.2015.00187

27. Dimeloe S, Frick C, Fischer M, Gubser PM, Razik L, Bantug GR, et al. Human regulatory T cells lack the cyclophosphamide-extruding transporter ABCB1 and are more susceptible to cyclophosphamide-induced apoptosis. *Eur J Immunol* (2014) 44(12):3614–20. doi: 10.1002/eji.201444879

28. Sun JM, Shen L, Shah MA, Enzinger P, Adenis A, Doi T, et al. Pembrolizumab plus chemotherapy versus chemotherapy alone for first-line treatment of advanced oesophageal cancer (KEYNOTE-590): A randomised, placebo-controlled, phase 3 study. *Lancet* (2021) 398(10302):759–71. doi: 10.1016/S0140-6736(21)01234-4

29. Chang CY, Park H, Malone DC, Wang CY, Wilson DL, Yeh YM, et al. Immune checkpoint inhibitors and immune-related adverse events in patients with advanced melanoma: A systematic review and network meta-analysis. *JAMA Netw Open* (2020) 3(3):e201611. doi: 10.1001/jamanetworkopen.2020.1611

30. Lu Z, Zhang X, Liu W, Liu T, Hu B, Li W, et al. A multicenter, randomized trial comparing efficacy and safety of paclitaxel/capecitabine and cisplatin/capecitabine in advanced gastric cancer. *Gastric Cancer* (2018) 21(5):782–91. doi: 10.1007/s10120-018-0809-y

31. Hall PS, Swinson D, Cairns DA, Waters JS, Petty R, Allmark C, et al. Efficacy of reduced-intensity chemotherapy with oxaliplatin and capecitabine on quality of life and cancer control among older and frail patients with advanced gastroesophageal cancer: The GO2 phase 3 randomized clinical trial. *JAMA Oncol* (2021) 7(6):869–77. doi: 10.1001/jamaoncol.2021.0848

32. Hall PS, Lord SR, Collinson M, Marshall H, Jones M, Lowe C, et al. A randomised phase II trial and feasibility study of palliative chemotherapy in frail or elderly patients with advanced gastroesophageal cancer (321GO). *Br J Cancer* (2017) 116(4):472–8. doi: 10.1038/bjc.2016.442

33. Hwang IG, Ji JH, Kang JH, Lee HR, Lee HY, Chi KC, et al. A multi-center, open-label, randomized phase III trial of first-line chemotherapy with capecitabine monotherapy versus capecitabine plus oxaliplatin in elderly patients with advanced gastric cancer. *J Geriatr Oncol* (2017) 8(3):170–5. doi: 10.1016/j.jgo.2017.01.002

34. Reck M, Rodríguez-Abreu D, Robinson AG, Hui R, Csőszi T, Fülöp A, et al. Pembrolizumab versus chemotherapy for PD-L1-Positive non-Small-Cell lung cancer. *N Engl J Med* (2016) 375(19):1823–33. doi: 10.1056/NEJMoa1606774

35. Yamashita K, Iwatsuki M, Harada K, Eto K, Hiyoshi Y, Ishimoto T, et al. Prognostic impacts of the combined positive score and the tumor proportion score for programmed death ligand-1 expression by double immunohistochemical staining in patients with advanced gastric cancer. *Gastric Cancer* (2020) 23 (1):95–104. doi: 10.1007/s10120-019-00999-9

36. Zhao JJ, Yap DWT, Chan YH, Tan BKJ, Teo CB, Syn NL, et al. Low programmed death-ligand 1-expressing subgroup outcomes of first-line immune checkpoint inhibitors in gastric or esophageal adenocarcinoma. *J Clin Oncol* (2022) 40(4):392–402. doi: 10.1200/JCO.21.01862

37. Morad G, Helmink BA, Sharma P, Wargo JA. Hallmarks of response, resistance, and toxicity to immune checkpoint blockade. *Cell* (2021) 184(21):5309–37. doi: 10.1016/j.cell.2021.09.020

38. Rizvi NA, Hellmann MD, Snyder A, Kvistborg P, Makarov V, Havel JJ, et al. Cancer immunology. mutational landscape determines sensitivity to PD-1 blockade in non-small cell lung cancer. *Science* (2015) 348(6230):124–8. doi: 10.1126/science.aaa1348

39. Le DT, Uram JN, Wang H, Bartlett BR, Kemberling H, Eyring AD, et al. PD-1 blockade in tumors with mismatch-repair deficiency. *N Engl J Med* (2015) 372 (26):2509–20. doi: 10.1056/NEJMoa1500596

40. Tumeh PC, Harview CL, Yearley JH, Shintaku IP, Taylor EJ, Robert L, et al. PD-1 blockade induces responses by inhibiting adaptive immune resistance. *Nature* (2014) 515(7528):568–71. doi: 10.1038/nature13954

41. Wen T, Wang Z, Li Y, Li Z, Che X, Fan Y, et al. A four-factor immunoscore system that predicts clinical outcome for stage II/III gastric cancer. *Cancer Immunol Res* (2017) 5(7):524–34. doi: 10.1158/2326-6066

42. Chen PL, Roh W, Reuben A, Cooper ZA, Spencer CN, Prieto P, et al. Analysis of immune signatures in longitudinal tumor samples yields insight into biomarkers of response and mechanisms of resistance to immune checkpoint blockade. *Cancer Discov* (2016) 6(7):827–37. doi: 10.1158/2159-8290.CD-15-1545

43. Wen T, Barham W, Li Y, Zhang H, Gicobi JK, Hirdler JB, et al. NKG7 is a T-cell intrinsic therapeutic target for improving antitumor cytotoxicity and cancer immunotherapy. *Cancer Immunol Res* (2022) 10(2):162–81. doi: 10.1158/2326-6066

44. Zhang C, Fan Y, Che X, Zhang M, Li Z, Li C, et al. Anti-PD-1 Therapy response predicted by the combination of exosomal PD-L1 and CD28. *Front Oncol* (2020) 10:760. doi: 10.3389/fonc.2020.00760

45. Nejman D, Livyatan I, Fuks G, Gavert N, Zwang Y, Geller LT, et al. The human tumor microbiome is composed of tumor type-specific intracellular bacteria. *Science* (2020) 368(6494):973–80. doi: 10.1126/science.aay9189

46. Sasaki A, Kawazoe A, Eto T, Okunaka M, Mishima S, Sawada K, et al. Improved efficacy of taxanes and ramucirumab combination chemotherapy after exposure to anti-PD-1 therapy in advanced gastric cancer. *ESMO Open* (2020) 4 (Suppl 2):e000775. doi: 10.1136/esmoopen-2020-000775

47. Kankeu Fonkoua LA, Chakrabarti S, Sonbol MB, Kasi PM, Starr JS, Liu AJ, et al. Outcomes on anti-VEGFR-2/paclitaxel treatment after progression on immune checkpoint inhibition in patients with metastatic gastroesophageal adenocarcinoma. *Int J Cancer* (2021) 149(2):378–86. doi: 10.1002/ijc.33559

48. Kato K, Narita Y, Mitani S, Honda K, Masuishi T, Taniguchi H, et al. Efficacy of cytotoxic agents after progression on anti-PD-(L)1 antibody for pre-treated metastatic gastric cancer. *Anticancer Res* (2020) 40(4):2247–55. doi: 10.21873/anticanres.14187

49. Hara H, Shoji H, Takahari D, Esaki T, Machida N, Nagashima K, et al. Phase I/II study of ramucirumab plus nivolumab in patients in second-line treatment for advanced gastric adenocarcinoma (NivoRam study). *J Clin Oncol* (2019) 37(Suppl 4):129. doi: 10.1200/JCO.2019.37.4_suppl.129

50. Fukuoka S, Hara H, Takahashi N, Kojima T, Kawazoe A, Asayama M, et al. Regorafenib plus nivolumab in patients with advanced gastric or colorectal cancer: An open-label, dose-escalation, and dose-expansion phase ib trial (REGONIVO, EPOC1603). *J Clin Oncol* (2020) 38(18):2053–61. doi: 10.1200/JCO.19.03296

Advantages of publishing in Frontiers

OPEN ACCESS
Articles are free to read for greatest visibility and readership

FAST PUBLICATION
Around 90 days from submission to decision

HIGH QUALITY PEER-REVIEW
Rigorous, collaborative, and constructive peer-review

TRANSPARENT PEER-REVIEW
Editors and reviewers acknowledged by name on published articles

Frontiers
Avenue du Tribunal-Fédéral 34
1005 Lausanne | Switzerland

Visit us: www.frontiersin.org
Contact us: frontiersin.org/about/contact

REPRODUCIBILITY OF RESEARCH
Support open data and methods to enhance research reproducibility

DIGITAL PUBLISHING
Articles designed for optimal readership across devices

FOLLOW US
@frontiersin

IMPACT METRICS
Advanced article metrics track visibility across digital media

EXTENSIVE PROMOTION
Marketing and promotion of impactful research

LOOP RESEARCH NETWORK
Our network increases your article's readership